THESE DE DOCTORAT

Présentée à

UNIVERSITE DJILLALI LIABES DE SIDI BEL ABBES
FACULTE DE TECHNOLOGIE
DÉPARTEMENT DE GÉNIE MÉCANIQUE

POUR OBTENIR

LE DIPLOME DE DOCTORAT 3 éme CYCLE EN GÉNIE MÉCANIQUE

Option : Comportement mécanique des matériaux et des structures

Par

Salheddine AYAD

Intitulée :

Contribution à la rééducation d'un membre d'un être humain par un robot

---

Devant le jury composé de :

Mr.	**HAMDAOUI HABIB**	MCA	U. Sidi Bel Abbes	Président
Mr.	**HADJ ABDELKADER MOHAMMED AMINE**	Professeur	U. Tlemcen	Examinateur
Mr.	**ARDJOUN SID AHMED EL MEHDI**	MCA	U. Sidi Bel Abbes	Examinateur
Mr.	**BOUCHIKHI ABOUBAKAR SEDDIK**	Professeur	U. Sidi Bel Abbes	Directeur de thèse

---

Laboratory of Mechanics of Structures and Solids (LMSS), Département Génie Mécanique,
UDL/ Sidi Bel Abbes, Faculté de Technologie,
BP 89, Cité Larbi Ben Mhidi, Sidi Bel Abbès 22000, Algérie
ANNÉE UNIVERSITAIRE 2023-2024

ABSTRACT

Due to the increase in the number of patients with significant gait deficits, the need for sophisticated tools to assist patients with performing different kinds of locomotion training exercises is highly relevant. Ground walking platforms are among the new robotic gait rehabilitation systems that aim to simulate different ground trajectories for a patient (e.g., level ground, hill, etc.) with different haptic materials (e.g., water, sand, ice, etc.). The system targeted in this thesis aims to provide the user with simulated ground reaction forces based on the user's movements in a virtual reality environment by deploying two six-degrees-of-freedom robotic footplates. Each footplate consists of two mechanisms: a XYZ mechanism and the Stewart platform. Overall, the Stewart platform consists of light parts, while the parts of the XYZ mechanism are heavy. The aim of the XYZ mechanism is to simulate translation movements, while the objective of the Stewart platform is to simulate rotational movements as well as to increase the precision of the translational movements.

A position-based admittance/impedance control was adopted for controlling the system. This allows us to define the suitable relation between position and interaction forces for the ground walking platform. The admittance/impedance control strategy was first tested under the assumption of using an ideal hardware (the output from the hardware follows the input well). Using real data, the results show good detection of interaction between the foot and different mediums, while the simulation of the robot gives results concerning the properties of simulated mediums. The admittance/impedance control was also tested by including the dynamic parameters of the XYZ mechanism and Stewart platform. Results show that while the XYZ mechanism performed well in simulating low-frequency movements, some residual inertia appeared when simulating high-frequency movements. Nevertheless, the simulation of high-frequency movements using the Stewart platform exhibited better performance in simulating the desired virtual environment. This demonstrates that the bandwidth of both systems combined is large enough to simulate most types of movements.

ملخص

نظرًا للزيادة في عدد المرضى الذين يعانون من عجز كبير في المشي ، فإن الحاجة إلى أدوات متطورة لمساعدة هذه الفئة من المرضى في أداء أنواع مختلفة من تمارين التدريب على إستعادة حركة المشي المعتادة هي مهمة غاية في الأهمية. تعتبر منصات المشي على الأرض من بين أنظمة إعادة التأهيل الروبوتية الجديدة التي تهدف إلى محاكاة مسارات أرضية مختلفة للمريض (على سبيل المثال ، المشي على أرض مستوية ،صعود درج ، إلخ) و كذلك محاكاة المشي على أسطح بمواد لمسية مختلفة (مثل الماء والرمل والجليد وما إلى ذلك). يهدف النظام المستهدف في هذه الرسالة إلى تطبيق قوى رد فعل أرضية بناءً على تحركات المستخدم في بيئة الواقع الافتراضي و ذلك عن طريق منصتين روبوتيتين توضعان أسفل قدمي المستخدم. تتكون كل منصة من جزئيين مختلفين:جزء يسمى منصة XYZ و الآخر يسمى منصة Stewart. تتكون منصة Stewart من أجزاء ميكانية خفيفة ، بينما تتكون آلية XYZ من أجزاء ثقيلة. الهدف من آلية XYZ هو محاكاة حركات الازاحة

المستقيمة ، بينما الهدف من منصة Stewart هو محاكاة الحركات الدورانية بالإضافة إلى زيادة دقة محاكاة حركات الازاحة المستقيمة.

تم اعتماد نظام التحكم المعروف ب admittance/impedance control كأداة رئيسية للتحكم في في طريقة عمل نظام المحاكاة. يتيح لنا نظام التحكم الآنف ذكره تحديد العلاقة المناسبة بين موقع المنصة الروبتية و القوى التفاعلية التي تطبقها المنصة من أجل محاكاة عملية المشي على الأرض. تم اختبار نظام التحكم admittance/impedance control أولاً تحت فرضية استخدام جهاز مثالي (مخرجات النظام تتبع جيدا مدخلات النظام) باستخدام مدخلات بيانية حقيقية. أظهرت النتائج وجود تنسيق جيد بين موقع قدم المستخدم و القوى القوى التفاعلية المطبقة. كذلك أظهرت النتائج كفائة المنصة الروبوتية على محاكاة المشي على مواد لمسية مختلفة. تم أيضًا اختبار التحكم admittance/impedance control من خلال تضمين الخصائص الديناميكية للمنصتين الروبوتيتين XYZ و Stewart. أظهرت النتائج أنه بينما كان أداء آلية XYZ جيدًا في محاكاة الحركات المنخفضة التردد ، ظهر بعض القصور عند محاكاة الحركات عالية التردد. ومع ذلك ، أظهرت محاكاة الحركات العالية التردد باستخدام منصة Stewart أداءً أفضل في محاكاة البيئة الافتراضية المطلوبة. يوضح هذا أن عرض النطاق الترددي لكلا النظامين مجتمعين كبير بما يكفي لمحاكاة معظم أنواع الحركات.

Résume

En raison de l'augmentation du nombre de patients présentant des déficits de marche importants, le besoin d'outils sophistiqués pour aider le patient à effectuer différents types d'exercices d'entraînement à la locomotion est très pertinent. La plateforme de marche au sol (GWP) est une des nouveaux systèmes robotiques de rééducation de la marche qui visent à simuler différentes types de sol pour un patient (par exemple, sol plat, colline ... etc.) avec différents matériaux haptiques (par exemple eau, sable, glace, etc. ..etc.). Le système visé dans cette thèse vise à fournir à l'utilisateur des forces de réaction au sol simulées basées sur les mouvements des utilisateurs dans un environnement de réalité virtuelle en déployant deux repose-pieds robotiques à 6 degrés de liberté. Chaque plaque de base se compose de deux mécanismes nommés: mécanisme XYZ et plate-forme Stewart. Dans l'ensemble, la plate-forme Stewart se compose de pièces légères, tandis que les parties du mécanisme XYX sont lourdes. Le but du mécanisme XYZ est de simuler les mouvements de translation tandis que l'objectif de la plate-forme Stewart est de simuler le mouvement de rotation ainsi que d'augmenter la précision des mouvements de translation.

Une commande d'admittance / impédance basée sur la position a été adoptée pour contrôler le système. Cela nous permet de définir la relation appropriée entre la position et les forces d'interaction pour la plateforme de marche au sol. La stratégie de contrôle d'admittance / impédance a d'abord été testée sous l'hypothèse d'utiliser une plateforme idéal (la sortie de la plateforme suit bien l'entrée). À partir de données réelles, les résultats montrent une bonne détection de l'interaction entre le pied et les différents milieux, tandis que la simulation du robot donne des résultats concernant les propriétés des milieux simulés. Le contrôle d'admittance / impédance a également été testé en incluant les paramètres dynamiques du mécanisme XYZ et de la plate-forme Stewart. Les résultats montrent que si le mécanisme XYZ a bien fonctionné dans la simulation des mouvements à basse fréquence, une certaine inertie résiduelle est apparue lors de la simulation de mouvements à haute fréquence. Néanmoins, la simulation de mouvements à haute fréquence à l'aide de la plateforme Stewart a montré de meilleures performances dans la simulation de l'environnement virtuel souhaité. Cela démontre que la bande passante des deux systèmes combinés est suffisamment grande pour simuler la plupart des types de mouvements.

TABLE OF CONTENT

LIST OF TABLES

LIST OF FIGURES

General Introduction

According to the World Health Organization [1], 15% of the global population is estimated to be living with some form of disability as of 2010, of which 2.2% have very significant functional difficulties and 3.8% have severe disabilities. This is an increase of 50% over the last 40 years [1]. Neurological disorders are the leading cause of permanent disability worldwide. They can occur as a result of damage to any part of the nervous system, such as the brain, spinal cord or other nerves and tissues, from disease (e.g., stroke or multiple sclerosis) or injury (e.g., spinal cord injuries or brain trauma) [2]. Besides the depressing pain that these individuals suffer, they may also experience physical complications such as muscle atrophy, numbness and loss of sensation [3], [4]. Hence, various functions necessary for daily living are affected [5], such as one's walking abilities, which are the focus of this thesis.

There are two approaches for helping individuals with neurological disorders to perform locomotion for activities of daily living (ADLs). This can be achieved either with the assistance of assistive devices or simply by the patient regaining gait function through rehabilitation. The latter is more desirable, as functionality can never be compensated by any assistive device. However, the success of rehabilitation faces several challenges, such as how to provide a patient with quantitative and qualitative training methods. The physical rehabilitation of gait is to a large extent based on executing high-intensity and repetitive tasks in a motor learning approach [6]. With consideration of one fundamental gait rehabilitation determinant [7] [8], the specificity [9] [10] of regaining full walking functionalities, the patient has to train on two broad gait oriented takes: simple gait training (functional exercises) and ADL-related gait training (occupational exercises). In an early stage of rehabilitation, functional exercises should be conducted to help the patient to improve movement ability and to reduce muscle atrophy [11]. The movements performed in this type of exercise are relatively similar to walking on a typical surface (flat ground). At an advanced stage of rehabilitation, and after the patient gains a certain amount of strength, the focus turns toward teaching the patient to interact with more real-world environments. This corresponds to walking on uneven ground. For most clinical programs, this usually means helping the patient up and down stairs. Nevertheless, one of the basic requirements for realizing the specificity motor learning principle is to provide a diversity of environments in association with different training movements [12]. In addition, providing the patient with feedback on the movements not only helps in enhancing sensitivity, but it also increases the motivation to do so [13]. Thus, a direct effect of the patient's effort can be detected, which is another determinant for a successful rehabilitation [6].

Since the beginning of this century, gait rehabilitation has heavily relied on the use of robotic devices [14] [15]. These systems have shown significant advantages in terms of accuracy and reliability [16]. However, recent clinical studies show no difference between robotic and conventional manual therapy in terms of motor recovery [17]. One of the reasons for this may be related to the uniform ground reactions obtained when using gait robots [18], thus unfirming the specificity of the gait training. Most of these systems are designed with the main goal of providing the patient with reciprocal stepping assistance [19] [20]. Less interest is given to the inclusion of environmental properties. These current systems reveal different limitations in providing an advanced environmental simulation. Among these are the restriction of patient movement on the sagittal plane, the simulation of one type of ground only and the lack of visual feedback on patient movements.

We propose a new robotic gait rehabilitation called the Three-Dimensional Interactive Robotic Rehabilitation System (3D-IRS), which can give the patient a sensation of walking on different types of ground and further provide visual feedback to the patient. The integrated robotic system aims to simulate different types of ground that are not only simple but also complex and which are difficult to realize at clinical centers. The simulation can be realized with a combination of robotic techniques and virtual reality (VR). The system consists of two programmable footplates which have continuous contact with the patient's feet during use. These plates are controlled based on the patient's movements in a VR environment.

The organization of the thesis is as follows. The first chapter presents the state of the art of physical rehabilitation. The chapter discusses in detail fundamental topics related to physical rehabilitation including gait analysis, neurological disorders contributing to gait deficits and principles of physical rehabilitation. In addition, the chapter reviews different techniques that are followed to improve the locomotion ability of patients with neurological disorders.

Data shows that even with the development of some advanced robotic rehabilitation systems, the ability of patients to have a good-quality gait is still limited. Chapter 2 describes the systematic research we performed to investigate the limitations of current robotic gait rehabilitation systems. In addition, the chapter presents an approach for graphically representing different gait rehabilitation systems. Such a representation could be introduced to standardize the evaluation of rehabilitation robots which can help with developing systems with advanced features.

In Chapter 3, our project to improve the quality of gait for patients with neurological disorders is presented. In addition, an overview of how we can make rehabilitation processes motivating for patients is introduced. Moreover, the chapter discusses in detail the technical characteristics and presents a kinematic analysis of the new robotic system we propose with the project.

As an important part of improving the gait rehabilitation experience, we develop a robotic system with two main parts for simulating different gait environments for the patient. The first part has the objective of simulating translation gait movements along *x*-, *y*- and *z*-axes. Thus, the associated system is given the name XYZ mechanism. The second part has the aim of simulating the rotation movements with respect to the *x*-, *y*- and *z*-axes as well as of compensating for the translation movements that cannot be attained with the XYZ mechanism. We propose that the tasks of this mechanism should be done using a Stewart platform.

In Chapter 4, various impedance control methods used to simulate different virtual environments are discussed. The stability and performance of these methods are investigated and tested on the XYZ mechanism. Finally, the limitations of the impedance control, which is selected as the best method for rendering virtual environments, are discussed.

In Chapter 5, the most development type of Stewart platform and a description of different possible configurations are presented. In addition, the characteristics of the optimized Stewart platform we developed to meet certain requirements are covered. Finally, the results of testing the ability of the platform to simulate high-frequency movements are discussed.

Chapter 1: STATE OF THE ART

1.1. Introduction

Gait is a foundational component of independent human function. It involves highly coordinated movements that allow for adaptability to task demands and interaction with the environment. Unfortunately, some people, especially individuals suffering from neurological disorders such as stroke, spinal cord injury or traumatic brain injury, can lose this function. Physical therapy can play an important role in helping these individuals reach significant recovery. This chapter provides a review of the literature related to the physical therapy of gait. Terminologies related to the term "gait," characteristics of its cycle and the most common forms of gait disorders are identified in Section 2. Section 3 discusses the key facts related to the most common neurological disorders. Symptoms, causes and complications of these disorders are extensively explained. Section 4 addresses a rehabilitation-related topic. In this section, principles, methods and clinical tasks of rehabilitation are identified. In Section 5, the state of the art in robotic gait rehabilitation systems is presented, and a broad classification based on rehabilitation principles is given. The chapter summary is provided in the last section.

1.2. Gait

Gait can be defined as: 'a particular way of walking, running, or moving along on foot', or shorter 'a manner of walking'. In literature of rehabilitation, gait is usually a synonym for 'walking' [21]. Human gait is defined as bipedal, biphasic forward propulsion of center of gravity of the human body, in which there are alternate sinuous movements of different segments of the body with least expenditure of energy.

1.2.1. Gait cycle

The gait cycle is the largest element used to describe human gait [22]. The gait cycle can be broken down into two primary phases, the stance and swing phases, which alternate for each lower limb. Figure 1-1 shows phases of a gait cycle.

- Stance phase: is the portion of the cycle when the foot is in contact with the ground (constitutes 60% of the cycle).
- Swing phase: is the portion of the cycle when the limb is off the ground and moving forward (or backward) to take a step (constitutes 40% of the cycle).

Another important term in the gait cycle is the "double support time". This term refers to the period when both feet are simultaneously in contact with the ground as weight is transferred from one foot to the other.

In order to describe the elements of gait, the cycle can be broken down further into 8 sub phases [23], five of them are stance functional phases and two of them are swing functional phases. The sub stand and sub swing phases are: initial contact, loading response, mid stance, terminal stance, pre-swing, initial swing, mid swing and terminal swing.

1.2.1.1. Stance functional phases

- Initial contact (0–2%): initial contact or as known heel strike starts when the heel comes in contact with the floor. The ankle is in a neutral position, the knee is slightly flexed and hip is approximately in 30 degrees of flexion. The aim of hell strike is to stabilize the limb in order to take the impending forward translation of body weight.
- Loading Response (0–10%): The foot flattens on the floor through pronation. The ankle moves into approx. 5-10 degrees of plantar flexion and knee moves into 15 degrees of flexion. The hip moves into extension allowing trunk and body to catch up to the limb. The aim of this phase is to absorb shock, to stabilize weight bearing and to preserve progression.
- Mid stance (10–30%): During mid stance, the shank rotates forward over the supporting foot, creating the second rocker motion of the cycle. This maintains the forward progression of gait.
- Terminal stance (Heel Off) (30–50%): Heel off occurs when the heel just begins to lift off the floor and the body weight moves forward past the forefoot, as the hip increases in extension. The knee is extended and prepares to flex.
- Pre-swing (Toe Off) (50–60%): 'toe off' is the final phase of stance phase. The opposite foot begin a new stance phase and is in the initial contact phase. The foot is rapidly off loaded with a forward push to transfer the weight onto the opposite foot. The knee is flexed and the ankle plantar flexes as the toe leaves the ground.

1.2.1.2. Swing functional phases

- Initial Swing (60–70%): start of single limb support for opposite limb. The foot is lifted off the ground by the flexion of the hip and knee, at the time the ankle begins to dorsiflex. The other foot will be in mid stance phase. When the offloading limb is level with the leg in stance phase the initial swing phase is complete
- Mid Swing (70–85%): This phase involves the shortening of the limb to clear ground. The ankle is in a neutral position and knee in maximum flexion. Hip continues to flex [24].

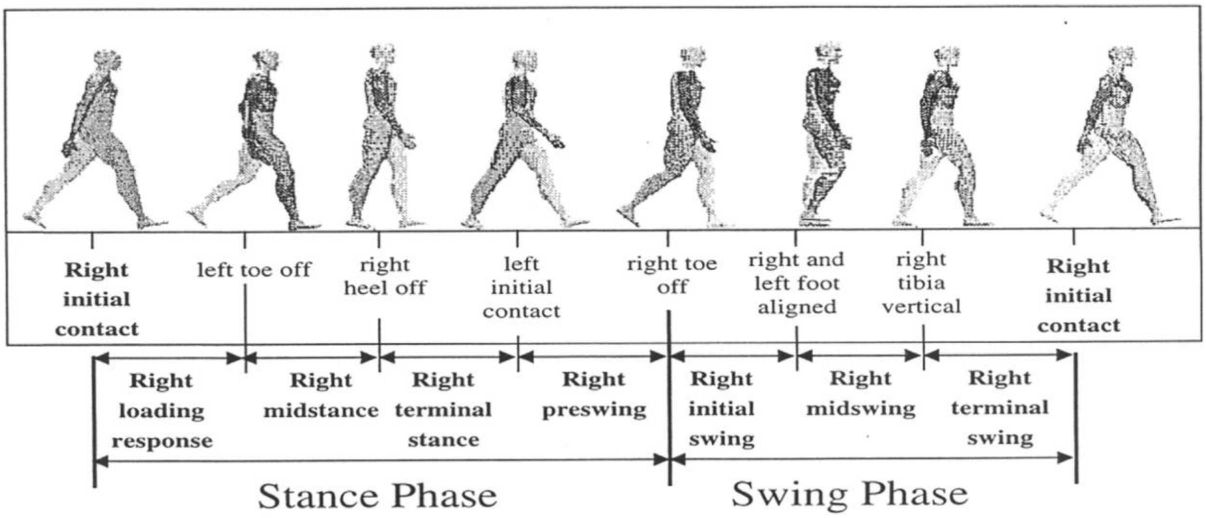

Figure 1-1. Phases of a gait cycle

- Terminal Swing (85–100%): At this phase the knee becomes fully extended and the ankle dorsiflexes to neutral as the foot prepares to make contact with the floor.

1.2.2. Gait disorders

Gait disorders are common, data shows that more than 50% of patient with neurological disorders, and 20% of geriatric patient have movement disorders associated with their lower limbs. Disorders in the central nervous system is one of the major causes of gait dysfunctions that vary from motor weakness and sensory loss, to loss of automaticity to cognitive decline. Details on most common neurological will be further discussed in the next section.

Gait deficits can have deleterious effects on the patient’s health in which: the patient with gait abnormality can sometimes fall and get secondary injury, and in some other situation, walking with an effected limb can be slow and insecure with a ‘fear of falling’ and need for assistive devices. All these effects are ultimately resulting in social isolation and reduced activity. Most gait disorders can be diagnosed and classified after performing a detailed physical and neurological exam including a gait analysis. In many situations the result of the diagnosis can be straightforward just by analyzing temporal, spatial, kinetic and kinematic parameters (Table 1.1 [25] gives a detailed description to the major parameters in gait) of the subject. However, in some other situation, the cause is not clear and seems to have features of different types of problems and anatomic origins (multifactorial gait disorders) or has a strange character, and the diagnosis is not clear.

Overall, abnormal gait can be classified into five different types: spastic gait, scissors gait, steppage gait, waddling gait, propulsive gait.

Table 1.2 [26] gives a detailed description to the different types of gait deficits. Physical therapy is one of the efficient methods that can help improving the patient walking’s ability and reducing any uncomfortable symptoms. A Detailed description on physical therapy in case of gait deficits is given in section 1.4.

Table 1.1. major parameters in gait [25].

Type	Parameters
Temporal parameters	Gait cycle time, stride time, step time, stance phase (% gait cycle), swing phase (% gait cycle), single support (% gait cycle), double support (% gait cycle), cadence, speed, average speed, mean normalized velocity and stride velocity
Spatial parameters	Stride length, step length, base width, toe in/toe out, distance traveled, step/extremity ratio, step width and stride width.
Kinetics parameters	Pressure distribution, vertical force, shear force, joint movement, joint power and center of pressure.
Kinematics parameters	Joint angles and foot clearance of ground

Table 1.2. Different types of gait deficits.

Type	Description
Spastic gait	Spastic gait occurs when a person drags his or her feet while walking. This type can also make someone appear to be very stiff when walking.
Scissors gait	A person whose legs bend inward will often have a scissors gait. With this type, a person's legs cross and may hit each other while walking. The crisscross motion may resemble scissors opening and closing.
Steppage gait	Steppage gait occurs when a person's toes point towards the ground while walking. Often, the toes will scrape against the ground as the person steps forward.
Waddling gait	As the name suggests, a person with a waddling gait moves from side to side when walking. Waddling involves taking short steps as well as swinging the body.
Propulsive gait	Propulsive gait is when a person walks with his or her head and neck pushed forward. It can appear as though the person is rigidly holding a slouched position.

1.3. Most common neurological disorders

1.3.1. Stroke

Stroke is a major cause of disability in all the world population, and it is the fifth leading cause of death in the United States, behind diseases of the heart, cancer, chronic lower respiratory diseases, and unintentional injury. A Stroke occurs when the oxygen-rich blood stops to flow to any portion of the brain. Therefore, the brain cells start to die after a few minutes. There are two main types of stroke: ischemic (obstruction of a blood vessel; occurring in approximately 85%) which is the more common type, and hemorrhagic (rupture of a blood vessel; occurring in approximately 15%) [27].

Stroke often leads to various types of disabilities symptoms, caused by destruction of brain cells in the damaged area, and that may include: variety of sensory and in severest cases, patient can loss sense of touch, muscle weakness, spasticity, limited movement coordination, attention and memory deficits, depression and behavioral changes [28].

Based on the time elapsed after the incidence of stroke, patients may be classified as being in sub-acute (initial weeks), acute (between few weeks and six months) or chronic (past six months) stage. Therefore the rehabilitation therapy should start at the early stage after stroke [29]. It aims to help the stroke survivors to regain functional independence and resume self-care activities as much as possible [30]. Time duration required for stroke patient to recover motor function varies. It may take several weeks up to several months and can halt at any stage [31], [32]. Therefore, that rehabilitation devices can play a crucial role to safeguard patient's life and retrieve normal functions.

1.3.2. Spinal Cord Injury (SCI)

Spine is made of many bones called vertebrae. Spinal cord runs downward through a canal in the center of these bones. The spinal cord is a bundle of nerves that carries messages between the brain and the rest of the body for movement and sensation [33].

A spinal cord injury results from any damage to any part of the spinal cord or nerves at the end of the spinal canal. This often causes permanent changes in strength, sensation and other body functions below the site of the injury [34]. Most spinal cord injuries are caused by direct or indirect trauma such as: falls, motor vehicle accidents, sports injuries, violence (gunshot or stab wounds), etc. Data bellow shows some of important facts about the leading causes to spinal cord injuries in the United States [35]:

- The incidence of SCI is highest among persons age 16-30, in whom 53.1 percent of injuries occur; more injuries occur in this age group than in all other age groups combined.
- Males represent 81.2 percent of all reported SCIs and 89.8 percent of all sports-related SCIs.
- Among both genders, auto accidents, falls and gunshots are the three leading causes of SCI, in that order. Among males, diving accidents ranked fourth, followed by motorcycle accidents. Among females, medical/surgical complications ranked fourth, followed by diving accidents.
- Auto accidents are the leading cause of SCI in the United States for people age 65 and younger, while falls are the leading cause of SCI for people 65 and older.
- Sports and recreation-related SCI injuries primarily affect people under age 29.
- Spinal cord injuries are one of the most common disorders within youth generation.

The severity of an injury depends on the part of the spinal cord that is affected. The higher the SCI on the vertebral column is, or the closer it is to the brain, the more effect is on how the body moves and how the patient sense. Generally, subjects with injuries at lower levels are more able to move, to feel and to voluntary control their actions [35]. Figure 1-2 illustrates different types of gait deficits classified according to the level of the injury on the vertebral column.

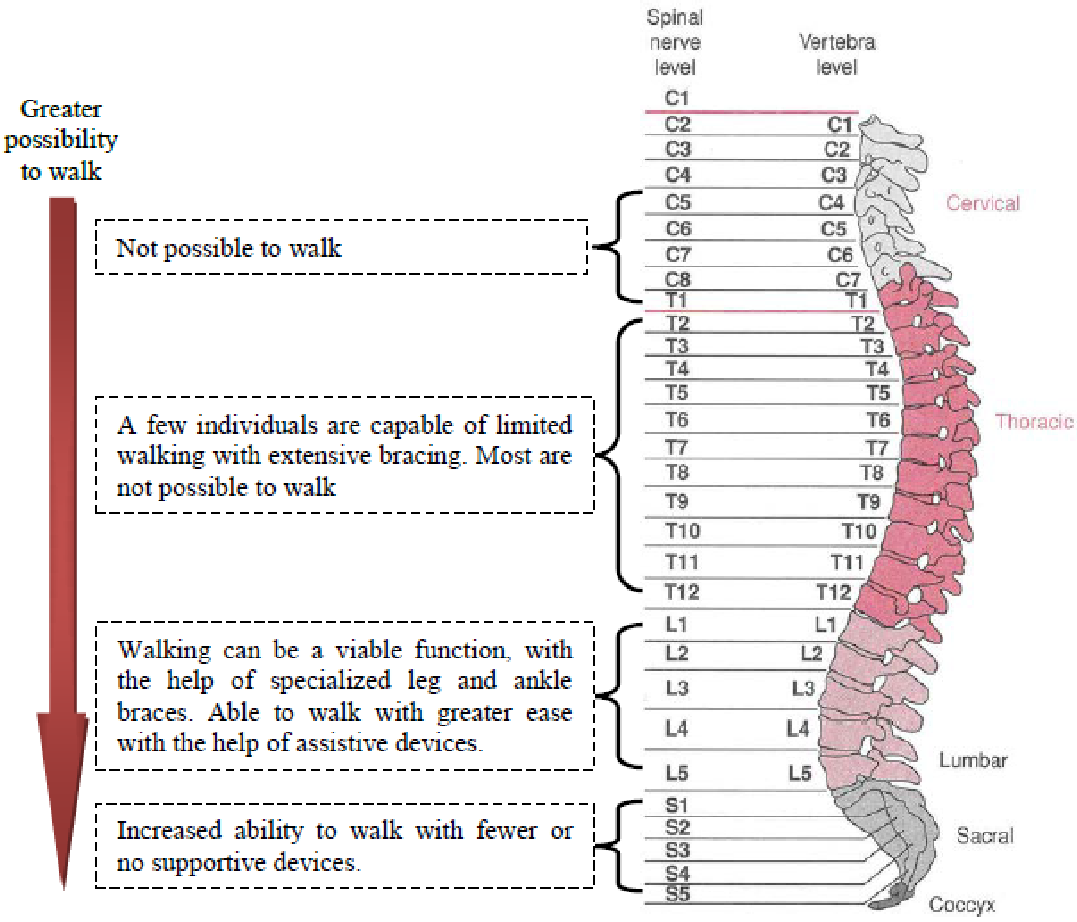

Figure 1-2. Gait disability of SCI patient [36]

The severity of the injury is classified as either of the following [34]:

- **Complete**. If all feeling (sensory) and all ability to control movement (motor function) are lost below the spinal cord injury, your injury is called complete.
- **Incomplete**. If you have some motor or sensory function below the affected area, your injury is called incomplete. There are varying degrees of incomplete injury.

Additionally, paralysis from a spinal cord injury may be referred to as:

- **Quadriplegia:** results from injuries to the spinal cord in the cervical (neck) region with associated loss of function in the arms and legs.
- **Paraplegia** results from injuries to the spinal cord in the thoracic or lumbar areas, resulting in loss of function in the legs and lower body.

1.3.3. Cerebral palsy (CP)

Cerebral palsy (CP) is one of the major causes of childhood disability with an estimated global incidence between 2 and 3 per 1000 live births [37]. The linguistic definition of Cerebral palsy is: the term "cerebral" is an adjective that means "of the brain" and "palsy" is a noun which means "paralysis" [38].The scientific definition of CP refers to a set of neurological disorder caused by non-progressive disturbance that occurs while the brain of the fetus or child is under development. Most leading causes to cerebral palsy occur before the child birth, and these may include: oxygen deprivation during birth, brain injuries during pregnancy, in addition to infection reasons like the rubella.

Damages that is caused by CP include: physical impairment that often lead to movement dysfunction, sensory, perceptual, cognitive and communication disturbances, and epilepsy [39]. The rehabilitation of cerebral palsy may involve: physical therapy, occupational therapy, speech therapy and recreational therapy [40].

1.3.4. Parkinson's disease (PD)

The Parkinson's disease is a chronic movement disorder and one of the most common neurologic troubles. Generally, it occurs beyond the age of fifty five. Neurological researcher outcomes show that PD is a result of either a dysfunction of the dopamine production process which is a chemical mediator responsible for neurotransmission and coordination of movement, or a presence of Lewy bodies and Lewy neuritis. Parkinson's disease is associated with motor symptoms, including tremor, postural instability, rigidity, bradykinesia and dysphonia [41]. In some advanced cases, patient becomes unable even to walk. Until nowadays, there is no really an efficient cure that can stop it to progress, however, rehabilitation exercises may significantly slow it down.

1.3.5. Multiple sclerosis (MS)

Multiple sclerosis (MS) is a central nervous system autoimmune disease that is disrupted through the brain and spinal cord [42]. In MS, the immune system attacks the protective sheath (myelin) that covers nerve fibers and causes communication problems between the brain and the rest of

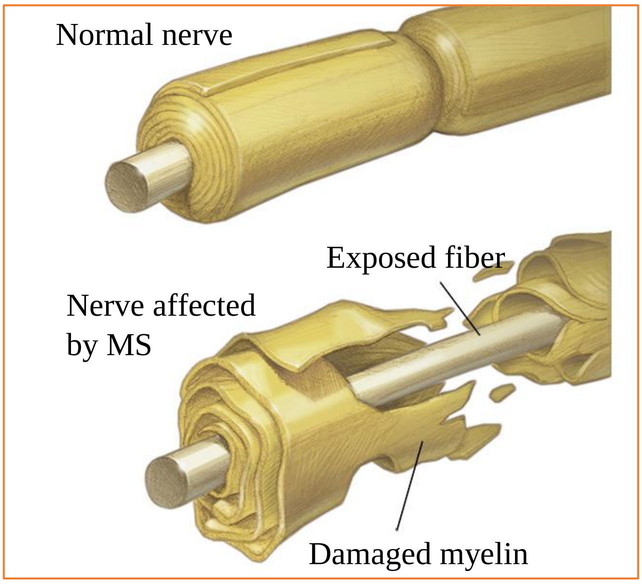

Figure 1-3: Multiple sclerosis

the body (Figure 1-3) [43]. It can cause a wide range of potential symptoms depending on the affected nerve and the amount of damages. People with MS typically show different sorts of neurological deficits such as motor and sensory impairments, cerebellar symptoms, fatigue, impaired vision, cognitive deficits, speech and swallowing problems, bladder and bowel disorders, and sexual dysfunction [44], [45].

Unfortunately, there's no cure for multiple sclerosis. Waiting for the day that an invention of an efficient pharmacological treatment becomes available, the current treatment strategy focuses on slowing down the MS as possible by providing a pharmacological treatment in combination with (multidisciplinary) the rehabilitation [46].

1.4. Rehabilitation

Rehabilitation from a neurological disorder is one of the main methods used for recovering and improving a patient's quality of life [47], which aims to help patients with physical impairments to restore their abilities to control their muscles and nervous systems normally [22]. From a therapeutic perspective, the rehabilitation process to regain meaningful mobility in the event of a neurological disorder can support or involve the application of any method or technique aiming to stimulate the nervous system to create new neurological pathways to replace the damaged pathways [48]. The process known as "neural plasticity" was the basis for proposing various gait recovery approaches [49], with rehabilitation for gait recovery heavily reliant on the "physical 54 exercises" approach.

1.4.1. Principles

Motor learning for neurological disorder rehabilitation relies on three main determinants: practice, specificity and effort [6]. Practice is related to the duration and intensity of training. More practice will result in more learning. Specificity describes a set of specific oriented tasks that aim to teach patients some or all functions generally involved in human locomotion so that the patient should ultimately be able to walk in a more natural way [9]. Effort indicates the degree of patient self-participation in the training, which is required for facilitating motor learning [50].

1.4.2. Clinical tasks

The clinical-based gait rehabilitation program implies the execution of five major tasks [51] and involves enhancing muscle strength, maintaining balance control, training gait, providing pelvic control and assisting for performing various types of locomotion for ADLs. It is supposed that the application of those specific tasks with respect to the two other gait rehabilitation principles (practice and effort) will result in significant motor recovery.

- **Enhancing muscle strength**: Muscle weakness can lead to immobilization or to markedly reduce physical activity [52]. Thus, minimum muscle force is required to perform locomotion training. Activities targeting enhancing muscle force include joint movement of the lower extremities. The assessed voluntary function of the 10 key lower-limb muscles (e.g., left and right hip flexors, knee extensors, ankle dorsiflexes, long toe extensors and ankle plantarflexions) is used as a key predictor of the potential for recovery of locomotion [53]. Once the patient regains the minimum muscular power, allowing them to control their joint movements, repetitive and resistive exercises are the next training target and have the aim of increasing muscle endurance.

- **Maintaining balance control**: Balance control is the foundation of the human ability to move and function independently. Standing or moving the human body are mechanically unstable activities. The body will usually fall over after a short time, unless it is actively stabilized by activating muscles in a controlled, goal-directed manner [54]. In maintaining balance exercises, the patient is trained to keep their upper body upright when sitting or standing, through which they can relearn controlling their trunk. Center of mass is an essential part in human balance control. It is used as a reference to measure the patient's progression toward maintaining balance control [25].
- **Training gait**: Walking forward and backward are some of the essential gait training activities. These activities consist of hip extension and a knee flexion and are particularly useful for patients with hemiplegia who are synergy affected in the lower extremities [55]. Patients with earlier stages of recovery (who usually have weak muscular strength) often need assistance in lifting their bodies. Therefore, locomotion training is usually done with the assistance of body-weight support or a therapist. Figure 1-4 shows a therapist exercising a patient to walk, while assisting them to maintain balance.
- **Pelvic control**: Walking properly without abnormalities is a task essentially maintained by good pelvic control. Patients with significant motor deficits often need assistance with controlling their pelvic movements. The assistance usually consists of a therapist placing their hands on the patient's hips to correct the error that may occur on the patient's pelvic trajectory while walking.
- **Locomotion types of ADLs**: After a significant gait recovery, a patient is often trained to walk in more actual types of environments to prepare them for getting by themselves in their own places of interest such as school, a worksite, etc... The training involves different types of exercises that vary in difficultly, such as walking on uneven ground, climbing stairs as well as turning and stumbling.

Figure 1-4. Patient having locomotion exercises with the assistance of a therapist [36].

1.4.3. Methods

To achieve the five aforementioned clinical tasks, many rehabilitation methods have been proposed. These methods can be classified into two main categories: compensation and recovery models. Accordingly, different tools used in physical training are grouped according to these categories. It is important to notice that some tools can be used in both rehabilitation models because they support multiple characteristics.

- **Compensation model**: This model consists of using tools or devices that are employed for non-remediable deficits of paralysis, weakness and balance. These tools have no therapeutic purpose. In other words, they are not used for preventing brain plasticity. However, the main goal of their use is to assist the patient in ambulation and mobility. Compensation models have two main advantages:
    - Improving the independence of patients who are at the initial stage of rehabilitation or those who have less potential for recovery.
    - Enhancing the patient's ability to ambulate safely by increasing the base of support and preventing the patient from having any injury [56].

  Compensation models include many types of tools such as parallel bars, standing frames, tilt tables, walking frames, crutches and wheelchairs.
- **Recovery model**: Because the aim of physical rehabilitation is to perform specific tasks that allow the brain to restore lost motor function, the rehabilitation recovery model is a model that consists of assistive tools that facilitate the performance of therapeutic exercises. The assistive tools are arm swing assistance training, the rehabilitation cage, the balance training machine, the balance ball, parallel bars, the treadmill and others.

The passage below gives a brief description of some of the most common tools used in the compensation and recovery models.

Figure 1-5. Parallel bar

Parallel bars: Parallel bars have been used for years by therapists as a base to assist patients to perform a set of rehabilitation exercises including exercises for regaining balance, strengthening muscles, increasing the range of motion of joints in the lower extremities and improving mobility [57]. Being permanent or portable, parallel bars can be platform mounted, floor mounted or wall mounted and can be height adjustable with electric power or with manual manipulation. Assist with parallel bars is provided by support from the upper extremities. This helps therapists with coordination exercises, requiring patients to repeat concise movements that work more than one joint and one muscle. Parallel bars are also used for ambulation exercises to improve a patient's ability to walk independently or with assistance [58]. Figure 1-5 shows a patient training to walk with the assistance of a parallel bar.

Canes: In general, canes provide the least support for gait stability [59]. They do not offer bilateral support and thus cannot be used for patients with weight-bearing restrictions [56]. Patients are typically instructed to hold a cane in the opposite hand of the affected extremity. During walking, the cane moves forward simultaneously with the affected or disabled lower limb. Canes are very helpful for patients especially when they need balance or body weight support. Standard canes are light, are made of aluminum, wood or plastic and have a half-circle (crook) handle. There are many types of canes, the most common of which are straight and quad canes.

- **Straight cane**s have one point touching the ground. This kind of cane is quite advantageous for decreasing the weight on an arthritic joint (most commonly a hip or knee) and reducing the pain at the level of the hip joint.
- **Quad canes** consist of four supporting points with the floor. Compared to straight canes, quad canes provide more support to the patient, and they are quite useful for climbing stairs.

Different types of canes are shown in Figure 1-6 [59].

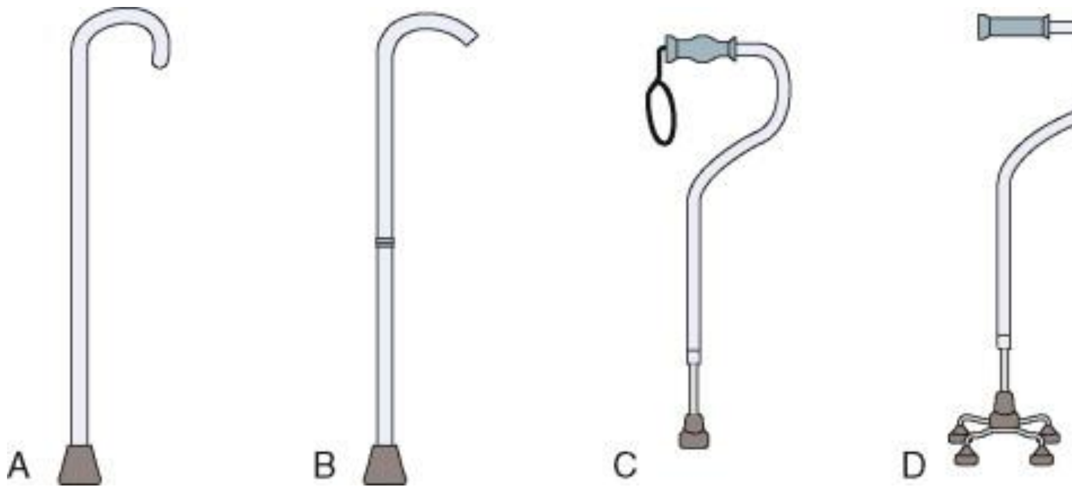

Figure 1-6. A. Standard wooden cane. B. Adjustable aluminum cane. C. Adjustable aluminum cane with offset handle. D. Four-point quad cane.

Rehabilitation cage: The rehabilitation or therapy cage is a unique dynamic device consisting of a system of pulleys, straps and splints utilized to perform several types of lower-limb exercises. It is mainly used to help patients with strengthening muscles, increasing muscle flexibility and augmenting the range motion of lower extremity joints [60]. Furthermore, it allows therapists to isolate certain muscle groups and to target specific muscle tones. As a result, the quality of gait and the balance and coordination of a patient’s movements increase rapidly.

The universal exercise unit, or cage, can be utilized in two different ways: the monkey cage and the spider cage (Figure 1-7).

- The monkey cage consists of a three-dimensional rigid metal cage in which a system of pulleys and weights is used to stretch and strengthen specific muscle groups. In addition to helping strengthen weak muscles while preventing compensatory use of others, the monkey cage can also be used for vestibular activities such as "flying" and swinging.
- The spider cage uses a belt and bungee cords to provide dynamic assistance to maintain an upright position. The spider cage is an effective tool for implementing neuro-development. With it, the patient can stand without a therapist's assistance and can safely learn to weight shift, kneel, jump, half-kneel and step up and over objects.

A B

Figure 1-7. Rehabilitation cages: (A) monkey cage; (B) spider cage [61].

1.5. Modalities of gait rehabilitation

Gait rehabilitation can broadly be divided into two different modalities: conventional physiotherapy and robot-assisted gait training.

1.5.1. Conventional physiotherapy

Conventional therapy is the modality that involves implementation of rehabilitation methods that are not based on integrating programmable automatic devices. Historically, the following two modalities of conventional gait rehabilitation can be individuated.

1.5.1.1. Conventional manual gait rehabilitation

Conventional manual therapy is based mainly on the therapist's experience and on the implementation of several basic assistive tools that help the patient to perform exercises. In the clinical setting, a physiotherapist develops exercises that help the patient practice walking. Usually, these exercises are determined by the ability and character of the patient as well as the preferences and experience of the therapist [62]. Conventional manual gait rehabilitation has the capacity to train the patient for a single type of training during the rehabilitation session. Most of these exercises focus on strengthening the patient's muscles because such exercises do not require the involvement of many therapists or therapists with advanced experience. The therapist can use different types of manual tools such as parallel bars, a rehabilitation cage and others.

1.5.1.2. Partial bodyweight support treadmill gait rehabilitation with manual assistance

Since the beginning of this century, body weight-supported treadmill training (BWSTT) has been used to enhance locomotor function in individuals with neurological disorders, especially those with stroke and spinal cord injuries (Figure 1-8. [A]). This technology originated from basic scientific research on the neural control of vertebrate locomotion. Figure 1-8. (B) is an expressive image of a mouse being trained to walk with the assistance of BWSTT. Basically, it is a new method that has been proposed after the positive results of experiments conducted on cats with spinal cord injuries. These cats have been trained to step with their hind limbs on a treadmill while their body weight is partially supported [36]. In the field of physical therapy, this technology consists of a suspension system that provides a proper upright posture, balance and safety for patients. The suspension of the patient's body weight is accomplished through a harness that can be adjusted to remove a portion of the weight off the legs, and this redistributes it to the trunk and groin. Meanwhile, the system allows for the free movements of the patients' arms and legs. Body

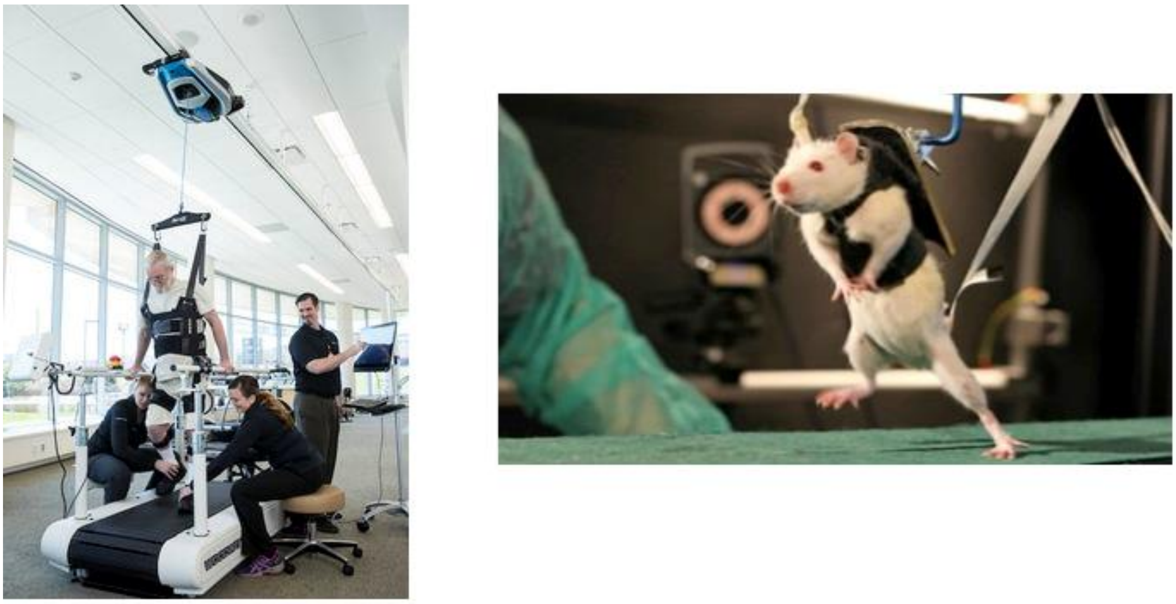

A B

Figure 1-8. Body weight-supported treadmill training: (A) a patient being trained to walk; (B) expressive image of a mouse being trained locomotion.

weight-supported treadmill training requires a team of three or more physical therapists to guide the patient's legs on predefined paths as well as to stabilize the patient's pelvis.

Partial bodyweight-supported treadmill training technology has shown great success compared to the former conventional physiotherapy modality. Many studies have documented the efficiency of this technology to assist individuals who have had a spinal cord injury [63, 64] or stroke [65, 66] to restore their walking ability [67]. For instance, it has been shown that 80% of wheelchair-bound patients with chronic incomplete spinal cord injury gained functional walking ability after training [36].

The interpretation of such positive outcomes relative to the three motor learning determinants can be summarized as the following:

- Increase the practice rate: The combination of the treadmill with partial body weight support offers a good framework for increasing the number of repetitions and functional gains [68], [69].
- Ability to perform more than one specific task simultaneously: Patients in the early stage of rehabilitation can perform many specific tasks at the same time due to the body weight support that allows the therapist to assist the pelvis motion and leg swing, while maintaining balance and stability [70].

Nevertheless, the use of BWSTT in most rehabilitation settings has been limited because it relies on physiotherapy procedures that are extremely labor intensive. It becomes increasingly difficult to provide an optimum gait training pattern, and it becomes challenging to maintain the high quality of therapy across a full training session. Therefore, there is a pressing need for more sophisticated technology to relieve therapists from the burden of manual assistance and to help patients attain greater locomotion recovery.

1.5.2. Robot-assisted gait training

Robotic rehabilitation is an emerging field that is expected to provide more advanced solutions to current physiotherapy problems [15]. Robotic rehabilitation has many advantages compared to conventional therapy, allowing more intensive repetitive motions, relieving therapists from heavy burdens and providing measuring tools to quantitatively assess the level of motor recovery.

In the last two decades, several lower-limb rehabilitation robots have been developed to assist patients with restoring mobility. According to rehabilitation principles, these robots can be classified into four classes [15]: *exoskeleton robots* which include (1) treadmill-based devices and (2) orthosis-based devices and *end-effector robots* which include (3) footplates-based devices and (4) platform-based devices.

1.5.2.1. Treadmill-based devices

Treadmill-based devices consist of three fundamental sub-robotic systems: body weight support, treadmill and gait orthosis. Lokomat (Figure 1-9) is a typical treadmill-based exoskeleton device that is commercially available. It involves the following features: a driven orthosis with electric motors for knee and hip joints with four force transducers and four amplifiers. The speed range of the Lokomat treadmill varies from 0 to 10 km/h. The maximum patient weight supported by the body weight support is 135 kg (LokomatPro). Lokomat has a live screen for displaying biofeedback to the patient (Figure 1-11). This has the advantage of motivating the patient to activity participate in the training.

LOPES is another treadmill-based device robot that is commercially available. It consists of a translatable two-degrees-of-freedom-actuated (two-DOFs-actuated) pelvic assistive orthosis and two-DOFs leg assistive orthosis [16]. The leg orthosis can move in parallel with the patient's legs while the patient walks on the treadmill [19]. Recently, a new version of LOPES has been developed called LOPESII (Figure 1-10). This version has an eight-powered DOFs exoskeleton (hip flexion/extension, hip abduction/adduction, knee flexion/extension, pelvis forward/aft and pelvis mediolateral) [71]. This has the advantage of supporting more specific tasks and

Figure 1-9: Lokomat

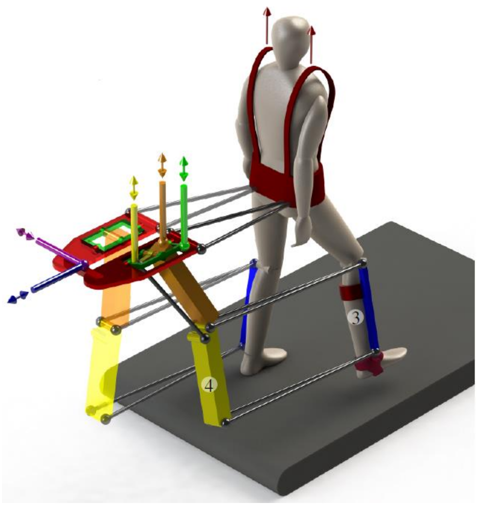

Figure 1-10: LOPESII

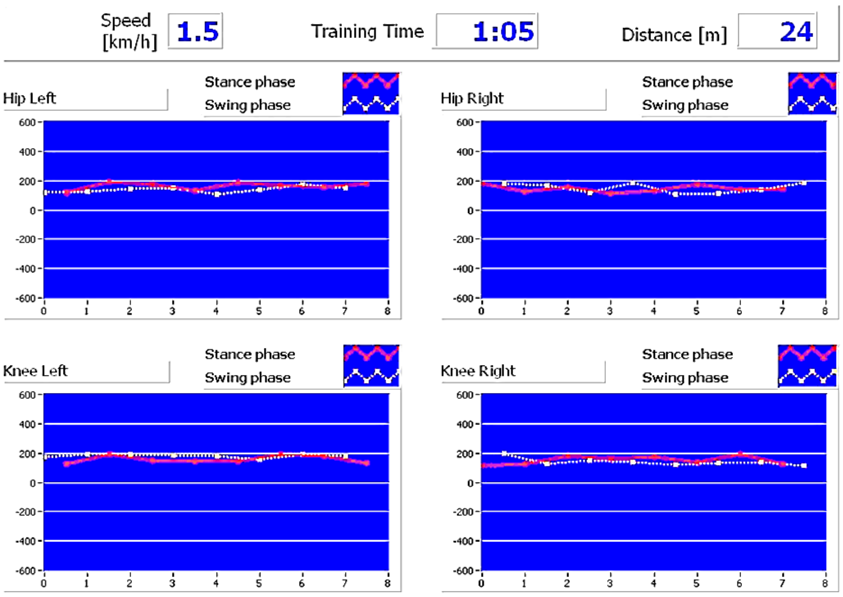

Figure 1-11. Screen displaying biofeedback.

facilitating the control of the patient's balance. Moreover, LOPESII uses an assist-as-needed approach [72], [73], which encourages the patient to actively participate in the training.

1.5.2.2. Footplates-based devices

With footplates-based devices, a patient's feet are placed on two separated programmable footplates that simulate various gait patterns. Gait Trainer GTI (Figure 1-12) [74] is one of the most common footplate systems. It consists of actuated foot-supporting plates, resembling the well-known fitness "cross-trainers." These plates are connected to a linkage system and move the patent's feet through a defined trajectory. The system allows the therapist to select different speeds and gait trajectories based on the patient's needs. However, the continuous contact of the patient's foot with the footplates is one of its disadvantages. The reciprocal loading and unloading of the body weight of each leg during walking may, as a consequence, not occur [75]. A redesign of the Gait Trainer GTI has led to the HapticWalker [76], a system that involves simulating various gait patterns that resemble more natural walking trajectories.

1.5.2.3. Platform-based devices

Platform-based device robots consist of a stationary platform attached to a patient's feet, allowing the patient to perform rehabilitation exercises while sitting in a chair. The objective of this type of systems is to enhance the force of lower-limb muscles and to increase the range of motion of lower-extremity joints. Unlike the previous type of rehabilitation systems consisting of complex mechanisms, platform-based devices have simple mechanisms. Ankle rehabilitation is one of the main applications of platform-based device robots. Rutgers Ankle (Figure 1-13) [77] is one of the pioneer ankle rehabilitation systems that uses the Stewart platform hardware. It is also a haptic interface that applies resistive forces on the patient's foot in response to VR-based exercises [51] [20].

Figure 1-12: Gait Trainer GTI.

Figure 1-13: Rutgers Ankle.

1.5.2.4. Orthosis-based devices

Leg orthoses are actuated wearable exoskeletons that provide powered walking assistance [16]. ReWalk (Figure 1-14) [78] is one of the most common wearable robotic exoskeleton systems.

It was developed at the Moss Rehabilitation Hospital in Philadelphia, and it is commercially available. ReWalk comprises a light wearable brace support suit, which integrates DC motors at the joints, rechargeable batteries, an array of sensors and a computer-based control system [15].

ReWalk provides powered assistance to hip and knee joints which enables individuals with a spinal cord injury to stand upright, to walk, to turn and to climb and descend stairs.

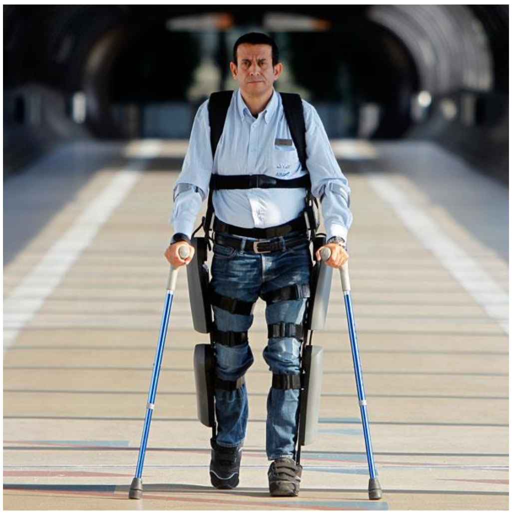

Figure 1-14. ReWalk.

1.6. Conclusion

Over the last 20 years, rehabilitation have greatly developed in correlation to the increase in the number of disabilities. The use of these sophisticated tools in the field of physical therapy can offer advanced solutions for helping patients achieve a significant gait recovery and for relieving therapists from the burden of manual assistance. This chapter has given a review of the basic issues related to physical therapy. It has been shown that the kinematic, kinetic, temporal and spatial parameters related to gait analysis can provide important information about the type and nature of a patient's gait deficits. Most gait disorders are the result of a disease or an accident that affect the central or peripheral nervous system. Rehabilitation is the most promising method to help patients regain their walking ability. Understanding physical therapy principles is an important step in assessing current gait rehabilitation modalities and in defining their limitations. Accordingly, robotic rehabilitation systems with advanced specifications can be developed.

Chapter 2: INVESTIGATION

2.1. Introduction

Initially, robotic therapy appeared to overcome the limitations of conventional therapy in terms of motor recovery. However, many meta-analysis studies have shown no difference between robotic and conventional gait therapy in promoting the motor recovery of neurological disorders [17]. Statistics show that only 65–70% of stroke survivors learn to walk independently 6 months after a stroke [79]. Among them, few can be described as having a good quality of gait. The goal of this research is to define limitations of current clinical rehabilitation interventions. Therefore, the research has the objective of answering these two main questions: Why are current conventional and robotic therapies still not sophisticated enough to provide for a significant gait recovery? Why has technology represented by rehabilitation robots not succeeded yet in producing better outcomes compared to conventional therapy?

To find answers to these two main questions, we performed two different studies. First, we visited two rehabilitation centers and interviewed several physiotherapists, rehabilitation physicians and patients with physical deficits. Second, we conducted a review of current gait rehabilitation robots, and we compared the features of about 25 systems among them. In the first and the second sections of this chapter, the objectives and outcomes of the studies we performed are presented. The summary of this chapter is provided in the last section.

2.2. University hospital visit

2.2.1. Objectives

In the context of the author's PhD project, the author had the opportunity to visit the rehabilitation unit of the university hospital of SidiBelabbess. Below are the objectives of this visit.

Interviewing patients with neurological disorders to achieve the following:

- Define difficulties facing patients from their own point of view.
- Have a critical view of the existing techniques and search for potential solutions.

Interviewing therapists to achieve the following:

- Define the efficiency of existing rehabilitation methods based on their experience.
- Define difficulties facing therapists and discuss potential solutions for improving the recovery level of patients.

2.2.2. Observations

Through the visit to the rehabilitation center, the author met with many therapists and different patients with neurological disorders. Below are the resulting main observations.

- Patients are not active within the training: The patient usually participates actively at beginning of the training, then after a short period of time, they find difficulties continuing at the same pace. This is because the therapist cannot be present all the time to motivate and guide each patient. There are more patients than therapists.
- Many patients withdraw from the rehabilitation program: For many patients, the rehabilitation program sounds very exhausting, especially in the first days when the patient feels very depressed because of the dramatic changes occurring in their life. Moreover, rehabilitation exercises sound quite challenging to patients because they include tasks that are repetitive and boring.
- Robotic systems are not very efficient: Although there are many robotic systems in the rehabilitation center, they are not more advantageous than conventional therapy is. These systems do not support a wide range of motion and DOFs with which they cannot support side walk. Instead, they only assist movements along the sagittal plane. In addition, they do not provide any type of visual feedback to the patient while walking. The patient, as a consequence, does not find a relationship between the movements they are performing and the surrounding view. Moreover, although the robotic systems in the rehabilitation center provide some temporal feedbacks on the patient's performance, most of the data provided does not include an analysis report on the patient's progression. Therapists often need these kinds of reports to plan and design future exercises.

2.3. Review

2.3.1. Objectives

Many systematic reviews have compared the engineering aspects (e.g. mechanical, control etc.) of current robotic systems [15, 16, 80, 81]. Although most of these studies succeeded in including and describing current systems, they failed to illustrate the position of each system in the global field. Therefore, we questioned whether it was possible to generate a graphic representation of the systems to allow the reader to perceive and compare the main aspects of each system.

The main goal of this review is to classify different rehabilitation systems, graphically and simply representing the main aspects without too much textual description. Such a representation could be introduced to standardize the evaluation of robotic gait rehabilitation systems, thereby helping researchers to identify the system weaknesses, thus make improvements.

The process of classifying robotic gait rehabilitation systems is performed in four steps, which are also the four main sections of this review:

- Step 1 Systems identification: the first step concerns collecting data on current gait systems for the analysis, standardization and evaluation. The next section describes the method we followed to achieve this. A detailed technical description of most current gait systems are shown at the end of the section in a comprehensive table.
- Step 2 Features analysis involves two main steps:
    - Global features analysis which consists of analyzing the three main aspects of the gait robotic intervention (patient, rehabilitation approach and environment) and describing them relevant to a technical characteristic representation. Accordingly, the key elements of rehabilitation interventions required for gait robotic systems to provide can clearly be defined and classified.
    - Robotic features analysis which involves analyzing the current robotic gait systems and suggesting the best robotic module classification to incorporate the set of the defined features (defined in the previews step).
- Step 3 Classification which comprises:
    - Elementary characteristics description, whereby the elementary characteristics measuring the ability of each robotic module to execute the predefined feature are defined.
    - Weighting, due to the difference in importance of different elementary characteristics of robotic modules relevant to the set of required features, each characteristic should be weighted. Therefore, we have proposed two approaches for weighting.
- Step 4 Application: In this step, the different steps described in different rehabilitation robotic systems are applied for a classification.

An overview of the review methodology process in shown in Figure 2-1, in which the relation between the pre-mentioned steps is described using a bock diagram.

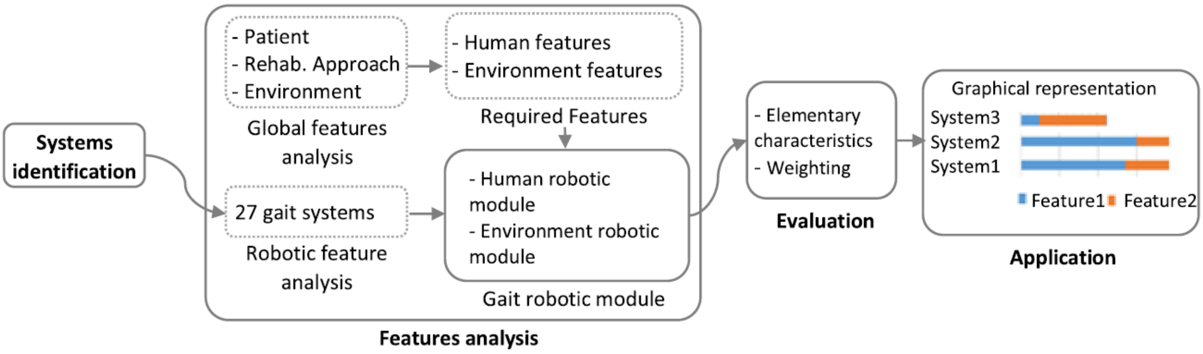

Figure 2-1. Review methodology process.

2.3.2. Gait robotic rehabilitation systems: Data collection

2.3.2.1. Identification

For a quantitative and qualitative database of most existing robotic systems for gait rehabilitation, a total of 35 reviews of different lower limb rehabilitation robotics where selected [15], [82]. Then, an automatic algorithm was applied using relevant keywords classified according to four defined issues: “related to robot description”, “related to limb location”, “related to rehabilitation”, and “related to the patient case”. For the keyword “Robotic”, “Systems”, “Robot” refer to “Related to robot description” class…etc. The search function was based on the keyword classification and created the best search request formula relevant to the desired criteria, for example, *“(New OR novel) AND (Robotic OR Robot OR Device OR Manipulator OR End-Effector OR Orthosis OR Treadmill OR biomechanical OR Locomotion OR Platform-Based OR Bio-Robotic OR Prosthetics) AND (Lower limb OR Lower limb OR Lower Extremity OR hip OR ankle OR leg)*”). The databases Scopus, PubMed, Science Direct, Google scholar, IEEE Xplore, MEDLINE, SpringerLink, Compendex, and EMBASE were searched using different search phrases generated by the search function.

2.3.2.2. Inclusion and exclusion criteria

The scope of this review is generally limited to the devices mainly designed for regaining gait function through physical rehabilitation, which target patients with neurological disorders. This review excluded passive systems mainly used for stretching muscles, such as those used for specific types of exercises, like isometric etc., since they cannot supply the affected limbs with the required energy to complete the rehabilitation task. Also, assistive systems not clinically supervised or not developed for a therapeutic goal were excluded.

2.3.2.3. Selection result

In total, 27 gait robotic systems were selected for this study. These systems can be classified into three mechanical groups, treadmill-based devise, and footplate-based devices and over ground based devices, as shown in Table 2.1.

2.3.2.4. Table notes

All system characteristics are presented relevant to the technical characteristic representation described in the next section to compare the extent of such system in supporting features of the basic gait robotic modules, that is, human robotic modules and environment robotic module (separated with a thick bold row lines).

The identity information section contains basic and general information describing the systems, including the name of the system (marked in bold), year of development, country of origin, stage of development, i.e., is it a prototype or commercial system (followed by their producer names), total of active actuated Degree Of Freedom (DOF) and type of the system (treadmill, footplates or over ground based system).

The human robotic modules section contains information about the three robotic modules, body weight support, reciprocal stepping mechanism and pelvis mechanism, used for assisting the patient gait movement (separated with a dark black line), in addition to information about body weight shifting. The BWS (row) indicates the type of the mechanical designed supported, cable body weight support (cBWS) and structure body weight support (sBWS). Body weight shifting (row) indicates if the system supports the feature of BWS or not (Yes/No). The reciprocal stepping and pelvis mechanism robotic parts contain information regarding the degrees of freedom of the robotic module (DOF) and Mechanical design. There are four states of DOF, A:

active, P: passive (i.e. exerting only resistive force), F: free (neither active nor passive force is exerted), and R: restricted certain criteria. For movements designation: FE: flexion/extension, AA: abduction/adduction, IE: indorotation/exorotation. LR: left/right, FB: forward/backward, UD: up/down, PR: pelvis rotation, PT: pelvic tilt, PM: pelvic rotation about the mediolateral axis.

Two features were considered for the mechanical design, type of actuation (if no actuator is introduced to support movement in a certain direction, the "No" mark is filled, other designation are AC: alternating current, DC: direct current) and power of transmission (note: for lack of data, this features has not described the pelvis mechanism).

The environment robotic module contains physical properties and visual properties, Yes/No marks are used for checking if the system simulates different types of grounds and if it can complete the physical properties of simulated terrain with visual feedback (VR: virtual reality, AR: actual reality).

2.3.3. Features analysis

2.3.3.1. Gait based elements (patient, robot, environment)

For the integration of robots in rehabilitation, engineers depended largely on their designs to imitate therapist movements [15], [16], [83]. The movements that the robots tried to perform were originally set by rehabilitation programs to satisfy the requirements of the period of the pre-robotic age. Consequently, many weaknesses not addressed by conventional therapy were also inherited by robotic therapy. Robotic therapies could benefit from different rehabilitation philosophies that are independent of the conventional therapy way of thinking.

Firstly, the relationship between the walker and the environment should be well understood with respect to the set of characteristics defined by a descriptor. The different rehabilitation and engineering aspects could then be described from the perspective of maintaining this natural relationship.

The actual walking process in the case of a healthy person can be described as a direct relationship between the walker and the environment in which the walker performs a set of movements, while the ground responds with a set of physical reactions allowing the walker to change their location. However, due to the disability, this reciprocal relationship can be missing or weakened from the patient side, which could be repaired either with assistive tools (such as crutches or assistive robotic devices) [84–86] or simply by restoring the damaged function through therapeutic rehabilitation. The latter consists of two main elements, approach and executive. The approach is the "software", while the executive is the "hardware" (Figure 2-2).

Table 2.1. Robotic devices for gait rehabilitation.

					LOPES II [71]	LOPES [19, 87–89]	PAM & POGO [90–92]
Identity information				System	**LOPES II [71]**	**LOPES [19, 87–89]**	**PAM & POGO [90–92]**
Identity information				Year	2014	2007	2003
Identity information				Country	Netherland	Netherland	USA
Identity information				Development stage	Commercial (Moog)	Prototype	Prototype
Identity information				Total DOF	8	8	9
Identity information				Type	Treadmill	Treadmill	Treadmill
Human Robotic Modules	**Body Weight Support**				BWSc	BWSc	BWSc
Human Robotic Modules	Reciprocal stepping mechanism	DOF		Hip (FE-AA-IE)	A-A-F	A -A -R	A-P-R
Human Robotic Modules	Reciprocal stepping mechanism	DOF		Knee (FE)	A	A	A
Human Robotic Modules	Reciprocal stepping mechanism	DOF		Ankle (FE-AA-IE)	P-P-P	F-F-F	F-F-F
Human Robotic Modules	Reciprocal stepping mechanism	Mechanical design	Actuation	Hip	Servo motor 40N.m, gear ratio (2/3)	Servo motor (max speed: 8000rmp; power: 567 W; continuous torque 0.87Nm; peak torque 2.73 Nm) gear ratio (64/1)	Pneumatic cylinders (Length =25cm)
Human Robotic Modules	Reciprocal stepping mechanism	Mechanical design	Actuation	Knee	Servo motor 100N.m, gear ratio (3/2)		
Human Robotic Modules	Reciprocal stepping mechanism	Mechanical design	Actuation	Ankle	No	No	No
Human Robotic Modules	Reciprocal stepping mechanism	Mechanical design	Power transmission		Push-pull rods	Bowden cable drive + springs (at hip and knee flexion) (Stiffness 35.1 KN/m) (hip abduction)	Pneumatic cylinders
Human Robotic Modules	Pelvis mechanism	DOF	Translation	LR	A	A	A
Human Robotic Modules	Pelvis mechanism	DOF	Translation	FB	A	A	A
Human Robotic Modules	Pelvis mechanism	DOF	Translation	UD	P	P	A
Human Robotic Modules	Pelvis mechanism	DOF	Rotation	PR	P	R	A
Human Robotic Modules	Pelvis mechanism	DOF	Rotation	PT	P	R	A
Human Robotic Modules	Pelvis mechanism	DOF	Rotation	PM	R	R	P
Human Robotic Modules	Pelvis mechanism	Mechanical design – Actuation	Translation	LR	Servomotor (torque 40Nm) (gear ratio 0.2)	DC motor (max speed: 6000rmp; power: 690 W; peak torque 2.2 Nm) gear ratio (8/1) + springs (stiffness 3.98 KN/m)	Pneumatic cylinders (Length =25cm)
Human Robotic Modules	Pelvis mechanism	Mechanical design – Actuation	Translation	FB	Servomotor (torque 100 N.m)	Linear actuator (power: 250 W; peak force 204 N)	
Human Robotic Modules	Pelvis mechanism	Mechanical design – Actuation	Translation	UD	No	No	
Human Robotic Modules	Pelvis mechanism	Mechanical design – Actuation	Rotation	PR	No	No	
Human Robotic Modules	Pelvis mechanism	Mechanical design – Actuation	Rotation	PT	No	No	
Human Robotic Modules	Pelvis mechanism	Mechanical design – Actuation	Rotation	PM	No	No	No
Human Robotic Modules	**Body weight shifting**				No	No	No
Environment Robotic Module	Physical properties			Simple ground	Yes	Yes	Yes
Environment Robotic Module	Physical properties			Complex ground	No	No	No
Environment Robotic Module	Physical properties			Challenges	No	No	No
Environment Robotic Module	Visual property			VR	No	No	No
Environment Robotic Module	Visual property			AR	No	No	No

Table 2.1. Robotic devices for gait rehabiliation (Continued)

LOKOMAT [14, 93–95]	ALEX [96–99]	ALEX II [20]	UoA PMAbot [100, 101]	ARTHuR [102–104]	STRING-MAN [105]
2000	2007	2011	2012	2002	2003
Switzerland	USA	USA	New Zealand	USA	Germany
Commercial (Hocoma)	Prototype	Prototype	Prototype	Prototype	Prototype
4	4	4	4	2	6
Treadmill	Treadmill	Treadmill	Treadmill	Treadmill	Treadmill
BWSc	BWSs	BWSs	BWSc	BWSc	Developed BWSc
A(50)-P-R	A-P-R	A-P-R	A-P-R	A_F_F	F-F-F
A(50)	A	A	A	A	F
P-P-P	F-F-F	F-F-F	A-P-P	F_F_F	F
DC motor	Linear actuator	Rotary motor + gear ratio (1/50 integrated with motor) + (1/60)	PMA	Coil linear motor	No
	Linear actuator (peak torque 100 N.m)		No	No	No
No	No	No	No	No	No
Precision Ball Screw	Linear actuator	Gear drive	PMA (length: 34cm) (braid diameter: 3cm) (Peak torque at the joint 50 N.m)	Rigid links	wires
P	R	P	R	F	A
R	R	P	R	F	A
P	P	P	P	F	A
R	R	P	R	F	A
R	R	P	R	F	A
R	R	R	R	F	A
No	No	No	No	No	Electrical motor
No	No	No	No	No	
No	No	No	No	No	
No	No	No	No	No	
No	No	No	No	No	
No	No	No	No	No	
No	No	No	No	No	_
Yes	Yes	Yes	Yes	Yes	Yes
No	No	No	No	No	No
No	No	No	No	No	Yes
Yes	No	No	No	No	No
No	No	No	No	No	No

Table 2.1. Robotic devices for gait rehabilitation (continued)

RGR [69, 106, 107]	MIT-Skywalker [108–110]	HapticWaker [18, 111–113]	G-EO- system [114–116]	ULRF [117–120]	LOKOIRAN [121, 122]
2010	2010	2004	2010	2007	2013
USA	USA	Germany	Germany	Korea	Iran
Prototype	Prototype	Prototype	Commercial (Rehatechnology)	Prototype	Prototype
1	4	6	6	6	4
Treadmill	Treadmill	Footplates	Footplates	Footplates	Footplates
No	BWSc passive	BWSc	BWSc	BWSc	BWSc
P-P-P	F-F-F	A-R-R	A-R-R	A	A-R-R
P	F	A	A	A	A
F-F-F	A-A-P	A-R-R	A-R-R	A-R-R	R-R-R
No	No	Linear motor + Electrical motor	1500W Servo motor 400 W Servo motor	Linear actuators + AC servo motor	AC motor
No	No	No	No	No	No
No	Brushless servomotor	No	No	No	No
No	Treadmill belt	Rails + parallel arm	Rail + parallel arm	Parallel Mechanism + Sliders	Parallel arm
P	R	F	F	F	F
P	R	F	F	F	F
F	F	F	F	F	F
F	R	F	F	F	F
A	F	F	F	F	F
F	R	F	F	F	No
No	No	No	No	No	No
No	No	No	No	No	No
No	No	No	No	No	No
No	No	No	No	No	No
Linear actuator	No	No	No	No	No
No	No	No	No	No	No
_	No	No	No	No	Yes
Yes	Yes	Yes	Yes	Yes	No
No	No	Yes	Yes	Yes	No
No	Yes	No	No	No	No
No	No	Yes	Yes	Yes	No
No	No	No	No	No	No

Table 2.1. Robotic devices for gait rehabilitation (Continued)

ICARE [123–125]	GM5 [126]	Gait Master 2 [127]	GT (Gait Trainer) [74, 128–130]	DSP [131]	WalkTrainer [132, 133]
2010	2010	2002	1999	2005	1st version (2006) 2nd version (2009)
USA	Japan	Japan	Germany	USA	Switzerland
Commercial (sportsartamerica)	Prototype	Prototype	Commercial (Reha-Stim)	Prototype	Commercial (Swortec SA)
4	4	4	4	12	12
Footplates	Footplates	Footplates	Footplates	Footplates	Over ground
BWSc	Safety frame	BWSc	BWSc	BWSc	BWSc
A-R-R	A-R-R	A-R-R	A-R-R	A-A-P	A-R-R
A	A	A	A	A	A
P-R-R	P-P-R	R-R-R	R	A-A(40)-A(25)	A-R-R
Electric motor	Linear actuator + AC servomotor	AC servomotor	Electric motor	Pneumatic pistons	DC motors
No	No	No	No		
Crank-rocker	Parallel arms	Crank-rocker	Double crank + rocker gear	Pneumatic pistons	Precision ball screw
F	F	F	F	F	A
F	F	F	F	F	A
F	F	F	F	F	A
F	F	F	F	F	A
F	F	F	F	F	A
F	F	F	F	F	A
No	No	No	No	No	DC motors
No	No	No	No	No	
No	No	No	No	No	
No	No	No	No	No	
No	No	No	No	No	
No	No	No	No	No	
No	No	No	No	No	Yes
Yes	No	Yes	Yes	No	Yes
No	Yes	Yes	No	No	No
No	No		No	No	No
No	Yes	Yes	No	Yes	No
No	No	No	No	No	Yes

Table 2.1. Robotic devices for gait rehabilitation (Continued)

NaTUre-gaits [51, 134–136]	BAR [137]	KineAssist [138, 139]	WHERE-II [140]	WHERE-I [140]	GaitEnable [141]
2011	2016	2005	2009	2009	2012
Singapore	Slovenia	USA	Korea	Korea	Canada
Prototype	Prototype	Commercial (Kinea Design LLC)	Prototype	Prototype	Prototype
11	3	_	_	_	_
Over ground	Over ground	Over ground	Over ground	Over ground	Over ground
BWSs	BWSs	BWSs	BWSc	BWSs	Passive BWS
A-R-R	No	No	No	No	No
A	No	No	No	No	No
A-R-R	No	No	No	No	No
DC brushless motors	No	No	No	No	No
			No	No	No
	No	No	No	No	No
Gears	No	No	No	No	No
A	A	P	F	R	R
A	A	P	F	P	F
A	P	P	F	P	F
A	A	P	F	R	F
A	P	P	F	R	F
P	P	P	F	R	F
DC brushless motors	Linear actuators	No	No	No	No
		No	No	No	No
		No	No	DC motor, gear ratio (150:1)	No
		No	No	No	No
		No	No	No	No
	No	No	No	No	No
Yes	Yes	_	Yes	Yes	_
Yes	Yes	_	Yes	Yes	Yes
No	No	No	No	No	No
No	Yes	Yes	No	No	No
No	No	No	No	No	No
Yes	Yes	yes	yes	yes	yes

In addition, the environment where the executive executes the approach could have more importance. For instance, the type of ground on which the executive tries to teach the patient to walk may affect the quality of the result. An ideal program should account for different ground shapes (plane, stairs…etc.), considering the patient's situation as well as the environment. An ideal system should be able to simulate the environment with all its complexity. Then, the relationship between the patient and the environment should be managed throughout the approach. Figure 2-2 describes graphically the relation between the different gait elements in the case of a healthy person and a paralyzed subject.

The different elements of the chain Patient-Rehabilitation-Environment will be discussed in the following sections

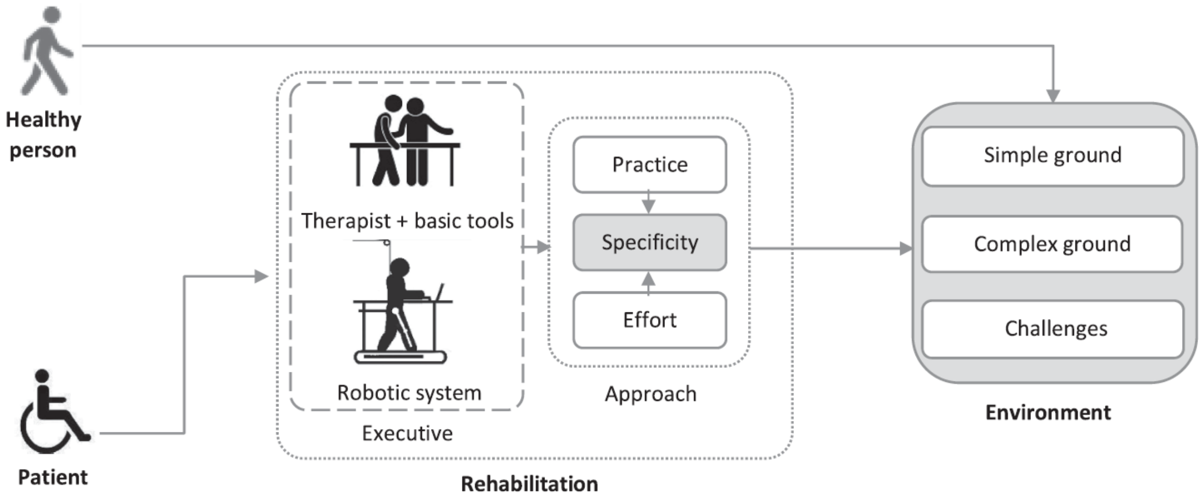

Figure 2-2. Basic relation patient, environment and robot.

A) Approach

a) Specificity

The specificity can be described by a set of movements that should be supported in order to imitate natural gait movements. In conventional therapy, this sets to five specified oriented tasks, whereas the terms features and activities are used in robotic rehabilitation [51]. The features are simply the characteristics the gait robotic system should provide to help implement the activities. Five different features are selected based on the theoretical basis of locomotor training: body weight support, balance and truck stability, reciprocal stepping, pelvic motion and body weight shifting [142].

For the governing conditions of their implementation, these can be elected in association with the biomechanics of movements of the supported activity. The activities are just a set of associated locomotion movements prescribing the type of gait patterns allowing the walker to navigate through the different types of ground.

b) Practice

The practice determinant can be easily measured using two benchmarks emphasized by both rehabilitation interventions, duration, which refers to the time involved in one training session, and intensity, which is the number of training sessions within a time period e.g. week, month or year.

c) Effort

This part of the approach refers to the degree of patient self-participation within the training. Generally, at the beginning of the rehabilitation, the patient is not able to participate in the exercise, instead, he is moved by the robot. However, over time, the robot should persuade the patient to participate in the action, thus becoming progressively active and independent. In other words, the robot must have the ability to control and adjust the degree of assistance given to the patient, based on their progress [71].

B) Environment

While both interventions (robotic and manual therapies) support the movement of the patient, they do not provide the patient with the perception of walking on natural ground [107, 136]. The key environment characteristic elements that the rehabilitation interventions should provide must be clearly defined. They include physical properties, which are important for the patient to experience during the training process. Walking on simple ground, for example, must provide a reaction force when touching the ground. Also, sight (visual property) is important as patients can neglect most signals provided by other senses if they contradict the sight. Therefore, used properly, this property could be very beneficial by enhancing the stimulation of the nervous system for completing the physical properties or for motivating the patient.

With respect to these elements, the robotic systems summarized by this review are compared by their efficiency to simulate for the user, three levels of ground shaping forms selected based on the environment types involved in the clinical program of gait rehabilitation: simple ground which refers to the referential ground supported by the task of gait locomotion, such as walking on a flat plane [14]; complex ground which could be any form of the ground experienced in daily living environments. However, to be more precise and respecting what exists in clinical programs, this should refer to the ability of teaching the patient to go up/down stairs [143]. Thirdly, challenges, which does not refer to a specific type of ground but is important to improve locomotor functions by challenging the patient’s level of comfort, for example, subjecting the patient to an actual fall experiment [134] or unstable ground by teaching the patient balance exercises.

C) Patients

The effectiveness of robotic gait rehabilitation largely depends on the ability of the system to provide different type of assistance according to patients’ different recovery stages [144]. The rehabilitation process can broadly be divided into three stages: the preliminary, intermediate and advanced stages [16]. Patients can be classified into eight main groups [12]:

0 = normal

1 = mild disability (no visible gait abnormality)

2 = moderate disability (abnormal gait but no aids)

3 = early cane (patient can walk about 8 m without cane)

4 = late cane (dependent on unilateral support)

5 = bilateral support (scooter for distance)

6 = confined to wheelchair (patient cannot walk about 8 m)

U = unclassifiable (significant cognitive, visual, fatigue, bowel/bladder impairment).

2.3.3.2. Gait robotic modules

In order to respond to the pre-mentioned approach and environment features requirements, the gait robotic rehabilitation systems support two different robotic modules: human robotic modules (since their role consists of assisting or completing the patient movements) and environment robotic modules (since they simulate different ground reaction forces). Figure 2-3 describes in detail the relation between the required features and the associated robotic modules developed to help to incorporate these features.

1) Human robotic modules

Gait rehabilitation systems can use a combination of three different robotic modules for assisting patient gait movements, of which there is more than one mechanical design, thereby providing a diversity of solutions. These robotic modules are Body Weight Support (BWS), reciprocal stepping mechanism, pelvis mechanism, and body weight shifting cited in the order of their use in gait rehabilitation robots.

a) Body Weight Support

BWS is a mechanical system used to help the patient carry some or the full weight of their body during standing [62, 145]. It provides stability to the trunk and the pelvis during movement, so that the patient performs gait training safely. BWS can be sorted according to the mechanical design into two types:

- cBWS supports the patient’s weight through an overhead attachment cable, distributing unweighting assistance equally on both sides of the body through the harness fastened around the hip and the abdomen of the patient. In an active dynamicBWS, the attachment of the cable is adjustable to maintain the amount of the prescribed force assistance. Examples of a gait rehabilitation robot that uses the cBWs system include Lokomat [14], LOPES [87], and G-EO system [111].
- sBWS is less commonly used compared to cBWS. For supporting the subject’s weight, these systems use a robotic arm holding the patient’s waist or back. Examples of gait rehabilitation robots that use cBWS system are KineAssist [138], NaTUre-gaits [51], PAM and POGO [92].

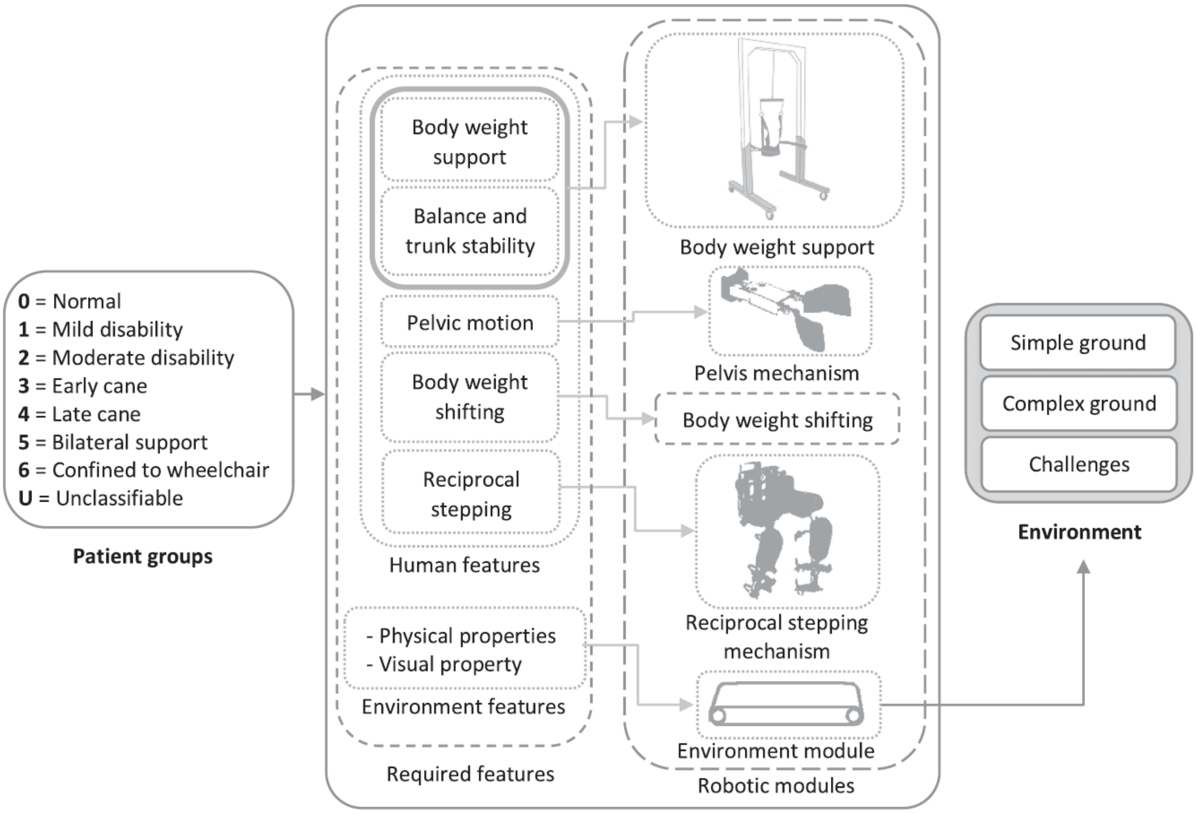

Figure 2-3. Gait robotic systems.

b) Reciprocal Stepping mechanism

The reciprocal stepping robotic modules are mechanisms for assisting the movements of the body lower extremities involved in the walking process or other gait patterns. The joints motorized by reciprocal stepping mechanism comprise all the leg joints including the hip, knee, and ankle [146]. It is important to note that the largest proportion of the robotic research on gait rehabilitation systems have focused on developing and enhancing the characteristics of this specific module. In addition, its design is considered very complex due to the number of mobile parts, the Degree of Freedom (DOF), Range of Motion (ROM), and the forces for each of the parts.

The reciprocal stepping mechanisms for assisting in gait locomotion are exoskeleton and end-effector.

- Exoskeleton: the exoskeletons are wearable mechanical parts that move in parallel to the skeleton of the patient in a way that no additional active DOF will be required to follow patient movements [19]. In such devices, the exoskeleton is attached to the BWS frame of the gait system at the pelvis level, where the advantage of weight-compensation to the exoskeleton.
- End-effector: in this system, the leg movements are controlled by moving the distal parts instead of moving the thigh and shank of the subject. This can be at the foot level using programmable footplates. Based on the trajectory generated, two mechanisms can be distinguished:

- Fixed trajectory: This class groups all the systems where the trajectory is adjusted before starting the exercise. Generally, the trajectory is elliptic and adjusted by changing the size of each member of the crank-rocker mechanism e.g. GT [74] and ICARE [123].
- Dynamic trajectory: This class groups all the systems where the trajectory is not predefined. Typically, it can take any shape within limited ranges according to certain directions e.g. HapticHaker [111] and G-EO system [114].

c) Pelvis mechanism

Pelvis is the center of the body weight and the link point between the lower limbs and the trunk, thus it is very important for maintaining balance and transferring forces during walking. Therefore, it is not surprising that three of the six gait determinants are related to pelvis motion, and the lack of control of this part will likely disturb the quality of gait rehabilitation. The problems can manifest as secondary gait deviations [69], which may result from abnormal pelvic obliquity.

The pelvis mechanism is a robotic system usually placed at the back of the patient attached to the gait system frame, developed to assist the six pelvis DOF. The comparison between different systems is based on the number of DOF they support. Despite its high importance and impact on quality of gait recovery, few studies have attempted to develop it [69]. Earlier gait robotic systems, such as Lokomat, focused on controlling leg movement, while the pelvis was restricted. Later, it was given more importance and can also be found as a separate system for correcting the deviation from normal pelvic motion.

d) Body Weight Shifting

One of the important concepts in the rehabilitation process for a well-trained neurological system is body weight shifting, without which a patient may lose the ability to maintain balance during walking [69]. Body weight shifting can be provided by assisting the pelvis forward translation. Actually, it is difficult for a fixed system to provide such a sensation using limited local motions, for example, a pelvis mechanism with motorized forward and backward motion. However, movable systems can partially provide that.

A) Environment robotic Modules

Three known types of mechanisms are used for simulating the environment [15, 16]: treadmill, footplates and over ground. The first two are static systems where the simulation of ground reaction is performed by moving the ground under the patient’s feet, while the latter is a movable system, in which the user interacts directly with the ground without simulation. In such a system, the patient travels on real ground, while the system plays the role of assistance or guidance.

- Treadmill is a popular progress method used for locomotor devices, consisting of generating an opposite movement to which the subject is walking or running toward, so he or she stays in the same place. The walker’s foot is not in permanent contact with the device, it can be only during the stance phase. With this type of progression method, only a typical flat ground can be simulated.

- Footplates in addition to their role in assisting the patient stepping reciprocal movements as previously mentioned, can be setup to act as an environment simulator [18]. By changing the type of executed control, the footplates can switch from the mode of foot guide assistance to ground simulation. This can be realized by exerting a low impedance force to the patient's feet when they are supposed to be in the air (swing phase), while a high impedance is executed when the feet are in contact with the virtual ground (stand phase) [143]. In a similar way, this mechanism can simulate complex grounds rather than a typical flat ground such as stairs, slope...etc.
- Over ground systems consist of a mobile platform allowing the patient to navigate into the clinical environment. The mobile platform generates the movements through motorized wheels and can be a guide following a straight or curved path [139].

2.3.4. Evaluation of Gait Robotic systems

As mentioned earlier, the aim of this review is to make it easy to perceive different gait robotic systems, by classifying them according to certain properties. This classification emphasizes the differences between systems, evaluating the gait systems through the robotic modules comprising the system with coefficients defining the weight of every module. The evaluation of each module is achieved by assessing elementary characteristics (features measuring the ability of each robotic module to execute the predefined feature) with coefficients determining the weight of every element. It is important that weight coefficients can change according to the activity and the patient recovery stage, since the conditions governing these features have changed. The first part of this section discusses the methodology employed for weighting and scoring the features of the different robotic modules. The second part describes the elementary characteristics defined to technically describe the different gait robotic modules.

2.3.4.1. Scoring and weighting

One of the biggest challenges in this study is the evaluation of the systems for a specific feature and the weight of each feature for calculating the global evaluation. The team discussed and analyzed the problem, finally defining two main issues: evaluating the score of the system for a specific feature; and the evaluation of the weight of the feature for a robotic module.

2) Scoring

Three levels of authenticity where determined when scoring a system:

- High, when the information was provided directly from the developer, e.g., a precise value of DOF and ROM (this can be found in catalogs, articles etc.).
- Medium, when the information can be extracted from the description provided by the developer or from other studies.
- Low, when a subjective evaluation of the system was made based on the mechanical design basic elements (type of actuation, power transmission and mechanical configuration).

A) Weighting approaches

Two approaches were adopted for weighting, different features or different robotic modules, where both were based on descriptive evaluations provided by many studies of robotic gait rehabilitation. For instance, if studies confirmed that for a specific stage S1, feature F1 (e.g. balance support) is more important than feature F2 (e.g. pelvic motion assistance), the weight W1 for feature F1 is higher than weight W2 for feature 2. It was observed that the descriptive evaluation could be implicit, for example studies focus more on F1.

The next step was numeric evaluation, and the two approaches were:

- Approach 1: An approximate intuitive value was based on the rank of the features using the descriptive evaluation. The descriptive evaluation is a numeric evaluation with a very low resolution, therefore providing a numeric evaluation is nothing more than increasing the resolution with an amount sufficient to make the scale of evaluation capable of distinguishing differences between systems. Nonetheless, this does not mean that this evaluation is as authentic as measurements.
- Approach 2: After sorting features according to descriptive evaluations, the first feature is awarded the highest value of the scale. The value for the second one is the value of the first multiplied by a factor lower than 1 (for example 0.75), and so on. The goal of this is to make the differences uniform, since actual data is unavailable.

The following expressions are examples of some of the descriptive evaluations used to provide an approximate intuitive value to some features:

“the *main* requirements of the gait rehabilitation robot concern *weight beaning* and *balancing*, as well as *posture control* [105]”,

“a robot, in the *first place*, should allow for a “patient-in-charge” mode where healthy subjects are able to walk unconstrained by the device. This concerns the choice of DOF and the quality of low impedance control” [87],

“the reason to *omit* an actuated robotic *ankle joint* was that it is not *necessary* to provide an external “*ankle push-off*” in the device in order to walk safely” [87].

2.3.4.2. Elementary characteristics

Two different groups of characteristics associated with the two types of robotic modules were defined, human and environment modules:

3) Human robotic module characteristics

Dynamic and adjustability: While walking or practicing any exercise, the body moves locally in all directions. A BWS is supposed to carry the body within the exercise, providing constant support of the patient’s body weight [67] during all walking phases. The amount of support provided may be adjusted according to different subject weights and recovery stages. Therefore, the “Dynamic and adjustability” factor assesses the extent to which the system verifies the terms “constant support” and “adjustable support”.

Back-drivability: During rehabilitation exercises, it is possible that the patient suddenly loses control or the ability to move a limb, as well as any unexpected event. Therefore, if the system is not ready to cope quickly with the new situation, it may cause damage to the patient [147]. Moreover, the back-drivability allows the therapist to easily apply certain maneuvers, that is, back-drivability is the ability of the system to show low intrinsic endpoint impedance toward certain force sources [92], thus the patient does face an inertia that could delay the response of the system. Back-drivability can be realized using different methods.

Free movement: This feature verifies whether any part of the system disturbs or prevents the motion of other parts. It is important to notice that the movement of the upper limbs and the trunk are the main concern. Commonly, restriction of the trunk movement occurs by the harness of the cBWS type, and the exoskeleton restricting the arm swinging [71].

DOF: This is one of the basic characteristics for describing the gait system capabilities [71] and refers to the number of independent displacements and rotations. In order to satisfy the movement requirements, the robotic system must be able to support a sufficient DOF, which may change according to the activity. Some activities rely more on certain degrees, while others do not [143]. Any lack in the DOF affects more or less the agility and the comfort according to its importance for the activity [92, 102]. Therefore, this can be defined with regard to pelvis and reciprocal stepping robotic modules as:

- Pelvis mechanism allows six pelvis movements, three translations: mediolateral (left/right), anteroposterior (forward/backward) and superior-inferior (up/ down), and tree rotations: pelvis rotation, pelvic tilt and pelvic rotation about the mediolateral axis.
- Reciprocal stepping mechanism considers the three main joints of the lower body, hip, knee, and ankle. The hip is a 3 DOF joint, consisting of flexion/extension, abduction/adduction, and internal/external rotation. Although the knee consists of 2 DOF [148], only the flexion and extraction are considered. For most activities, the second one (internal/external flexion) is less important [146, 149]. The ankle joint has 3DOFs dorsiflexion/plantar flexion, abduction/adduction and internal/external rotation [150].

There are three main states possible for a DOF, free, restricted or assisted. The evaluation in this case, involves restriction and assistance, which can be represented in a two-dimensional space like polar coordinates. The restriction axis corresponds to the impedance the limb is experiences, while the assistance axis corresponds to the acting force. For an assisted system, the motion is provided by the system, while it is a resistive force if it is restricted. As the “free” point is approached, the difference between “restricted” and “assisted” becomes unclear, explaining why this representation was selected. The evaluation is a combination of the two coordinates “restriction” and “assistance”, with coefficients defining the weight of each of them, which vary according to the recovery stage. Figure 2-4 describes the relation between the 3 states of DOF. The different robotic assistance modes are derived from this relation [144].

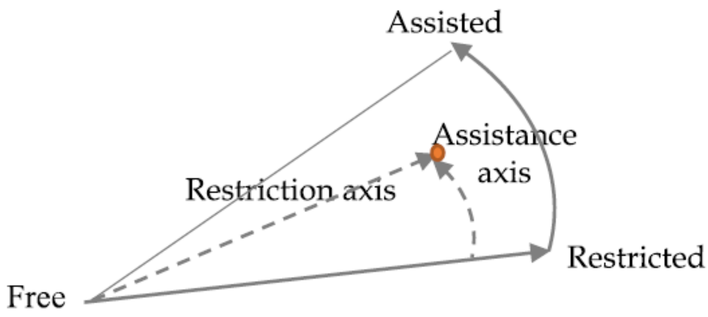

Figure 2-4. Basic relation between the 3 states of DOF.

ROM: ROM is a concept strongly correlated to the DOF: knowing that the DOF means the possibility to move or rotate in a certain direction, the ROM determines the extent the motion could reach. A limited ROM may cause many disadvantages according to the DOF [151]. For example, in addition to critical balance, restricted motion in the sagittal plan limits the step length and the speed, which may affect the quality of gait training. Therefore, a well-designed system for the ROM [20] should take into account different patient anthropometrics [87], especially the thigh and shank lengths, since they have a direct impact on the step size.

A) Environment robotic module characteristics

The evaluation of the environment robotic module can be achieved through an assessment of three characteristics, diversity of grounds, synchronization, and visualization. The first characteristic aims to the check the ability of robotic devices to simulate different type of grounds as discussed previously. The visualization defines the extent of systems in providing real or virtual feedbacks to patient movement while walking. Since most gait robotic systems use ground simulators, then the system should ensure the walker receives a reaction force the moment he steps on a virtual ground [143]. Therefore, the synchronization term is introduced to evaluate the capacity of different environment modules to realize this requirement.

2.3.5. Application

In order to achieve the goal of classifying and graphically representing the different robotic gait systems, the final step applied the different evaluation steps mentioned in the previous section on the 27 gait systems included in this review. The features of each robotic module were sorted relevant to the methodology described in section IV. Furthermore, the coefficients describing the weights of the features, as well as the weights of the robotic modules were define relevant to *approach 2* described in section 2.3.4.1.A).

The first part of this section presents an overview of the sorting of the different feature characteristics. The second part analyses the results of the graphical representation of the modular and global evaluation, providing the review classification.

2.3.5.1. Features ranking

The evaluation of every module is the combination of the relevant elementary characteristics with their coefficients. To define the weight coefficients, the features of the different robotic modules including BWS, reciprocal stepping mechanism, pelvis mechanism and body weight shifting, were sorted as follows:

4) BWS

Three elementary characteristics important for describing the BWS robotic module were defined: dynamic, back-drivability, and free movement. The importance of these three features could vary according to the level of recovery stage. It was determined that most designs give more importance to “dynamic and adjustability” and free movement, with less to back-drivability. Moreover, free movement becomes more important in the latest stages of rehabilitation since the subject has recovered the ability to move without the need for assistance [152]. Therefore, the features were sorted as follows:

- Early stage: (dynamic, free movement, back-drivability)
- Latest stage: (free movement, dynamic, back-drivability)

A) Reciprocal stepping mechanism and pelvis mechanism

The evaluation of the reciprocal stepping and pelvis mechanisms robotic modules was performed through the evaluation of 4: DOF, ROM, back-drivability and free movement. Usually, designers develop their systems to have more DOF and wide ROM [71, 93, 96], than developing a lightweight and high dynamic driving mechanism [90], while the free movement has the lowest priority. Therefore, these features were sorted as follows:

- (DOF and ROM, back-drivability, free movement).

B) Body weight shifting

For body weight shifting, we only determined if the system supported this feature or not, assigning a Boolean value accordingly.

C) Environment robotic module:

Three elementary characteristics for evaluating the environment robotic module were defined, two of which related to the physical properties of the simulated environment (diversity of grounds and synchronization) and one to visual feedback. Typically, designers give more importance to physical properties as they directly impact the physical condition of the patient. For the differentiation between the two physical properties, designers give a high priority to enable their system to simulate one or more types of ground [18, 111], while for the synchronization, only a few designers highlighted the importance of such features. Therefore, the environmental features were sorted as follows:

- (diversity of grounds, synchronization, visualization)

Degree of authenticity: There were three levels of authenticity when scoring, the degree of authenticity for each feature in shown in Table 2.2.

D) Global evaluation

The global evaluation is a combination of the modular evaluation with coefficients describing the weight of each robotic module. The robotic modules were included on the basis that they were basic, support more features or support more complex and dynamic movements, so they were sorted as follows:

- (reciprocal stepping, environment module, BWS, pelvis orthosis, body weight shifting).

Table 2.2. Authenticities of different elementary characteristics.

Authenticities	High	Medium	Low
Features	DOM	Dynamic and adjustability	Back-drivability
	ROM	Free movement	Synchronization
	visualization	Diversity of grounds	

2.3.5.2. Results

The weights and scores are shown in Table 2.3 and the results of the evaluation are shown in Figure 2-5, while the global evaluation is shown in Figure 2-6. It is important to notice that result of evaluating the BWS is relevant to earlier stage (the more important one [16, 144]) conditions.

2.3.5.3. Results analysis

5) Modules analysis

The evaluation of each robotic module based on specific characteristics showed diverse tendencies. For the reciprocal stepping, setting a threshold of 3.5, approximately 63% of the systems could be described as having a good result. In contrast, the pelvis mechanism had a poor average score compared to the other modules, even with a threshold of 2.5, only 22% of the systems satisfied this requirement. For the environmental modules, all the systems satisfied the basic requirements of environment ground for assisting sample locomotor training, of which only 19% were able to support more advanced ADL training. All systems were dynamic trajectory footplates based devices.

Dynamic and adjustability property: overall, 25 out of the 27 systems provide high dynamic support to different patient weights and groups. Two different strategies were used to achieve the dynamic properties in these systems, active dynamic and passive elastic mechanisms. The more common active dynamic is a suspension mechanism that controls the dynamic weight using a force feedback, e.g. Lokolift found in Lokomat [153], whereas the amount of unloaded weight is adjusted in the passive elastic mechanism by changing the springs displacement using an electrical motor, e.g. Lokoiran [122]. Two systems showed a low dynamic property, specifically WHERE-I and UoA PMAbot, due to the use of powerless BWS.

Back-drivability property: most systems presented medium to good back-drivability either for BWS, reciprocal stepping or pelvis robotic modules. In addition, some systems obtained a better score because they used pneumatic actuators, expect LOPES II in which the back-drivability was achieved by a light innovative parallel mechanical configuration.

Free movement property: For BWS, STRING-MAN provided the best free movement since it used six driven cables, which provide 6 DOF. The medium performance class used BWSs and provided good results because of the absence of a suspension harness, which allowed free movement of the trunk. For reciprocal stepping mechanism, all footplate-based devices allowed free upper extremities movement because of the absence of any intersection area. In addition, two systems scored highly for free movement as they utilized an exoskeleton, the parts of which were placed on the patient's back.

DOF/ROM property: for reciprocal stepping mechanism, 74% of systems scored between medium and high, with no maximal scores since no system presented a full DOF and ROM. Most defects were due to lack of ankle joint control and assistance to abduction/adduction of the hip. The dynamic trajectory footplate-based devices had more promising mechanisms because of their abilities to assist the movement of three different joints (hip, knee, and ankle), and to provide an appropriate stride width. Similarly, two over ground systems also scored highly for their abilities to assist for the same three mentioned joints using wearable exoskeletons.

The two versions of LOPES showed the most important treadmill-based devices reciprocal stepping mechanism. An exoskeleton was developed, not only for assisting movement in the sagittal plan, but also for allowing left and right stepping. This was realized by motorized hip ab/ad. The rest of treadmill devices and elliptical footplate devices had low-quality mechanisms mainly due to the constraints and limitations in ROM.

The remaining 26% of the systems had very low scores due to the absence of reciprocal mechanisms, only receiving a score for free movement of the lower limb extremities. It was evident that most systems (about 72%) were over ground based devices because they were developed for assisting patients in later recovery stages, where the focus is more on promoting balance. For the pelvis mechanism, 15% of systems obtained a high score for DOF/ROM property. Among them, two systems (NaTUre-gaits and WalkTrainer) had maximum scores because they offered mechanisms assisting the 6 DOF pelvis of motion with full ROM. Also, 15% of systems obtained a medium score, as 3 DOF pelvis movements were assisted, mostly L/R, F/B, and PR movements. Approximately 40% of systems obtained a low score. Most of these systems were footplate-based devices in which there was no pelvis mechanism. However, they obtained a basic score because they allowed free movement. The remaining 30% of systems had a very low score, as they provided no assistance to the pelvis. Moreover, they restricted some important movements.

Environment module

Diversity of grounds: dynamic footplate-based devices scored highly because of the simulation of different training grounds. Applying forces on both feet and controlling the impedance, facilitated training the patient, not only to climb the stair, but also to stumble, thereby improving balance. Twenty-five systems got a medium score, most of which were over ground systems. They offered the possibility to train patient for challengeable exercises such as actual fall experience. Overall, 59% of systems only simulated one type of ground, except for GMT5 that was designed for climbing stairs, the rest simply simulated flat ground. It is important to note that most systems were treadmill-based devices.

Table 2.3. Assessement of robotic gait systems.

System			LOPES II	LOPES	PAM & POGO	LOKOMAT	ALEX	ALEX II	UoA PMAbot	ARTHuR	STRING-MAN	RGR	MIT-Skywalker	HapticWaker	G-EO- system	ULRF	LOKOIRAN	ICARE	GM5	Gait Master 2	GT (Gait Trainer)	DSP	WalkTrainer	NaTUre-gaits	BAR	KineAssist	WHERE-II	WHERE-I	GaitEnable
Human Robotic modules	BWS (0.125)	Dynamic (0.5)	5	5	5	5	5	5	2	5	5	5	0	5	5	5	5	5	0	5	5	5	5	5	5	5	5	3	1
	BWS (0.125)	Back-drivability (0.1)	4	4	4	4	4	4	4	4	4	4	0	4	4	4	4	4	0	4	4	4	4	4	4	4	5	4	0
	BWS (0.125)	Free movement (0.4)	2.5	2.5	2.5	2.5	4	4	2.5	2.5	5	2.5	1	2.5	2.5	2.5	2.5	2.5	2.5	2.5	2.5	2.5	3	4	4	4	2.5	4	0
	Reciprocal stepping mechanism (0.45)	DOF (0.3) – Hip (0.5) – FE (0.6)	5	5	5	5	5	5	5	5	2	2	2	5	5	5	5	5	5	5	5	2	5	5	0	0	0	0	0
	Reciprocal stepping mechanism (0.45)	DOF (0.3) – Hip (0.5) – AA (0.3)	5	5	1	1	1	1	1	1	1	1	1	0	0	0	0	0	0	0	0	2	0	0	0	0	0	0	0
	Reciprocal stepping mechanism (0.45)	DOF (0.3) – Hip (0.5) – IE (0.1)	1	0	0	0	0	0	0	1	1	1	1	0	0	0	0	0	0	0	0	2	0	0	0	0	0	0	0
	Reciprocal stepping mechanism (0.45)	DOF (0.3) – Knee (0.3)	5	5	5	5	5	5	5	5	2	2	2	5	5	5	5	5	5	5	5	2	5	5	0	0	0	0	0
	Reciprocal stepping mechanism (0.45)	DOF (0.3) – Ankle (0.2) – FE (0.6)	1	1	1	1	1	1	1	1	1	1	5	5	5	5	1	1	0	0	0	2	5	5	0	0	0	0	0
	Reciprocal stepping mechanism (0.45)	DOF (0.3) – Ankle (0.2) – AA (0.3)	1	1	1	0	1	1	1	1	1	1	5	0	0	0	0	0	1	0	0	2	0	0	0	0	0	0	0
	Reciprocal stepping mechanism (0.45)	DOF (0.3) – Ankle (0.2) – IE (0.1)	1	1	1	0	1	1	1	1	1	1	1	0	0	0	0	0	0	0	0	2	0	0	0	0	0	0	0
	Reciprocal stepping mechanism (0.45)	ROM (0.3) – Hip	4	4	1.5	4	2.5	4	4	4	4	4	4	4.5	5	2	4	4	4	5	4	0	4	4	5	5	5	5	5
	Reciprocal stepping mechanism (0.45)	ROM (0.3) – Ankle	2	2	2	2	2	_	_	_	_	_	_	5	5	5	2	2	5	0	2	1	5	5	_	_	_	_	_
	Reciprocal stepping mechanism (0.45)	Back-drivability (0.25)	5	4	5	3	3.4	3	5	4	0	_	3	4.5	5	5	4.5	4.5	4.5	4	4	5	3	3	_	_	_	_	_
	Reciprocal stepping mechanism (0.45)	Free movement (0.15)	5	2.5	5	2.5	2.5	2.5	4	3	0	0	5	5	5	5	4	4	4	5	5	5	2.5	3.5	0	0	0	0	0
	Pelvis mechanism (0.175)	DOF/ ROM (0.8) – LR (0.2)	5	5	5	1	0	1	0	1	5	1	0	1	1	1	_	1	1	1	1	1	5	5	5	1	1	0	0
	Pelvis mechanism (0.175)	DOF/ ROM (0.8) – FB (0.13)	5	5	5	0	0	1	0	1	5	1	0	1	1	1	_	1	1	1	1	1	5	5	5	1	1	1	1
	Pelvis mechanism (0.175)	DOF/ ROM (0.8) – UD (0.13)	1	1	5	1	2	1	1	1	5	1	1	1	1	1	_	1	1	1	1	1	5	5	1	1	1	1	1
	Pelvis mechanism (0.175)	DOF/ ROM (0.8) – PR (0.2)	1	0	5	0	0	1	0	1	5	2	0	1	1	1	_	1	1	1	1	1	5	5	5	1	1	0	1
	Pelvis mechanism (0.175)	DOF/ ROM (0.8) – PT (0.2)	1	0	5	0	0	1	0	1	5	5	1	1	1	1	_	1	1	1	1	1	5	5	1	1	1	0	1
	Pelvis mechanism (0.175)	DOF/ ROM (0.8) – PM (0.13)	0	0	1	0	0	0	0	1	5	1	0	1	1	1	_	1	1	1	1	1	5	1	1	1	1	0	1
	Pelvis mechanism (0.175)	Back-drivability (0.1)	5	3	5	_	_	_	_	_	_	_	_	_	_	_	_	_	_	_	_	_	_	_	_	_	_	_	_
	Pelvis mechanism (0.175)	Free movement (0.1)	5	2.5	5	_	_	_	2.5	_	4	4	_	_	_	_	_	_	_	_	_	_	4	4	4	5	5	_	_
	Body weight shifting (0.05)		0	0	0	0	0	0	0	0	0	0	0	0	0	0	0	0	0	0	0	0	5	5	5	5	5	5	5
Environment robotic module (0.2)	Diversity of grounds (0.6)		2.5	2.5	2.5	2.5	2.5	2.5	2.5	2.5	4	2.5	5	5	5	5	2.5	2.5	2.5	5	2.5	4	2.5	2.5	4	4	4	4	2.5
	Synchronization (0.3)		2.5	2.5	2.5	2.5	2.5	2.5	2.5	2.5	2.5	2.5	2.5	5	5	5	5	5	5	5	5	5	5	5	5	5	5	5	5
	Visualization (0.1)		0	0	0	5	0	0	0	0	0	0	0	5	5	5	0	0	5	5	0	4	5	5	2.5	5	5	5	5

( ) Coefficient defining the weight of a feature or of a robotic module, FE: flexion/extension, AA: abduction/adduction, IE: indorotation/exorotation. LR: left/right, FB: forward/backward, UD: up/down, PR: pelvic rotation, PT: pelvic tilt, PM: pelvic rotation about the mediolateral axis.

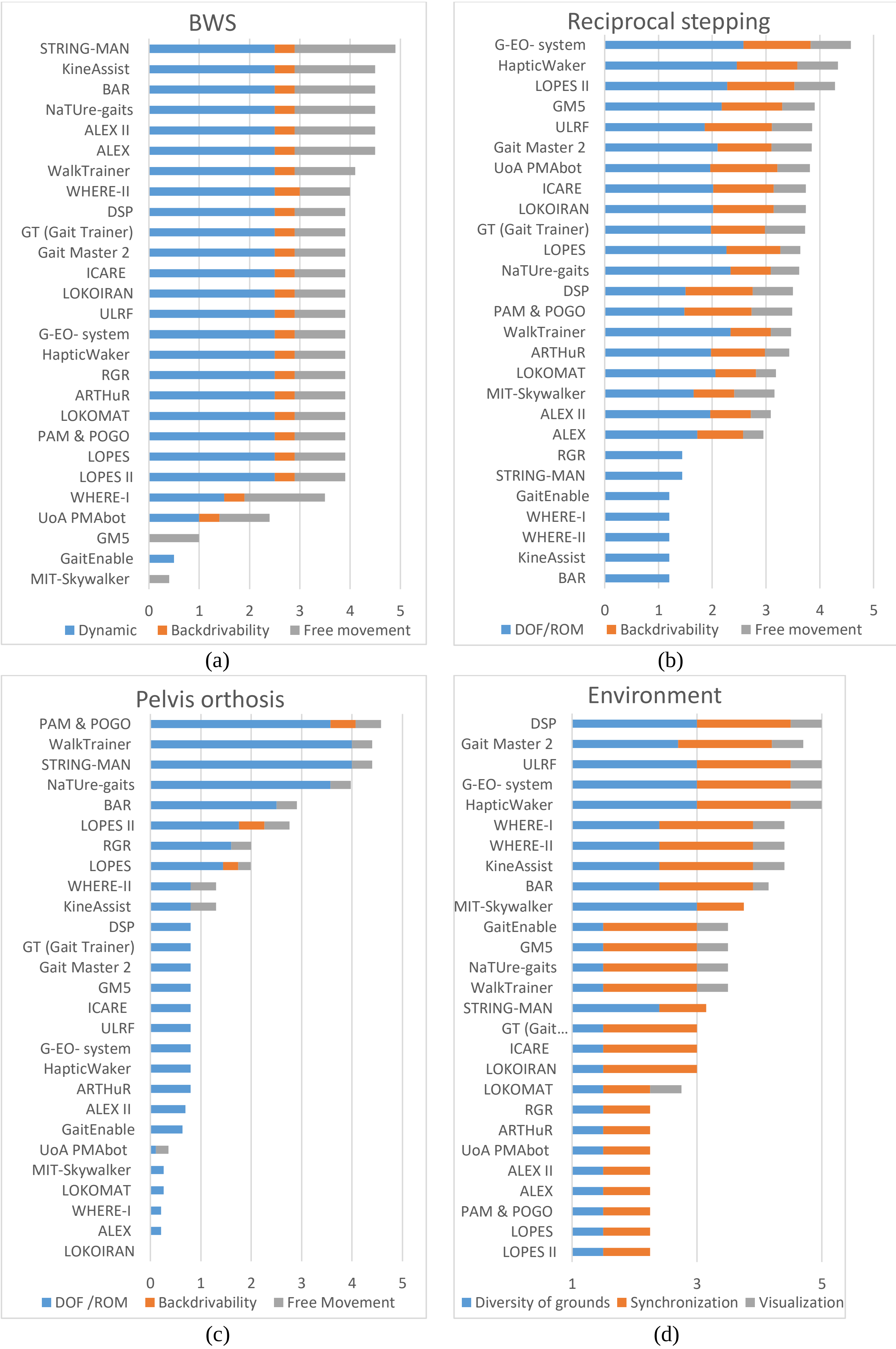

Figure 2-5. (a) Assessment based on BWS evaluation. (b) Assessment based on reciprocal stepping mechanisms evaluation. (c) Assessment based

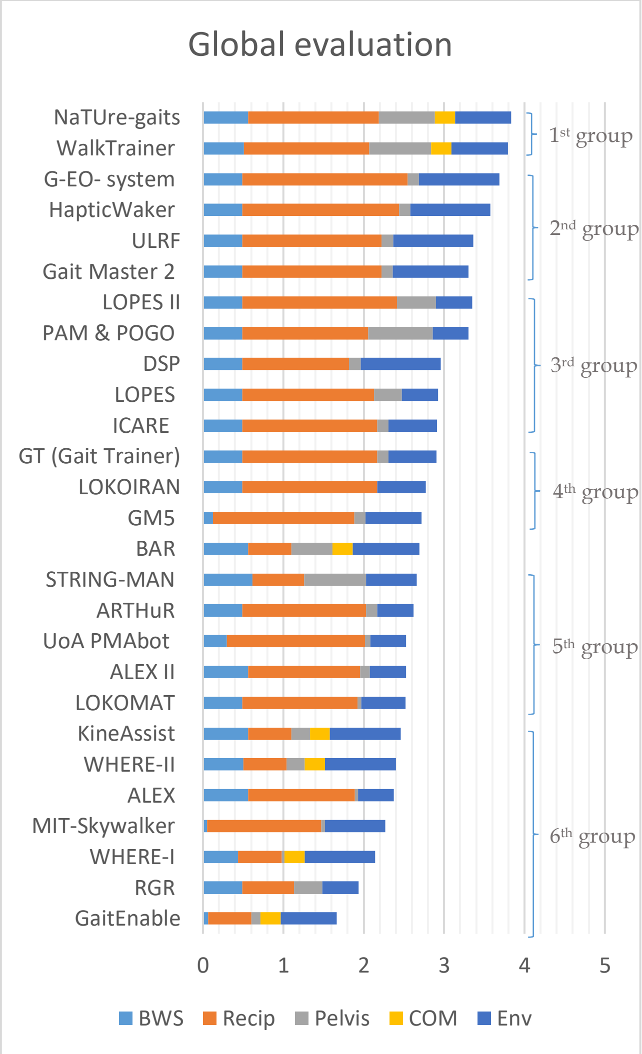

Figure 2-6. Global evaluation (Recip: reciprocal stepping mechanism, Pelvis: pelvis mechanism, Env: environment robotic module, BW: body weight shifting).

Synchronization property: 67% of the systems provided a clear stepping for a real sensation of the actual world. Of the 33% of systems that did not, most were treadmill-based devices, in which there was a shift of speed between the treadmill belt and the foot, resulting in foot drag, except for Mit-Skywalker where this was overcome by two rotational treadmills for each foot.

Visualization property: approximately 48% of systems did not provide any type of visual representation. Most of these systems were treadmill-based devices and fixed trajectory footplate-based devices, in which patients may be confused since there is no correspondence between the movement performed and the scenes.

A) Global evaluation analysis

The global evaluation revealed a mediocre performance for robotic rehabilitation, with the outcome distribution heavily dependent on differences in mechanical design groups. The analyses differentiated six groups, from top to bottom:

- 1st group (2 systems): an excellent score was given to two of the over ground systems NaTUre-gaits and WalkTrainer. This was achieved by an excellent score in BWS and pelvis mechanism, as well as the assistance for body weight shifting. In addition, good reciprocal stepping and environment mechanisms were presented. These 2 systems are designed to assisted a large groups of patients.

- 2nd group (3 systems): a high score was achieved by the dynamic trajectory footplate-based devices groups, due to the development of sophisticated environment robotic modules allowing the simulation of simple and complex grounds. In addition, there were good results for the reciprocal stepping and BWS robotic modules. These systems are mostly designed for assisting patients in intermediate and advanced stage of recovery.
- 3rdgroup (4 systems): this group of five gait systems mostly include dadvanced robots of treadmill-based devices. In these systems, a medium to high score was achieved by the reciprocal stepping and pelvis robotic modules, good scoring BWS system and low-quality environment module. These systems are designed mostly for patients in earlier stage of recovery.
- 4thgroup (4 systems): the three fixed trajectory footplate-based devices performed satisfactorily, with a good BWS, a medium score for reciprocal stepping mechanism and low-quality pelvis and environment robotic modules. These systems are designed mostly for patients in intermediate stage of recovery
- 5thgroup (5 systems): From STRING-MAN to Lokomat. This group of systems consisted only of treadmill-based devices. Except for the good BWS systems, this group had low score in the following robotic modules (reciprocal stepping mechanism, pelvis mechanism and environment).Most of these systems are developed for assisting patients in earlier stage of recovery.
- 6thgroup: the rest ofthe26% systems were considered having low score in almost each robotic module. This group included a mix of treadmill and over ground systems, with very low-quality BWS, reciprocal stepping and pelvis mechanisms being their most important characteristics. These robots are designed for assisting patients in advanced stage of recovery.

2.3.6. Visit outcomes

Overall, the visit clearly showed that current rehabilitation therapies are still not efficient at producing better physical outcomes. Current robotic rehabilitation systems still need more development. Although they succeeded to some extent in relieving therapists, they still do not offer an advanced solution for patients. The most important outcomes of the visit are the following:

- Current rehabilitation methods are based on applying high-intensity and repetitive exercises. This type of training makes the patient exhausted and less motivated to continue the training. The training should support some kinds of entitlements and challenges.
- The duration of the training can be optimized to perform more than one specific task during one rehabilitation session. Strengthening muscle force, controlling balance,

supporting weight and other tasks can be better if done simultaneously with an advanced robotic system.

- Future robotic gait rehabilitation systems should give a larger role to VR technology to provide the patient with visual feedback. The performance of the patient can also be provided using VR technology. In addition, VR can be used to give instructions to the patient in a way that decreases the patient's dependence on the therapist.
- Future robotic systems should provide therapists with analysis reports on the patient's performance. In addition, they should allow therapists to adjust the training based on recovery stage requirements.

2.3.7. Review of outcomes

According to our method of comparing rehabilitation systems, the simulation of the ground seems important for better outcomes (only four of the gait systems identified in this study were able to support more advanced training for daily activities). Some commercialized systems are still commonly used (e.g., Lokomat), but they are outdated and do not use a comprehensive strategy. Some prototypes are quite interesting (e.g., NaTUre-gaits), but as they are not commercialized, their safety, efficiency and efficacy have not yet been confirmed. Furthermore, optimal rehabilitation systems should focus on many aspects rather than one specific task. In addition, it is recommended that further research on gait robotic design be conducted to enhance the properties of pelvis mechanisms as this robotic module had a poor average score compared to the other modules.

The evaluation of the different characteristics and weights of the features was challenging due to the lack of quantitative data, probably due to the absence of standards that show quantitatively the importance of features within the different stages. Therefore, we call for a review of these standards and the addition of more, as well as new methods for evaluation. This could be achieved by collating the results from different studies already conducted, as well as conducting specific studies for evaluating the needs of patients according to the stage and the importance of each the stage's features.

2.4. Conclusion

Data from the visited rehabilitation center show that although there is an increase in the number of patients with neurological disorders at the rehabilitation center, few of them pursue the training to the end. One of the reasons that push patients to not pursue the training is that training is difficult and boring. Meanwhile, robotic gait rehabilitation systems support few types of entertainment such as visualizing the movement of the patient in video games. However, most of these games are not interactive and are not designed to serve a therapeutic purpose.

Most of the existing gait robotic systems are not designed to assist patients in performing natural walking movements. This can be expressed in many forms such us restricting the movement of some parts of the body (e.g., pelvic tilt) or serving as just a passive assistance to the movement of some joints (e.g., passive assistance to the ankle joint using straps). In addition, these devices train patients to walk on typical ground surfaces (e.g., plane ground). However, a real environment may contain more than a simple ground surface. It includes complex ground surface forms such as stairs, hills and ground surfaces that comprise some small details like pebbles and cracks found in real soil.

Chapter 3: THREE-DIMENSIONAL INTERACTIVE ROBOTIC REHABILITATION SYSTEM

3.1. Introduction

The research we performed on different techniques and approaches used in rehabilitation provides valuable information about actual difficulties facing patients with neurological disorders. The research outcomes illustrate that current robotic rehabilitation devices have many drawbacks that hamper providing a better rehabilitation experience to the patient. We believe that the main contribution of these systems is the automation of the repetitive rehabilitation exercises. Thus, instead of a therapist assisting the patient in performing the training, the robot carrying this out. On the other hand, little work has been done to motivate patients to perform the training. On this basis, we propose developing a new robotic rehabilitation system of which one of its main objectives is making the rehabilitation process interactive and motivating to the patient by integrating robotic and VR techniques. Thus, we named our project the Three-dimensional Interactive Robotic Rehabilitation System (*3D-IRS*). The project broadly presents a vision of what the rehabilitation robot of the future should include as features. Overall, the 3D-IRS consists of two hardware components. One has the objective of assisting the patient with performing locomotion exercises while the other has the objective of simulating to the patient different walking ground surfaces. In this thesis, we focus on developing the second hardware component of the 3D-IRS, which is named the ground walking platform (GWP). This chapter is organized as follow: in the first section, a broad description of the objectives and the sections of the 3D-IRS are given. In the second section, objectives, the design specifications and the kinematic of the GWP is presented. The summary of this chapter is provided in the last section.

3.2. Three-dimensional Interactive Robotic Rehabilitation System

The 3D-IRS targets patients who have had strokes or spinal cord injuries or those who have partially lost the ability to move or walk. The major goals of the project are the following:

- Make rehabilitation training entertaining for the patient by integrating challenging VR tasks.
- Create an adjustable environment with the possibility of designing different rehabilitation scenarios according to the patient's case and rehabilitation purpose. For example, the therapist or the expert can create a scenario that targets the points below.
    - Strengthening muscles and augmenting joints' range of motion. For example, the system can be used to strengthen specific weak muscles of the leg as well to increase the range of motion of the ankle joint.
    - Teaching the patient to walk on complex ground surfaces such as a plane floor, hill, slope and others.
- Compare data of different rehabilitation sessions to help create reports and follow the progress of the patient over the long term.

Based on these objectives, the project is divided into three main sections:

- Developing a hardware simulation of the GWP and the orthosis.
- Developing a VR environment.
- Establishing analysis tools.

Section 1: Developing a hardware simulation of the GWP and the orthosis

In this section, we propose developing the hardware components of the robot. To use VR and create different scenarios, we would have to design a hardware platform that allows the simulation of the GWP and the exoskeleton orthosis limb that performs the rehabilitation functions. Figure 3-1 illustrates the 3D-IRS, with a Ground-Walking platform and an exoskeleton orthosis.

- **Simulation of ground walking.**

  To create a system that simulates the process of walking on the ground or climbing stairs, we suggest designing a system of two manipulators fixed under each foot and provided with necessary sensors. Their role is to generate force that corresponds to the reaction of the ground that one is walking on. A modified parallel robot seems to be convenient for this purpose. Position and force sensors are necessary to realize the interaction between the feet and the simulated ground. This system is called the GWP.

- **Exoskeleton orthosis limb.**

  We intend to use or to design an exoskeleton orthosis limb to assist in performing tasks for rehabilitation. Many modes may be integrated into the system: passive mode, active mode, active assist mode, active resist mode and others.

Section 2: Developing a VR environment.

Virtual reality seems quite important to stimulate the neurological system. By combining it with the hardware components we have described, we can create a virtual environment that surrounds the patient, helping them to be at ease and comfortable. Moreover, moving a limb or just having the intention to move it and getting the sensation that one is doing it through VR helps the brain to create new neurological pathways. Drawing on psychology, we propose to design different environments and scenarios, taking into account the patient's degree of disability, the progress made with treatment and especially how to motivate the patient.

Section 3: Establishing analysis tools.

This section is important for the therapist since it offers the possibility to control the patient's performance and progress in the long term. It consists of a set of records of different activity responses, such as forces generated by the impaired limb, range of motion and perhaps

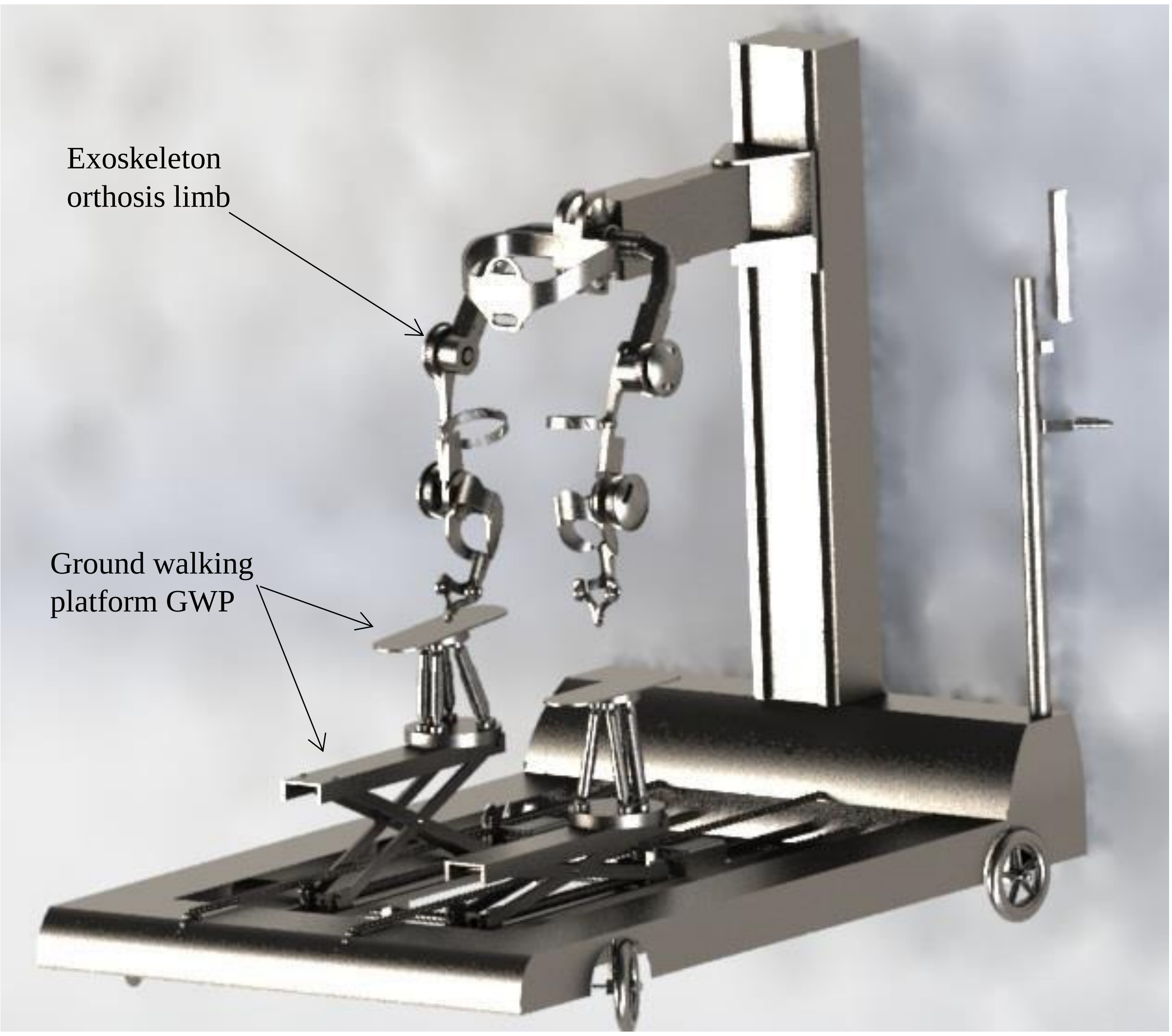

Figure 3-1. Three-Dimensional Interactive Robotic Rehabilitation System.

neurological activity. Comparing the data of different rehabilitation sessions helps to create reports and to follow the patient's progress.

It is important to note that because it is difficult to realize all the mentioned objectives within this paper, we focus on achieving the most important objective of the 3D-IRS which concerns developing the GWP. Therefore, the rest of this thesis will focus on studying the characteristics of the GWP system.

3.3. Ground Walking Platform

3.3.1. Objectives

The GWP system is the part of the system that simulates the relationship between the walker and the ground. Like a flight simulator, applying forces and mechanical laws on both feet and controlling impedance, we can make the user feel as if they are in a real environment. The GWP system aims to meet all the physical and visual requirements that make the simulation of walking on different ground surfaces as realistic as possible. Therefore, the key environmental characteristics that make the simulation seem to be realistic are defined in the following:

- Physical properties: During the simulation of walking, the subject must receive two different kinds of forces as follows.
  - Reaction force: The system should provide reaction forces in response to the foot movements in any direction and along all the walking path.
  - Body acceleration force: Generating necessary acceleration gives the user the real sensation of walking, which makes a major difference with static systems.
- Visual properties: This is a quite important property since it works in harmony with the physical part to provide a visual perception that corresponds to a physical sensation. In addition, it provides the user with a virtual world that should be attractive, challenging and motivating. This can be a crucial point for patients that find physical exercises difficult and boring.

3.3.2. System description

To provide the patient with the relevant reaction forces and the visual feedback corresponding to the type of simulated ground, the GWP system was established with three main parts: a control unit, a hardware unit and a VR unit. Figure 3-2 describes the GWP’s units and shows the relationship among them.

- The control unit coordinates the task of the different units to simulate the ground reaction forces generated in response to walking on a ground surface with different degrees of hardness (e.g., walking on concrete or on mud) and on a ground surface with different gradients (e.g., walking on a plane ground, walking uphill or walking downhill).
- The hardware unit is the mechanical part of the system. It will support each foot while simulating the above-mentioned ground reaction forces.
- The VR environment unit visualizes the environment simulated by the control unit and applied by the robotic platform.

The ground reaction force can be simulated in three dimensions or more or less. The control system will take a set of measurements from the hardware unit (robot), describing the state of the robot as well as the physical state of the walker’s foot. These state measures can be forces, positions or angles. Further, the VR unit will provide the control unit with a set of information

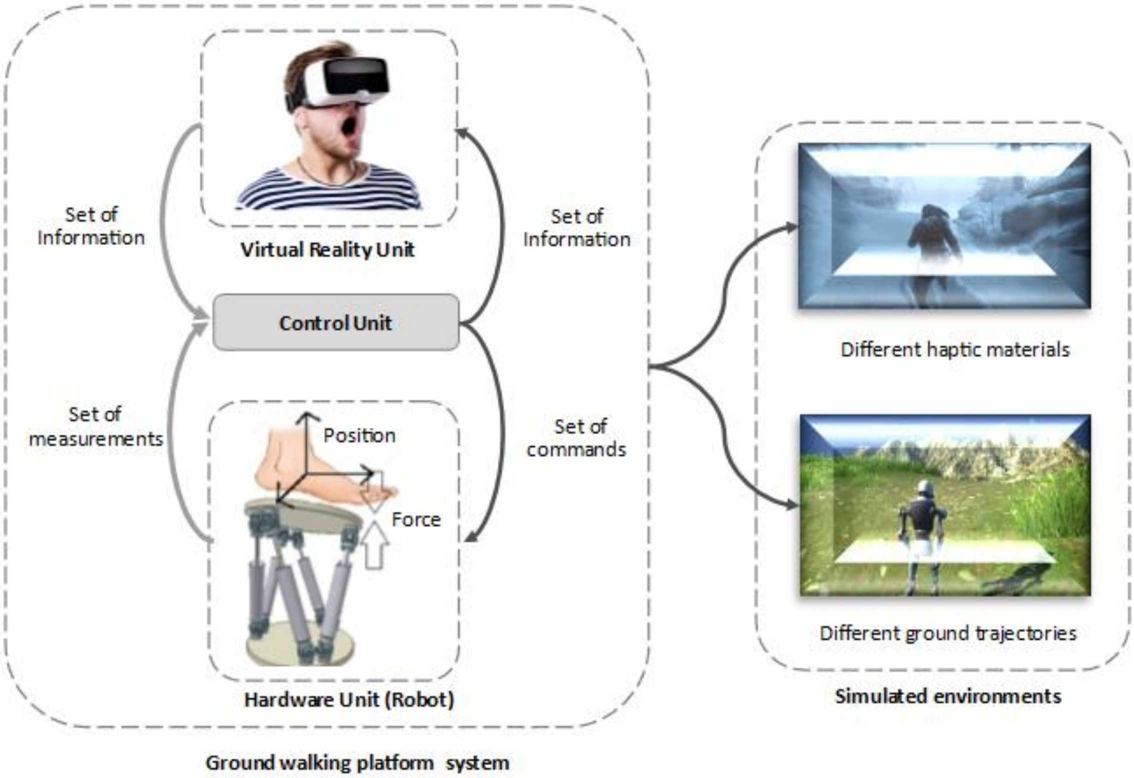

Figure 3-2. Block diagram of the ground walking platform.

describing the physical state of the virtual avatar that simulates the patient's motions. This set of information includes relative feet position, body position and features of the ground (slope and hardness).

Combining these data, the system generates a set of commands for the robot such as forces, positions, angles and voltages for the actuators. The platform will then follow the feet of the patient during the swing phase of walking, and move the feet during the stand phase to simulate walking in the VR environment, while the user stays at the same place in the real world. At the same time, the system updates the VR state elements (relative feet position, body position, etc.). The VR environment will then display and simulate an environment and an avatar.

3.4. Design

3.4.1. Specifications

To meet the aforementioned physical requirements, the hardware part of the system has to solve the following mechanical problems:

- **Degree of freedom and range of motion**: To realize a comprehensive simulation of the different types of ground surfaces, natural movements of the foot should be allowed and supported in full degree of freedom (six DOFs) and wide range of motion (no movement restriction).
- **Support of different walking speeds**: One of the criteria to detect the quality of the driving system implemented in a locomotion system consists of defining the capacity

of the system to execute different walking speeds (low, normal and fast walking speed).

- **Back-drivability**: During rehabilitation exercises, it is possible the patient may suddenly loses control or the ability to move a limb or may execute unexpected movements. Thus, if the systems is not ready to cope quickly with the new situation, this may cause injury to the patient. Therefore, the back-drivability of the driving system of the robot should be high.

3.4.2. Method

To define the best mechanical structure that meets our kinematic and dynamic requirements, we analyzed designs of various mechanisms. We found that the hybrid parallel mechanical design has more advantages over the ordinary types of designs. The hybrid design benefits from serial robots to increase workspace and from parallel robots to preserve stiffness and to provide a driving system with high back-drivability. The fundamental definition related to parallel, serial and hybrid robots are as follows. A robot is called a serial or open-loop manipulator if its kinematic structure does not make a loop chain. A robot is called a parallel or closed-loop manipulator if its structure makes a loop chain. A robot is a hybrid manipulator if its structure consists of both open and closed-loop chains [154].

The system proposed consists of two main parts: an XYZ mechanism (this also includes two subsystems, X & Y translation rails and a mechanism for Z translation) and a Stewart platform (Figure 3-3).

1. X & Y translation rails: The movements of the walker on the XY plan are provided using two independent rails. For each foot, a rail is introduced to simulate movements along the *x*-axis, and another rail is introduced to simulate movements along the *y*-axis.
2. A mechanism for Z translation: To support the translation movements of the foot along the *z*-axis, a pantograph mechanism is used. The pantograph mechanism is a parallel high stiffness mechanism, which has the advantage of providing a wide range of motion along *z*-axis.
3. A Stewart platform: This type of parallel robot is chosen specifically to simulate the rotation movements of the user. We also aim to use this platform with high precision with the translation movements. A detailed description of the characteristics of the selected Stewart platform is presented in Chapter 5:

3.4.3. Power transmission

Choosing the proper power transmission type for the system is a challenging task. There are advantages and disadvantages to each kind of power transmission. There are numerous elements that affect the transmission type selection, including: torque, temperature, and maintenance concerns. The majority of these factors will only become clear once a system has been tested in practice.

Since our study is theoretical in nature, we chose the well-known conditions the system is meant to be implemented for. The well-known factors that affect our choice of power transmission are described in relation to the characteristics of the walker's gait speed and acceleration.

Human gait speed and acceleration in the sagittal plane are more significant than along the transverse and frontal planes. In accordance with the characteristics of the movements along each plan, a distinct mechanical power transmission system has been chosen.

A belt drive is chosen along the X axis because of the large movement speed. The belt drive is used in high-speed applications because it performs effectively at both moderate and extremely high speeds. Meanwhile, a reliable and more accurate power transmission, such as Power screws (lead screws), is used for the Y and Z axes, where the speed movement is respectively slow".

3.4.4. Actuators and sensors

The GWP system is actuated using two types of power steering Electric and Hydraulic. The translation movements along X, Y, Z axes, are actuated by electrical motors. The motors rotate the lead screws of Z, and Y mechanism and also the driving belt of X mechanism. The electrical motors are smooth and easy to control and fits well the application of the X, Y, Z mechanism of supporting slow and moderate frequency movements. However, to compensate for high frequency movements a hydraulic actuator on Stewart platform is implement as they can provide pic power.

A 6 DOF sensor is positioned just beneath the footplate between the Stewart platform and the user's foot to sense the interaction forces between the foot and the platform. The GWP mechanism's actuators and force sensor are depicted in Figure 3-4.

3.4.1. Advantages of the selected design

The design of the GWP system has the advantage of adding and enhancing many characteristics:

- **Degree and range of motion**: The system is able to simulate more complex contours of virtual ground surfaces to the user because it consists of two nine-DOFs platforms (one platform for each foot). The GWP allows movement of feet in wide range of motion without restriction on any DOFs. Therefore, the user will be free to walk in any direction they want.

- **Low user entry**: The GWP provides easy access to its foot plates, thanks to the Z mechanism that offers the possibility of landing the footplates to a level close to that of the clinical floor.

- **High back-drivability:** The GWP mechanism employs hydraulic actuators for the Stewart platform part of the system. This feature allows controlling the system to respond quickly to the user's different actions.

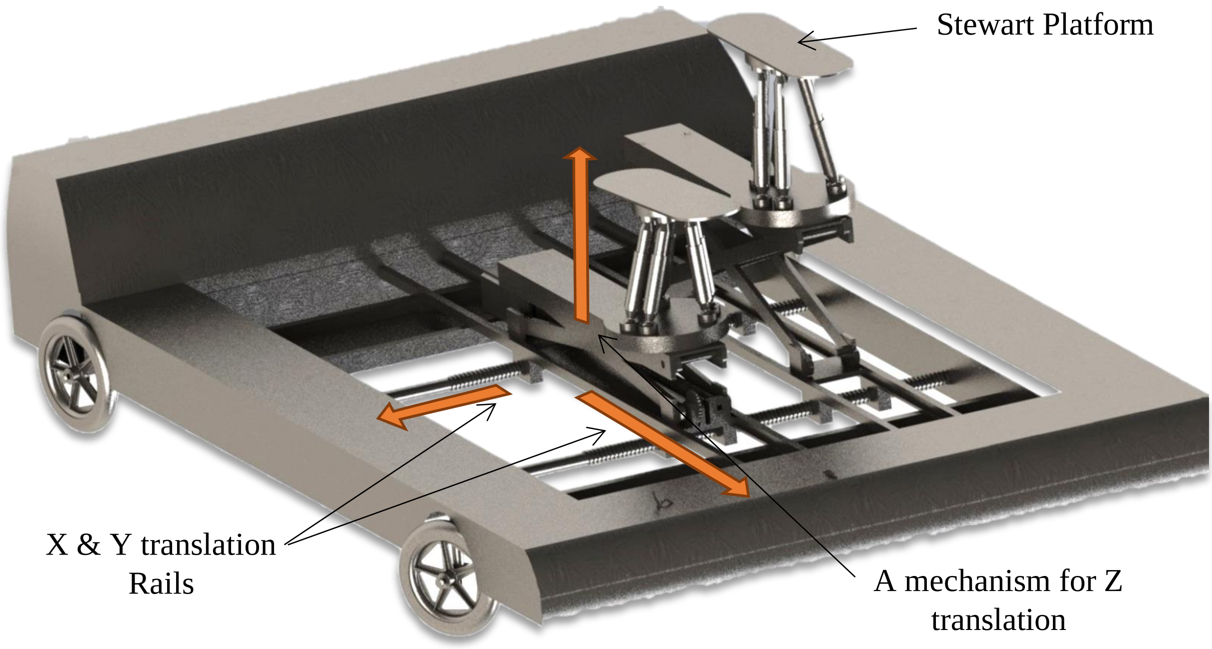

Figure 3-3. Ground Walking Platform.

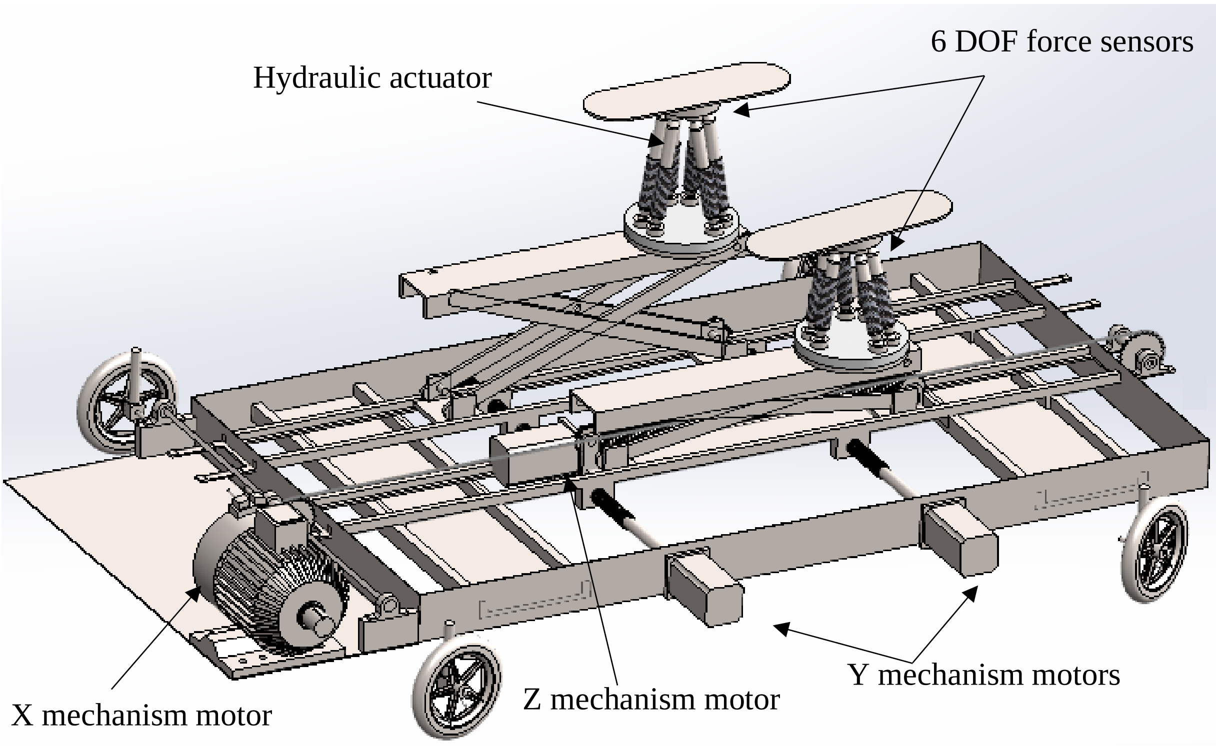

Figure 3-4. Placement of the actuators and force sensors of GWP.

3.4.2. Dimension

The basic work space parameters of the GWP system are defined according to the follow criteria.

- Rotational range of motion of the footplate has been primarily selected and calculated based on the ankle's maximum allowable motion (Table 3.1).

- The maximum allowable translation movements of the feet on a GWP footplates are calculated as follows: thigh range of motion multiplied by functional leg length. The thigh range of motion is described in Table 3.2, while the functional leg length is illustrated in Table 3.3.

The selected GWP basic workspace is illustrated in Table 3.4 and in Figure 3-5.

N.B: To cover a wide population, the functional leg length is selected relevant to a maximum length of the man. It is also worth mentioning that the workspace selected for the GWP system is an initial one. After performing the kinematic and dynamic study, the workspace will be adjusted to consider the constraints defined.

Table 3.1. Ankle maximum allowable motion.

Motion	Maximum allowable motion.
Dorsiflexion	20.3°–29.8°
Plantarflexion	32.6°–40.8°
Inversion	14.5°–22.0°
Eversion	10.0°–17.0°
Abduction	15.4°–25.9°
Adduction	22.0°–36.0°

Table 3.2. Thigh range of motion.

Motion	Approximately motion
Flexion	120°–125°
Hyperextension	10°–15°
Abduction	30°–45°
Adduction	15°–30°

Table 3.3. Functional leg length, seated.

	Female	Male
Mean (cm)	101.20	108.21
Maximum (cm)	118.00	129.10
Minimum (cm)	81.90	88.10

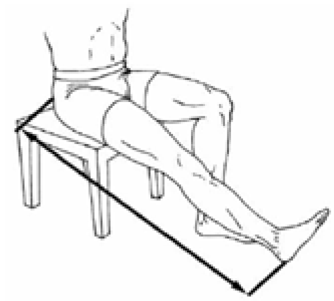

Table 3.4. GWP basic workspace.

Step length (cm)	Step width (cm)	Step height (cm)	Rotation about X	Rotation about Y	Rotation about Z
140	45	40.6	26 _ 36	-40 _ 30	-50 _ 50

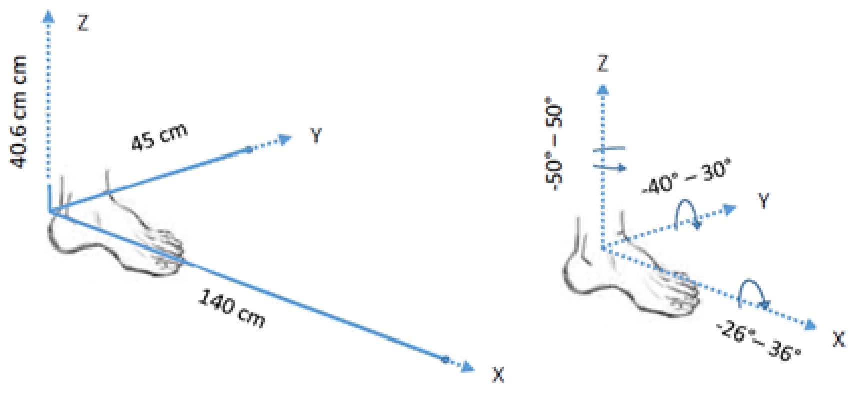

Figure 3-5. Ground walking platform basic workspace.

In this section, the kinematic of only the XYZ mechanism is discussed first as it is central mechanical part of the GWP, while the kinematic of the Stewart platform is discussed in a separate Chapter 5:.

3.4.3. Kinematic of the XYZ mechanism

The robotic mechanism we selected for simulating the translation movements in the three-dimensional Cartesian space consists of three subsystems (pantograph mechanism for translational movements along the *z*-axis, a rail to drive the translation movements along the *x*-axis and another rail to drive the translation movements along the *y*-axis). Each of the mentioned mechanisms are independent and so are their kinematic and dynamic equations.

The kinematic equation that describes Z-mechanism movement is straightforward. While Figure 3-6 illustrates the front view of the pantograph mechanism, the equation of the movement along the *z*-axis can be derived by applying the Pythagorean theorem.

$$l^2 = h^2 + \left(\frac{b}{2}\right)^2$$
$$l^2 = h^2 + \frac{b^2}{4} \qquad (3.1)$$
$$h^2 = l^2 - \frac{b^2}{4}$$

$$h = \sqrt{l^2 - \frac{b^2}{4}} \qquad (3.2)$$

where l is the length of one arm of the pantograph measured from the center of one revolute joint of the fixed base to one revolute joint of the top platform, h is the vertical distance between revolute joints of the fixed base and the revolute joint connecting both arms of the pantograph mechanism, H is the horizontal distance between revolute joints of the fixed base and joints of the top platform and b is the vertical distance separating the centers of the revolute joints of the fixed base.

The movement of the pantograph mechanism is driven using a lead screw and rotational electrical motor. Accordingly, the distance b can written as follows:

$$b = \theta_3 . L_2 \tag{3.3}$$

where θ_3 is the angular position of the motor and L_2 represents the translation distance covered by a unit rotation angle (its unit is m/rad).

Knowing that,

$$H = 2h \tag{3.4}$$

by adding the distance separating the motor shaft and the fixed base d as well as by adding the distance separating the top revolute joint of the platform and the top edge of the top platform to the previous equation d. (Both distances are equal.) The horizontal position of the footplate can be written as

$$Z = H + 2d \tag{3.5}$$

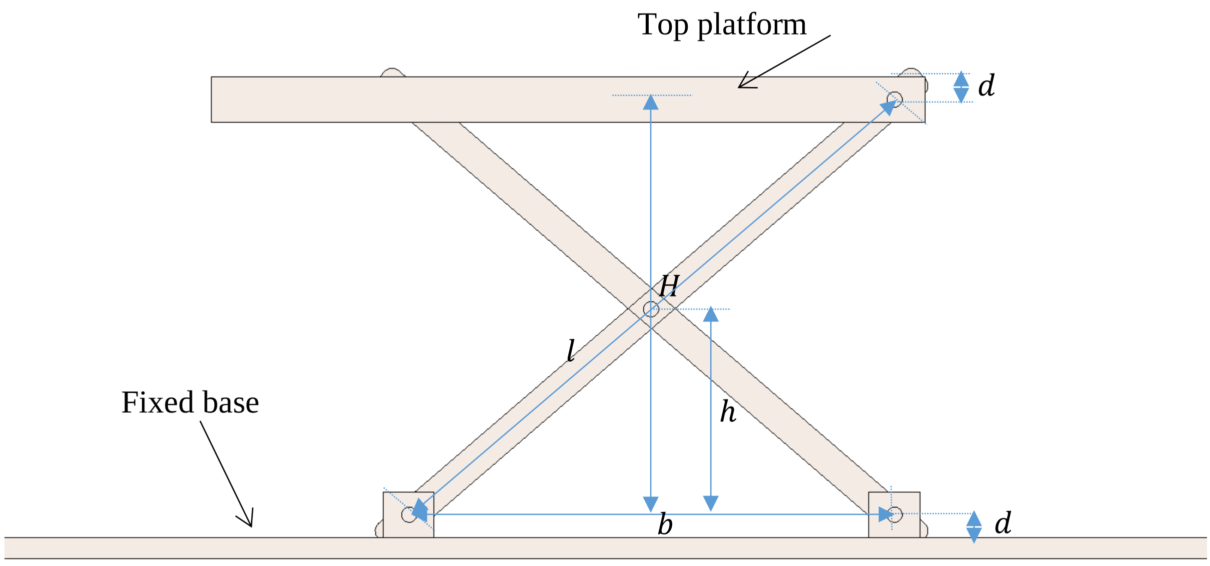

Figure 3-6. Front view of the pantograph mechanism.

The derivative of the previous equation with respect to time gives the velocity of the end-effector along the z-axis as a function of the articular velocity. All the previous parameters are constant with respect to time except θ_3, which gives the following velocity equation:

$$\dot{Z} = \frac{-L_2^2\theta_3^2}{\sqrt{l^2 - \frac{L_2^2\theta_3^2}{4}}}\dot{\theta}_3 \tag{3.6}$$

Let us denote the term multiplied by $\dot{\theta}_3$ in the preview equation as $J[3,3]$. This term refers to the third diagonal element of the Jacobean matrix. We can then write Equation (3.6) as follows:

$$\dot{Z} = J[3,3].\dot{\theta}_3. \tag{3.7}$$

The acceleration $\dot{Z}$ with respect to $\dot{\theta}$ can be obtained in a similar manner by deriving the preview equation with respect to time, which gives

$$\ddot{Z} = \dot{J}[3,3].\dot{\theta_3} + J[3,3].\ddot{\theta_3}. \tag{3.8}$$

The movement of the XYZ mechanism along the *x*-axis is generated using a driving belt. This belt transforms the movement from a driving pulley fixed at one of the extremities of the system to the moving XYZ platform. The kinematic equation connecting the motion of the end-effector in the horizontal axis with respect to the motor shaft displacement of the driving pulley is given as

$$X = k_r.R.\theta_1 \tag{3.9}$$

where X, k_r, R and θ_1, are, respectively, the Cartesian position of the end-effector in the horizontal direction, the pulley radius, the gear reduction ratio and the articular position (angle of rotation) of the shaft of the motor.

The derivative of the previous equation with respect to time gives the velocity of the end-effector $\dot{X}$ as a function of the angular velocity of the motor shaft $\dot{\theta}_1$. This gives

$$\dot{X} = k_r.R.\dot{\theta_1}. \tag{3.10}$$

Let us denote the term multiplied by $\dot{\theta_1}$ in the preview equation as $J[1,1]$. This term refers to the first diagonal element of the Jacobean matrix. The acceleration $\ddot{X}$ with respect to $\ddot{\theta}$ is obtained in a similar way. This gives

$$\ddot{X} = \dot{J}[1,1].\dot{\theta_1} + J[1,1].\ddot{\theta_1}. \tag{3.11}$$

The movement of the XYZ platform along the *y*-axis is driven by a lead screw mechanism. The screw is driven by an electric motor. The kinematic equation describing the left and right motion of the end-effector with respect to the motor shaft displacement can be describe as

$$Y = L_1.\theta_2 \tag{3.12}$$

where θ_2 is the angular position of the motor shaft and L_1 is the translation distance covered by a unit rotation angle.

The derivative of the previous equation with respect to time gives the velocity of the end-effector $\dot{Y}$ as a function of the angular velocity of the motor shaft $\dot{\theta}_2$. This gives

$$\dot{Y} = L_1.\dot{\theta_2}. \tag{3.13}$$

Similarly, the acceleration of the platform along the *y*-axis can be given as

$$\ddot{Y} = \dot{J}[2,2].\dot{\theta_2} + J[2,2].\ddot{\theta_2} \tag{3.14}$$

where $J[2,2]$ refers to the second diagonal element of the Jacobean matrix.

The velocity and the acceleration of the XYZ mechanism in three-dimensional space can be written in a matrix form as follows:

$$\dot{P} = J.\dot{\theta} \qquad \ddot{P} = \dot{J}.\dot{\theta} + J.\ddot{\theta} \tag{3.15}$$

where the elements of $\dot{P}$ and $\ddot{P}$ vectors represent, respectively, the Cartesian velocities and the Cartesian accelerations of the XYZ mechanism, while the elements of θ, $\dot{\theta}$ and $\ddot{\theta}$ vectors represent, respectively, the articular movements of shafts of the motors of the mechanism.

Expressions of the following vectors P (vector describing the Cartesian coordinates of the center of the end-effector), $\dot{P}$, $\ddot{P}$, θ, $\dot{\theta}$, $\ddot{\theta}$ and the expression of the Jacobin matrix J of the XYZ mechanism are given as

$$P = \begin{bmatrix} X \\ Y \\ Z \end{bmatrix}, \dot{P} = \begin{bmatrix} \dot{X} \\ \dot{Y} \\ \dot{Z} \end{bmatrix}, \ddot{P} = \begin{bmatrix} \ddot{X} \\ \ddot{Y} \\ \ddot{Z} \end{bmatrix}, \tag{3.16}$$

$$\theta = \begin{bmatrix} \theta_1 \\ \theta_2 \\ \theta_3 \end{bmatrix}, \dot{\theta} = \begin{bmatrix} \dot{\theta}_1 \\ \dot{\theta}_2 \\ \dot{\theta}_3 \end{bmatrix}, \ddot{\theta} = \begin{bmatrix} \ddot{\theta}_1 \\ \ddot{\theta}_2 \\ \ddot{\theta}_3 \end{bmatrix}, \tag{3.17}$$

$$J = \begin{bmatrix} k_r.R & 0 & 0 \\ 0 & L_1 & 0 \\ 0 & 0 & \frac{-L_2^2\theta_3^2}{\sqrt{l^2 - L_2^2\theta_3^2}} \end{bmatrix}, \dot{J} = \begin{bmatrix} 0 & 0 & 0 \\ 0 & 0 & 0 \\ 0 & 0 & \dot{\left(\frac{-L_2^2\theta_3^2}{\sqrt{l^2 - \frac{L_2^2\theta_3^2}{4}}} \right)} \end{bmatrix}. \tag{3.18}$$

3.5. Conclusion

The 3D-IRS is a project that aims to overcome current robotic rehabilitation drawbacks and aims to improve the rehabilitation experience. The main idea of the project focuses on developing a new robotic system that can support the active participation of the patient during the training by mean of motivating the patient. To realize this, the patient should receive the physical and virtual feedback that make the simulation of gait process realistic. While meeting the visual feedback requirements can be an easy task to achieve using the VR technique, meeting the physical requirement is a challenging task. Proving the user with physical feedback is a problem of an appropriate selection of the mechanical design, the actuation system and the control design of the hardware. This section has shown that the hybrid serial parallel mechanical design offers many advantages over the traditional mechanical designs. This would benefit the system from both the advantages of serial and parallel robots. In addition, to have a flexible dynamic system that can coupe quickly with dynamic changes, we designed a driving system consisting of electric and hydraulic actuators. This combination provides us with a high back-drivability driving system.

Chapter 4: GROUND WALKING PLATFORM CONTROL APPROACH

4.1. Introduction

The GWP robot can be classified as a system with haptic locomotion interfaces (HLIs). An HLI system creates a sense of walking in a virtual environment without damaging the sense of distance and orientation during walking, while a user's true position is maintained in the real word [155]. The HLI can be given a set of different walking tasks to be simulated, including training of dis-mounted operators, the basis of systems for indoor track and field training, [161].

After the GWP's mechanical design is established, the next step aims to achieve a realistic simulation of different type of environments. Apparently, defining the proper control strategy is key to achieve this specific objective. Among numerous sorts of control systems, "impedance control" is the most proper control strategy for simulating a wide range of mediums. In this chapter we invest the GWP system's potential to deliver accurate simulation utilizing an impedance control approach.

The first section provides a state or arts and discusses the different techniques used to analyze the stability and performance of haptic systems. These methods serve as the criteria by which we would assess the GWP's capacity to accurately simulates various types of situations. In the second section, different strategies of controlling contact forces between the user and the system are introduced. In the third section, three studies on the control structure of the GWP are presented. The summary of this chapter is provided in the last section.

4.2. Stability and performance

Stability and performance are two related key features that can effectively be used to describe the behavior of the system. Stability depends on the performance and vice versa. It is the goal of haptic interfaces to first be stable and second be transparent [156].

Stability:

Stability is critical in haptic interfaces, in which this problem arises when there is a dynamic interaction between the user, robot and environment [157]. Stability depends on all three elements that comprise the haptic interfaces: hardware, human operator and the virtual environment. The last two elements are highly unpredictable, and this makes proposing a stable controllable system difficult [158]. Figure 4-1 illustrates the relation between the three elements that comprise a haptic interface. In the literature, there are many suggested ways to stabilize a haptic system; two of them are the most used, which are defining the transfer function of the human operator and controlling the transfer of energies in the haptic system.

- Controlling the transfer of energies: This method consists of studying the transfer of energies between the three basic elements that constitute the haptic interface and applying the law of passivity to guarantee stable operation [159]. Passivity is a fundamental property of many physical systems which may be roughly defined in terms of energy dissipation and transformation. It is an inherent input-output property in the sense that it quantifies and qualifies the energy balance of a system which, stimulated by external inputs, generates an output [160]. A system is stable if the energy following in yields following-out energy at all times. The passivity concept in control was originally used in terms of electric circuits which was then used as a generalized analogy for robotic control. In the electric circuit, the energy of a system is defined by the relation between voltages and currents following in and out. In a mechanical system, the energy is set to the relation between efforts (forces) and flows (velocities) [161]. Hence, a haptic interface can be represented by a network block with two ports. There are two types of passive systems which are passive and active systems. A system is passive when its energy is equal to or greater than zero. This type of system consists of passive elements such as spring, damper and others, and it is stable all the time. A passive system is stable by nature, and this is mainly due to the existence of friction between its elements in which this has the effect of dissipating the initial energy the system receives for moving. Opposite of this, an active system can provide energy in which the energy of its output is greater than its input which may destabilize the system. In a haptic system, the virtual environment and human operator are passive systems while the hardware is active. The presence of an active component in the system can introduce more energy flowing, which may destabilize the system if it is not well controlled. Therefore, to ensure that the system is stable during the walking simulation process with respect to the stability law previously mentioned, a passive controller can be introduced. Figure 4-2 shows two different types of passive controllers that can be introduced to the system.

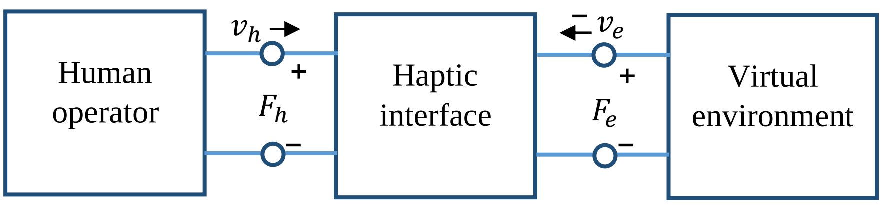

Figure 4-1. Haptic interface [161]

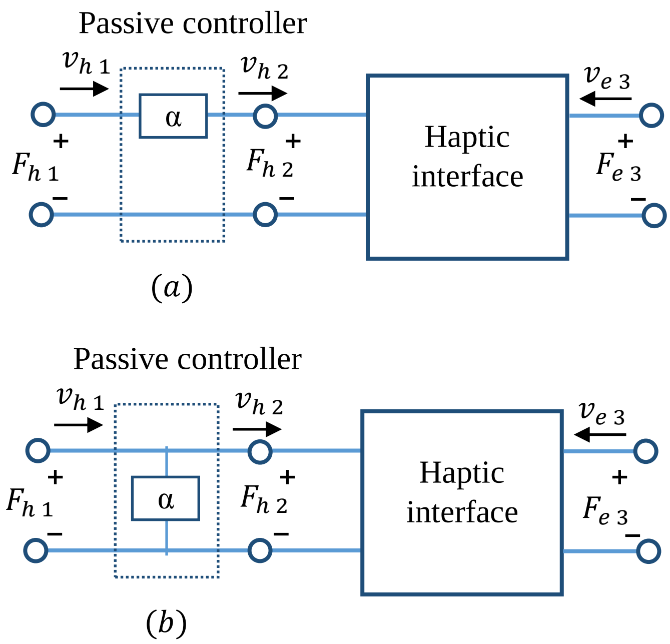

Figure 4-2. Two different types of passive controllers [159].

- Defining the transfer function of the human operator: This method consists of defining the transfer function of the user by creating a model representing the muscles of the human operator. In this way, the effort that the users may apply on the platform as well as the movements that they intend to perform can be predicted. Therefore, the appropriate control elements that guarantee a stable response of the system can be well defined. The stability of the system can be analyzed using different tools, including Root locus, Routh-Hurwitz, Bode plot, Nyquist, Lyapunov and others.

Performance:

The performance of a haptic interface can be described by how well the system renders a virtual environment to the user. Robotics researchers often use the term “transparency” to describe the qualitative measurement of the performance. Different methods are used to defined the transparency of haptic interfaces. The most common of them are Z-width and M-width. Colgate and Brown [162] define “Z-width” as the dynamic range of impedance that can be rendered passively for a desired bandwidth. Nevertheless, in simulations of free foot movements (swing phase) for instance, this can be described by the amount of impedance the system applies on the user’s foot that prevents the user from realizing the desired movement. The formula of transparency Z_T, with respect to this definition, can be written as the ratio between the measured Z_M and the desired impedances Z_D. This relation is given by Equation (4.1) (Figure 4-3 shows the relation between different impedances of haptic interface):

$$Z_T = \frac{Z_M}{Z_D}. \tag{4.1}$$

In relation to forces and velocities, this can be written as

$$Z_T = \frac{F_M V_D}{F_D V_M} \tag{4.2}$$

where V_M is the measured velocity, V_D is the desired velocity, F_M is the measured force and F_D is the desired force.

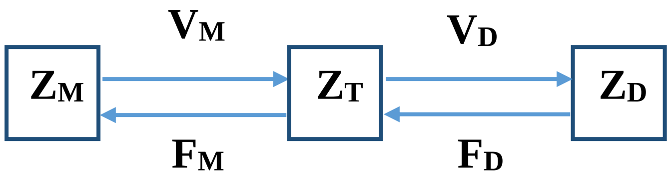

Figure 4-3. Block diagram of haptic interface [156].

The most transparent system is that which has a transparent ratio equal to 1. It is difficult with existing haptic interfaces to achieve this high-transparency precision. The total value of the impedance of the system depends on two main factors: frictions and inertia. Friction can affect the movement of the platform at low frequencies in which the force required to be applied to overcome the static friction is significant. The value of the static friction depends on the amount of the normal force applied by the mass of the moving object. The heavier the object is, the more difficult it is to move it. On the other hand, at high frequencies, the impedance of the system depends on the inertia of the platform in which it would be difficult to change, for instance, the direction of a moving object. Therefore, to obtain good transparency, it is important to use light mechanisms.

Depending on the amount of the impedance generated, haptic interfaces are broadly divided into two classes: light and heavy systems. The first class characterizes systems using light mechanical components. These systems have the advantage of having low friction and low interaction forces. Thus, these systems can show a high transparency. Opposite of this, most relevant gait haptic interfaces that utilize electric motors can be classified in the second class. Usually, these systems use reductions (gear box or lead screw, etc.) to increase the high torque required for moving their complex, heavy mechanical parts. However, this solution has the disadvantage of providing a non-reversible effect on the force applied by the user on the motors in which it is difficult for the user to turn them *[163]*. Most systems of this type of haptic interface exhibit inadequate transparency. The user, as a consequence, can feel a resistance load at the bottom of their foot.

Dealing with the appearing inertia is among the most important problems these systems try to solve. Removing the reduction gear from the driving system could be a critical solution since the actuators will probably not be able to provide the necessary force to simulate different virtual environments to the user. Our approach consists of using a hybrid mechanism that uses a light Stewart platform to support fast movements and a rail mechanism with an electric motor to satisfy the movement requirement when we need to provide a wide range of motion. Dynamic control of the Stewart platform is investigated in the next chapter. The impedance appearing in the system does not only depend on its inherited dynamic parameters, but also on other factors related to the integrated parameters such as the precision of sensors used and frequency of communication between different elements of the system. Tackling these problems is a control problem. In the next section, we discuss in detail the most common control strategies used to deal with dynamic interactions between a human and robot.

4.3. Interaction control

Interaction control provides a fundamental approach to control the dynamic interaction between the robot and the environment or between the robot and the human [157]. Interaction control strategies can be broadly classified into those performing indirect force control and those performing direct force control [164]. The main difference between the two strategies is that the first one controls the interaction forces without an explicit force feedback. Instead, it modifies the force signal measured either directly or after transforming to a position or velocity signals, while the second one achieves force control by a close feedback force loop to the input. The two categories also differ in the sense of the objectives in which the main goal of indirect force control is not to ensure that the output force follows the reference input, but to introduce a reference target model specifying the interaction between the robot and environment [157]. Nevertheless, indirect force control imposes a specific dynamic behavior on the interaction between the user or the environment and the robot end-effector. The second type of control is suitable for haptic interface applications especially when the task involves simulating various types of virtual environments. The most common type of interact force control used in haptic interfaces is "the impedance control." With impedance control, the desired performance can be specified through a generalized dynamic impedance that is represented by a mass-spring-damper mechanical system. Figure 4-4 shows an example of a model of impedance control, which is expressed by a second-order mass-damper system defined by Equation (4.3):

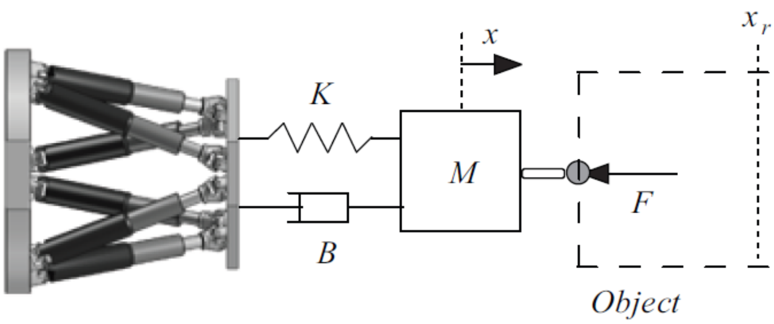

Figure 4-4. Virtual second-order mass-damper-spring system between a robot and object [165].

$$M(\ddot{x} - \ddot{x}_r) + B(\dot{x} - \dot{x}_r) + K(x - x_r) = F \quad (4.3)$$

where M is the virtual mass, B is the virtual damping coefficient, K is the virtual spring constant, F is the force applied to the system, x is the real position and x_r is the desired position of the virtual mass. In the s-domain, the desired impedance of the system can be expressed as

$$Z(s) = Ms^2 + Bs + K. \quad (4.4)$$

Two main types of impedance control are used for providing task-specific impedance via feedback control, namely "force (torque) mode control" and "position (velocity) mode control." It is important to notice that in the field of haptic devices, various given names could be found referring to these two types of impedance control. The most common of them are impedance control with force feedback or simply "impedance-controlled class" (for the first type) and admittance control with position feedback or simply "admittance-controlled class" (for the second type) [166–168]. The main differences between the two classes are the following:

The impedance-controlled class is as follows.

- It accepts displacement or velocity as input and responds with force or torque output.
- The controller is an impedance while the robot is an admittance.
- It is more suitable for the tasks that involve simulating high compliant environments. This allows stable dynamic interaction with a stiff environment; however, there is poor position accuracy in free space which subjects the system to instabilities when the user releases their foot.

The admittance-controlled class is as follows.

- It accepts a measured force or torque as input and responds with a displacement or velocity to the output.
- The controller is an admittance while the robot is an impedance [169].
- It simulates unyielding environments. Thus, the system is stable with non-contact tasks and unstable during dynamic interaction with stiff environments or when the stiffness of the user's legs increases [170].

In addition to these basic differences, impedance-controlled class is mainly implemented by robotic systems that involve a high causality between joint and end-effector, the characteristic that describes robots driven by direct actuators. Opposite of this, systems with significant inertia show a poor causality due the increase of non-linear friction because of the use of high gear ratios [157]. Another control strategy that consists of a hybrid impedance/admittance control can be used to render various types of virtual environments such as suggested in Christian [169]. Using the same robot, the impedance control can be implemented when the user's foot is in the swing phase in contact with solid ground while the admittance control is used when the foot is in the free space in contact with the air.

Our objective is to the define the most sufficient control strategy that meets our requirements and which guaranties the user gets the real sense of walking in different types of environments. Therefore, it is important to test the mentioned haptic control strategies using the GWP system and to determine the strategy that fits well with our application. First, we study the GWP system with respect to a simplified control strategy that consists of considering the system that has no inertia. The aim is to test the ability of the system to behave in the indented way. Second, with the presence of a hardware model of the system supported with dynamic actuators and linkages, we study the performance of the system under the impedance and admittance control classes.

The objective is to define the appropriate control strategy for our application when the dynamic effects of the hardware are included.

4.4. Ground walking platform control structure

Since the GWP aims to provide the subject with a reaction force based on their foot's position in a virtual environment, the position of the robot is ruled by the contact forces (between the foot and the platform) and the relative position of the foot in the VR environment. This section aims to, first, define the kinematics and dynamic elements acting on the GWP system and, second, to present the control model that matches these requirements.

The equation that describes the motion of the GWP robot is

$$B(q)\ddot{q} + C(q,\dot{q})\dot{q} + F_m\dot{q} + g(q) = u - J^T(q)H \quad (4.5)$$

where q is a vector of the robot's joint positions, $B(q)$ represents the inertia matrix, $C(q,\dot{q})$ describes the centrifugal and Coriolis coupling reaction forces between the joints of the robot, F_m describes the friction coefficients of the manipulator, $g(q)$ is the gravity torque, u is the vector torque applied by the robot, J is the Jacobian matrix and H is the contact force exerted by the manipulator's end-effector on the user's foot and vice versa.

As previously mentioned, there are two types of impedance controls, namely the impedance control with force feedback and admittance control with position feedback. The admittance control with position feedback is based on sensing the interaction force at the contact point between the robot and the user's foot and transforming it into a desired impedance position x_{A_foot} according to the desired virtual admittance ${Z_A}^{-1}$. The relation between the desired impedance position and interaction force H is given by Equation (4.6). The aim of this type of control is to lead the position error vector $\tilde{x}$ between foot position x_{foot} and x_{A_foot} given by Equation (4.7) to 0:

$$x_{A\_foot} = {Z_A}^{-1}H, \quad (4.6)$$

$$\tilde{x} = x_{foot} - x_{A\_foot}. \quad (4.7)$$

The impedance control with force feedback is based on reading the actual position of the foot. It provides a desired force F_A (Equation (4.8)) according to the desired virtual impedance Z_A. The objective of this control is to lead the force error vector $\tilde{F}$ (Equation (4.9)) between the foot force applied on the end-effector (interaction force) and the force vector of the desired impedance F_A to 0:

$$F_A = Z_A x_{A\_foot} \quad (4.8)$$

$$F_A = K_P x_{A.p\_foot} + K_D \dot{x}_{A.D\_foot}$$

where K_P and K_D are, respectively, the stiffness and damping matrices of the virtual environment and $x_{A.p\_foot}$ and $\dot{x}_{A.D\_foot}$ are vectors of which the elements respectively represent position/rotation and translation/rotation velocities, verifying the desired stiffness and damping values of the virtual environment.

$$\tilde{F} = H - F_A. \tag{4.9}$$

The block diagram of the admittance control with position feedback and impedance control with force feedback are respectively illustrated in Figure 4-13 and Figure 4-14. It is important to notice that this admittance or impedance control does not mean leading the admittance or impedance to 0, but it means imposing a certain value which is the admittance or the impedance of the simulated medium.

It is essential to notice that the admittance control with position feedback strategy could be achieved using two different models: one with one feedback [167] and one with two feedbacks [168]. The model control with two feedback loops uses measurements from a position and force sensors. The outer control loop is named a Cartesian loop, and it is used for controlling impedance. The inner control loop is called joint servo loop, and it has the objective of controlling joint position (it ensures tracking of the reference position from the impedance and admittance control) [157, 168, 171]. The admittance control with one feedback includes only the Cartesian loop that controls the impedance. The error regulated in the feedback loop is a force/torque signal that is fed directed to a joint actuator.

Both the impedance and admittance control models are divided into four different parts that are associated with different functions. The hardware unit represents the dynamic properties of the GWP robot. In fact, in such a system, the output of the manipulator may be seen having two sides: position and/or force. In the impedance control with force feedback (Figure 4-14), the force sensor provides the admittance unit by the contact force between the user's foot and the manipulator end-effector. Thus, this unit generates the position x_{A_foot} which is supposed to verify the desired admittance. In the admittance with position feedback, the position sensor provides the impedance unit by the position of the foot. Thus, this unit computes the force F_A associated with the desired impedance.

For the first type of control, the GWP control unit is provided by the difference between the user's foot position x_{foot} and the x_{A_foot}, while for the second one, it is provided by the difference between F_A and F. For both controls, the aim is to keep the difference close to 0.

The procedure for obtaining the inverse kinematic block shown in Figure 1-2 is described in the passage. To assist clarify how the inverse kinematic model is obtained, the distribution of the essential frames in the GWP is shown in Figure 4-5.

The inverse kinematic blocks compute the joint parameters given the GWP's end effector position as input. The joint parameters of GWP are calculated based on the joint positions of the XYZ mechanism and Stewart platform. Equations describing the inverse kinematic model of the XYZ mechanism are derived from equations ((3.5), (3.9)and, (3.12)), which give:

$$\theta_1 = \frac{X_B}{k_r.R} \tag{4.10}$$

$$\theta_2 = \frac{Y_B}{L_1} \tag{4.11}$$

$$\theta_3 = \sqrt{\frac{4}{L_2^2}\left[l^2 - \left(\frac{Z_B}{2} - 2\right)^2\right]} \tag{4.12}$$

Where, X_B, Y_B, and Z_B are the coordinates of the center point of the upper platform of the XYZ mechanism defined with respect to the {A} frame.

The inverse kinematics of the Stewart Platform is the calculation of the leg length of the platform given the required position of the platform. The inverse kinematic model of the Stewart platform is given by equation (5.4). details of obtaining this equation are given in section 5.5

$$L_i = H + R.P_i - B_i \tag{4.13}$$

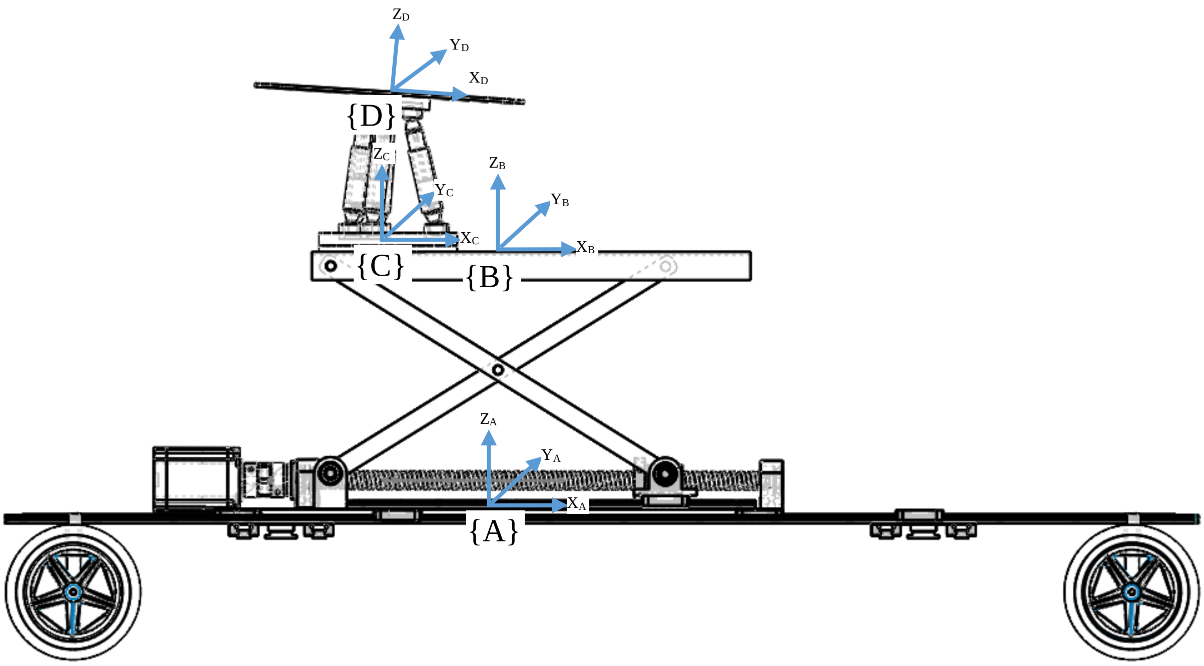

Figure 4-5. Main references for coordinates of GWP

It is important to notice that in equations (3.5), (3.9), (3.12) and, (4.13), the inverse kinematic models of the XYZ mechanism and the Stewart platform are described in relation to their respective end-effector frames. This implies that the XYZ mechanism's end-effector position is at the origin of frame {B}, and its coordinates are written with respect to frame {A}, while the end-effector position of the Stewart platform is at the origin of frame {D}, and it is described with reference to frame {C}.

It is now necessary to define the inverse kinematics of the entire GWP system using the relative inverse kinematic models that extracted from the XYZ mechanism and the Stewart Platform.

Assume that the poses (position and rotation) of the end-effector of the GWP with respect to the global reference of the GWP are located at the {A} frame, and are written as follows: (H, and R) where the H is the position of the end effector sitting exactly at the origine of the reference {D}, while R is the rotation matrix that describes the orientation of the end-effector.

In fact, simply knowing the poses of the end-effectors is insufficient to define the inverse kinematic model of the GWP system. This is due to the fact that the Stewart Platform and XYZ mechanism can be set up in several ways to produce the same end-effector poses.

To help solve the inverse kinematic problem, we propose that the position of the GWP's end-effector should remain at a constant distance from the Stewart platform. Thus, the constant term $H_{const} = [H_x, H_y, H_z]$ can be used to define the term in equation (5.4) that denotes the Cartesian coordinates of the end-effector frame with respect to the Stewart platform base frame {C}.

Once the end-effector position of GWP has been used to define the inverse kinematic of the Stewart platform, all that is left to do is dedicate the joint positions of the XYZ mechanisms. These can first be determined by determining the position of the base frame of XYZ mechanism {A}, which is also the global frame of GWP, in relation to the center upper platform of XYZ mechanism B. The homogeneous transform, which enables specifying the positions of the end effectors in relation to the global frame and is given by the flowing equation, can be used to determine this position.

Once, the inverse kinematic of Stewart platform is defined given the end-effector position of GWP, it remains just to dedicate the joints positions of the XYZ mechanisms. These can be obtained first by defining the position of the center upper platform of XYZ mechanism {B} with respect to the base frame of XYZ mechanism {A}, and which is also the global frame of GWP. This position can be obtained from the homogeneous transform, which allows describing the end effector's positions with respect to the global frame and is given by the flowing equation:

$$T_{AD} = T_{AB} T_{BC} T_{CD} \tag{4.14}$$

The frame {C} is a fixed distance away from the frame {B}. Thus, we can describe the homogenous transform matrix T_{BC} as follows:

$$T_{BC} = \begin{bmatrix} 1 & 0 & 0 & b_x \\ 0 & 1 & 0 & b_y \\ 0 & 0 & 1 & b_z \\ 0 & 0 & 0 & 1 \end{bmatrix}$$

$$T_{CD} = \begin{bmatrix} \cos\alpha\sin\beta & \sin\alpha\sin\beta\cos\gamma - \cos\alpha\sin\gamma & \cos\alpha\sin\beta\cos\gamma + \sin\alpha\sin\gamma & H_x \\ \cos\beta\sin\gamma & \sin\alpha\sin\beta\sin\gamma + \cos\alpha\cos\gamma & \cos\alpha\sin\beta\sin\gamma - \sin\alpha\cos\gamma & H_y \\ -\sin\beta & \sin\alpha\cos\beta & \cos\alpha\cos\beta & H_z \\ 0 & 0 & 0 & 1 \end{bmatrix}$$

$$T_{AD} = \begin{bmatrix} \cos\alpha\sin\beta & \sin\alpha\sin\beta\cos\gamma - \cos\alpha\sin\gamma & \cos\alpha\sin\beta\cos\gamma + \sin\alpha\sin\gamma & X \\ \cos\beta\sin\gamma & \sin\alpha\sin\beta\sin\gamma + \cos\alpha\cos\gamma & \cos\alpha\sin\beta\sin\gamma - \sin\alpha\cos\gamma & Y \\ -\sin\beta & \sin\alpha\cos\beta & \cos\alpha\cos\beta & Z \\ 0 & 0 & 0 & 1 \end{bmatrix}$$

$$T_{AB} = \begin{bmatrix} \cos\alpha\sin\beta & \sin\alpha\sin\beta\cos\gamma - \cos\alpha\sin\gamma & \cos\alpha\sin\beta\cos\gamma + \sin\alpha\sin\gamma & X_B \\ \cos\beta\sin\gamma & \sin\alpha\sin\beta\sin\gamma + \cos\alpha\cos\gamma & \cos\alpha\sin\beta\sin\gamma - \sin\alpha\cos\gamma & Y_B \\ -\sin\beta & \sin\alpha\cos\beta & \cos\alpha\cos\beta & Z_B \\ 0 & 0 & 0 & 1 \end{bmatrix}$$

Where α, β, and γ are the Euler angles about axes x, y, z.

From the equation above, we can extract the T_{AB} as follow:

$$T_{AB} = T_{AD}T_{CD}^{-1}T_{BC}^{-1} \tag{4.15}$$

Thus, we can write the equations describing the inverse kinematic model of the GWP as follows:

$$L_i = H_{const} + R.P_i - B_i \tag{4.16}$$

$$\theta_1 = \frac{T_{AB}[1,4]}{k_r.R} \tag{4.17}$$

$$\theta_2 = \frac{T_{AB}[2,4]}{L_1} \tag{4.18}$$

$$\theta_3 = \sqrt{\frac{4}{L_2^2}\left[l^2 - \left(\frac{T_{AB}[3,4]}{2} - 2\right)^2\right]} \tag{4.19}$$

It is noteworthy that determining the forward kinematics of the GWP is a challenging problem. We find that employing position sensors makes it easier to obtain the end-effector positions.

4.5. GWP control studies

- **Method**

To examine the GWP system's capacity to simulate various types of environments under an impedance control strategy, we performed three studies. In the first study we investigated the system's behavior under perfect circumstances. we assumed that there are no frictions or inertia in the system. This is to help us better grasp the concept of the impedance control we want to implement. In the second study, the system is studied under the same assumption while tested using real data as input. The test's data inputs are the foot positions of an actual subject. In the third study we investigate the system's stability and performance while accounting for friction and inertia effects.

- **Assumptions and simplifications**

The GWP system is made up of two mechanisms: the XYZ mechanism and the Stewart Platform mechanism. In studies 1 and 2, and for purpose of simplicity, the GWP system is studied using a simplified model (one DOF) that assumes there are no frictions and inertia forces. On the other hand, because the two primary mechanisms of the GWP system have distinct mechanical properties (the Stewart platform has light components while the X,Y,Z mechanism has heavy components), the mechanisms are independently examined when accounting for friction and inertia forces.

Since the XYX mechanism is the core component of the system, we first conducted a control study on it. The study's findings outlined the XYZ mechanism's shortcomings. In particular, the XYZ mechanism's primary shortcomings were the residual inertial and frictional forces. The issue of the apparent residual friction and inertia forces is what we want to address next. Therefore, we suggest the Stewart Platform (SP), which we think is the best way to solve the issue. We conducted control research on SP and sought to identify the best SP type.

To simplify the study of the two mechanisms, we concentrated on our study to investigate stimulating the following medium and taking the flowing DOF into account:

- The medium to be simulated: among the different types of environments, free air or a simulation of the swing phase of walking is the most challenging environmental situation that is difficult to simulate. The difficulty in simulating the swing phase is in overcoming and canceling the system's friction and inertia forces so that the user experiences no resistance. Therefore, we prioritized and restricted our objectives to simulating the swinging phase of walking.
- DOF to be investigated: we concentrated our efforts on studying the most crucial DOF in the swing phase. The foot's most crucial and challenging DOF during the swing phase is along the X axis. This is so because the majority of movements take place along this axis, which also includes a large range of frequencies of movement. As a result, we focused just on this axe's movement in our research.

4.5.1. Study1

In order to facilitate the study of the GWP system, we suggested in this step studying the system relative to some approximations in order to understand or expect the system behavior without getting deeply in some system complexities. The simplification consists of the use of ideal hardware that ensures that the output position follows well the input command, in addition to the use of approximated date as input (No real or virtual human foot position will be provided (no type of sensor will be used and no virtual reality data will be provided).

4.5.1.1. Simplified simulink model

In order to facilitate the study of the GWP system as well as to get a view of the required, the simplified Simulink model represented in Figure 4-15 was proposed. The model controls the motion on 1DOF only. The robot was supposed to be ideal which means that the output follows well the input. (The Simulink subsystem for simulating an ideal robot is depicted in the figure below)

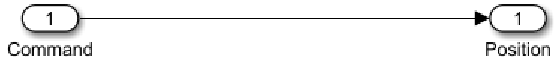

Figure 4-6. Robot's Simulink block.

A) Force sensor

In order to get force value necessary for the simulation, a Simulink block was introduced to provide us with the intended data using force sensor simulator. The sensor consists of implanting the Hooke's law (equation (4.20)).

$$K_S\left(x_{foot} - x_{robot}\right) \tag{4.20}$$

With K_S is the stiffness of the force sensor. In our case we consider manipulating a rigid sensor, hence we give a very high value K_S .

The following figure defines the Simulink sub-system for the force sensor.

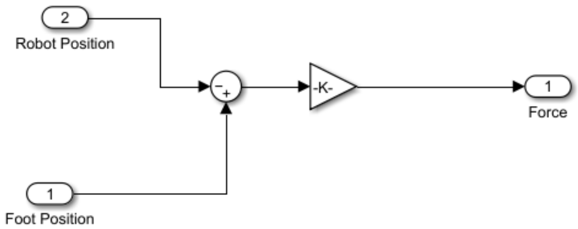

Figure 4-7. Force sensor's Simulink block.

B) Motion command and generator impedance block

To simulate a foot motion in Simulink, foot position data must be provided. Using an ideal signal block generator for simulating the user's foot position is practically incorrect, since the foot position is influenced by the contact forces value. To solve this problem, we implemented a system for generation of foot position with regard of the amount of the contact forces. The system generates the position by fitting "movement command" and "generator impedance". The command generator is equivalent to an ideal position generator followed by a spring. The "generator impedance" bloc's content is shown in the figure below.

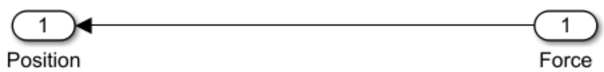

Figure 4-8. generator impedance's Simulink block

C) Virtual admittance

The admittance control with position feedback is based on sensing the interaction force at the contact point between the robot and the user's foot and transforming it into a desired impedance position x_{A_foot} according to the desired virtual admittance ${Z_A}^{-1}$. The relation between the desired impedance position and interaction force H is given by Equation (4.6). The Simulink block we used to simulate the virtual admission is depicted in the figure below.

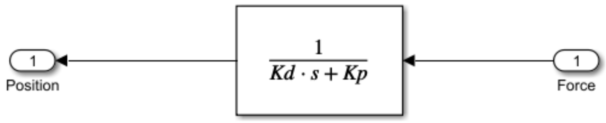

Figure 4-9. Virtual admittance's Simulink block.

4.5.1.2. Test of the model

In order to test the Simulink model of the admittance/impedance control for the GWP, a step signal of amplitude 1 was applied to the "motion command" block to simulate the ground and air, while for the liquid a sinusoidal signal with an amplitude of 1 and a frequency of 1 Hz was applied. Three kinds of environments (ground, air and liquid) have been simulated by setting different values of stiffness and damping. Table 4.1 presents stiffness and damping values sets for different environments. The selection of different selected values was based on our estimation to three states of matter in which we usually interact with. We know that the air has a very high admittance, ground has very low admittance, while the liquid shows an intermediate admittance relative to the velocity. We notice that these values represent theses three states (very high, very low, and intermediate).

Table 4.1. Stiffness and damping values of different environments.

Environment	K_P (N/m)	K_D (N.s/m)
Ground	1e6	1e-2
Air	1e-2	1e-2
Liquid	1e-1	1e+2

4.5.1.1. Results

The foot position and force data obtained from the simulation of different environments are illustrated in Figure 4-10, Figure 4-11, and Figure 4-12. The simulation of the ground shows a record of high force position ratio (impedance). On the contrary, the air simulation exhibits lower force position ratio. That means that ground exerts reaction forces to prevent your foot to dive in, while the air allows free foot motion with weak resistance. For the liquid simulation, there are both significant amplitude values of force and position. However, there is a phase-shift of π/2 rad between them. In the same way, this can be illustrated by the fact that the liquid force is proportional to the velocity rather than position.

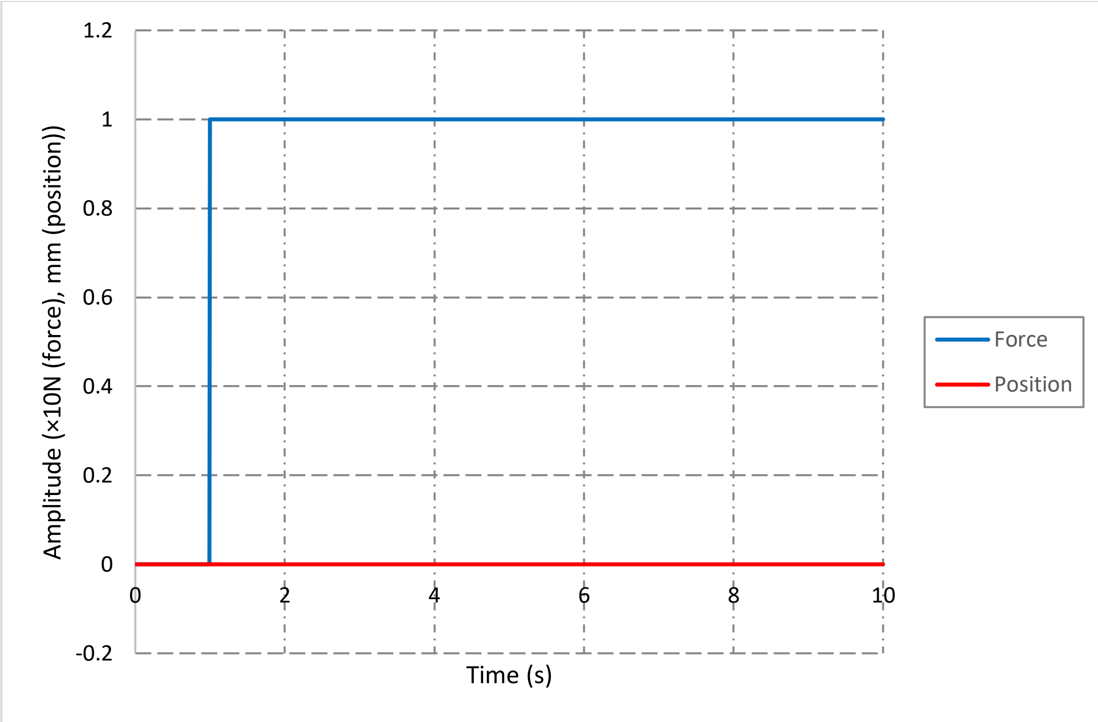

Figure 4-10. Ground

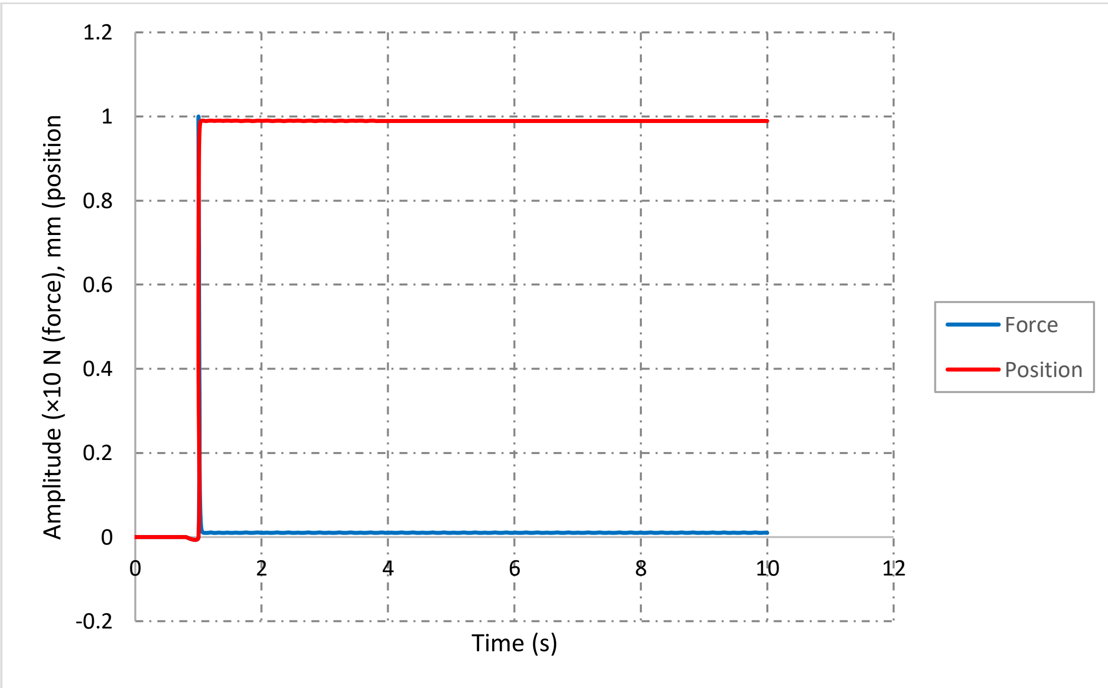

Figure 4-11. Air

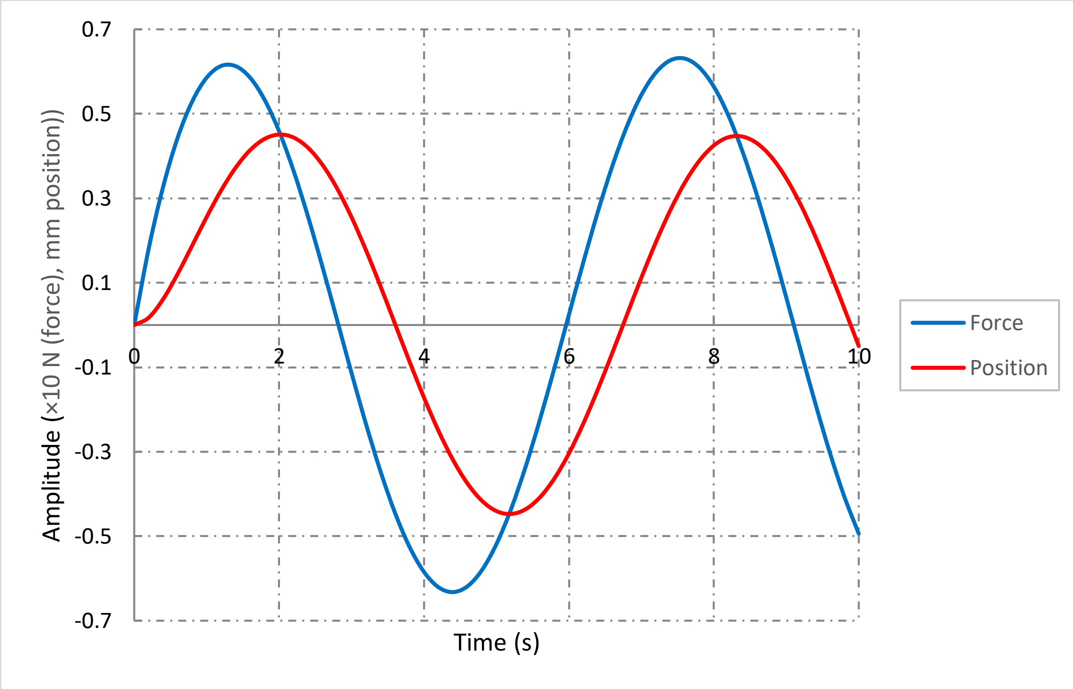

Figure 4-12. Liquid.

4.5.2. Study2

This study aims to test the control model we already defined to simulate the behavior and the interaction of the user, GWP, and virtual reality environment using real data as input. This consists of implementing a 3D virtual environment with an avatar using Unity 3D, and providing the system with data about real foot position using Kinect. The reset of the simulation can be realized using a Unity 3D Simplified Control model.

4.5.2.1. Unity 3D Simplified Control model

We have limited our study to one dimension, Z, which is the most important when interacting with the ground. It is important to note, that this does not mean that the subject is stepping instead of walking. However, this signifies that the study consists of tracking the Z position of the subject's foot while walking and simulating the reaction force resulting from the walking on different types of mediums on Z direction only. The simulated GWP is composed of 3 main modules: The user, the robot, and the virtual reality environment.

- Robot: it is mainly the mechanical part that interacts physically with user, and it needs 3 inputs: foot position, force between the foot and the robot's manipulator, and the coefficients of the ground which are retrieved from the virtual reality. In this study, we simulate the force sensor as a very stiff spring where the displacement is very low.

User: in order to apply realistic data to our model, we used Kinect to record position data of the human foot during walking and applied them to animate the avatar in real time. Since the force was the result of the interaction of the foot with the virtual medium, it was rather

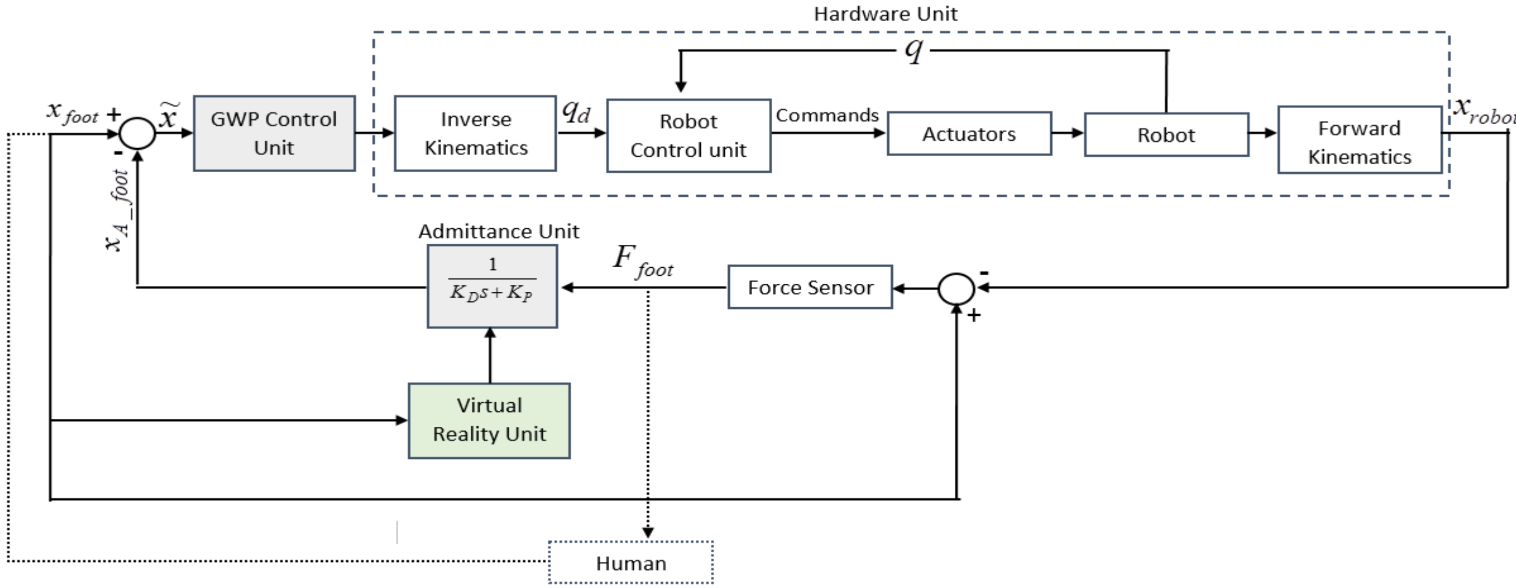

Figure 4-13. Admittance control with position feedback

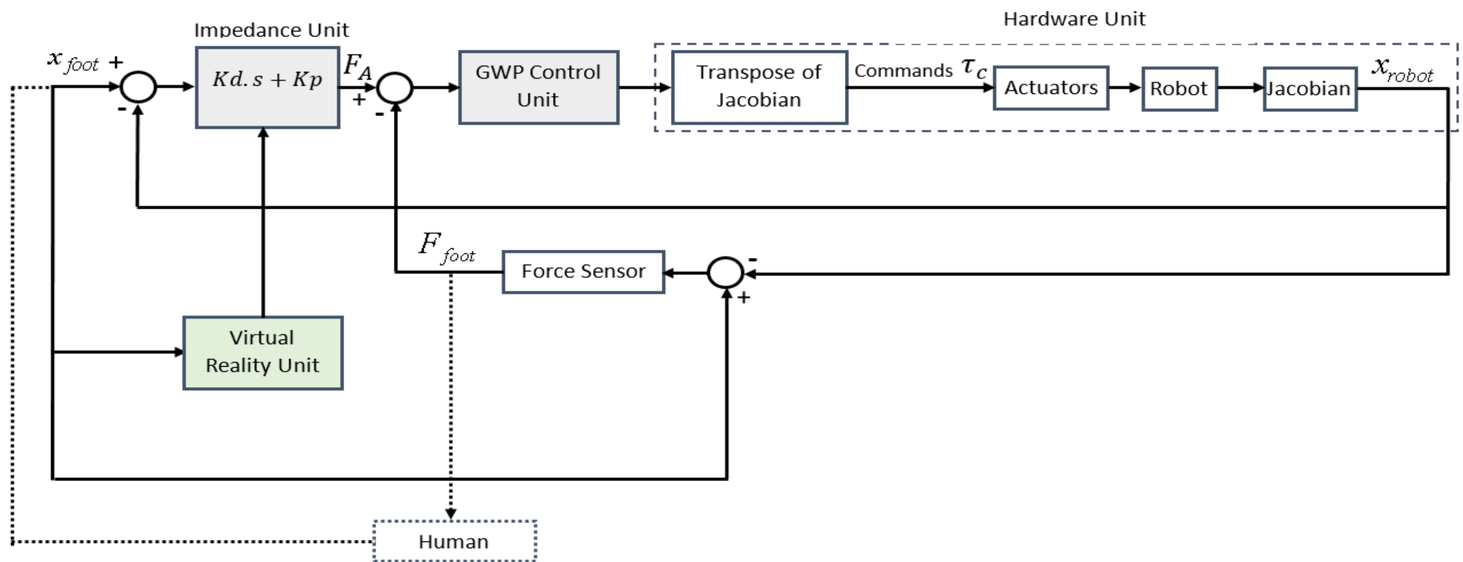

Figure 4-14. Impedance control with force feedback.

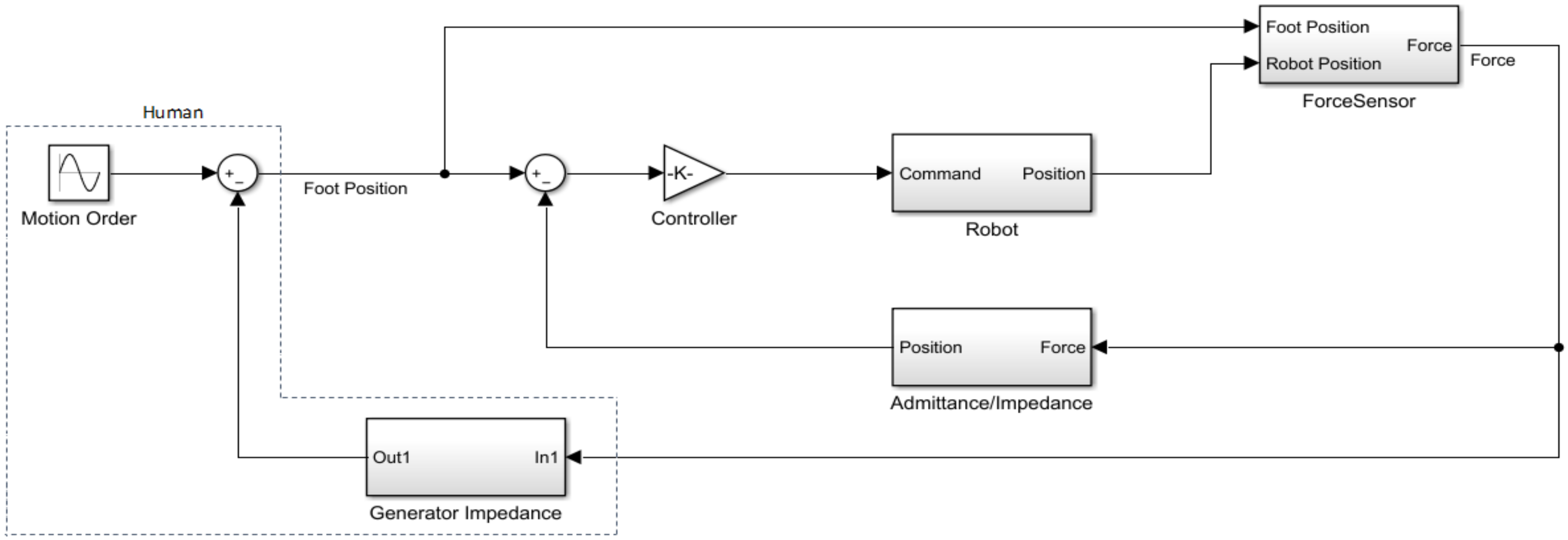

Figure 4-15. Simplified Simulink model of GWP

- an output not an input. Since we have not used the robotic hardware yet, and thus we could not apply the forces that interact with the foot, the forces were inferred using a model that takes into account the limitation of foot motions when exposed to high impedances [19]
- Virtual reality: we have used the recorded data from the human foot to animate an avatar representing the user in virtual environment. According to the position of the avatar, the software for the virtual environment generates the medium's parameters to be used by the robot.

In Figure 4-16 a detailed description of the simplified “impedance/ admittance" control diagram implemented in Unity3D [20] is given.

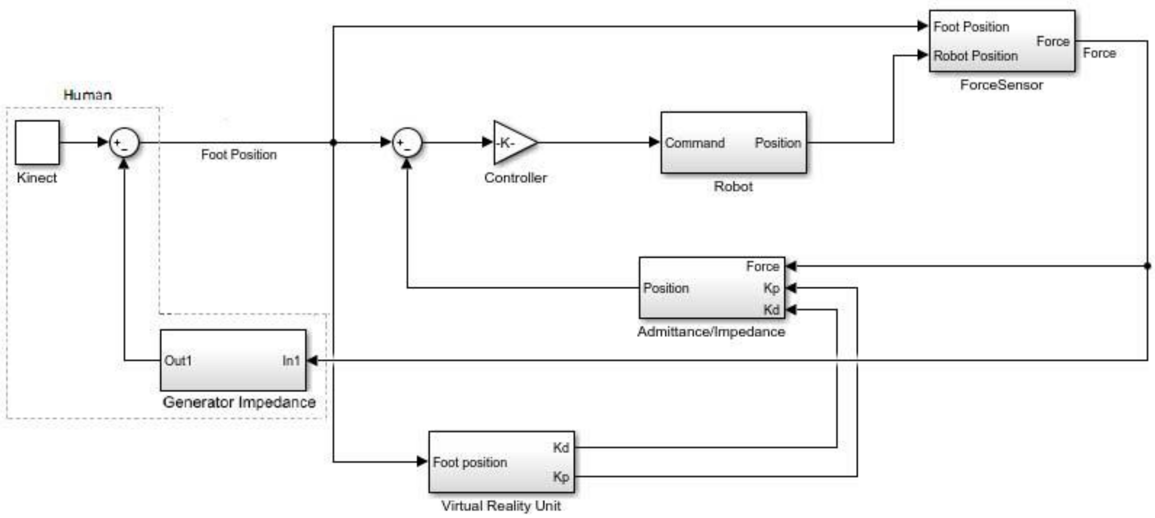

Figure 4-16. Unity3D control diagram described using Simulink blocks.

4.5.2.2. Unity3D Virtual reality interface

The virtual reality internal scene created for testing the “impedance/ admittance" control approach consists of two main Unity3D game components (objects) (Figure 4-17): avatar and terrain. Based on the interactions between these two objects, set values of stiffness and damping coefficients are dynamically generated and sent the “impedance/ admittance" control block. Thus, the kinematic and kinetic of parameters of the GWP robot are then calculated. Bellow a characteristic description is given to the object consisting of the VR scene:

- Avatar: the avatar was the embodied model of the human in VR. It allowed us to visualize and follow the real movements of the walker in the virtual environment. The outer shape of the avatar has a form of a cartoon character. Its internal configuration consists of a “bony” structure that is similar to the basic parts of a human skeleton. Based on the linking joints between each bone, the movements of the avatar segments can be generated and controlled. This can be done either by giving or reading the position and rotation values of the joint transform property in Unity3D. Detailed description of the joints supported by the avatar game object is shown in Figure 4-18. In the previously mentioned real time simulation of walking using Kinect, the kinematic data of each of the walker's joint was detected and analyzed and transferred to each relative avatar joint. Hence, the avatar mirrored the human walking.

- Terrain: the terrain is the VR part that defined the shape, appearance and physical properties of the simulated ground. The virtual environment (Terrain) chosen for the simulation consisted of a landscape that was selected to provide an attractive scenery for the user. The environment was constructed with 2 different type of elements. The first type consisted of components that were made with animated texture images only (e.g. Grass, stones, etc..) and that had no effect on the calculations of the parameters resulting from the interaction between the avatar and the virtual ground. It was introduced, just to provide visual effects. The second type, was the type where the elements are defined with some specific physical quantities (mesh definition, stiffness etc.)(e.g. sole, water, etc.). This type of elements was the target of the control simulation. The interaction between the avatar and the elements consisting this type can be measured and sent to the GWP control unit.

Figure 4-17. Unity3D Virtual Reality Scene.

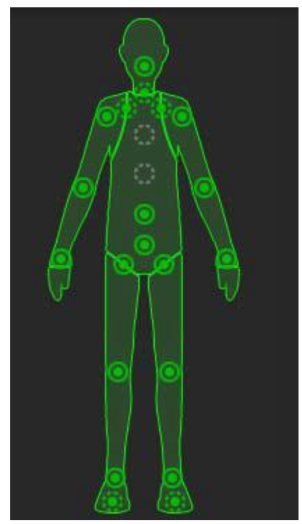

Figure 4-18. Configuration of the joints supported by the avatar.

4.5.2.3. Basic calculation of interaction between "terrain" and "avatar'

The basic process of calculating the interaction between "impedance/ admittance" was achieved using raycasting [21] method. The process consists of shooting an invisible ray, from an origin point (just beneath the foot of the avatar), in a specified direction (vertical), of length (a distance of 0) to detect whether) colliders (e.g. sole, water, etc..) lay in the path of the ray. In this way, VR unite (Unity3D provides the control unit with dynamic information about the environment where the current position of the foot of the avatar is in. Hence, the relevant values of the stiffness and damping coefficients are set based on this information.

4.5.2.4. Test Model

The scene we have designed in virtual reality contains different mediums: air which has a very low impedance, ground with a very high impedance, and liquid where the impedance is relative to speed. The parameters of the three different mediums are listed in table-I. The selection of different selected values was based on a physical estimation of the three states of matter in which we usually interact with.

Input data: As previously mentioned, Input data are recorded using Microsoft Kinect. The Figure 4-19 shows the gait cycle, where the foot (or foot platform of the robot) follows a swing phase, moving in the air, then stops for a while when touching the ground (stand phase) and so on. Data recorded by the Kinect represent the position of the real foot (the subject foot) where the ground is the reference. The virtual foot is the foot of the avatar in virtual reality that tries to follow the real foot. However when it interacts with the virtual ground, it cannot continue, and that is what makes our model generate the proportional force which is proportional to the difference between the real and the virtual foot. The virtual reality module has well detected the interactions between the foot of the avatar and the ground and the water. Subsequently, the simulated robot could update the medium parameters to induce the sensation of the VR environment on a patient's foot.

Figure 4-19 shows the characteristics of each medium. In the air, the robot (real foot) follows the foot position. The force diagram shows very low values, which means a very low impedance. While simulating ground walking, the robot shows a reaction force proportional to the foot position relative to the ground. In the water, the force is rather proportional to the speed, which is the derivative of the position.

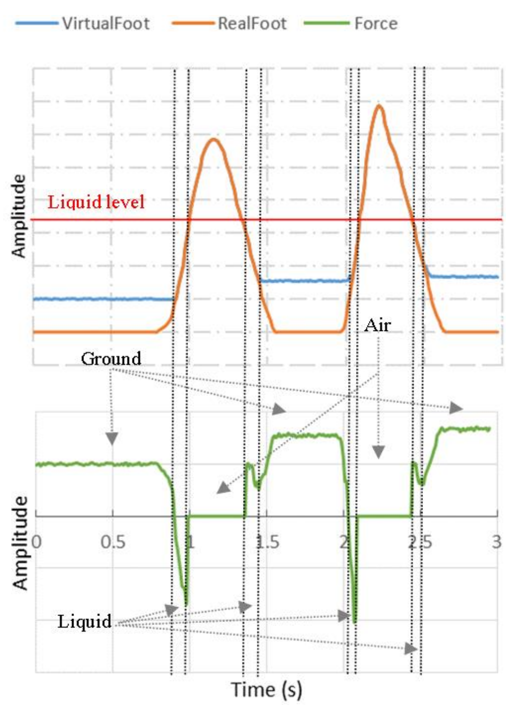

Figure 4-19. Foot positions (Human and Avatar) and force data obtained from the simulation of different environments

4.5.3. Study 3

The previous experiments we performed showed that the system behaved in the desired way as long as we considered the robot is an ideal position block that just assigns the value of the input position to the output position without making any errors. However, this would not be the case with a real hardware where the dynamic parameters related to high values of inertia and friction forces are considered. It is the role of the actuators, then, to compensate for the values of these parameters by providing relevant forces that guarantee simulating different environments to the user. However, it is still expected that with the XYZ mechanism (consisting of heavy parts), the dynamic impedance of the system will not be completely compensated. Therefore, the objective of this study is to define the stability and performance bandwidth of the XYZ mechanism. The limitations defined can then be compensated by a light Stewart platform which is discussed in the next chapter.

4.5.3.1. System simplification

To describe the performance of the XYZ mechanism under the impedance and admittance control, it is important we define first the transfer function of the robot and then eliminate it by the good selection of control parameters. The translation movement of the XYZ mechanism along one axis of the Cartesian space is independent of the movement along the other axes. This allows us to propose studying the movement of the user along one selected axis. The result of this study can then be generalized for the movement along the other axes. The movement direction we decided to study is X. This direction has been selected due to the fact that the X direction has the main contribution to the forward propulsion of the user, and it also is the direction in which the dynamic effort of the user is significant.

The formula describing the movement of the XYZ mechanism along the *x*-axis is

$$M(k_r.R)^2.\ddot{\theta} + F_m\dot{\theta} = u_x - J^T(\theta)H \tag{4.21}$$

where M is the mass of the mechanism; θ, $\dot{\theta}$ and $\ddot{\theta}$ are, respectively, the angular position, velocity and acceleration of the robot; R is the radius of the driving pulley of the XYZ mechanism along the *x*-axis; k_r is a parameter that describes the gear reduction ratio of the shaft of the motor driving the pulley; J is the Jacobian matrix; H is the contact force exerted by the manipulator's end-effector on the user's foot and vice versa; u_x is the vector torque applied by the robot on the x-axis and F_m describes the friction coefficients of the manipulator.

To simplify the study of movement of the robot, we propose transforming the mathematic model of the system described above into a physical model using Simscape so that it can be easy to deal with the system as if it were a real hardware component with different physical inputs and outputs.

Simscape is one of the tool boxes of Simulink's library that enables creating models of physical systems and simulating them. It allows building different physical models based on physical connections that are directly integrated with block diagrams and other modeling paradigms, including electric motors, bridge rectifiers and hydraulic actuators [172].

4.5.3.2. Hardware modeling

To quicken the simulation of our system in the Simspcape environment, we propose simplifying the dynamic model of our system. This can be achieved by representing the whole moving parts along the *x*-axis to one single moving part representing the mass and inertia of the all other parts. In this case, the new system we have consists of three main parts: one long rail (base platform), a moving platform (the total mass of it includes its proper mass and the mass representing the mass of the simplified parts of the system which are estimated to weigh 30 kg) and a driving mechanism consisting of two pulleys and a connecting belt to transform the movement to the moving platform. Static and dynamic friction forces F_m are by default calculated by Simscape.

The simplified model is modeled in Solidworks [173] by creating and assembling the four previously mentioned mechanical parts. These parts are connected by the use of two different types of joints: prismatic and revolute joints. One prismatic joint is used to connect the moving platform with the base platform while two revolute joints are introduced between pulleys and pulley holders fixed at the extremities of the base platform. The next step consists of implementing the CAD design of the robot on a Simscape model to do the simulation with the intermediate of SimMechanics Link (Figure 4-20). This step is achieved by exporting two main types of files from Solidwords to Simscape which are XML and STL files. The first type contains all the necessary information that defines the geometry and mechanical properties and the relation between different parts of the robot while the second one is used to represent surface geometries of the assembly bodies [174].

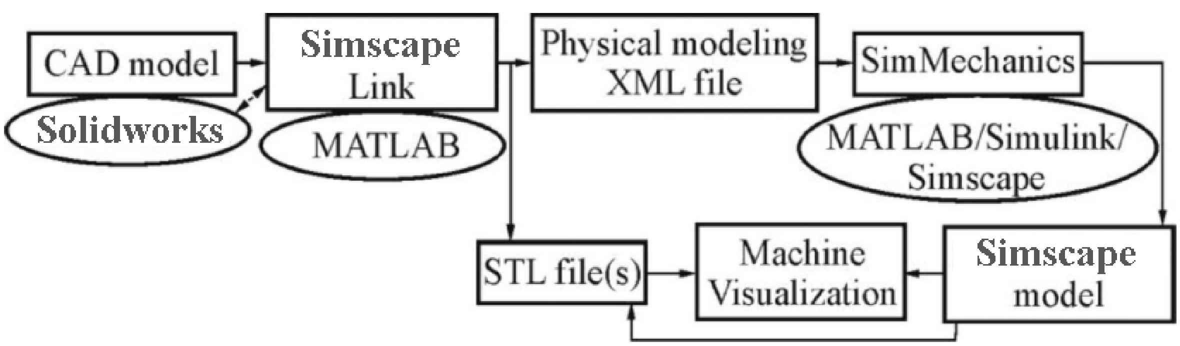

Figure 4-20. Implementation process of CAD model in MATLAB/Simulink environment [174].

Figure 4-21 shows the assembled X mechanism visualized in Simscape. The Simscape block diagram of the simplified mechanism is shown in Figure 4-23. It consists of three subblocks (X_slider_1_Rigid, moving platform and driving mechanism), which refer to the main parts of the system. The first two subblocks contain the geometry definition of the parts and the reference of their locations. The driving mechanism block includes the parts that contribute to driving the moving platform. A details of this sub-system block are illustrated in Figure 4-24. The movement of the platform can be generated by sending a torque signal to the resolute joint of the driving pulley.

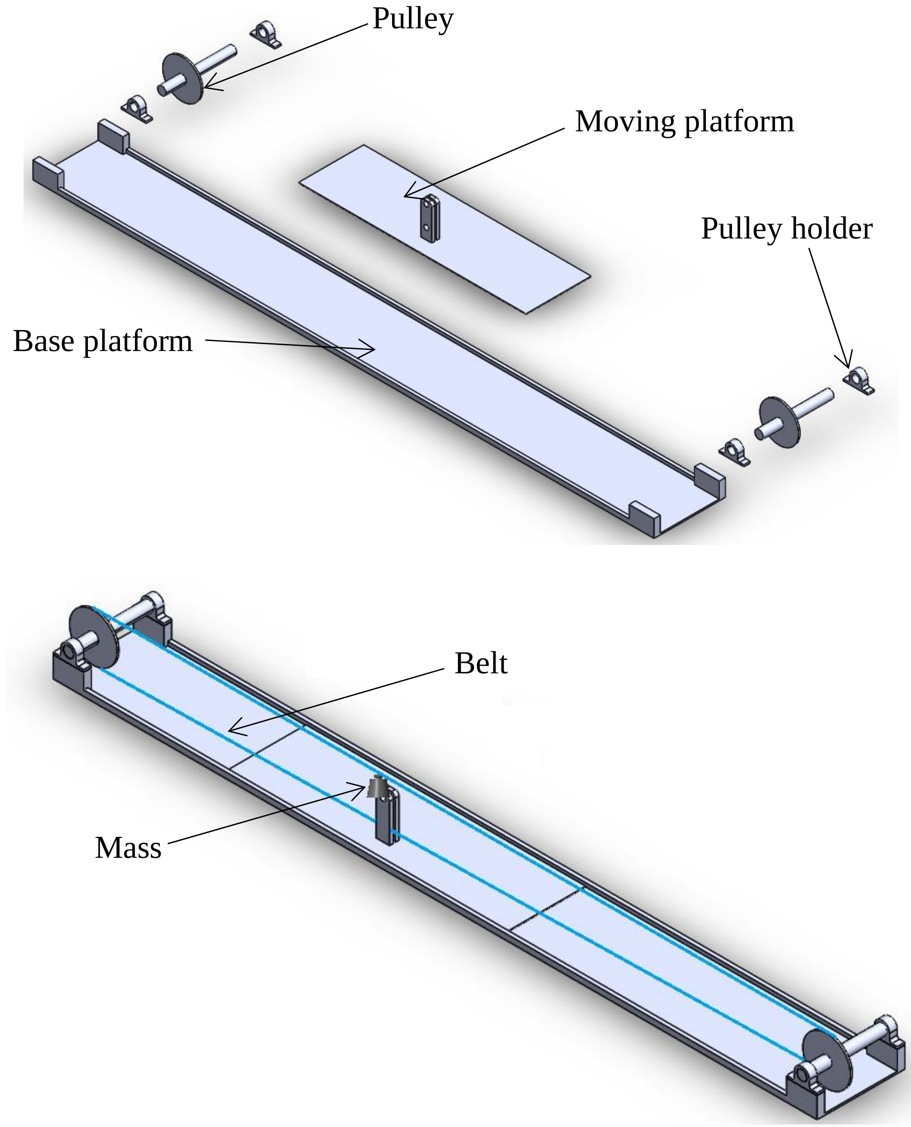

Figure 4-21. Simscape model of the simplified XYZ mechanism. (N.B: the "mass" shown in the figure represents the mass of simplified moving parts.)

4.5.3.1. User model

Walking is a quite complex behavior that requires cooperation of the human central nervous system and the rest of the body. Many dynamic paradigms have been proposed during the past decades for simulating and even predicting biped gait. These models have offered many advantages in many disciplines such as in medical diagnoses and treatments, design of medical devices especially prostheses and orthoses and particularly the control of haptic interfaces. As mentioned, using a human walking model to simulate the behavior of the user in response to interaction forces with the platform are one of common methods used to define suitable impedance control elements for the system.

Basically, research on human gait can be broadly divided into two areas: biomechanical gait and biped robotics. The first area has the interest of defining a complex human model that includes mostly everything found in the body of an actual subject including individual muscles, tendons and ligaments. Overall, this model is quite efficient for predicting mostly every detail of human gait. However, it is computationally intensive to be used in real-time robotic control. Opposite of this, the biped area has the objective of presenting a dynamic human model that can be utilized in conjunction with robotic systems. This area includes five sub-fields which are illustrated in the classification chart of the human gait research field (Figure 4-22) [175]. A detailed explanation of these subareas is given by Xiang et al. [176].

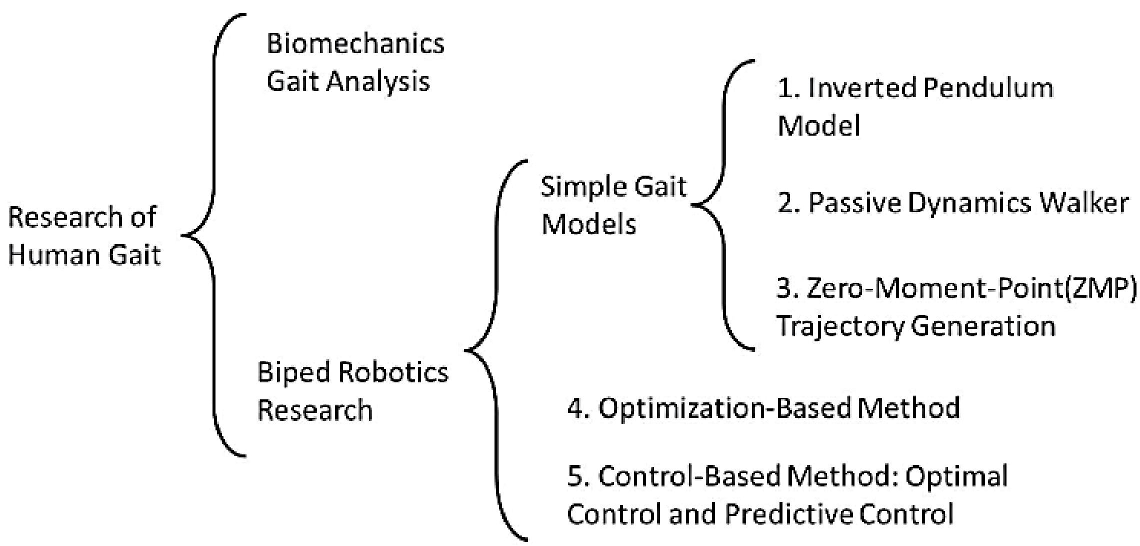

Figure 4-22. Classification chart of the human gait research field of [175].

In our research, we are interested in using what is called an inverted pendulum model (known in the literature also as a spring-loaded inverted pendulum SLIP [177, 178]) to simulate the behavior of the user while interacting with the system. SLIP is illustrated in Figure 4-25. Basically, the walking process is a relationship that involves transformation between potential and kinetic energy. Accordingly, this process can be simply represented by an inverted pendulum. This method reduces the whole body of the user to a point mass (body's center of motion) attached to a massless spring (representing the leg of the user).

To represent the friction forces better the parts of the body, a damper is included. As we intended to study the movement on the *x*-axis, we can simply represent the behavior of the user on this

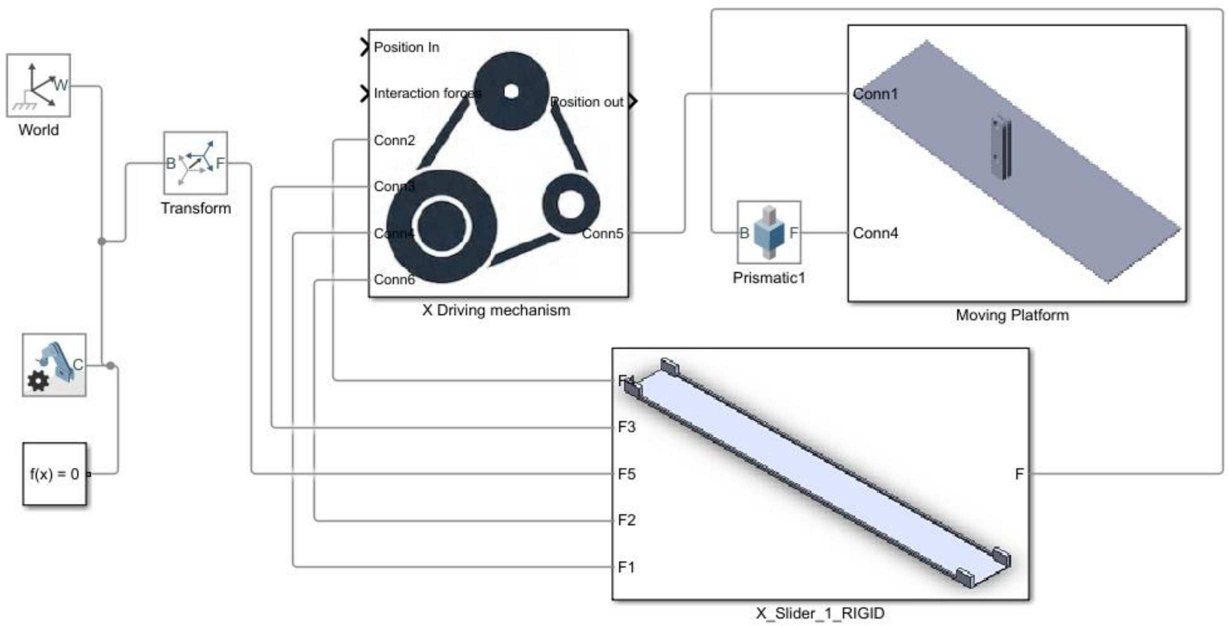

Figure 4-23. Simscape block diagram of the simplified XYZ mechanism.

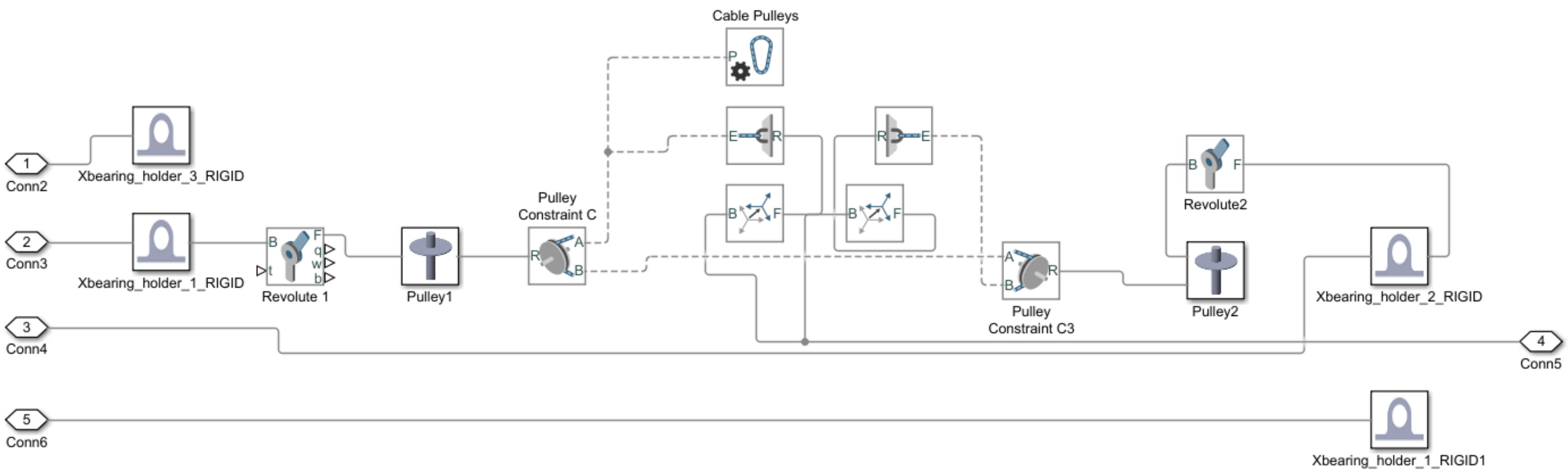

Figure 4-24. Simscape block diagram of X driving system block

direction by a horizontal mass-spring-damper attached to the system. The simplified SLIP model is illustrated in Figure 4-26

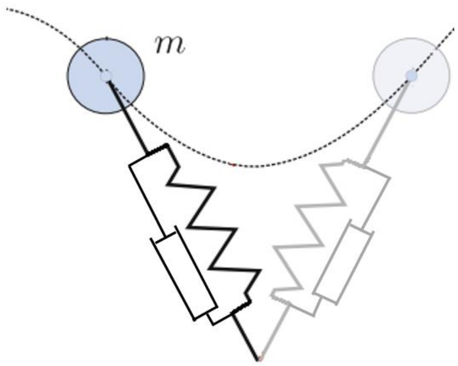

Figure 4-25. SLIP model.

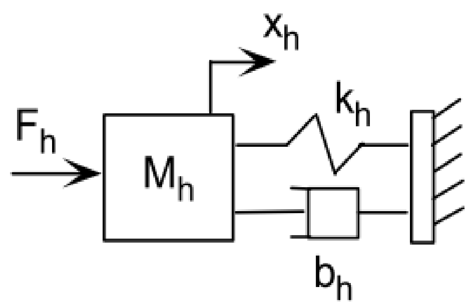

Figure 4-26. A simplified SLIP model.

The transfer function of the human model on the horizontal plane which accepts the interaction force as input and gives the position of the foot to the output can be written as follows:

$$G = \frac{1}{m_h s^2 + b_h s + k_h} \tag{4.22}$$

where m_h, b_h and k_h are, respectively, the mass, damping and stiffness of the human operator on the horizontal plane. Values of these parameters are selected based on the study performed by Dinh-Son Vu [179] on a three-DOFs locomotion interface, which allows us to rewrite the previous function as follows:

$$G = \frac{1}{3.25s+20}. \tag{4.23}$$

4.5.3.2. Controller design

To define the best control strategy that ensures that the GWP system behaves in the most transparent way, we propose studying both impedance control strategies, which are discussed in Section 4.3 (the impedance control with force feedback and admittance control with position feedback).

In this study, to obtain a more realistic performance of the different control strategies mentioned above, we need to define the type of controllers, and we need to define the communication rate between the different GWP modules.

A) Type of compensator

The proportional-integral-derivative (PID) and proportional-derivative (PD) controllers are widely used in the control of robotic manipulators, especially for industrial robots [180]. However, when the matter is related to interaction control with haptic interfaces as it is in our case, the integrated errors transmitted to the system can significantly affect the method of selecting the controller. Sensors used to transform position and force signals to the system are one of the main sources that add noise and disturbances. In addition, delays that can affect the communication between the different parts of the system can be a critical issue that has to be solved. Accounting for these errors, the following problem reflects some of the challenges that counteract the use of derivate and integration elements in the control of the system.

The proportional term is mostly used to amplify the error that results between a set point and an actual process to get a fast response. Overall, this element is simple to construct and implement and is mostly desirable [180]. The derivative term estimates the future trend of the error which helps improve the transient response through high-frequency compensation and reducing the over shoot response [180, 181]. However, this element can cause a difficulty that is primary related to the noise transmitted by sensors. The signal from the load cell is not transmitted to the controller as a continuous signal but as a desecrated signal. It can happen that the proportional gain amplifies the noise if the sampling rate is not small [156]. In addition, the derivative gain can significantly contribute to an undesired phase shift when obtaining the acceleration based on the double derivative of a sensed position. The integral term accounts for past values of the error and integrates them over time. It is beneficial for reducing the steady-state errors as well as beneficial for eliminating them. It can also allow imitating the effect of the noise by providing an average to the value measured. However, the difficulty of implementing it in haptic interfaces is related to the fact that there are no steady-state interactions. Therefore, the introduction of the integral element could lead the system to move into an unwanted position that can be defined as a reference or steady-state position.

B) Communication rate

It is clear that the above-described issues are related to practical problems that could be better solved with hardware implementation. However, due to the difficulty of satisfying this condition, it is important we account for the assumptions that may influence getting real performance from the simulation. Therefore, we propose studying the different control strategies in the discrete time as suggested in Colonnese [182]. This model is close to the reality in which the position and force sensor measurements are quantized, the control circuits run at different speeds and the control of a physical robot is performed through discrete controllers. The objective of this model is to study the effect of the sampling and the inherent dynamics of VR on achieving a desired impedance [162]. Figure 4-27 and Figure 4-28 show, respectively, the high-level and low-level control of the discrete time model in which the connection circuit in the GWP system is illustrated. The sampling time of each circuit is selected based on the available data of some haptic interfaces [162, 168, 183, 184].

Due to the above-mentioned issues related to the implementation of derivative and integration elements in a controller, a discrete proportional P controller has been selected to control the impedance loop of all different impedance control strategies already mentioned (the impedance control with force feedback and admittance control with position feedback, including one and two feedback models). The proportional gain should be given a high value to cancel the impedance of the system and to keep the desired impedance as well as to reject any disturbances [157].

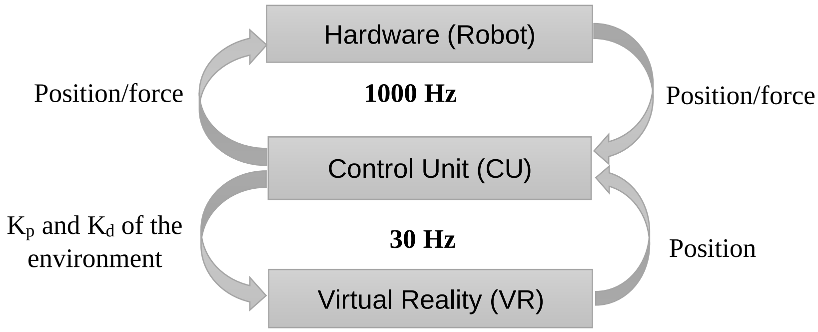

Figure 4-27. High-level control discrete time model of the gait walking platform system.

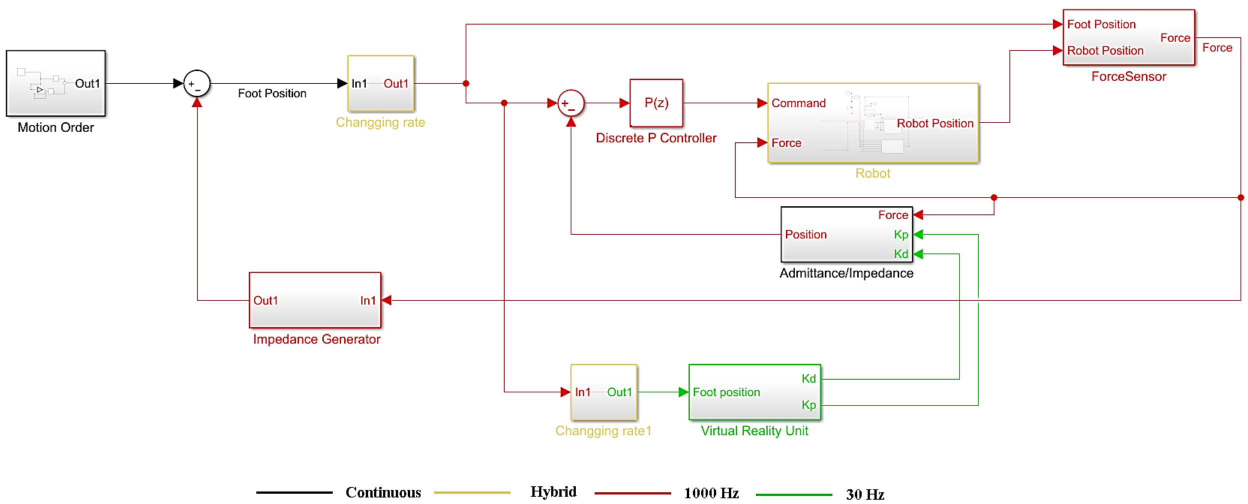

Figure 4-28. Low-level control discrete time model of the gait walking platform system.

On the other hand, to have an admittance control model with an inner position feedback where the sensed joint angle follows well the desired angle, a high PD controller is implemented. For this particular control model, to get the outer impedance loop stable, it is important to stabilize the open inner position loop [179]. Therefore, the gains of the loop's controller have to be selected by studying the stability of the open loop of the position around the plant of the robot.

The gains of the PD controller of the admittance control model with two feedbacks have been tuned using the MATLAB PID tuner app. The Bode plot corresponding to the open loop of the robot with particular PD controller gain values (P = 8.22, D = 0.12 and N = 57998.36) is shown in Figure 4-29. The resulted gain and phase margin values are, respectively, 10 dB and 38°, which demonstrates that the inner position loop of the impedance control of the XYZ mechanism is stable.

To derive characteristics of the closed loop of the XYZ mechanism, we drew the bode plot shown Figure 4-30. The plot illustrates that band width varies from $1e^{-10}$ Hz to 25 Hz in which all types of human movements can be supported. It is important to notice that the maximum frequency of the controlled movements of a human rarely exceed 2 Hz, while reflexes have a maximum bandwidth of 5 Hz [185].

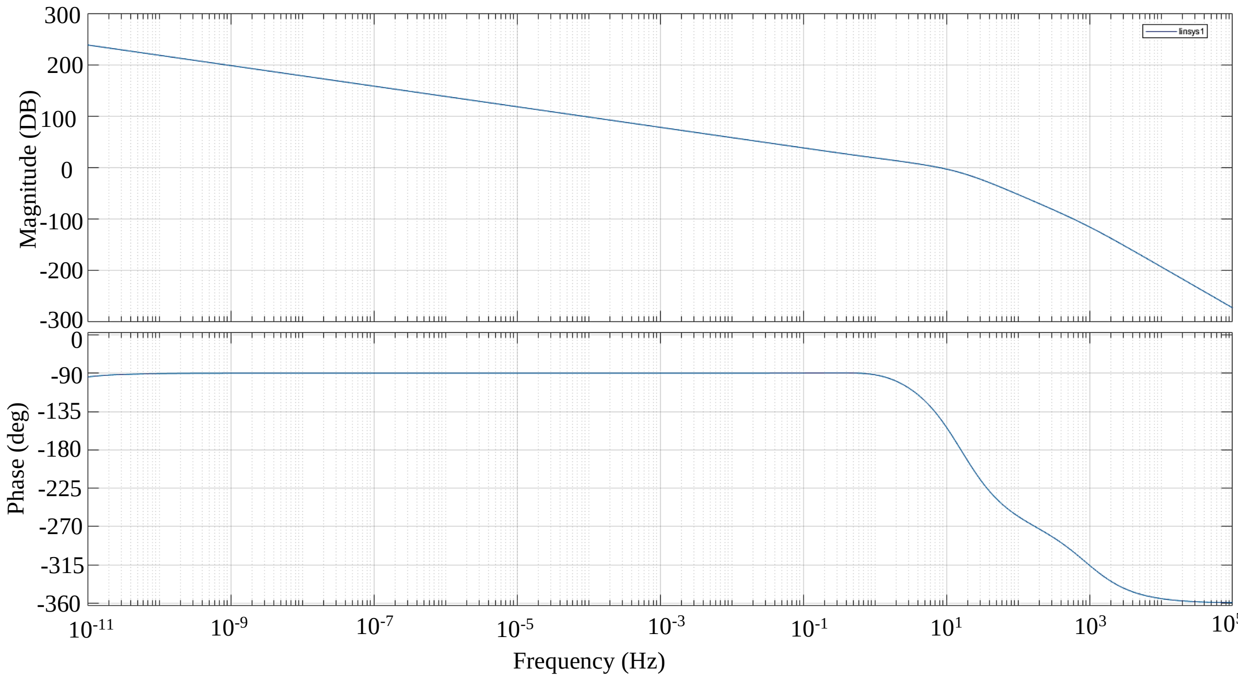

Figure 4-29. Bode plot of the open inner loop of the admittance control model with two feedbacks.

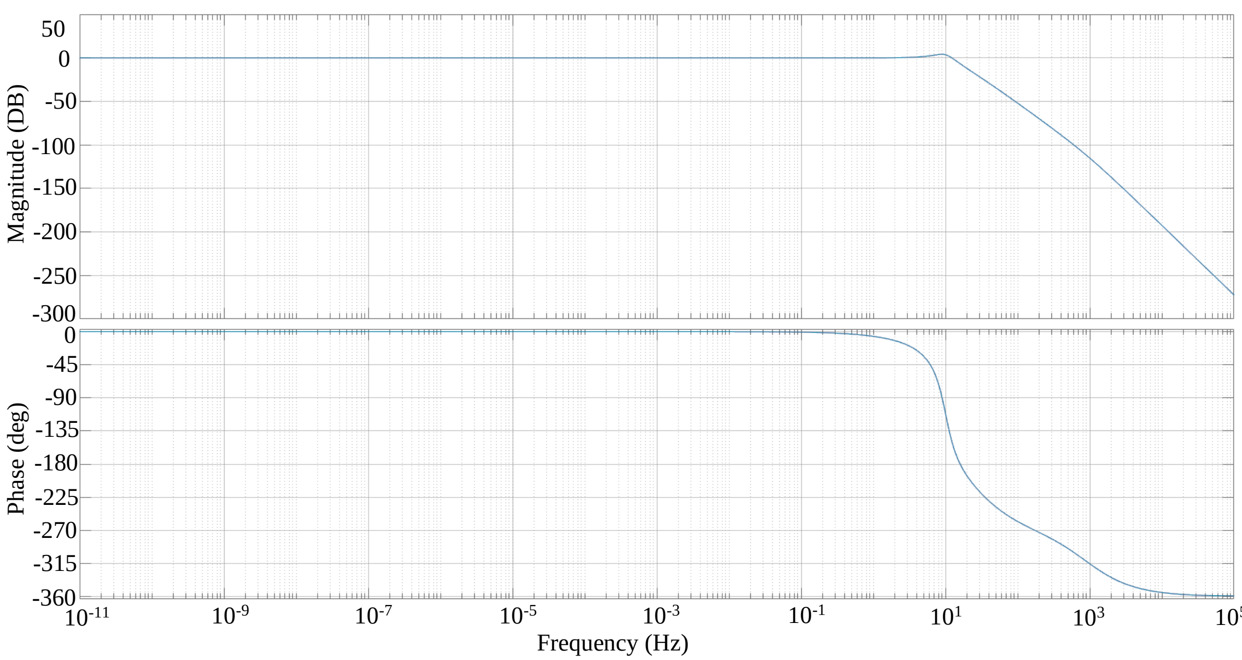

Figure 4-30. Bode plot of the closed inner loop of the admittance control model with two feedbacks.

As we ensured that the inner loop is stable, the proportional controller of the impedance outer loop was tuned, and it is given a value that ensures that the system stays stable (P = -5.82e-05). Figure 4-31 shows the behavior of the outer loop of the XYZ mechanism under the admittance control with two feedbacks. The gain margin is -91dB, and since the bode gain plot never crosses the limit of 0 dB, there is no phase margin. Therefore, the performance of the closed loop of the system is stable.

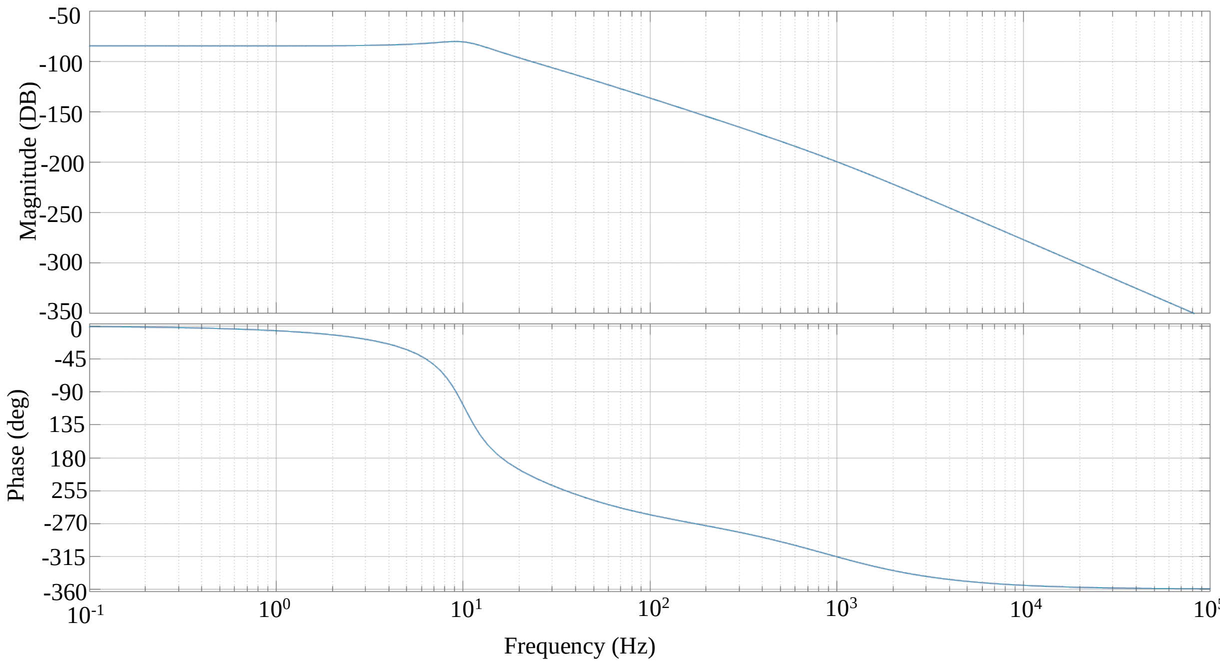

Figure 4-31. Bode plot of the open outer loop of the admittance control model with two feedbacks.

Similarly, proportional gains of the remaining control models (the impedance with force feedback and admittance with one feedback) were tuned using the MATLAB PID tuner app, and performance of their stability was analyzed using the bode plot. Gains selected for both control models are, respectively, P = -600 and P = 1.85e-06. Bode plots of the open loops of both impedance controls are respectively presented in Figure 4-32 and Figure 4-33.

The gain margins of both control models are, respectively, 91 dB and 56 dB. The phase margin of the plot of the admittance control with one feedback is 83.2°. There is no phase margin in the case of the impedance control with force feedback as the bode gain plot never crosses 0 dB. Therefore, the closed loops of these two control models are stable.

As we ensured that the system is stable, the next step in our study consisted of analyzing the performance of the system under different impedance control models. Transparency is the physical tool that provides us with a physical measurement of how well the system renders a selected virtual environment. It can be mathematically described as the ratio between the transmitted position X_M to the desired position X_D. Therefore, the first step required to define the transparency of the system is to define a way of extracting the desired position X_D. To achieve this, we constructed a Simscape physical model (Figure 4-34) that simulates the direct interaction of a user with a virtual environment without the intermediary of the robot. Such a model includes the physical model of the user as described in Section 4.5.3.1 (represented by mass1 and Damper1 blocks) and a virtual environment model described by the stiffness and damping value of the simulated environment (represented by Damper2 and Translational Spring blocks). The user's motion can be generated by applying force on the user's model (using force source blocks) while the output position can be measured using an ideal Simscape translational motion sensor. The measured position in this case also represents the desired position X_D parameter of the transparency equation.

As the reference signal of the transparency is defined, the next step consists of comparing this signal with the output signal positions of the different control impedance models.

4.5.3.1. Test

The aim of this test is to compare the transparency of the system under different impedance control strategies while simulating a wide range of frequencies. To study the transparency of the system in low frequencies, a sinusoidal force signal with an amplitude of 12N and a frequency of 0.16 Hz was applied to the human model of the different control strategies, while at high frequencies we applied a sin wave that had an amplitude of 12N and a frequency of 2 Hz. It is important to notice that the simulation of environments that have an important stiffness and damping values does not disturb the transparency of the system. Therefore, in this test, the performance of the system in rendering free movements is only tested (Swing phase). Parameters of the simulated environment (air) are listed in Table 4.1.

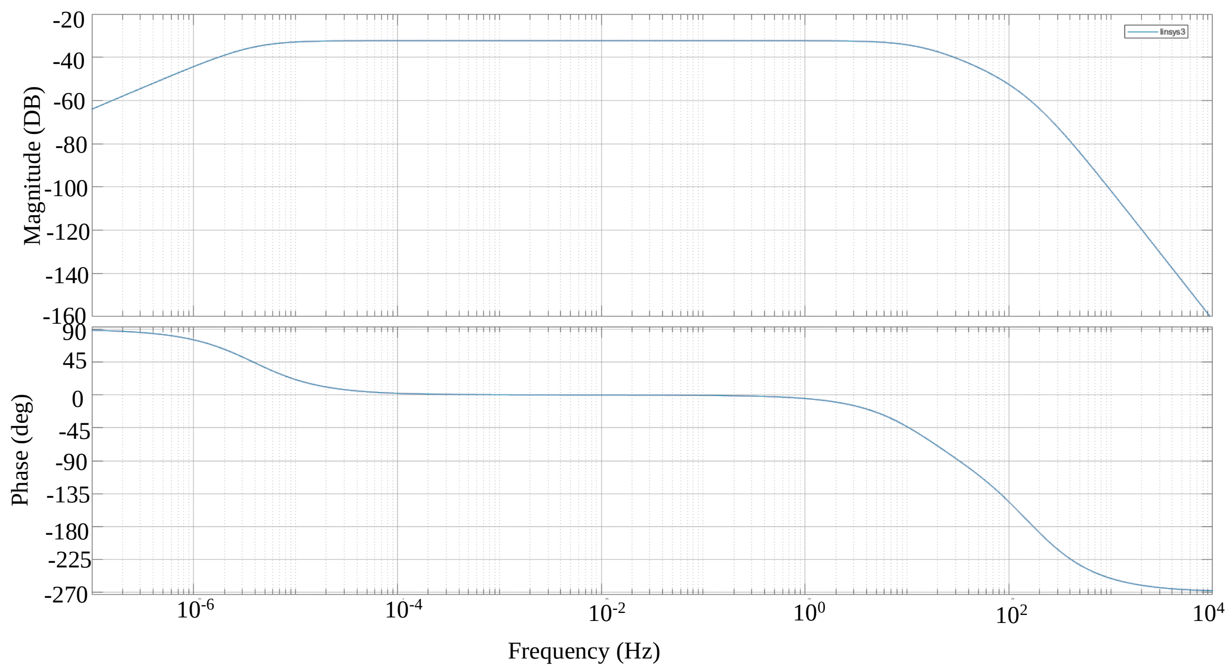

Figure 4-32. Bode plot of the open loop of the control impedance with force feedback.

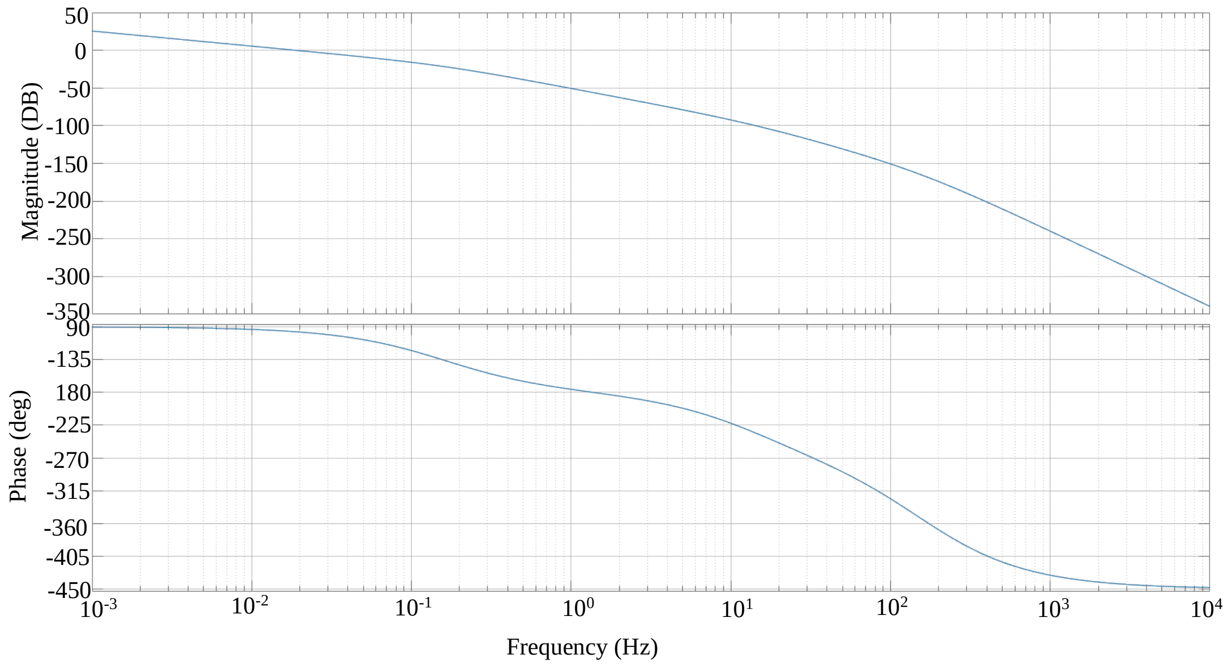

Figure 4-33. Bode plot of the open loop of the admittance control with position feedback.

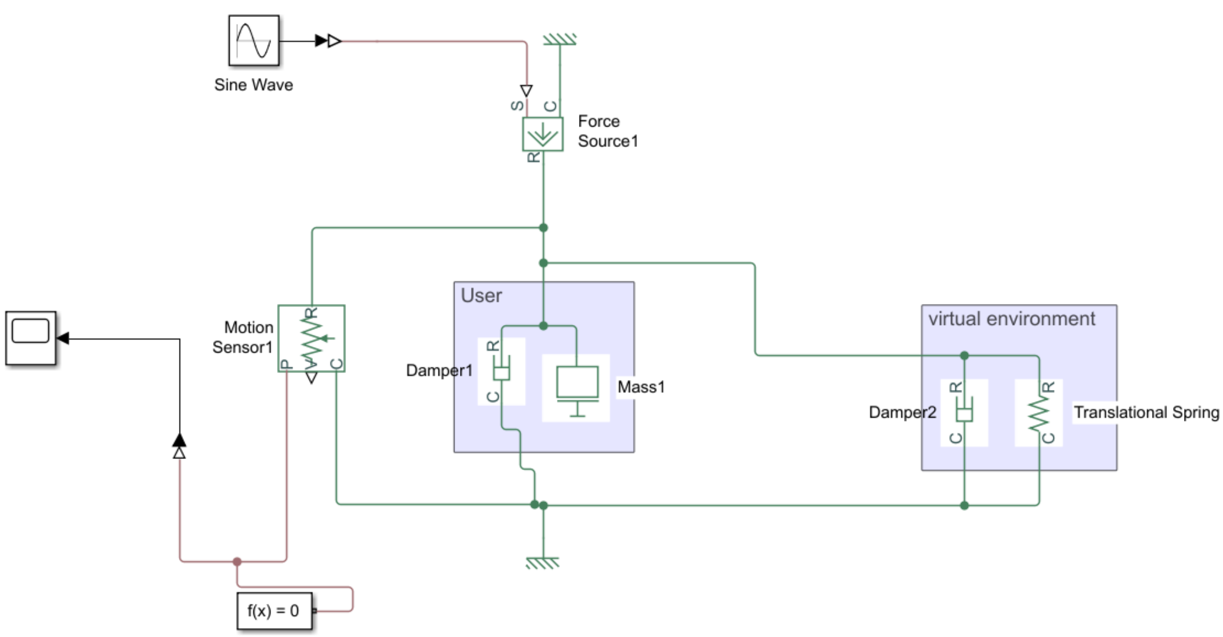

Figure 4-34. Simscape model of a user interacting directly with a virtual environment.

4.5.3.2. Results

Foot positions obtained from the simulation of low-frequency movements under different types of impedance controls are listed in Figure 4-35, while foot positions resulted from simulating high-frequency movements are listed in Figure 4-36. There are three main observations about the results obtained.

First, results show that at low frequencies the desired displacement of the user's foot obtained by applying the force signal input to human model is much higher in amplitude compare to the desired position resulting from high frequencies. At a low frequency, the amplitude of the desired position is about 1.2 m, while at a high frequency, it is about 0.07 m. This is because of the existence of a significant mass that describes the weight of the moving foot that would provide an important resistance when trying to move it fast.

Second, for both ranges of frequency, while the admittance control with one feedback and impedance control with force feedback show good performance in tracking the desired position, the admittance control with two feedbacks exhibits very poor performance. One possible explanation of the low performance of the admittance control with two feedback is that a control system with two feedbacks includes a human model that has an important moving mass. To understand better the performance of the admittance control with two feedbacks, we tested the system using a different dynamic model of the user. In this model, we included the elastic effects of the user, and we considered that the moving foot has no weight. Dynamic parameters of the new user's model are the damping coefficient = 2 N/(m/s) and spring stiffness = 1000 N/m. To test this model, we applied to the model a sinusoidal force signal with an amplitude of 12 and a frequency of 0.16 Hz, and we analyzed the performance of the system under the new conditions. The associated foot position recorded in response to this input signal is illustrated in Figure 4-37. The result illustrates that by changing the dynamic model of the user's foot, the system shows significant performance in tracing the desired position. In other words, the experiment demonstrates that the admittance control with two feedbacks can perform well with very specific dynamic models of users.

Third, results show that while the output position signal of the admittance control with one feedback is mostly identical to the desired position signal, the position signal of impedance control with force feedback is slightly smaller in amplitude compare to the desired one. This demonstrates that the admittance control with one feedback is better than impedance control with force feedback to render free movements as the transparency of the first one is higher than the last one. Having said that, it is worth mentioning that, at low frequencies, the difference between the position signal system under the admittance control with one feedback and the desired one is smaller than their difference at high frequencies. Although we do not expect the system will be perfect in rendering free movements, it is clear that the user would feel much resistance while moving their foot back and forth very fast. To see to what extent this resistance is, it is important at high frequencies to compare it to that of low frequencies. We put the diagram (Figure 4-38) of the force at the interaction point between the foot and the system at the a range of frequencies (0.16 Hz and 2 Hz). If we neglect the effect of transaction efforts present in the graph of movement of 2 Hz (points including sharp force increment), the ratio of forces at 2 Hz to forces at 0.16 Hz can be estimated to equal to 4.5. This means that the resistance that the user would feel while moving their foot very quickly is higher than four and half times that when moving it slowly. The value of the resistance is equivalent to moving an additional mass of 0.2 kg. This amount is important and makes the user feel uncomfortable while moving their foot. To solve this problem, we suggest introducing a light mechanism that could provide more transparency in simulating free movements at high frequencies. The details of this mechanism are the subject of the next chapter.

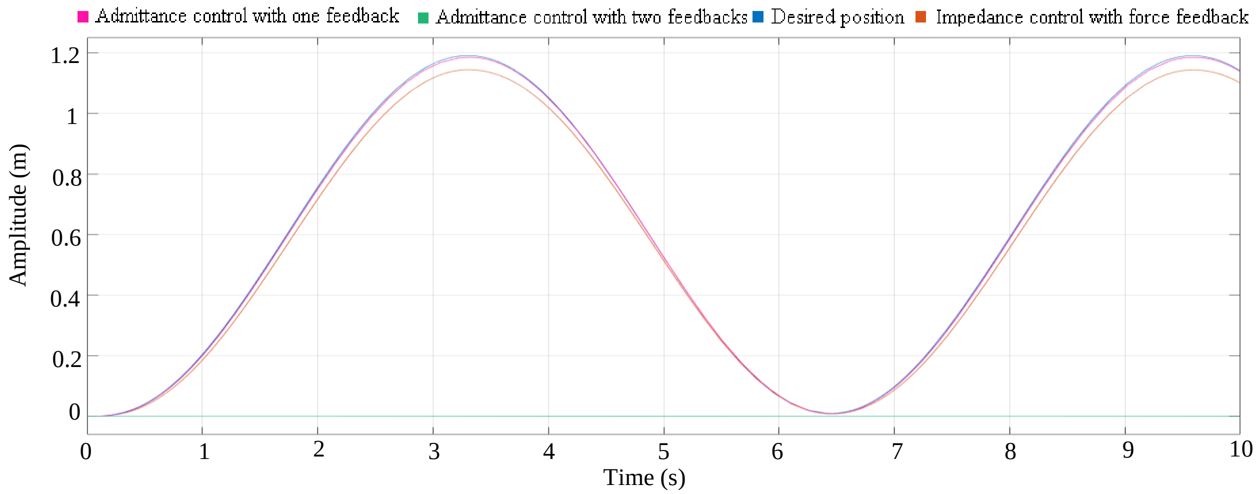

Figure 4-35. Foot positions obtained from the simulation of low-frequency movements under different control models.

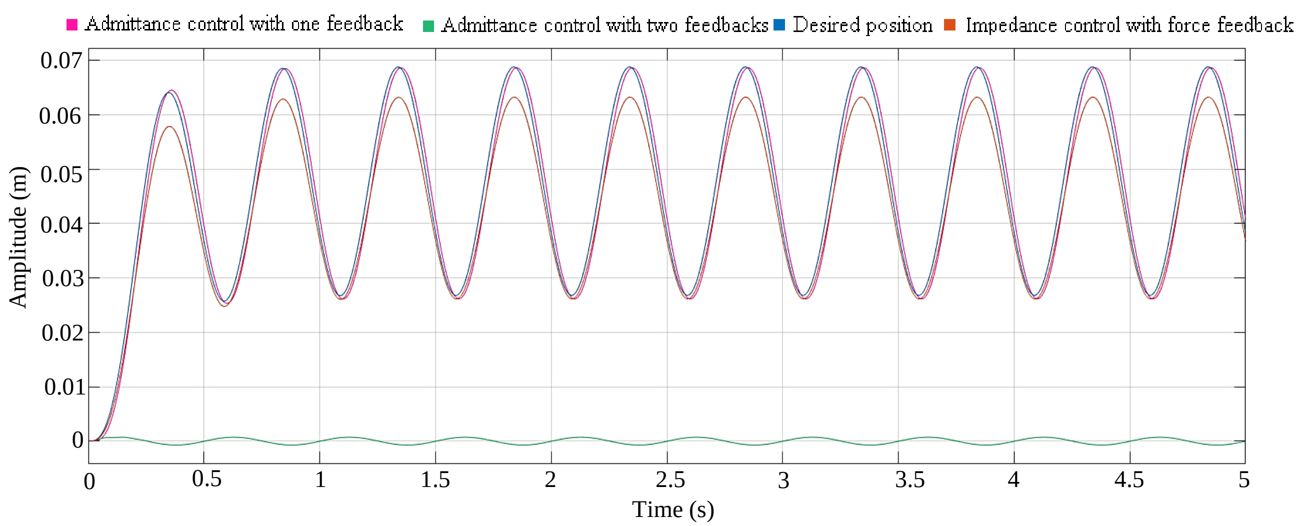

Figure 4-36. Foot positions obtained from the simulation of high-frequency movements under different control models.

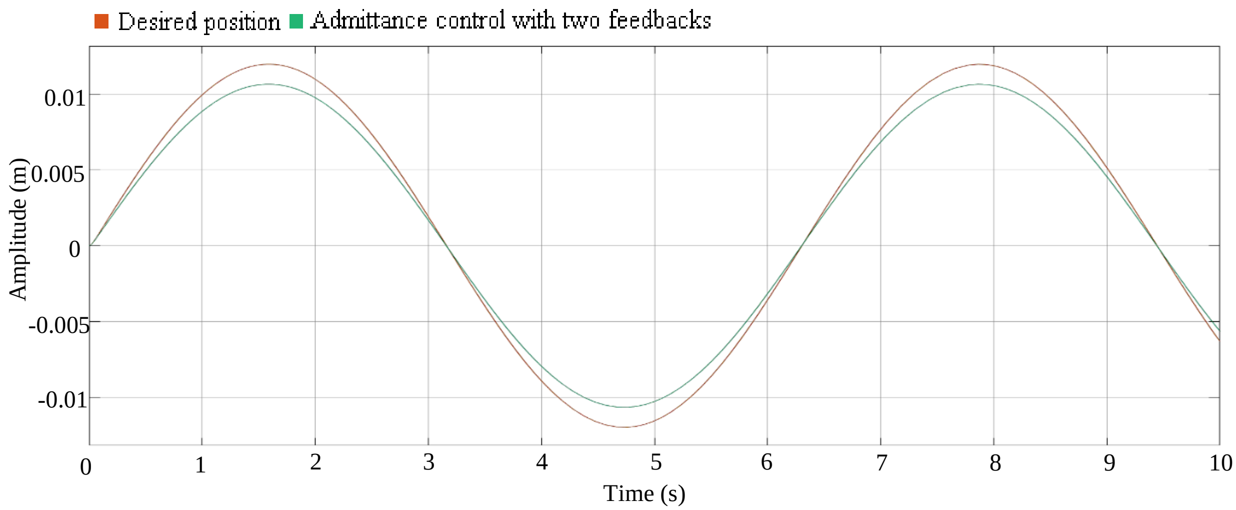

Figure 4-37. Foot positions obtained under the admittance control with two feedbacks and by using the new user model assumption.

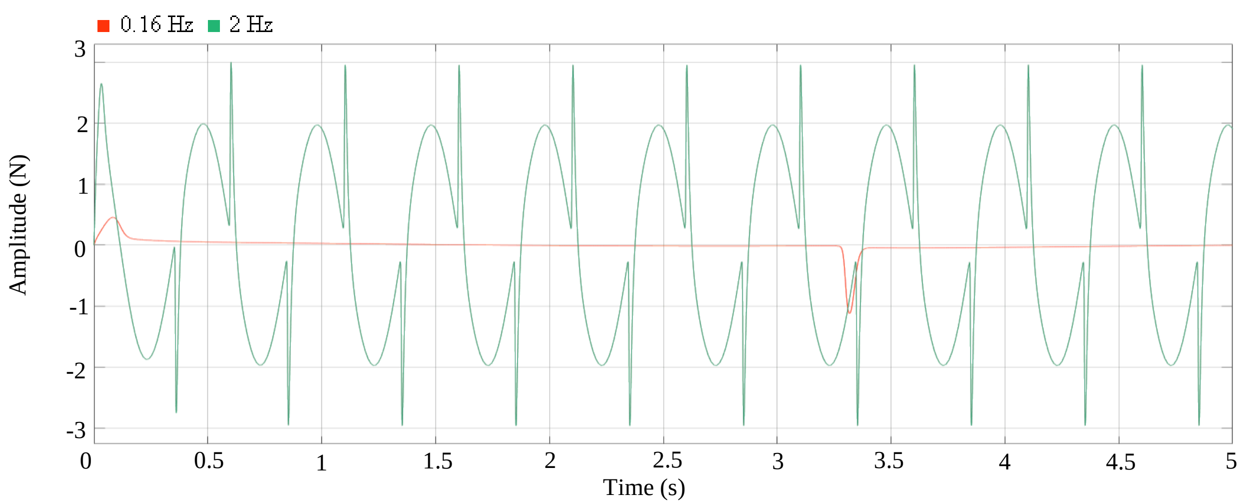

Figure 4-38. Comparing interaction force values obtained from simulating high- and low-frequency movements under the admittance control with one position feedback.

4.6. Conclusion

This chapter discussed various control strategies that define the relationship between the user, hardware and virtual environment. The relationship between the three elements that comprise the GWP system is a function of inputs and outputs of the positions and the forces communicated. It has been shown that since the objective of our system is to simulate virtual environments that have different stiffness and damping values impedance, the indirect force control strategy known as impedance control was adopted. This choice helps us in simulating environments that have different stiffness and damping values, such as water, sand and others.

Starting from a simplified control strategy is an important step to better understand the relation between the different parts comprising the GWP system. The aim of this step is to present a simplified model for the GWP that has the ability to be executed in VR with actual data. The control concept is based on the possibility of dynamically changing the properties of the system that represent different mediums. The success of the control strategy means that the system provides actual force relative to foot movements given by the equivalent simulated medium. The visualization is an important part in this concept because it addresses the visual perception that must be coordinated with the movement.

Adding the dynamic effects of the XYZ mechanism and the user to the system changes dramatically the way the system behaves. It also creates a difficulty at the control level as the behavior of the user and behavior of the virtual environment are unexpected. The type of feedback sent to the impedance control loop plays an important role in defining the stability and performance of the system. Results show that the impedance control with position feedback performs better than the admittance control with force feedback in simulating the movement of the user in the air. The impedance control with position feedback performed better although not all residual inertias of the system were successfully filtered out. we propose in the next chapter adding a mechanism to improve the transparency of the GWP system.

Chapter 5: STEWART PLATFORM

5.1. Introduction

The residual inertia and frictions that appear in haptic interfaces with heavy mechanical parts have a direct impact on the transparency of the system. The user as a result can feel resistance during the swing phase of walking. Thus, the user gets an unrealistic simulation of the movement visualized in the VR. To solve this problem and to improve the transparency of the system, two different approaches are proposed. The first approach consists of adding a passive mechanism to the system to allow the user to partially detach their foot from the system during the swing phase. The second approach consists of using a light active mechanism to flow up the movements of the user during the same phase. The system we propose is the Stewart platform. In the first section, the passive and active mechanisms for filtering apparent residual inertia are further discussed. The main focus of this chapter is discussing the kinematic and dynamic characteristics of the Stewart platform that we propose to use in the GWP system. Therefore, the rest of this chapter is organized as follows. Section 2 and 3 present a background about the Stewart platform and different possible configurations that can be shaped. Section 4 discusses the performance indices of the Stewart platform and presents criteria to obtain an optimized Stewart platform that meets our specific requirements. Section 5 discusses the performance of the selected optimized Stewart platform in rendering free user movements. The summary of this chapter is provided in the last section

5.2. Filtering residual inertias

Two types of mechanisms have been developed for filtering residual inertias: passive filtering mechanisms and active filtering mechanisms (Stewart platform).

5.2.1. Passive filtering mechanism

Opposite of an active system that is supported with motors, a passive system does not implement any external force to generate movement. It consists of passive elements that can partially disconnect the foot of the user from the platforms. To date, there are two main types of systems in this class in which they differ relative to the DOFs they support. These systems are the passive mechanism based on revolute joints and the passive cable mechanism.

5.2.1.1. Passive mechanism based on revolute joints

To deal with the apparent inertia in the two-dimensional haptic interface developed by Dinh-Son Vu [179], a hinge mechanism is proposed to provide unconstrained movement on the horizontal plane and to free the rotation of the dorsiflexion of the heal and toes of the foot. This mechanism has two DOFs and consists of two revolute joints (Figure 5-1). One joint connects the footplates of the whole robotic system to an intermediate plate so that the rotation of the toes is allowed. The other joint is attached between an intermediate plane and a plate made of Aluminum to support the rotation of the foot around the heel. The position and rotation of the foot are calculated based on the measurements provided by the potentiometers of each hinge. Although this mechanism can decrease the fall potential of the user, it encompasses two essential disadvantages. The first disadvantage is related to the restriction on movement on the horizontal plane, although small motions outside this plane are allowed for security by adjusting the distance between the hinge mechanism and shoe worn by the user. Moreover, the hinge mechanism's links are constructed in a way that force the feet to move in a parallel way and not as should happen in a real gait in which the user has the freedom to shift their foot left and right. Accordingly, the user has to put more effort to push their legs, which can result in losing balance. Therefore, the second disadvantage is about the system becoming less transparent. Adding extra joints to provide more freedom to the user could be an intricate solution to achieve transparency.

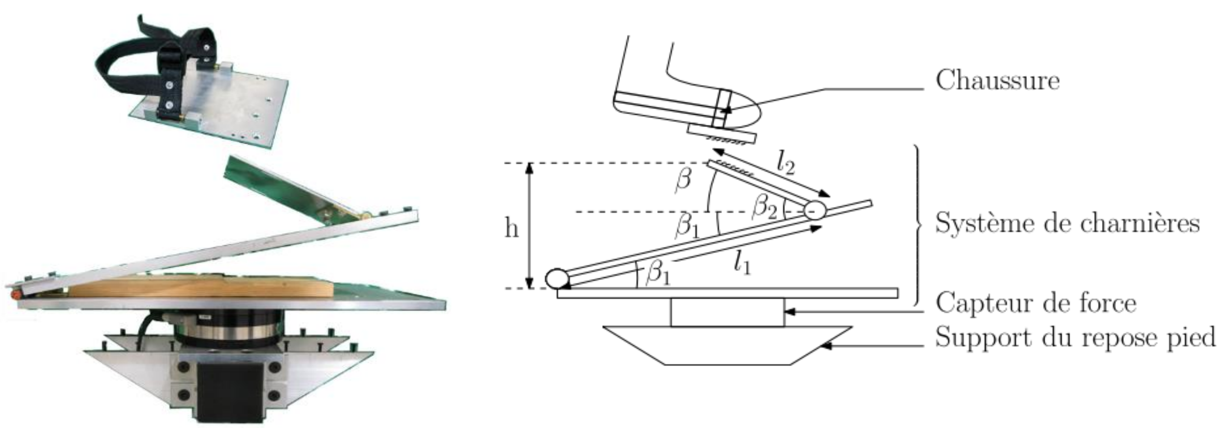

Figure 5-1. Passive interface with two revolute joints [179].

5.2.1.2. Cable-based passive mechanism

The cable-based passive mechanism is a system that consists of a set of extended strings attached to the user's foot and the platforms. Basically, this mechanism allows the free movement of the foot in any direction during the swing phase. Lengths of strings are calculated using potentiometers connected to the axis of the pulley around which strings are wrapped. Hence, the exact position of the foot could be simply defined by solving the trilateration problem. The first mechanism of this type of passive system was developed for Gait Master [186]. This system contains three tensioned strings attached to the sandal of the user as illustrated in Figure 5-2. Later, a more sophisticated mechanism using the same principle was developed by Dinh-Son Vu to provide more accurate measurements of the position of the foot. To achieve this goal, an optimized algorithm was introduced to define the best location of the potentiometers with respect to the foot. The cable-based passive system has the advantage of significantly reducing the inertia that the user can feel if their foot is rigidly connected to the platforms. This has the advantage of enlarging the frequency bandwidth of the system in which the user can feel with less impedance at high frequencies.

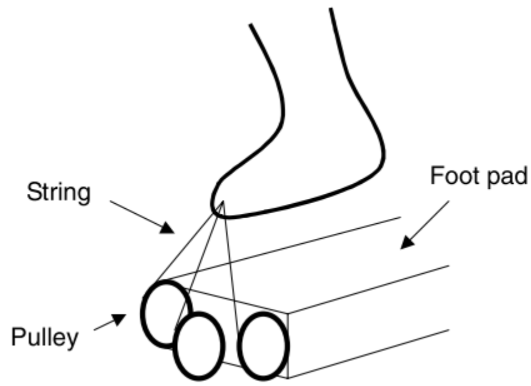

Figure 5-2. Cable-based passive mechanism for Gait Master.

5.2.2. Active filtering mechanism (Stewart platform)

The previously mentioned solutions for filtering residual inertias and friction forces could only applied in robotic systems where a healthy person is involved. In this case, the user themself is able to freely move their feet in any direction they want as well as deal with a potential risk of falling that could result from the disequilibrium of their body. However, our system is intended to be used as a rehabilitation device. Hence, we must consider that the system should actively support the movements of the patient who has weak muscles and whose movements are not fully controlled. In addition, the second objective of our system is presenting a platform for simulating different mediums to the user by implementing impedance control. In other words, the system has to support simulating walking in water, for instance. For this specific case, the user has to feel extra weight on their feet that is equivalent to water resistance. Therefore, solving all these problems can only be achieved using an active system. In an active system, the feet of the user are in permanent contact with the platforms. Thus, it is possible we could apply any type of desired impedance at any point in the space.

An active filtering system is a new type of mechanism in the field of haptic interfaces. To our knowledge, no previous work has investigated the implementation of such a solution. Overall, the main advantages of an active system over a passive one is that an active system can be both efficient in filtering apparent inertia and friction forces as well efficient in providing various desired impedances.

The design we propose for the implementation of an active filtering mechanism is a six-DOFs Stewart platform.

5.3. Background of the Stewart platform

A six-DOFs Stewart platform is one of the most common types of parallel robots which consists of two platforms connected by closed chains links (especially by using linear actuators such as pneumatic cylinders). The Stewart platform was first designed by Gough in 1956 to be used as a universal tire testing machine at a factory in England called Dunlop. Later, in 1965, the Stewart platform became widely popular when it was designed to be used as a flight simulator by Stewart [187]. Although the platform was invented by Gough, most researchers use the nomenclature "Stewart platform" to refer to this type of parallel robot, and a few researchers called it the "Gough/Stewart platform." Thus, for the purpose of convenience, we use in this thesis the most common nomenclature.

The Stewart platform offered a set of advantages over robotic systems with serial mechanical configurations. Overall, parallel robots and the Stewart platform in particular are very accurate and have high stiffness due to the lack of a cantilever-like structure [188]. Furthermore, they are able to support heavy loads due to the presence of many actuators in parallel rather than in serial. Accordingly, the Stewart platform has been extensively studied and developed so that it has been successfully implemented in many disciplines. The application of the Stewart platform includes:\ airplane simulators [189], pointing devices, adjustable articulated trusses [190] and mining machines [191]. The beginning of this century shows a significant interest in using the Stewart platform in the field of robotic rehabilitation. Regarding lower-limb rehabilitation, the Stewart platform is introduced to assist patients in performing two different rehabilitation training exercises, including rehabilitation of the ankle and full leg exercising. It is important to note that the Stewart platform is more commonly used for ankle rehabilitation because of the complex nature of the ankle that includes three rotation DOFs. The advantage of the Stewart platform for such applications is related to the ability of such robotic systems to assist the movement of the ankle joint around three different axes, a task that would be intricate if realized using a serial manipulator. The most popular robotic system for such applications is Rutger Ankle [192]. The system utilizes a typical six-DOFs Stewart platform to supply forces and torques required to perform the ankle rehabilitation. It is also supported with a visual screen that maps the movement performed in a VR world which can have major importance for giving the patient feedback on their performance. Another lower-limb robotic rehabilitation which uses Stewart platform involves assisting the patient with performing gait training exercisers. For such an application, the Stewart platform can be utilized as an end-effector robot attached to the foot of the user (as in our system). Accordingly, the platform has to move the foot with respect to different real gait patters. To achieve this task, the Stewart platform has to have a large workspace and has to support significant, heavy loads that the user can apply. In this situation, the optimal design solution could be given by a hybrid serial/ parallel system. An example of such a solution is presented by a nine-DOFs hybrid parallel robot [193, 194] to offer more advanced gait rehabilitation training. The robot contains nine linear actuators serially connecting two movable platforms and one stationary platform. This system benefits from serial robots to increase the work volume and from parallel robots to preserve stiffness.

5.4. Different configurations

Many different configurations of Stewart platform can be defined according to the type, arrangement and number of joints of the platform and according to the shape of the platform. As our application requires utilizing a six-DOFs Stewart platform, we are only interested in searching for logical configuration possibilities of Stewart platforms having six DOFs.

The degrees of freedom of a closed-chain robot can be defined using Chebychev–Grübler–Kutzbach as follows:

$$dof = m(N - 1 - J) + \sum_{i=1}^{J} c_i \tag{5.1}$$

where dof is the degree of freedom of the kinematic chain, m is the degree of freedom of each unconstrained single body (6 for special bodies and 3 for planar bodies), N: number of bodies or links including the ground, J: number of joints, and c_i: degrees of freedom allowed by the ith joint.

Considering a Stewart platform with six DOFs, the assumption of having these DOFs is given as follows. The number of known are only 2, including the base and the moving platform, while the number of legs and DOFs of each leg can vary so that we express them respectively as L and c_{L_i}. Since each leg has two links, there is a total of $2L$ legs, and adding the base and the top platform makes the number of bodies equal to $N = 2 + 2L$. Since each leg has three joints, the total number of joints is $J = 3L$. Accordingly, the previous equation can be rewritten as the following:

$$dof = 6 - 6L + \sum_{i=1}^{J} c_i. \tag{5.2}$$

Based on the previous equation, it is clearly noticed that thousands of possibilities for six-DOFs platforms can be found [195]. Thus, to limit the number of possibilities, some constraints are introduced.

For practical purposes, the number of legs in a Stewart platform has to have a maximum number equal to the DOFs of the mechanism (in our case, it is equal to $c_i = 6$) and has to have a minimum number of 3, which can be specified as the following:

$$6 \geq L \geq 3. \tag{5.3}$$

Once we defined the constraints on the number of possible legs for having a 6 DOF platform, the possible DOFs distributions can be enumerated as shown in Table 5.1.

Table 5.1. Possible DOFs distributions of Stewart Platform

Number of legs	c_{L_1}	c_{L_2}	c_{L_3}	c_{L_4}	c_{L_5}	c_{L_6}
3	6	6	6			
4	6	6	6	6		
5	6	6	6	6	6	
6	6	6	6	6	6	6

5.4.1. Joints arrangement

Typically, Stewart platforms support three different types of joints, including spherical, universal and prismatic (it is often given to hydraulic or pneumatic cylinders. To define the most possible practical configuration of a Stewart platform, three characteristics that describe the arrangement of joints are defined, which are the vertex structures, planarity and arbitrarily [196, 197].

5.4.1.1. Vertex structures

This characteristic defines the number of prismatic joints that share the same vertex in a platform. We can denote the vertex structure in a Stewart platform using two numbers separated by a dash in which the first number refers to the number of the vertices (joints) in the base, while the second number indicates the number of vertices on the mobile platform. Overall, there are about 36 different feasible combinations [196], such as 3-6, 4-6 and 6-6. The vertex structure combination 6-6, for instance, means that there are six joints in each platform, and each leg has its unique joint in the base and in the top platform. However, 3-6 means that we have three joints on the base and six in the top platform, and while each leg has an individual joint in the mobile platform, each two legs share one single joint in the base.

5.4.1.2. Planarity

This describes specifically whether the selected spherical or universal joints (of platforms) are located at the same plane of the platforms or at a different one. It can be decided for instance that not all joints of a certain platform be placed at an equal distance from the platform.

5.4.1.3. Arbitrarily

This describes the position of joints with respect to the center of each corresponding platform. Sometimes, all joints are positioned at an equal distance from the center, while in other cases they are not. As the number of possible legs in a Stewart platform is limited to 5, there are a maximum of six different configurations of joints (if each joint is placed at a proper distance from the center) and a minimum number of one configuration (if all joints are located at an equal distance from the center).

Using only these three joints criteria, a wide variety of six-legged Stewart platforms can be constructed. To reduce the number of possible configurations, some practical considerations have been taken in account, for example, it is difficult to manufacture a spherical joint that can be shared by more than two legs. Thus, after taking this fact into account as well as after reviewing all potential configurations that could practically be used and serve our application, it appears that five types of Stewart platforms are possible [198, 199]. One of them is a regular hexagon manipulator. It has regular and similar hexagonal mobile and base platforms. Another configuration is a semi-regular hexagons manipulator (SRHM), in which the joints are symmetric in pairs. The main characteristic of the SRHM is that the distance between the legs is greater than all other configurations. This feature has the advantage of reducing the potential of having interference between legs. The third structure is the simplified symmetric manipulator (SSM), which is characterized by having an axis of symmetry in the base and in the moving platform. The SSM is quite similar to the SRHM configuration with one major difference: the base and the mobile platforms are related to each other in shape with the same ratios. The fourth structure is triangular simplified symmetric manipulator (TSSM) which is similar to the SSM except that the mobile platform is triangular. The fifth configuration is the minimal simplified symmetric manipulator. It combines the TSSM with a 3-3 platform, and in this configuration, both the base and mobile platforms are similarly triangular. Figure 5-3 shows a top view of different configurations of Stewart platforms.

All these configurations have had extensity studies conducted on them during the last few decades. During the period from the invention of the Stewart platform to the mid-1980s, two types of configuration designs were widely utilized: 3-3 and 6-3 [187]. The main characteristics of these two types of configurations are that the Stewart platform can be constructed using a triangle shape for the construction of the base platform, for the structure of the mobile platform or for both platforms. Later, it was realized that legs that share the same spherical joints (as in the case of a triangle shape of platforms) severely hamper the mobility of the robot. Therefore, after the mid-1980s, 6-6 Stewart platforms have been considered as having the most practical configuration.

5.4.1. Kinematic modeling

The general assumption of a kinematic design of the Stewart platform consists that there is no restriction on what should be the number of the legs, vertex structures, degree of planarity and arbitrarily of joints of the platforms. However, some models, as we already discussed, have proved their limitations in providing high manipulability. Therefore, it is important to place some conditions that would help to find the optimal design that satisfies the kinematic requirements. These conditions are the following:

- **Vertex structures**: One of the most common issues related to the design of Stewart platforms is related to having limitations on providing a wide range of motion when there is a configuration consisting of one or more legs that share the same spherical joint. This type of configuration characterizes platforms having a triangular shape such as (e.g., 6-3, 3-6 or 3-3). Thus, we decided to avoid using this type of configurations.

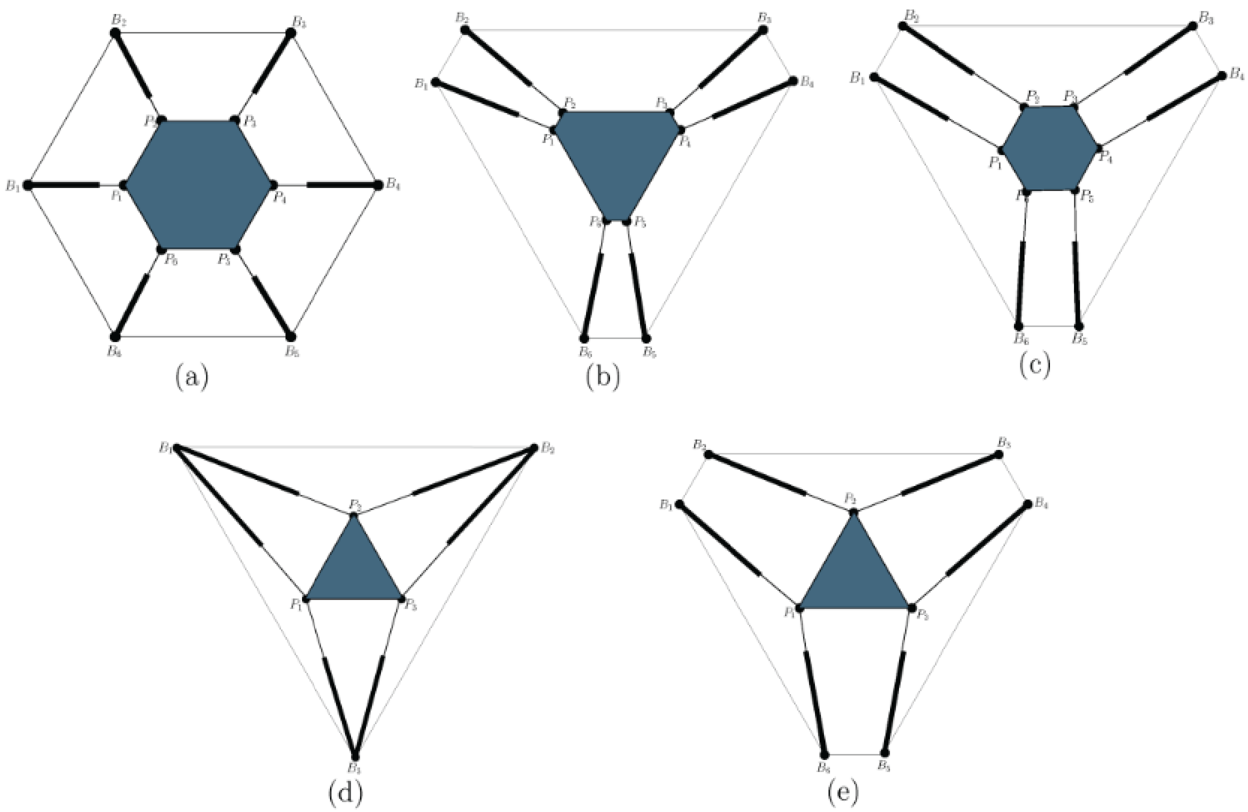

Figure 5-3. Top view of different configurations of Stewart platforms: (a) configuration with regular hexagon; (b) configuration with similar symmetric hexagons; (c) simplified symmetric manipulator; (d) minimal simplified symmetric manipulator and (e) triangular simplified symmetric manipulator [198].

- **Arbitrarity and planarity:** We are more concerned about studying 6-6 configurations because they have shown more advantages compared to other types of configurations. Although the semi-regular hexagons manipulator 6-6 SRHM is the most popular type of Stewart platform, it is important we make some changes to make the system feasible for our application. The first change consists of improving the configuration structure of a 6-6, single-circle Stewart platform by mounting joints located on the platforms on more than one concentric circle. The number of concentric circles can be decided with respect to an optimization analysis which is discussed later in this chapter. The second change consists of studying configurations that have joints that are not necessarily distributed in pairs. This will increase our odds of finding the best Stewart platform that meets our requirements when we solve the optimization problem.

5.5. Stewart platform kinematics

The six-DOFs Stewart platform consists of a moving platform and a base platform linked by six prismatic actuators with universal joints at the base and spherical joints at the moving platform. Figure 5-4 show a diagram of the 6-6-UPS Stewart platform.

In this diagram, two coordinate systems are established, including one global frame $\mathcal{R}: O - XYZ$ placed at a selected point on the static platform and a reference frame $\mathcal{R}': O' - X'Y'Z'$ located on the moving platform. Points $B_i(i = 1,2, \ldots \ldots, 6)$ are the universal joint centers on the base platform, and $P_i(i = 1,2, \ldots \ldots, 6)$ are the spherical joint centers on the moving platform. $\theta_i(i = 1,2, \ldots \ldots, 6)$ are the universal joints distributed angles of the base platform, and $\varphi_i(i = 1,2, \ldots \ldots, 6)$ are the spherical joints distributed angles of the moving platform. The Euler angles α, β and γ describe the orientation of the moving platform and respectively correspond to yaw, pitch and roll angles. We denote the vectors representing the prismatic actuators as L_i. The kinematics equation of the Stewart platform is

$$L_i = H + R.P_i - B_i \tag{5.4}$$

where H denotes the Cartesian coordinates of the end-effector frame with respect to the base frame and R is the rotation matrix, which can be written as

$$R = \begin{bmatrix} c\alpha c\beta & -s\alpha c\gamma + c\alpha s\beta s\gamma & s\alpha s\gamma + c\alpha s\beta c\gamma \\ s\alpha c\beta & c\alpha c\gamma + s\alpha s\beta s\gamma & -c\alpha s\gamma + s\alpha s\beta c\gamma \\ -s\beta & c\beta s\gamma & c\beta c\gamma \end{bmatrix} \tag{5.5}$$

where s and c denote the functions sine and cosine, respectively.

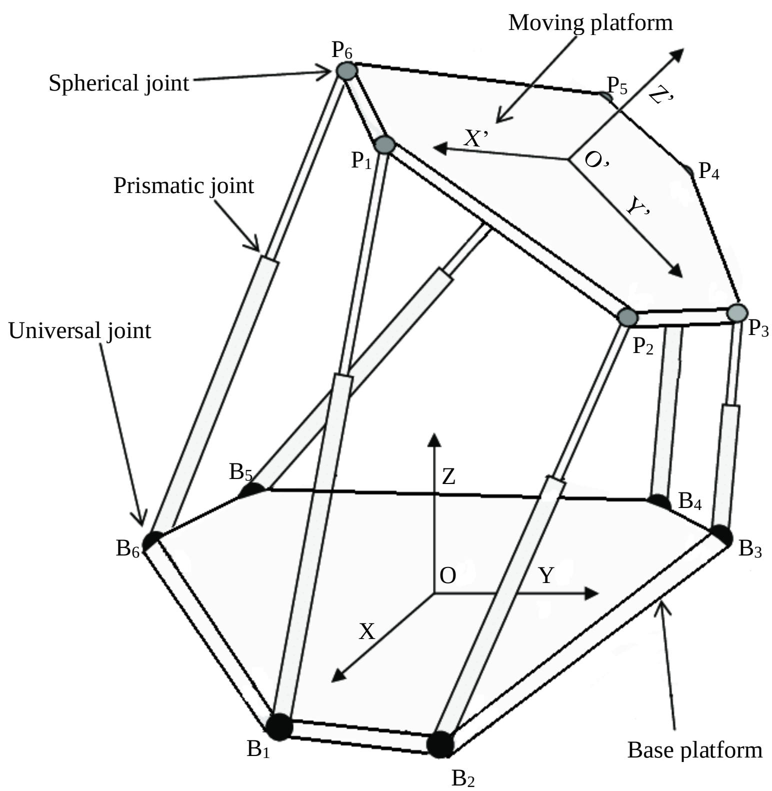

Figure 5-4. 6-6-UPS Stewart platform.

As the kinematic equation of the Stewart platform is defined, it is important to describe the kineto-statics of it. Kineto-statics describes the relationship between the *twist vector* containing the velocity of a point on the platform and its angular velocity [195] and the *wrench vector* containing forces and moments acting on the point when the system moves under static, conservative conditions [200]. This can be obtained using kinematic and static equations, both of which depend on a Jacobian matrix. Thus, to describe the kineto-statics of the Stewart platform, it is important to first derive the Jacobian matrix.

The Jacobian matrix of the Stewart platform relates the prismatic joints velocities of the legs $\dot{L}$ to Cartesian end-effector velocities $\dot{Q}$ (also known as *twist vector*). This relation can be deduced as

$$\dot{Q} = J^{-1}\dot{L} \tag{5.6}$$

where J is the Jacobian matrix.

This equation can be derived by differentiating Equation **Error! Reference source not found.** with respect to time, which gives

$$\dot{L_\iota}.u_i + L_i\dot{u_\iota} = \dot{H} + (\omega \times R.P_i) \tag{5.7}$$

where u_i is the unit vector corresponding with ith prismatic joints. Knowing that $u_i.u_i = 1$ and $u_i.\dot{u_\iota} = 0$, we can rewrite the previous equation as

$$\dot{L_\iota} = \dot{H}u_i + (R.P_i \times u_i).\omega. \tag{5.8}$$

We denote the vector P_i after applying the rotation as T_i, so that we have $T_i = R.P_i$, defining the vector of translational and angular velocities as

$$\dot{L} = \begin{bmatrix}\dot{H} & \omega\end{bmatrix}. \tag{5.9}$$

Equation (5.6) can be rewritten as

$$\dot{Q} = J^{-1}\begin{bmatrix}\dot{H} & \omega\end{bmatrix}, \tag{5.10}$$

from which the inverse Jacobian matrix is given by

$$J^{-1} = \begin{bmatrix} u_1^T & (T_1 \times u_1)^T \\ \vdots & \vdots \\ u_6^T & (T_6 \times u_6)^T \end{bmatrix}. \tag{5.11}$$

To obtain the static model of the Stewart platform, we have to relate the external forces and moments applied to the moving platform and the forces and moments to the actuators.

We denote $\tau = [f, M]$, the resultant wrench applied on the moving platform in which f and M are the total forces and moments applied on the moving platform. The static model can be written as

$$\tau = J^{-T}.g \tag{5.12}$$

where g is the resultant forces in the actuators. To g , we rearrange the previous equation as

$$g = J^T.\tau. \tag{5.13}$$

To obtain the resultant forces applied on the moving platform, we can multiply the first row of J^{-T} by the vector g, so that we get

$$f = u_1^T . f_1 + \cdots + u_6^T . f_6. \quad (5.14)$$

To obtain the resultant moments applied on the moving platform, we denote the rotation inverse Jacobean submatrix as:

$$J_R^{-1} = \begin{bmatrix} (T_1 \times u_1)^T \\ \vdots \\ (T_6 \times u_6)^T \end{bmatrix}. \quad (5.15)$$

This allows us to express the vector moment M as

$$M = J_R^{-1} . f^T. \quad (5.16)$$

5.6. Kinematic performance indices

Evaluation indices are a set of scale quantities used to describe the performance of a manipulator in a response to a given position and a given force. These indices have been widely investigated in the period from the 1970s to now, especially for the purpose of optimizing the mechanical properties of existing robotic systems. Kinematic performance indices that are based on the Jacobian matrix are as follows.

5.6.1. The singular value index

The singular value index has a major importance for analyzing the characteristics of mapping velocities from joint to Cartesian space using the Jacobin matrix, which is a linear transformation between the two spaces. Singular values of the transformation matrix tell one which direction in the space the Cartesian velocities are maximized with respect to the joint velocities. The term "eigenvalues" is usually associated with matrices that are diagonal. However, because Jacobian matrices are often not diagonal matrices, they can be diagonalized with the singular value decomposition method, and the associated eigenvalues are called singular values [201, 202].

The singular value decomposition considers any linear transformation as a set of three simple operations: rotation, stretch and rotation. For a given $(m \times n)$ matrix J^{-1} or rank r, and by using the singular value decomposition theory, the J matrix can be factorized as

$$J^{-1} = U \ \Sigma \ V^T \quad (5.17)$$

Where U is an $(m \times m)$ orthogonal matrix containing the eigenvectors of $J^{-T} J^{-1}$, Σ is an $(m \times n)$ diagonal matrix that contains a D $(r \times r)$ matrix which its diagonal elements are the singular values of J, and J^{-1} is an $(n \times n)$ orthogonal matrix that has the eigenvectors of J^{-1}.

The $(m \times n)$ matrix Σ has the following form:

$$\Sigma = \begin{bmatrix} D_{r \times r} & 0_{r \times (n-r)} \\ 0_{(m-r) \times r} & 0_{(m-r) \times (n-r)} \end{bmatrix}. \quad (5.18)$$

For an arbitrarily $J^{-1}(m \times n)$ matrix, the $J^{-T}J^{-1}$ is symmetric. Though to find the singular values of J^{-1}, we consider $\{U_1, \dots\dots, U_n\}$ as an orthonormal basis for $\mathbb{R}^n$, consisting of eigenvectors of $J^{-T}J^{-1}$, and we consider $\lambda_1, \dots\dots, \lambda_n$ as associated eigenvalues of $J^{-T}J^{-1}$. Then, for $1 \leq i \leq n$, we have

$$\|J^{-1}U_i\|^2 = (J^{-1}U_i)^T J^{-1}U_i = {U_i}^T J^{-T}J^{-1}U_i \\ = {U_i}^T(\lambda_i U_i) \tag{5.19}$$

since U_i is an eigenvector of $J^{-T}J^{-1}$, and

$$= \lambda_i I = \lambda_i$$

since U_i is a unit vector.

Singular values of J^{-1} are the square roots of $J^{-T}J^{-1}$ which can be denoted as $\sigma_1, \dots\dots, \sigma_n$. This gives

$$\sigma_i = \sqrt{\lambda_i}. \tag{5.20}$$

The singular values of J^{-1} are also the lengths of the vectors $J^{-1}U_1, \dots\dots, J^{-1}U_n$.

By substituting Equation (5.17) in (5.6), the kinematic model becomes

$$\dot{Q} = U \ \Sigma \ V^T \dot{L}. \tag{5.21}$$

To get the associated unite vector with both joint and Cartesian velocities, we multiply both part of Equation (5.21) by U^{-1} (since U is orthogonal, $U^T = U^{-1}$). This gives

$$U^T \dot{Q} = \ \Sigma \ V^T \dot{L}. \tag{5.22}$$

From this equation, we deduce that $\{V_1, \dots\dots, V_n\}$ and $\{U_1, \dots\dots, U_n\}$ form orthonormal bases for the subspace of $\dot{L}$ and $\dot{Q}$, respectively. In addition, it is important to notice that singular values σ_i represent the velocity transmission ratio from the joint space to the Cartesian space in the Stewart platform.

The kinematic model allows us to evaluate the performance of transforming joint velocities to workspace velocities. To do so, we consider that the length of the vector of the set velocities of all joint is not greater than the length of the unit vector:

$$\dot{L}^T \dot{L} \leq 1. \tag{5.23}$$

Then we can write the corresponding Cartesian velocities of the end-effector as

$$\dot{Q}^T J^{-T} J^{-1} \dot{Q} \leq 1. \tag{5.24}$$

Physically, this equation represents the equation of a hyper-ellipsoid which is, for the six-DOFs Stewart platform, an ellipse in six dimensions. The major half axial lengths of the ellipse are eigenvalues of $J^{-T}J^{-1}$ which represent singular values of J^{-1}. We suppose that joint velocities of the Stewart platform are limited in this way:

$$-\dot{L}_{min} \leq \dot{L} \leq \dot{L}_{max}. \tag{5.25}$$

Then, the associated Cartesian velocities of the end-effector can be expressed as the following:

$$\dot{Q}_{min} \leq \dot{L} \leq \dot{Q}_{max} \tag{5.26}$$

with

$$\dot{Q}_{min} = min\left(J^{-1}.\dot{Q}\right). \tag{5.27}$$

This signifies that the value of the largest value of the axis constituting the ellipse corresponds with the largest value of the joint velocities. Accordingly, we can use the singular value index to define the maximum velocity of the prismatic joints of the Stewart platform since these are associated with the maximum singular value σ_{max} of the Jacobian matrix. Moreover, we can easily not describe the relationship between the joint and Cartesian space velocities. For instance, we suppose for a given end-effector velocities that the maximums values of the singular values of the Jacobin matrix are large. Then we can deduce that the joint velocities will have significant values. Therefore, it is important to minimize the maximums of singular values when designing a Stewart platform.

5.6.2. Manipulability index

The concept of manipulability was first introduced by Yoshikawa [203] to describe how close a robot is to being singular by analyzing velocities that have the form of an ellipse. The volume of the velocity ellipsoid gives an indication of the ability of the robot to generate a velocity [201]. The manipulability of a robot is defined as

$$m = \sqrt{JJ^T} = \sqrt{\det\,[JJ^T]}. \tag{5.28}$$

This can also be expressed as the product of singular values of the Jacobian matrix, which gives

$$m = \sigma_1\sigma_2 \,\ldots.\, \sigma_n. \tag{5.29}$$

Accordingly, we can check if the robot configuration is close to being singular or not by analyzing the values of singular values of the Jacobin matrix we have. If at any position of the end-effector at least a singular value is equal to zero (the case when the Jacobian matrix is not invertible), then this means that the robot lost one or more DOFs in the Cartesian space. In addition, if singular values are not high (if the manipulability is close to 0), then it will be difficult to move the robot in one direction.

5.6.3. Condition number index

The condition number index evaluates how close the maximum and the minimum of the singular values of the Jacobian matrix are or how the maximum and minimum lengths of the axis of velocity ellipse are close to being equal. The condition number is defined as the following:

$$\kappa = \|J^{-1}\|_2\|J\|_2 = \frac{\sigma_{max}}{\sigma_{min}} \tag{5.30}$$

where $\|.\|_2$ is the 2-norm of a matrix.

The reciprocal of the condition number, also called the local condition index (LCI), is also often used to evaluate how singular values are close to being equal. The LCI is defined as

$$\kappa^{-1} = \frac{1}{\|J^{-1}\|_2 \|J\|_2} = \frac{\sigma_{min}}{\sigma_{max}}. \tag{5.31}$$

The condition number is another way to describe the degree of isotropy and dexterity of the manipulator. A kinematic system is isotropic if, for a given end-effector position, the resulting Cartesian velocities exhibit homogeneous behavior in all directions. In other words, this signifies that all singular values are identical. In a three-dimensional representation, this harmony of velocities can be visualized as a sphere. For a six-DOFs Stewart platform, this can be expressed as the following:

$$J^{-T} J^{-1} = \sigma^2 I_{6\times 6}. \tag{5.32}$$

However, it is important to notice that it is possible that the transformation from the joint velocities to the Cartesian velocities do not create a uniform sphere. Therefore, the term dexterity is used instead to measure the degree to which the unit sphere is distorted by the mapping [197] or to define the degree of isotropy in a given point for the robot. This can be achieved using the LCI which is defined by a scale from 0 to 1. A value of 1 signifies when there is an isotropic configuration [204].

The inverse condition index describes the dexterity of the robot only in a specific point in the Cartesian space. To measure the dexterity over the whole workspace, the global conditioning index is proposed. It is defined as follows:

$$GCI = \frac{\int_w (LCI) dw}{\int_w dw} \tag{5.33}$$

where w is the workspace of the manipulator.

The global conditioning index is useful for defining the global performance of the robot since it represents the average values of the LCI in the entire workspace. To have a more precise descriptive image to the degree of dexterity in the whole workspace, it is important to choose an adequate number of points to calculate the LCI.

5.7. Stewart platform design optimization

A typical Stewart platform is not appropriate for use in our application due to specific considerations we have. Our requirements include achieving a specific workspace and improving dexterity. Therefore, an optimized solution has to be searched for to meet our requirements.

5.7.1.1. Preferable workspace

The preferable workspace of the Stewart platform is defined according to two objectives.

First, the Stewart platform will be utilized for compensating the translation movements of the XYZ mechanism. As it is expected, the value of compensated movements is not high. Therefore, we accept that the boundary volume of 5 cm of a workspace of translation movements of a Stewart platform is a volume adequate for compensating all the movements of the XYZ mechanism.

Second, the system will be utilized to support the rotation movements of the user's foot. During the walking process, the rotation of the foot with respect to the sagittal plan is considered to be significantly large. Although the maximum range of motion of the ankle flexion is 20.3°–29.8°, the rotation of the foot is greater than that because the rotation of the knee is added to the initial rotation angle of the ankle. The total angle of rotation of the foot with respect to the horizontal axis is a function of the walking speed. The total rotation angle would be small at a normal speed and significantly large when sprinting. Figure 1-2 illustrates the range of motion of rotation of the foot according to different walking speeds.

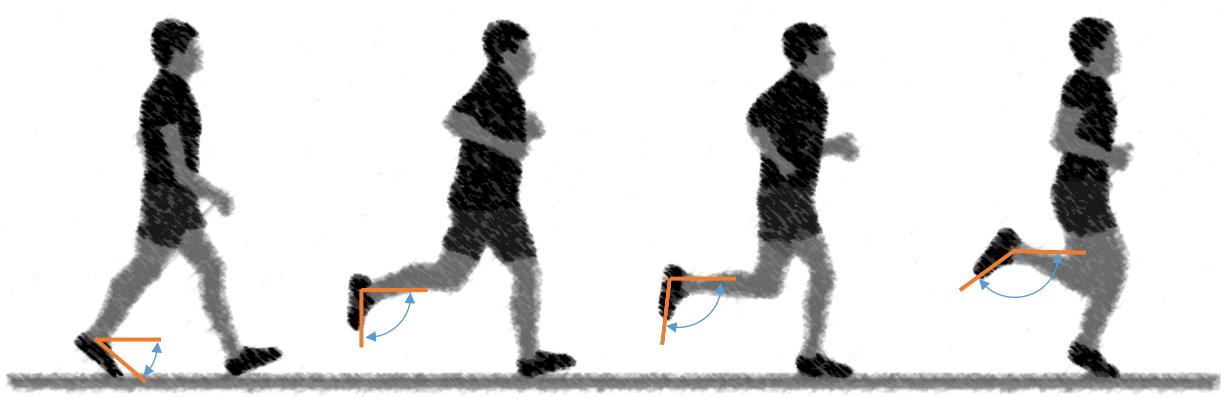

Figure 5-5. Range of motion of rotation of the foot according of different walking speeds.

Therefore, the preferable range of motion of the pitch angle of the Stewart platform we aim to optimize is selected to be as large as possible. The preferable range of motion of the roll and yaw angles of the platform we aim to optimize are respectively chosen with respect to the maximum angles provided by the planaflexion and dorsiflexion of the ankle.

5.7.1.2. Kinematic constraints consideration

The workspace of the Stewart platform involves three types of kinematic constraints which should be considered while searching for the optimal Stewart platform configuration. The three kinematic constraints are the link length limitations, joint angle limits and link interference.

A) Joint angle limits

The prismatic legs of the Stewart platform are attached to the base and the moving platforms, respectively, by universal and spherical joints. It is supposed that both of these joints are free to rotate about the axes, representing the degree of freedom they support. However, in practice, movements of these joints are restricted by their physical constraints. For instance, the motion of the boil joint is restricted by the maximum angle defined by its socket (Figure 5-6).

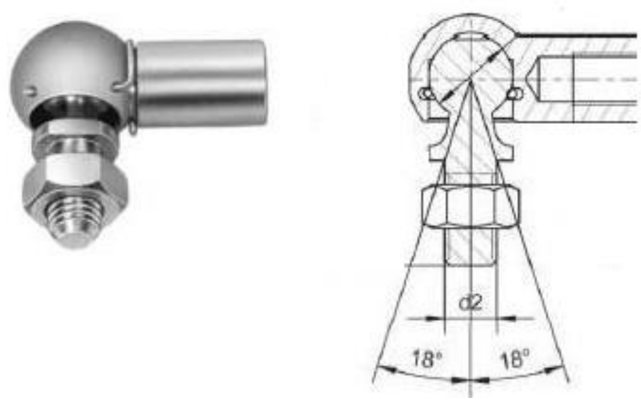

Figure 5-6. Boil joint having a maximum rotation angle of 18° [205].

The rotational angle and its limit can be computed as follows:

$$\theta_i = cos^{-1}\left(\frac{L_i . n_i}{|n_i|}\right) \leq \theta_{i(\max)} \tag{5.34}$$

where n_i is the unit vector that describes the rotational range of each leg with respect to a reference frame. $\theta_{i(\max)}$ is the maximum allowable rotational angle of the joint.

B) Link interference

Since the legs of the Stewart platform have physical dimensions, collision between them may occur. To avoid interference between legs, the shortened distance between two successive legs d_{legs} must be defined. This distance is given by the following equation:

$$d_{legs} = \frac{\left|\overrightarrow{B_\iota B_{\iota+1}} . \overrightarrow{(u_\iota \times u_{\iota+1})}\right|}{\left\|\overrightarrow{u_\iota \times u_{\iota+1}}\right\|} \tag{5.35}$$

where B_i and B_{i+1} are, respectively, the positions of joints connecting i and $i+1$ legs with the moving platform of the Stewart platform while u_i and u_{i+1} are the corresponding legs vector units.

To avoid any collision between the legs of a Stewart platform, the distance d_{legs} has to be greater than the outer diameter of the actuators.

C) Link length limitations

The legs of a Stewart platform include two main parts: the upper (which also called a stroke of the hydraulic cylinder) and lower legs. The link length limitation constraint describes the situation in which a position in the free workspace requires a link that has a total length either greater than the maximum length the link can provide or less than the length of the minimum length the link can provide [206]. This can be expressed as follows:

$$L_{i(\min)} \leq L_i \leq L_{i(\max)} \tag{5.36}$$

where $L_{i(\min)}$ and $L_{i(\max)}$ are, respectively, the minimum and maximum allowable length of the leg i.

5.7.1.3. Design configurations and variables

Selecting certain design variables of an optimization objective function rather than others can be crucial for finding the optimal Stewart platform configuration that satisfies our requirements. Design variables can influence the time required for finding the minimum or the maximum of the objective function. Certain variables allow the objective function to converge after a short number of iterations while others allow that after more iterations. Overall, the objective function can be influenced by the type of design variables selected, the number of these variables and the constraints placed on them. To increase the odds of finding better solutions, we suggest that we study two different types of Stewart platform configurations. This means that we will have two different types of design variables for the same objective function.

A) Three-circles Stewart platform

Although a single cycle Stewart platform design is the simplest and the widely used type of configuration, this design puts more restrictions on the ability to position joints in an arbitrary way on platforms. To solve this problem, we suggest that each pair of the six joints of each platform should vary independently of the two other pairs. This would give us a Stewart platform called a three-circles platform in which the actuators are located on three circular paths on each platform. The radius of the i circular paths (j varies from 1 to 3) of the base and the moving platforms are respectively denoted as $r_{b(j)}$ and $r_{p(j)}$. Angles separating one pair of joints on the base and the moving platform are respectively denoted as $\varphi_{b(j)}$ and $\varphi_{p(j)}$. In addition, h represents the height or the vertical distance separating the two platforms. Figure 5-7 shows a drawn model of the three-circles Stewart platform configuration where all of the variables mentioned here are described.

In the three-circles Stewart platform configuration, the legs are distributed evenly with respect to angles $\varphi_{b(j)}$ and $\varphi_{p(j)}$. To define the vector that describes the position of the six joints associated with each platform, we denote the position angles for the i *'th* actuators on the base and platform respectively as $\psi_{b(i)}$ and $\psi_{p(i)}$. These positions allow for an equal spacing between the pair joints located on the platforms, which can be calculated as follows:

$$\begin{aligned} &\psi_{b(i)} = \frac{i\pi}{3} - \frac{\varphi_{b(j)}}{2} \qquad \psi_{p(i)} = \frac{i\pi}{3} - \frac{\varphi_{p(j)}}{2} \qquad for\ i = 2,4,6\ and\ j = 1,2,3 \\ &\psi_{b(i)} = \psi_{b(i+1)} + \varphi_{b(j)} \qquad \psi_{p(i)} = \psi_{p(i+1)} + \varphi_{p(j)} \qquad for\ i = 1,3,5\ and\ j = 1,2,3 \end{aligned} \quad . (5.37)$$

Accordingly, we can calculate the position of the joints connecting the legs with the base and moving platforms as follows:

$$B = \begin{bmatrix} r_{b(j)}cos(\psi_{b(i)}) \\ r_{b(j)}sin(\psi_{b(i)}) \\ 0 \end{bmatrix} = \begin{bmatrix} b_{ix} \\ b_{iy} \\ b_{iz} \end{bmatrix} \quad for\ i = 1..6\ and\ j = 1,2,3$$
$$P_i = \begin{bmatrix} r_{p(j)}cos(\psi_{p(i)}) \\ r_{p(j)}sin(\psi_{p(i)}) \\ h \end{bmatrix} = \begin{bmatrix} p_{ix} \\ p_{iy} \\ p_{iz} \end{bmatrix} \quad for\ i = 1..6\ and\ j = 1,2,3 \quad . (5.38)$$

Since the base and moving platforms of the Stewart platform are rigidly connected with hydraulic cylinders, the kinematic characteristic of the Stewart platform will vary according to the selected minimum length of these cylinders l_{min}. Therefore, the minimum length of the cylinder is also introduced as a design variable. Accordingly, the number of variables for an objective function in the case of the three-circles Stewart platform is equal to 14. Variables of the objective function are the following:

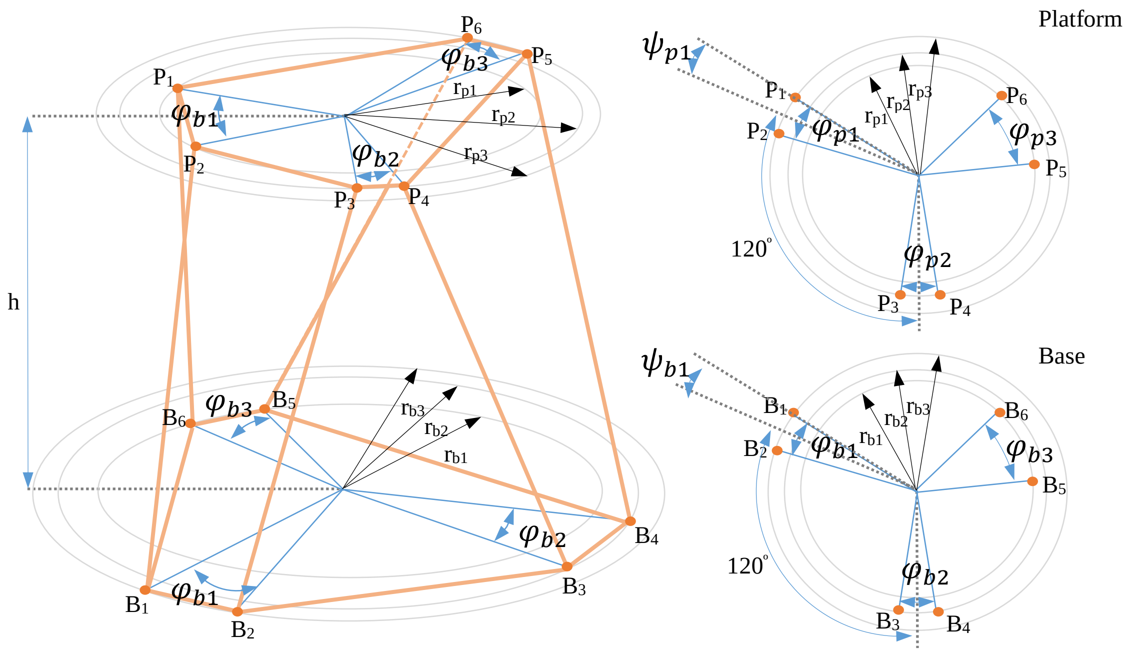

Figure 5-7. Three-circles Stewart platform.

$$\lambda = [r_{b1} \quad r_{b2} \quad r_{b3} \quad \varphi_{b1} \quad \varphi_{b2} \quad \varphi_{b3} \quad r_{p1} \quad r_{p2} \quad r_{p3} \quad \varphi_{p1} \quad \varphi_{p2} \quad \varphi_{p3} \quad h \quad l_{min}]. \quad (5.39)$$

B) Six-circles Stewart platform

In the six-circles Stewart platform design, actuators are placed on six circular paths on both platforms, which means that each position of the six actuators can be described by a vector independent of the other ones. The objective is to improve the dexterity and workspace indices compared to three-circles Stewart platform, as we have more independent design variables. Vectors that describe the position of joints on the base and on the moving platforms are denoted respectively as B_i and P_i where i varies from 1 to 6. Figure 5-8 shows a drawn model of the six-circles Stewart platform configuration where all the variables mentioned here are described.

Including the variable that defines the minimum cylinder length (l_{min}), the kinematic design of the six-circles Stewart platform can be then be described by 26 design variables as the following:

$$\lambda = [B_{1x} \quad B_{2x} \quad B_{3x} \quad B_{4x} \quad B_{5x} \quad B_{6x} \quad B_{1y} \quad B_{2y} \quad B_{3y} \quad B_{4y} \quad B_{5y} \quad B_{6y} \quad P_{1x} \quad P_{2x} \quad P_{3x} \quad P_{4x} \quad P_{5x} \quad P_{6x} \quad P_{1y} \quad P_{2y} \quad P_{3y} \quad P_{4y} \quad P_{5y} \quad P_{6y} \quad h \quad l_{min}] \tag{5.40}$$

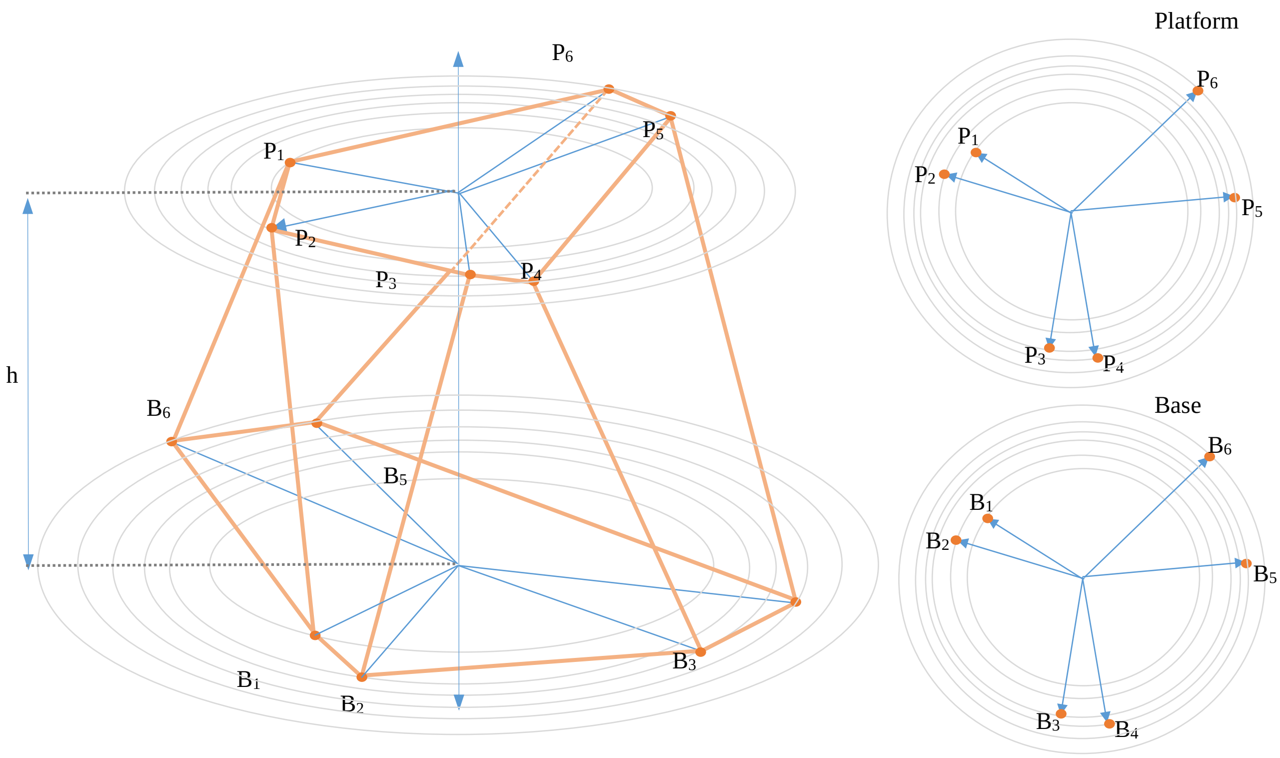

Figure 5-8. Six-circles Stewart platform.

5.7.1.4. Multi-objective optimization function

The optimization of the platform's structure can be done according to many criteria. The Stewart platform is implemented for two purposes:

- Compensating a small range of translation motions that the base cannot perform well due to the limited bandwidth.
- Performing different rotations according to the XYZ frame.

In such a configuration, the performance of the platform is affected by many factors. The singular values can well describe the behavior of the system according to certain directions in the workspace. Singular values give the ratio between the input and the output (velocities and forces). Therefore, a small singular value means a small ratio between the leg velocities and the platform velocities and a large ratio between forces. If the difference between the minimum and the maximum of the singular values is large, then the system not isotropic. Thus, in some directions we have high impedance, while in others we have low impedance.

The desired system may be anisotropic since there are some directions that are more important than others. However, extracting just singular values without their corresponding vectors makes them less important. Therefore, it is recommended to try to make the system isotropic to avoid complex criteria. Nevertheless, in an isotropic system, it is quite easy to reach a balance between the velocity ratio and the force ratio, which go in opposite directions.

Normalizing the units is one of the most important issues in this case. The dimension of the motion of the platform is evaluated in two units: length and angles. Therefore, the comparison of different dimensions in different units is not meaningful unless we normalize different units to certain properties where we can consider them as having the same impact. In our case, we have decided to normalize the angle to the linear motion resulting from a rotation made by a ray of about 1 foot. Therefore, we replace angles by their corresponding translations as follows:

$$Tran = Angle * L \text{ where } L = 30 \text{ cm} \tag{5.41}$$

where $Tran$ is the vector that describes the normalized $Angle$ resulting from a rotation made by the ray L of about 1 foot.

Therefore, the optimization has to do the following:

- Maximize the angular workspace, especially according to the x-axis.
- Minimize the difference between the minimum and maximum of the singular values of the Jacobian matrix.

5.7.1.5. Penalty function

Generally, the optimization function is made in a way that the optimal solution has the lower value. In a multi-objective function, the result is a weighted average of all the single functions as described in Equation (5.42) ($f_i(x)$ is a singular objective function and w_i is its weight):

$$\Phi = \sum_{i=1}^{k} w_i f_i(x) \tag{5.42}$$

Therefore, to exclude some undesirable solutions from an objective function because they are impossible, we should use a function that tends to infinity for the excluded solution. In our system, we have some kinematic constraints such as the link length limitations, the joint angle limits and the link interference. The best way to exclude these solutions from being part of the objective function results is by using a penalty. This penalty function should rise smoothly when approaching the limits, then rise rapidly at the very limits where the exponential function fits this condition well.

The main objectives of the optimization of the Stewart platform are to maximize the workspace and to increase the dexterity of the system. With the addition of the penalty condition to the sum of these two objectives, the multi-objective for our optimization problem can be written as follows:

$$\Phi = GCI.w + WorkInd(1 - w) + PntInx. \tag{5.43}$$

As mentioned earlier, the manipulability index represents the mean amplification of the system regardless of whether it is isotropy. Thus, if some configurations have the same manipulability, this does not mean that they have similar behaviors.

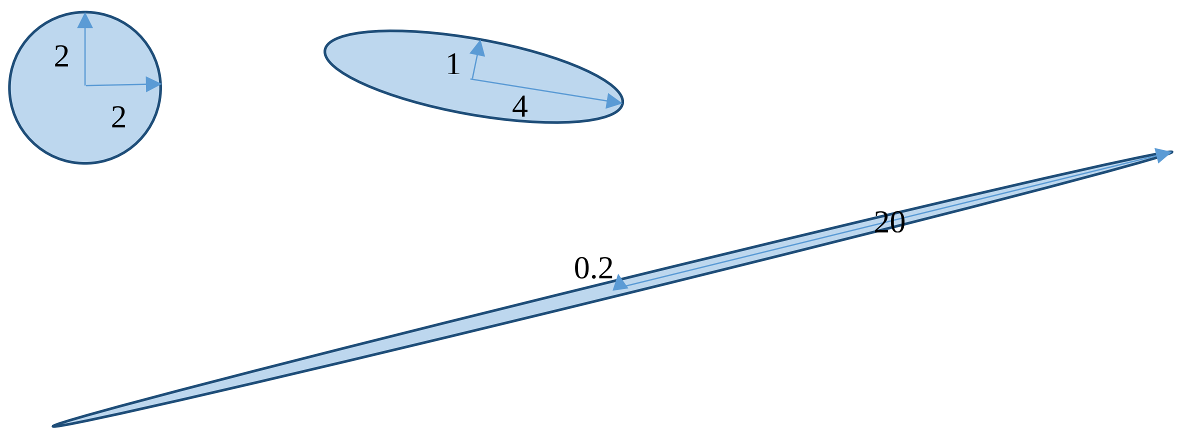

Figure 5-9. Diagrams having the same manipulability that is equal to 4.

Figure 5-9 shows an example of different diagrams having the same manipulability (= 4). However, it is quite difficult to conclude that these three systems have similar mechanical properties. The first system has an amplification of 2 in all directions, the second system has an amplification of 1 in the minimum singular value direction and 4 in the maximum singular value direction and the third system has an amplifications of 0.2 and 20 in the minimum and maximum directions. Therefore, we can easily conclude that the manipulability index does not contain an important significance. Multiplying the amplifications in different directions in not very intuitive, while considering the minimum and the maximum values of the singular values looks more intuitive. Therefore, we decided not to consider the manipulability index.

5.7.1.6. Results

The optimization of Stewart platform has been investigated for two different types of configurations: the three-circles and six-circles platforms. For both configurations, the objective function has been defined so that we optimize the dexterity and workspace of the platform, while ensuring a minimum distance between feet. The most desirable space between feet is zero which allows one to simulate walking more naturally. However, practically, the mechanical complexity of the design, primarily related to the selected length of actuators and the positioning of the actuators on the platforms, can impose a distance between feet that is greater than the desired one. Therefore, to define a feasible solution that can be physically achieved, we studied various types of configurations that are characterized by having different distances between feet. The genetic algorithm of the MATLAB Optimization Toolbox has been selected as the main solver for solving the optimization problem. However, in the case of results that contain no feasible solutions (the case when the penalty function returns a high value), we alternatively use the pattern search solver. Regarding the input parameters, the genetic algorithm does not require selecting an initial starting point as the initial generation of candidate solutions that are tested against the objective function, are initiated by the solver itself. In contrast to the genetic algorithm, in the pattern search solver, the initial starting point is selected manually, and results can change based on the values of the initial guess. Therefore, different initial guesses are tested, and we table values that lead to the most optimal solution (Table 3.4 and Table 5.3). Figure 5-10 and Figure 5-11 show solutions obtained from optimizing three- and six-circles Stewart platform configurations.

Overall, the dexterity obtained from different optimized configurations are with compatible values for having a platform in which the internal forces and velocities in any direction in the workspace are uniform. However, some of the solutions obtained are either difficult or impossible to realize.

Results show a significant difference between optimizing three- and six-circles platforms in terms of shapes. While most solutions obtained from optimizing the three-circles platform resulted in a base and moving platforms having shapes more or less regular as well as sizes that are approximately equal, optimizing the six-circles platform provided a platform with random shapes and important contrasts in size. For example, it is clear that among platforms with three circles illustrated in Figure 5-10 from (a) to (g), almost all of them have a base and moving platforms with a hexagonal regular shape of nearly the same size. Opposite of this pattern, the six-circles platforms shown in Figure 5-11 exhibit a sort of random hexagonal regular shapes that form groups of shapes significantly different than each other (the group of shapes the include [a], [e] and [f] is very different than the group of shapes that include [b], [c] and [d]). Practically, the implementation of solutions for six-circles platforms signifies the use of cylinders that are significantly different in length. These solutions are practically undesirable. Therefore, in terms of the elimination process, we excluded all solutions obtained by optimizing the six-circles Stewart platform. Moreover, and for the same purpose, we exclude the three last shapes of the three-circles platforms. This is because the six cylinders comprising these three platforms are considerably long and close to each other, which would result in an unstable system. Accordingly, the most appropriate solution for the three remaining circle platforms, (a), (b) and (c), is the platform represented in Figure 5-10 (c) because the distance between the user's feet in this design is the shortest one compare to that of the two other platforms, (a) and (b).

Table 5.2. Optimization of the three-circles Stewart platform in relation to a selected value of a minimum distance between feet (MinD).

MinD (cm)	Method	Results		
		Idx	Iterations	Configuration
20	Genetic algorithm	2.851	411	[20.000 20.000 20.000 49.644 49.634 55.994 20.000 19.994 20.000 7.181 7.470 7.181 33.268 26.755]
15	Genetic algorithm	4.264	336	[19.999 20.000 15.627 7.332 7.181 43.711 19.898 16.012 11.185 44.159 39.518 12.917 28.672 24.006]
10	Genetic algorithm	6.007	359	[17.983 10.244 10.841 44.226 47.479 37.282 20.000 13.615 14.107 16.043 10.582 10.208 29.474 24.000]
8	Genetic algorithm	2.753	579	[9.773 8.499 5.194 37.116 40.261 28.772 5.002 5.183 6.198 31.944 29.280 35.163 41.553 38.213]
7	Genetic algorithm	2.643	631	[5.437 7.590 7.583 31.343 37.256 37.372 6.464 5.033 5.047 37.785 30.215 30.308 26.556 24.180]
6	Genetic algorithm	8.123	679	[10.411 8.067 8.066 50.791 18.055 18.056 10.066 6.799 6.812 61.614 31.939 31.738 38.176 34.566]
5	Genetic algorithm	0.215	780	[3.206 5.296 5.363 12.774 40.737 38.785 1.800 1.226 1.204 36.636 20.456 19.093 50.124 35.397]

Table 5.3. Optimization of the six-circles Stewart platform in relation to a selected value of a minimum distance between feet (MinD).

MinD (cm)	Method	Results		
		Idx	Iterations	Configuration
30	Genetic algorithm	6.056	111	[2.104 -9.351 -14.262 8.731 19.376 15.440 20.336 9.676 -6.484 -20.406 -1.648 4.619 6.222 -13.239 -13.576 -4.435 0.189 1.589 9.426 15.406 0.768 -6.708 -6.760 -0.064 44.284 38.710]
30	Pattern search	0.871	1417	[2.319 -15.991 -10.751 25.259 25.376 21.055 13.826 7.635 -26.109 -30.000 11.110 11.619 7.225 -1.837 -6.576 -7.435 10.800 5.589 10.218 9.862 1.243 -6.708 -6.760 -3.670 31.176 30.710]

20	Pattern search	0.871	462	[2.319 -15.992 -10.751 25.259 25.376 21.055 13.826 7.635 -26.109 -30.000 11.110 11.619 7.225 -1.837 -6.576 -7.435 10.799 5.589 10.218 9.862 1.244 -6.708 -6.760 -3.670 31.176 30.710]
15	Pattern search	0.872	1412	[2.935 -15.000 -10.237 25.258 25.375 20.916 13.829 7.708 -26.126 -30.000 11.071 11.619 7.262 -1.777 -6.576 -7.435 10.653 5.589 10.098 9.834 1.165 -6.708 -6.760 -3.513 30.812 30.710]
10	Pattern search	8.310	102	[-7.157 -5.695 -0.834 7.561 10.299 0.125 11.421 -8.952 -14.420 -13.491 2.840 11.570 -5.085 -0.273 -3.138 4.737 11.746 -2.220 5.271 -1.184 -4.735 -5.692 2.287 9.533 63.639 50.482]
8	Pattern search	8.310	102	[-7.157 -5.695 -0.834 7.561 10.299 0.125 11.421 -8.952 -14.420 -13.491 2.840 11.570 -5.085 -0.273 -3.138 4.737 11.746 -2.220 5.271 -1.184 -4.735 -5.692 2.287 9.533 63.639 50.482]

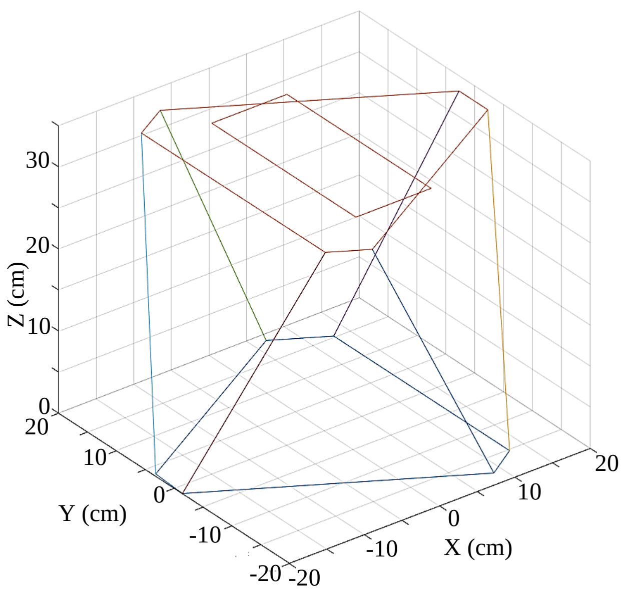

(a)

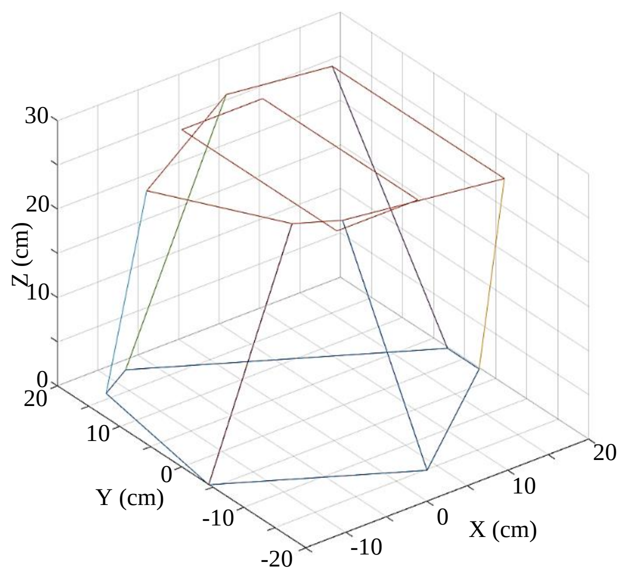

(b)

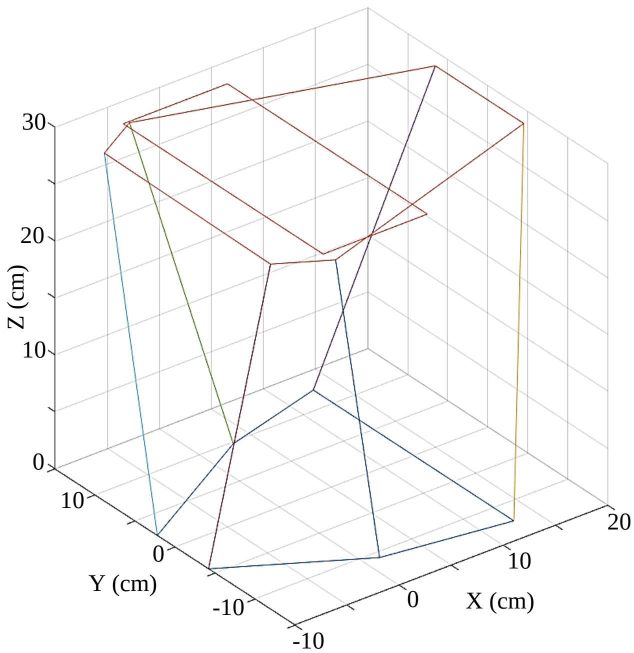
30
20
10
0
Z (cm)
10
0
-10
Y (cm)
-10
0
10
20
X (cm)

(c)

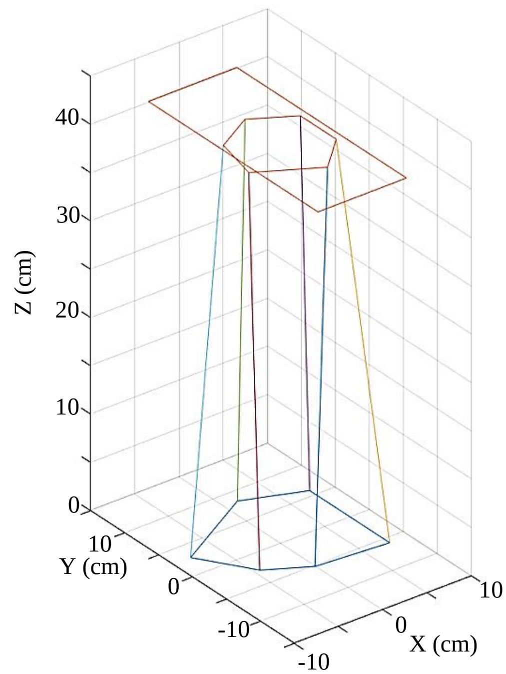
40
30
20
10
0
Z (cm)
10
0
-10
Y (cm)
-10
0
10
X (cm)

(d)

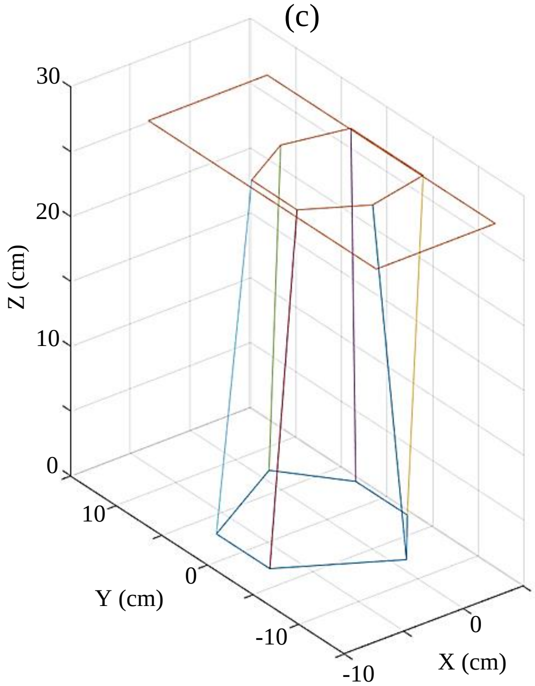
30
20
10
0
Z (cm)
10
0
-10
Y (cm)
-10
0
X (cm)

(e)

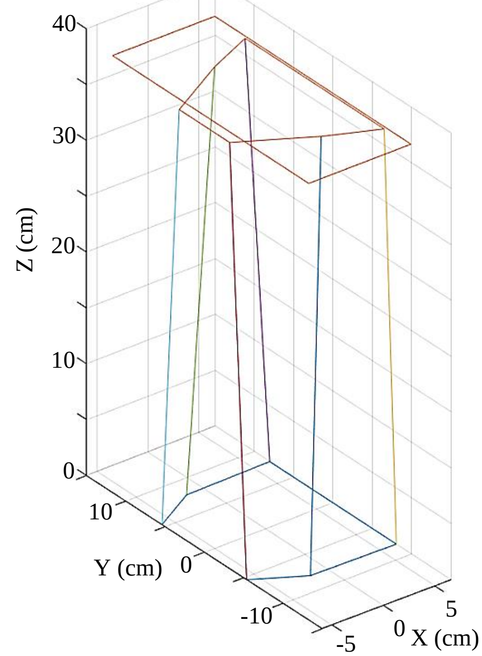
40
30
20
10
0
Z (cm)
10
0
-10
Y (cm)
-5
0
5
X (cm)

(f)

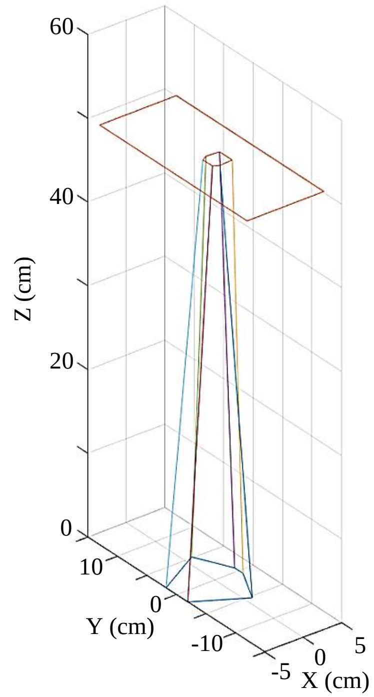

(g)

Figure 5-10. Optimization of the three-circles Stewart platform in relation to a selected value of a minimum distance between feet (MinD); (a) MinD = 20; (b) MinD = 15; (c) MinD = 10; (d) MinD = 8; (e) MinD = 7; (f) MinD = 6 and (g) MinD = 5.

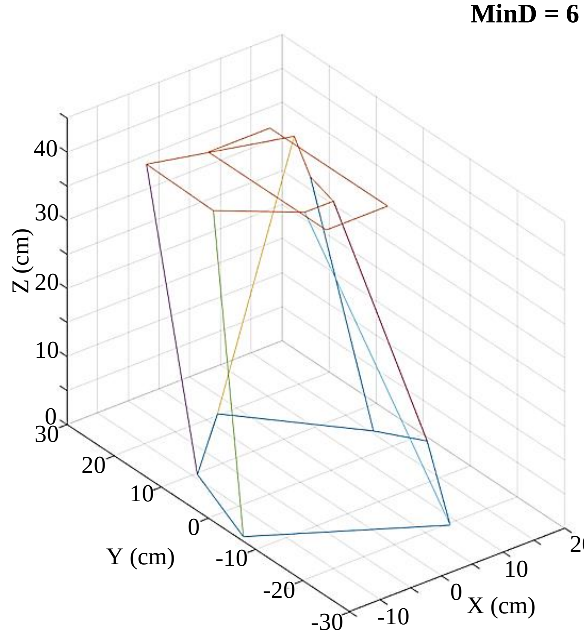

(a)

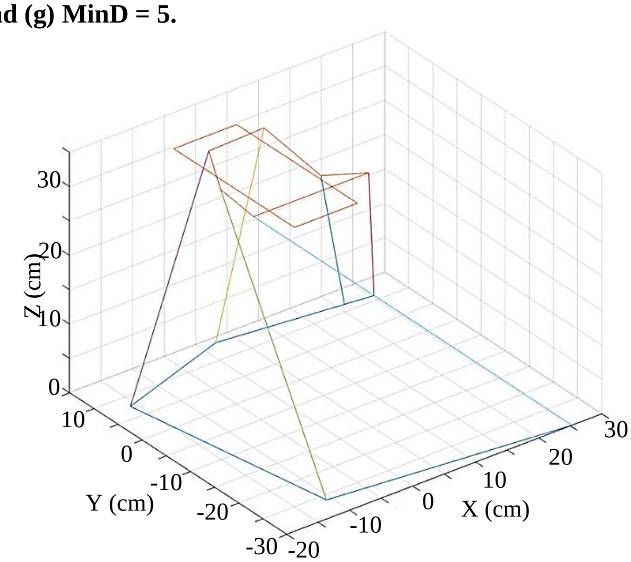

(b)

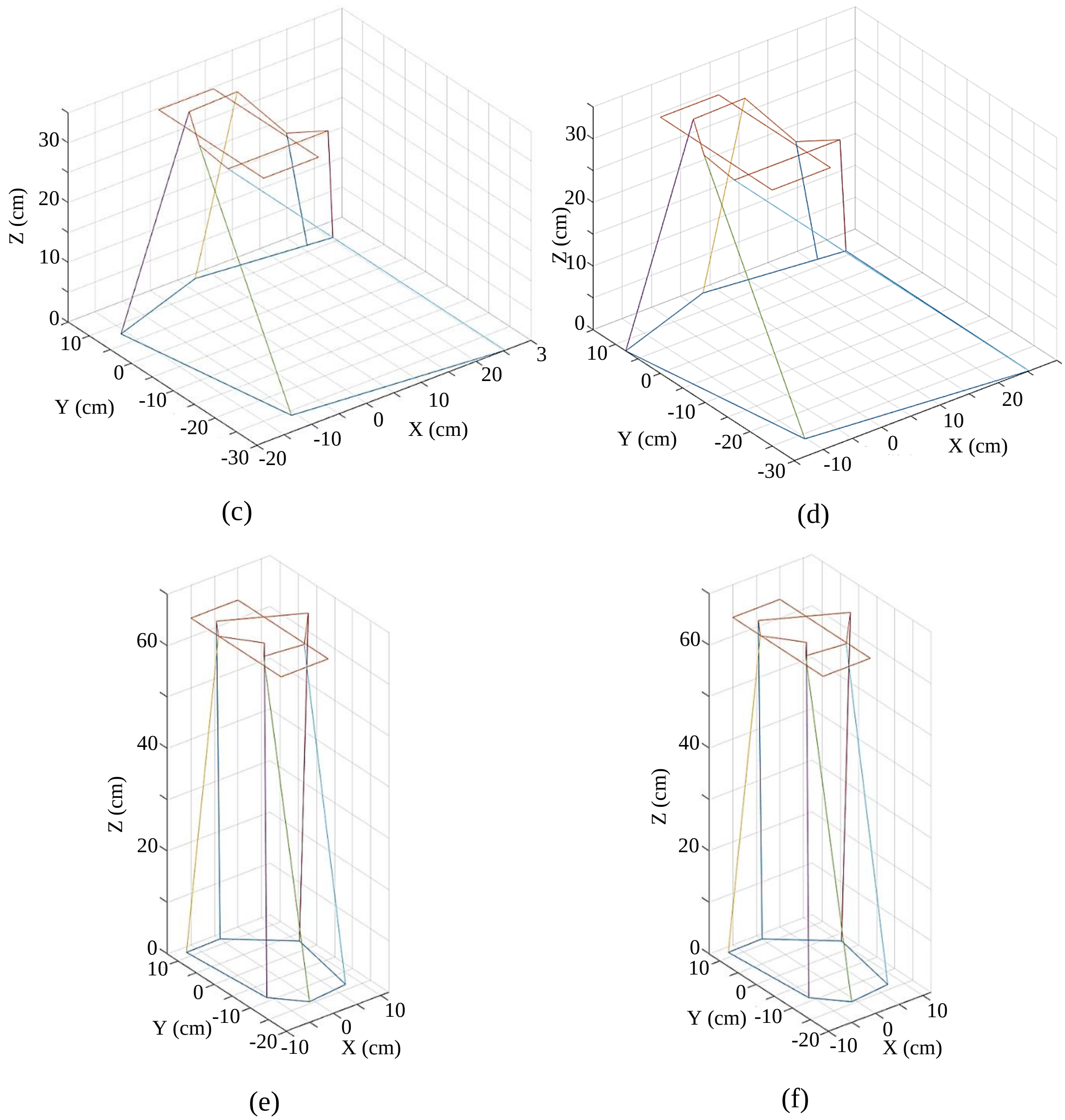

Figure 5-11. Optimization of the three-circles Stewart platform in relation to a selected value of a minimum distance between feet (MinD); (a) MinD = 30 using genetic algorithm; (b) MinD = 30 using pattern search; (c) MinD = 20; (d) MinD = 15; (e) MinD = 10 and (f) MinD = 8.

A MATLAB function was defined to compute the workspace of the selected optimized configuration of the Stewart platform. The upper and lower translation boundaries of the platform were calculated in relation to the maximum and minimum length of the cylinders. First, we selected an interval in the three-dimensional space in which we could check the condition of the cylinders' limits. This interval is defined as follows: X[-50 50], Y[-50, 50] and Z[0 100]; each direction is sampled at a constant step of 3. For each position in the search space, the inverse kinematic of the

Stewart platform is used to calculate the associated length of the cylinders. If the calculated lengths of the cylinders verify the physical limits of the real cylinders defined by Equation (5.36), then these lengths were included.The lower bound of the workspace is defined in relation to the first points that verify the condition length of the cylinders, while the upper bound is defined in relation to the points that lastly verify it. Figure 5-12 shows the resulted workspace of the optimized Stewart platform configuration.

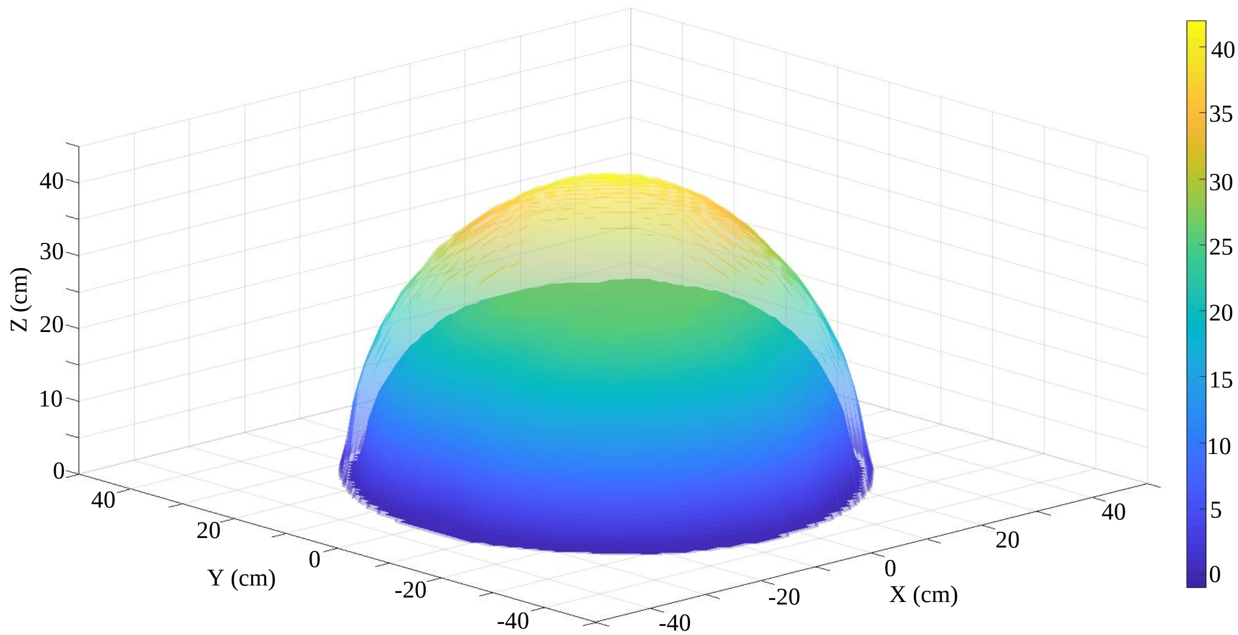

Figure 5-12. Workspace results of the selected optimized Stewart platform.

5.8. Control

The control objective of the Stewart platform compensates the translation movements that the XYZ mechanism could not provide as well as controls the rotation movements of the platform under the impedance control. The parameters of the impedance control that defines the reaction of the user with the virtual environment will be adjusted with respect to the properties of the simulated environment as discussed in the previous chapter. To achieve this, the control architecture of the Stewart platform is divided into two loops: an inter loop for controlling the position and force of each cylinder and an outer control loop for simulating a desired impedance.

5.8.1. Inner loop

In the model of the hydraulic actuation of the Stewart platform, the pressure exerted at both sides of each hydraulic actuator, is controlled through the movement of the spool of each corresponding controlling valve. The shaft of the pump is driven by a motor which provides constant pressure at the valve inlet. Meanwhile, a control system is used to adjust the position of the valve to get a desired position (length) of a hydraulic cylinder. The Simscape model of the selected optimized

Stewart platform is shown in Figure 5-13, while the block diagram of this model, including details about the hydraulic system of the Stewart platform, is represented in Figure 5-14 and Figure 5-15.

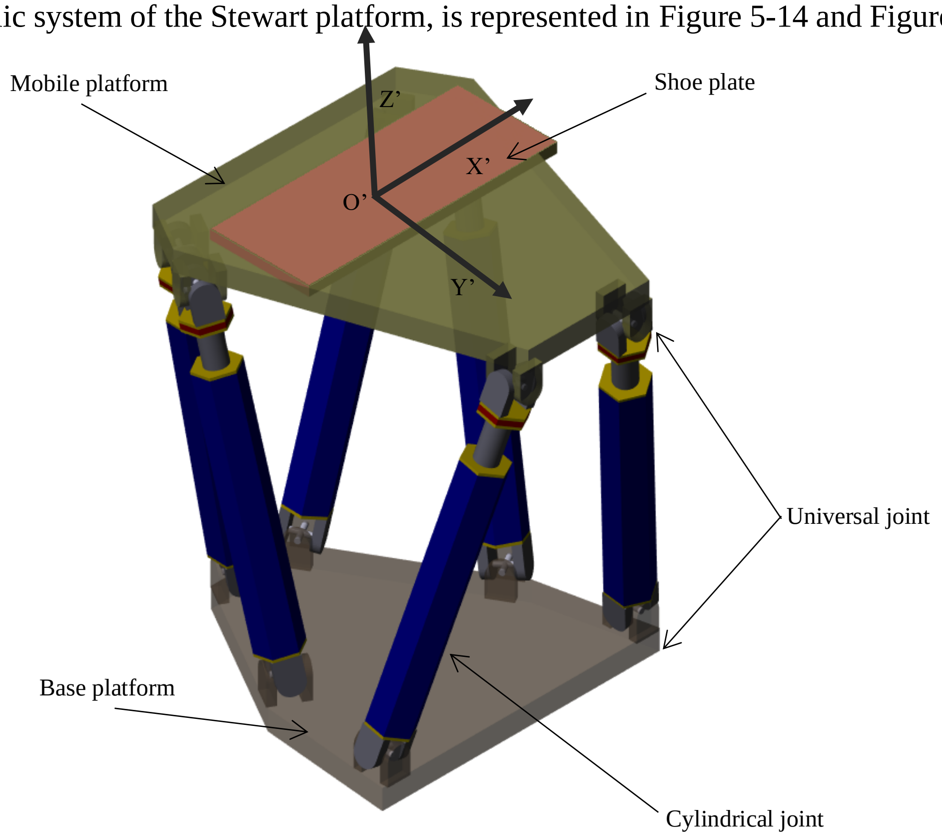

Figure 5-13. Three-dimensional Simscape model of the selected optimized Stewart platform.

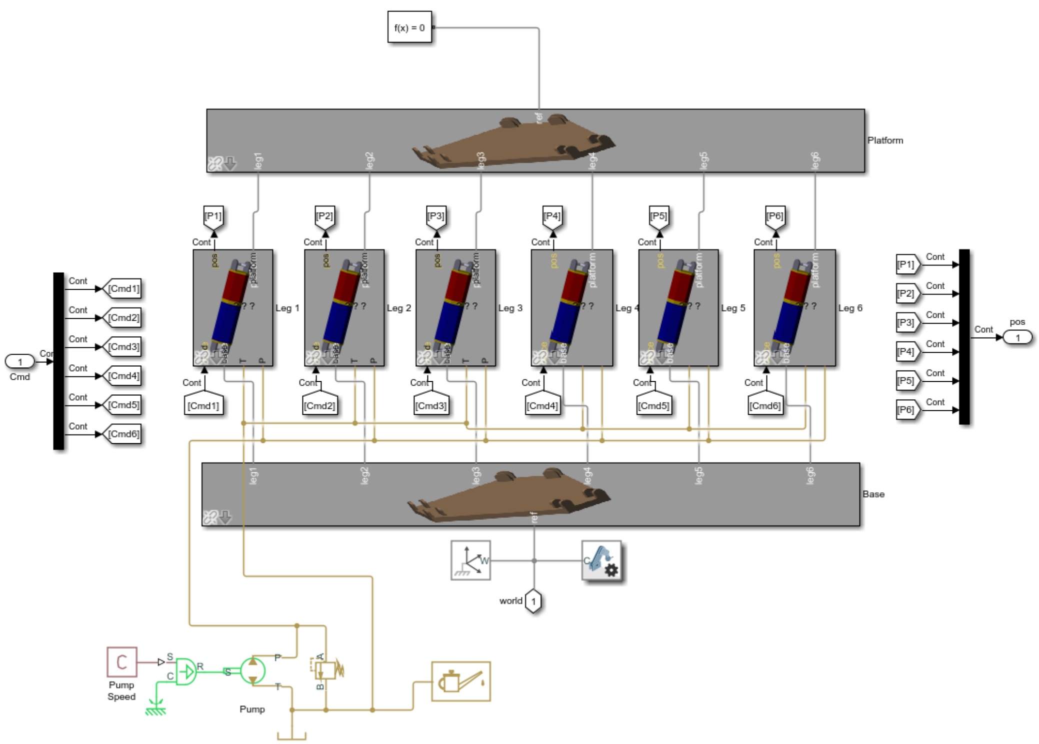

Figure 5-14. Simscape block diagram of the selected optimized Stewart platform.

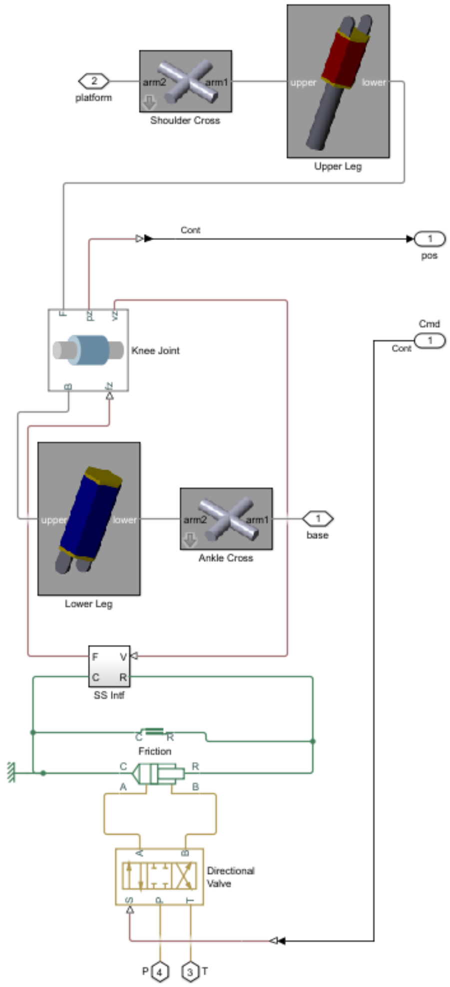

Figure 5-15. Simscape block diagram of one cylinder of the selected optimized Stewart platform.

The control problem of the inner loop addresses controlling the lengths of legs of the Stewart platform so that the position of the joint of each leg of the mobile platform follows the desired joint position imposed by the outer control loop. To simplify this process, we consider that inputs to cylinders are the six-leg forces while the displacement of them are the output. Our task then is creating a control strategy to control the lengths of the cylinders.

The input signal to the inner loop is the desired position and orientation of the moving platform x_{dp}. This signal goes through an inverse kinematic block to map the desired end-effector trajectory to the corresponding joint position trajectory defined by the actuator lengths q_{dp}. The desired actuator lengths are then sent to a controller to command the legs to follow the desired trajectory using a closed loop [193, 207]. This has the advantage of having a system in which the output position can follow the input position well without the need for solving the forward kinematic problem.

The controller we implemented for the control of the inner loop is a PID controller with a filter. The input to the controller is the actual position q_{ap} and desired position q_{dp} of the legs that are used for forming an error in the position while the outputs are spools position commands sent to the

hydraulic valves which are created based on the gain and integral of the error [207]. At end of the controller, a gain of 0.005 is added to convert the output signal of the controller to a spool displacement. Each hydraulic cylinder has its unique PID controller, allowing it to follow a desired position. Parameters of the six controllers of the hydraulic system of the Stewart platform were tuned using a MATLAB optimization tool box. The optimization problem consists of searching for parameter values that meet the requirement of having a minimum position error of the hydraulic cylinders. The selected gains of the controllers of the six hydraulic cylinders of the Stewart platform are given in Table 5.4.

Table 5.4. Gains of the controllers of the six hydraulic cylinders of the Stewart platform.

Cylinders	P	I	D	N
1	33518.57	42398.15	6945.47	34.69
2	230.33	101293.53	59.89	278.54
3	4282.35	-20842.79	0.24	0.03
4	7.26	2299077.85	328.45	4320.25
5	27.48	11130292.03	1217	560414.62
6	1362036.35	-5122230.65	-17145.49	70.59

5.8.2. Outer loop

The outer control loop (also known as the high-level control) describes the whole behavior of the Stewart platform. This corresponds to the implementation of an impedance control to simulate to the user different walking environments which are broadly discussed in the previous chapter. The control model selected for controlling the impedance of the system is described in the block diagram of Figure 5-16.

5.8.1. Test

The main goal of using the Stewart platform in our application is compensating for high-frequency movements, especially translation movements on the horizontal plane. To verify the ability of the optimized Stewart platform to simulate high-frequency movements along the *x*-axis, a sinusoidal force signal with an amplitude of 12 and a frequency of 2 Hz was applied to the human-made model of the selected impedance control model. Constant values of 0 were commanded to the movements along the *y*-axis as well as commanded to rotation movements, while the vertical movement of the Stewart platform was fixed at a height of 31.33 cm. A comparison between the desired foot position and the position obtained from the simulation of high-frequency movement along the *x*-axis under an admittance control of the Stewart platform is illustrated in Figure 5-17.

The interaction force sensed at the contact point between the user's foot and the system, with respect to the movement along *x*-axis, is show in Figure 5-18.

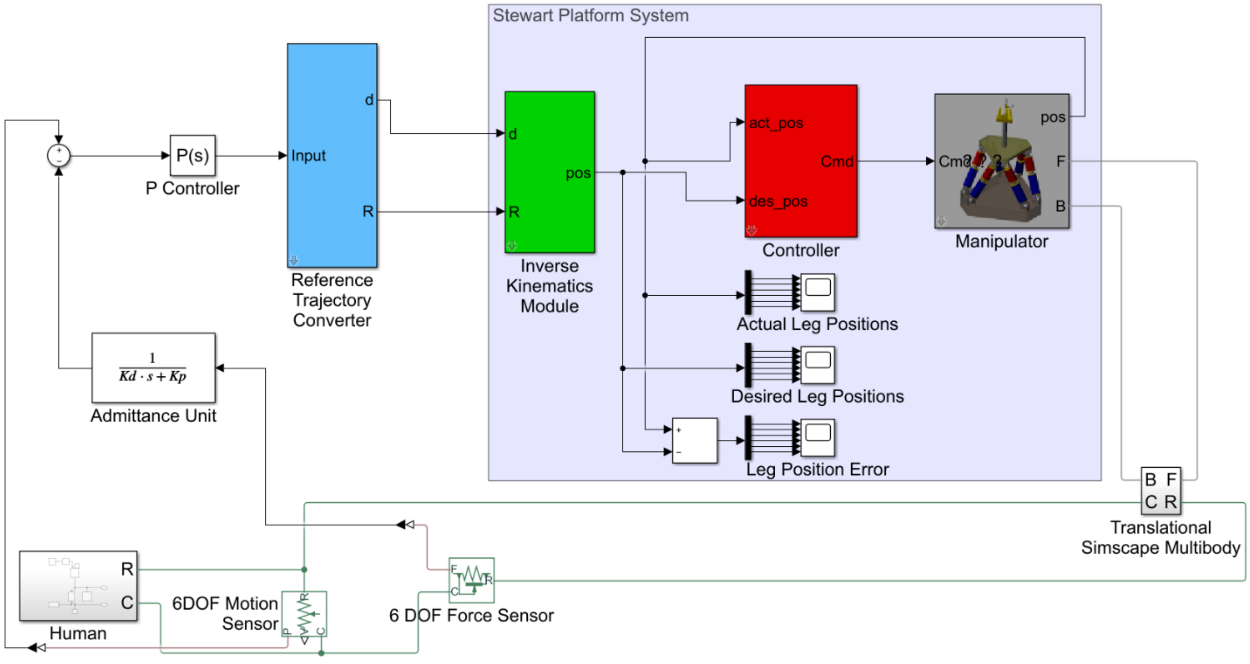

Figure 5-16. Control diagram of the Stewart platform.

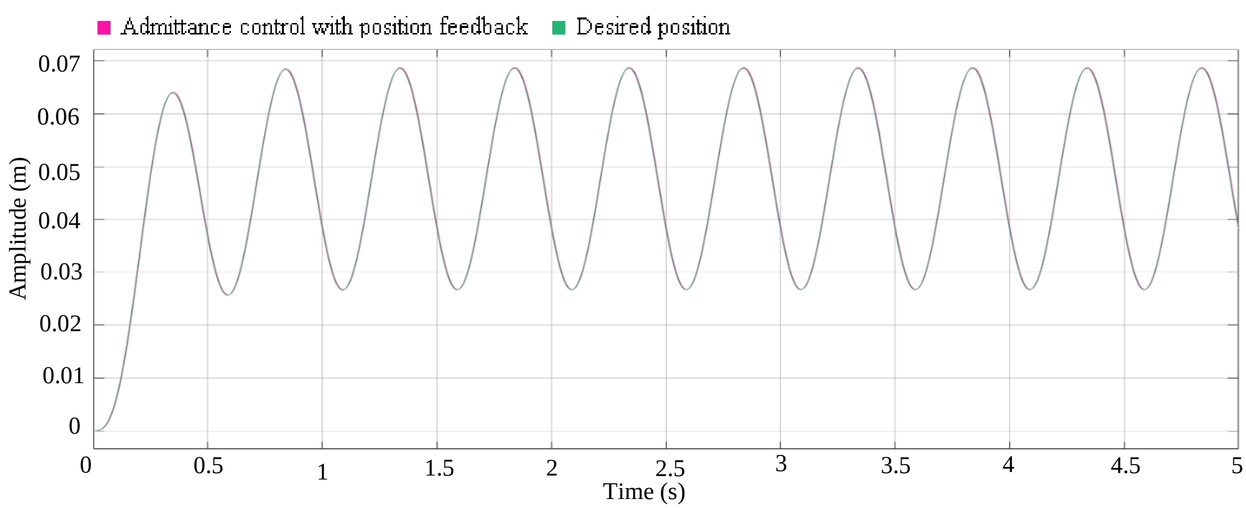

Figure 5-17. Comparison between desired foot position and position obtained from the simulation of high-frequency movement along the *x*-axis under the admittance control of the Stewart platform.

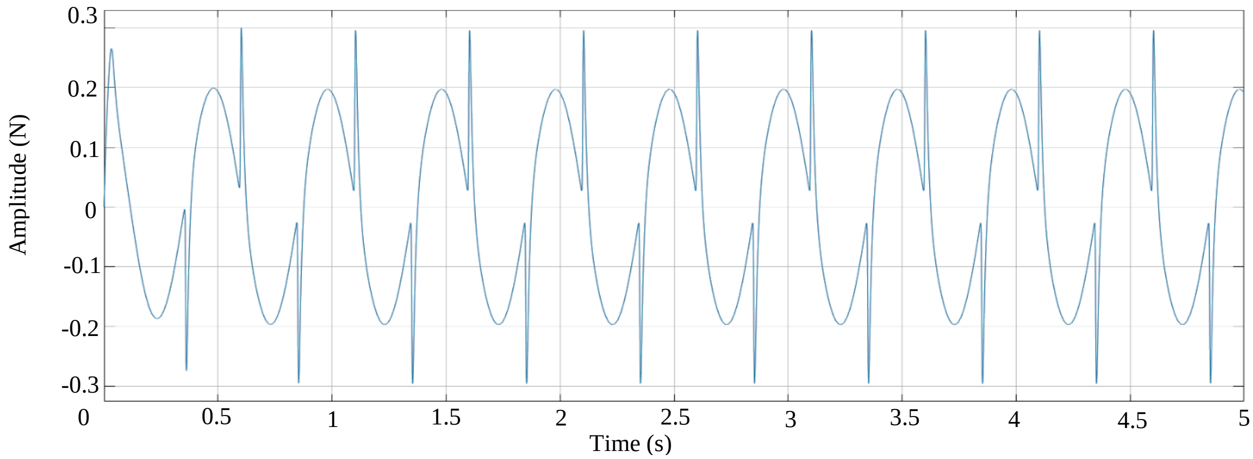

Figure 5-18. Interaction force sensed at the contact point between the user's foot and the system (Stewart platform) with respect to the movement along the *x*-axis.

Results show that the output position of the admittance control of the system and the desired position are almost identical. At the same time, the amplitude of the measured contact force between the user's foot and the interface is quite low. The contact force measured using the Stewart platform is about ten times less than the contact force measured using the XYZ mechanism. Although the system (Stewart platform) does still provide some resistance, this amount of resistance would not considerably affect the ability of the user to freely move their foot. Practically, it is difficult to have a system completely transparent, as there are always technical issues, such as tolerance errors and communication delays between different units of the system, which are difficult to eliminate.

5.9. Conclusion

This section has presented the process of developing an optimized Stewart platform that is intended to be used as hardware for compensating residual inertia and simulating rotation movements. The obtained structure has the following advantages:

- Increasing the angular workspace of the system, especially along the *x*-axis.
- Minimizing the distance between the user's feet.
- Increasing the dexterity of the structure.

These features make the system potentially suitable for simulating a wide variety of virtual environmental textures, solving some of current research problems and establishing a guideline base to achieve better performance in rendering different types of virtual environments for the user.

The performance study of the optimized Stewart platform has shown the ability of the system to largely filter the residual inertia associated with high-frequency translation movements. Although the filtering process did not completely eliminate the impedance of the system, this would not affect the simulation. The values of the interaction forces during the swing phase are quite and low.

GENERAL CONCLUSION

This thesis has focused on developing a new robotic system for assisting patients with neurological disorders, especially those who have suffered from a stroke, to perform physical rehabilitation exercises. Since the beginning of this century, the rehabilitation of these individuals has been heavily reliant on the use of robotic devices. Although robots demonstrate considerable advantages in terms of accuracy and reliability, data show that the use of assistive robotic devices does not significantly improve the quality of gait for patents with neurological disorders. The research we performed on gait robotic rehabilitation systems has allowed us to suggest two main explanations for the limitation of these devices which are the following:

- Gait robotic rehabilitation systems are mainly designed to assist patients with performing repetitive tasks and to relieve therapists from the burden of manual assistance. It is important to note that the physical tasks that these robotic systems assist with are strenuous and boring for the patient. The main problem with this is that the patient can lose interest in pursuing rehabilitation exercises if the patient is not motivated. Unfortunately, current gait robotic systems do not develop techniques to solve the problem of motivating the patient (such as the introduction of an interactive VR scenario for rehabilitation). Therefore, the patient would either stay passive or would spend inadequate effort during the rehabilitation session, which could result in insignificant gait improvement.
- Although most current rehabilitation robots provide the patient with the required assistance to perform basic gait movements, there are limitations associated with their abilities to support complex movements. Technically, drawbacks of robotic rehabilitation systems have different forms, such as a lack of DOFs, low back-drivability driving systems and inappropriate mechanical design. The consequences for the quality of gait gained by the patient can accordingly vary with respect to the type of drawback.

Our project has aimed to make the rehabilitation process more relaxing as well as to assist patents with performing complex gait training. To address these issues, GWPs have been employed as a part of a lower-limb robotic rehabilitation system to combine robotic devices with VR, thus making the gait simulation more realistic and more motivating. The robotic system that we propose allows for the simulation of walking on different terrains (e.g., walking on a flat plane, on stairs or on a hill) simultaneously with the performance of different rehabilitation training modes (for example, passive mode, active mode, active assisting mode and active resisting mode).

The mechanical design we propose for the GWP system is a hybrid parallel-serial mechanical system. This design has the advantage of adding and enhancing a set of properties. In terms of motion freedom, the system allows all six DOFs for the foot and supports movements requiring a wide range of motion. In terms of response, the system is able to simulate movements at different speeds and accelerations.

To get the appropriate control design for the GWP system, different control strategies were discussed, and an admittance control with position feedback was adopted for controlling both the mechanical parts of the system (the XYZ mechanism and Stewart platform). It is important to note that while we were searching for the appropriate control strategy for our system, a direct force control strategy was not investigated because it does not allow imposing a specific dynamic behavior for simulating VR environments. Therefore, the control solutions to our system were chosen to be within impedance control strategies only.

To study the behavior of the XYZ mechanism under different control strategies, concepts of stability and performance were introduced. Studying the stability of the XYZ mechanism was in particular a very challenging step because the behavior of the user is unpredictable. Therefore, one of the key solutions to stabilize the system is to create a dynamic model representing the user's behavior. The model allows one to define the transfer function of the user. Thus, the transfer function of the system as a whole can be well defined, and the stability of it can be easily analyzed using a bode plot. Transparency is an important concept to describe the performance of the system. Transparency allows one to define how well the system renders a selected VR environment. Among different methods used to define the transparency of haptic systems, Z-width is adopted for our system. With this method, the transparency can be easily described by comparing the measured impedance of the system with the desired one.

The results of studying the stability of the XYZ mechanism under impedance control with position feedback show that the stability bandwidth is large enough to support the whole range of frequencies of human-controlled movements that vary from 0 to 2 Hz. On the other hand, the performance of the same mechanism varied with respect to the frequency operating point. While at low frequencies the desired impedance and the measured impedance matched quite well in terms of amplitude, their amplitudes differed a bit at high frequencies. The XYZ mechanism is a mechanical system that has substantial inertia. Therefore, it is difficult to move it forward and backward quickly. This, as a result, led us to think about integrating a light mechanism for compensating for the delay in movements.

The Stewart platform is the type of light mechanism we suggested to compensate for the residual inertia as well as to simulate rotational movements. This design has the advantage of allowing all foot movements. Further, it is a stiff mechanism, and more importantly, it supports high speed movements. On the other hand, the singular value index, condition number index and manipulability index are important indices for describing the performance of the Stewart platform. They are very crucial for describing the ability of the platform to exert forces and generate velocities.

Designing the Stewart platform was a challenging task due to the fact that we had many objectives we needed to meet, including keeping short distances between the user's feet, providing a wide range of motion and having an isotropic system. Indeed, these are overlapping objectives, and meeting one single objective could affect achieving the others. Solving the optimization problem allowed us in the end to define the best Stewart platform configuration that balances between the different objectives we set.

The results of studding the impedance control of the Stewart platform show that the system is able to behave in a very transparent way while simulating a wide range of frequencies that correspond to moving a foot in the air. This proves the successful choice of the proper mechanical design for compensating the residual inertia that resulted from the XYZ mechanism..

One of the technical limitations that is difficult to bypass with this system is the range of motion of the whole body. In a real environment, our motion is unlimited (at least on the *x*-*y* plane). Keeping the user in the same real position does not give them the sensation of acceleration, which can cause some confusion for them since VR tells them that they are moving. We believe it is important to mitigate this fact through providing an acceleration, and slowly over time we could return the patient back to their point of origin. To realize this, we suggest a moving platform that provides the necessary acceleration on the *x*-*y* plane so that the user can get the sense of accelera

REFERENCES

[1] WHO, “World Report on Disability - Summary,” *World Report on Disability 2011*, no. 9789241564182, 2011.

[2] WHO, “What are neurological disorders?,” *Online Q&A*, May, p. 2016, 2007.

[3] A. Chaudhuri and P. O. Behan, “Fatigue in neurological disorders,” *Lancet*, vol. 363, no. 9413, pp. 978–988, 2004, doi: 10.1016/S0140-6736(04)15794-2.

[4] M. Matzo and D. W. Sherman, *Palliative Care Nursing: Quality Care to the End of Life*: Springer Publishing Company, 2015.

[5] Y. Moon, J. H. Sung, R. An, M. E. Hernandez, and J. J. Sosnoff, “Gait variability in people with neurological disorders: A systematic review and meta-analysis,” *Human Movement Science*, vol. 47, pp. 197–208, 2016, doi: 10.1016/j.humov.2016.03.010.

[6] C. Werner, S. von Frankenberg, T. Treig, M. Konrad, and S. Hesse, “Treadmill training with partial body weight support and an electromechinical gait trainer for restoration of gait in subacute stroke patients,” *Stroke*, vol. 33, (12), 2895--2895-, 2002.

[7] J. C. Outermans, R. P. S. van Peppen, H. Wittink, T. Takken, and G. Kwakkel, “Effects of a high-intensity task-oriented training on gait performance early after stroke: a pilot study,” *Clinical rehabilitation*, vol. 24, no. 11, pp. 979–987, 2010, doi: 10.1177/0269215509360647.

[8] D. P. Ferris, G. S. Sawicki and A. Domingo, “Powered Lower Limb Orthoses for Gait Rehabilitation,” *Topics in Spinal Cord Injury Rehabilitation*, vol. 11, no. 2, pp. 34–49, 2005.

[9] J. C. Bachman, “Specificity vs. generality in learning and performing two large muscle motor tasks,” *Research Quarterly of the American Association for Health, Physical Education and Recreation*, vol. 32, no. 1, pp. 3–11, 1961, doi: 10.1080/10671188.1961.10762064.

[10] H. Barbeau, “Locomotor training in neurorehabilitation: emerging rehabilitation concepts,” *Neurorehabilitation and Neural Repair*, vol. 17, no. 1, pp. 3–11, 2003, doi: 10.1177/0888439002250442.

[11] M. Wirz *et al.*, “Effectiveness of automated locomotor training in patients with chronic incomplete spinal cord injury: a multicenter trial,” *Archives of physical medicine and rehabilitation*, vol. 86, no. 4, pp. 672–680, 2005, doi: 10.1016/j.apmr.2004.08.004.

[12] K. H. Low, “Recent development and trends of clinical-based gait rehabilitation robots,” *Springer Tracts in Advanced Robotics*, vol. 106, pp. 41–75, 2015, doi: 10.1007/978-3-319-12922-8_2.

[13] H. Sveistrup, “Motor rehabilitation using virtual reality,” *Journal of NeuroEngineering and Rehabilitation*, vol. 1, no. 1, p. 10, 2004, doi: 10.1186/1743-0003-1-10.

[14] Colombo G, Joerg M, Schreier R, Dietz V., “Treadmill training of paraplegic patients using a robotic orthosis,” *Journal of Rehabilitation Research and Development*, vol. 37, pp. 693–700, 2000.

[15] I. Díaz, J. J. Gil, and E. Sánchez, “Lower-Limb Robotic Rehabilitation: Literature Review and Challenges,” *Journal of Robotics*, vol. 2011, i, pp. 1–11, 2011, doi: 10.1155/2011/759764.

[16] W. Meng, Q. Liu, Z. Zhou, Q. Ai, B. Sheng, and S. S. Xie, “Recent development of mechanisms and control strategies for robot-assisted lower limb rehabilitation,” *Mechatronics*, vol. 31, pp. 132–145, 2015.

[17] E. Swinnen, S. Duerinck, J. P. Baeyens, R. Meeusen, and E. Kerckhofs, “Effectiveness of robot-assisted gait training in persons with spinal cord injury: A systematic review,” *Journal of Rehabilitation Medicine*, vol. 42, no. 6, pp. 520–526, 2010, doi: 10.2340/16501977-0538.

[18] H. Schmidt, S. Hesse, R. Bernhardt, and J. Krüger, “HapticWalker---a Novel Haptic Foot Device,” *ACM Trans. Appl. Percept.*, vol. 2, no. 2, pp. 166–180, 2005, doi: 10.1145/1060581.1060589.

[19] J. Veneman, “Design and Evaluation of the Gait Rehabilitation Robot LOPES,” *97890365*, vol. 15, no. 3, p. 201, 2007.

[20] K. N. Winfree, P. Stegall, and S. K. Agrawal, “Design of a minimally constraining, passively supported gait training exoskeleton: ALEX II,” *97814244*, 2011, doi: 10.1109/ICORR.2011.5975499.

[21] Jan F Veneman, “Design and evaluation of the gait rehabilitation robot lopes,” Doctor of Philosophy, University of Twente, 2007.

[22] S. B. O'Sullivan and T. J. Schmitz, *Improving Functional Outcomes in Physical Rehabiliation*, 2010.

[23] Physiopedia, *Gait in prosthetic rehabilitation.* [Online]. Available: https://www.physio-pedia.com/Gait_in_prosthetic_rehabilitation (accessed: Aug. 27 2020.818Z).

[24] Bone and Spine, *Normal Gait Cycle and Abnormalilties of Gait | Bone and Spine.* [Online]. Available: https://boneandspine.com/normal-gait-cycle/ (accessed: Aug. 27 2020.845Z).

[25] WANG Ping, "Gait Locomotion Generation and Leg Muscle Evaluation for Overground Walking Rehabilitation Robots," Doctor of Philosophy, SCHOOL OF MECHANICAL AND AEROSPACE ENGINEERING.

[26] William Morrison, *Abnormal gait: Types, causes, and diagnosis.* [Online]. Available: https://www.medicalnewstoday.com/articles/320481 (accessed: Aug. 27 2020.919Z).

[27] N. L.A. Van and H. J. Hermens, "Revalidatietechnologie in Euregio," PhD Thesis, Netherlands.

[28] L. Duda, N. Lo van, S. Röseler, B. Greitemann, H. W. van, and N. S. Klazinga, "Rehabilitation in Germany and the Netherlands, A comparison of two," Netherlands.

[29] R. Chemuturi, "GENTLE/A - Adaptive robotic assistance for upper-limb rehabilitation," PhD Thesis, University of Hertfordshire.

[30] G. Kwakkel *et al.,* "Effects of augmented exercise therapy time after stroke: a meta-analysis," *Stroke,* vol. 35, no. 11, pp. 2529–2539, 2004, doi: 10.1161/01.STR.0000143153.76460.7d.

[31] J. Stein, H. I. Krebs, W. R. Frontera, S. E. Fasoli, R. Hughes, and N. Hogan, "Comparison of two techniques of robot-aided upper limb exercise training after stroke," *American journal of physical medicine & rehabilitation*, vol. 83, no. 9, pp. 720–728, 2004, doi: 10.1097/01.phm.0000137313.14480.ce.

[32] S. E. Fasoli, H. I. Krebs, J. Stein, W. R. Frontera, and N. Hogan, "Effects of robotic therapy on motor impairment and recovery in chronic stroke," *Archives of physical medicine and rehabilitation*, vol. 84, no. 4, pp. 477–482, 2003, doi: 10.1053/apmr.2003.50110.

[33] *Acute Spinal Cord Injury.* [Online]. Available: https://www.hopkinsmedicine.org/health/conditions-and-diseases/acute-spinal-cord-injury (accessed: Aug. 27 2020.991Z).

[34] Mayo Clinic, *Spinal cord injury - Symptoms and causes.* [Online]. Available: https://www.mayoclinic.org/diseases-conditions/spinal-cord-injury/symptoms-causes/syc-20377890 (accessed: Aug. 27 2020.336Z).

[35] *Spinal Cord Injury – Types of Injury, Diagnosis and Treatment.* [Online]. Available: https://www.aans.org/Patients/Neurosurgical-Conditions-and-Treatments/Spinal-Cord-Injury (accessed: Aug. 27 2020.095Z).

[36] H. B. Lim, "Study and implementation of a gait rehabilitation System with capability for mobility and gait pattern generation," Doctor of Philosophy, Nanyang technological university.

[37] Ozmen M, Calişkan M, Apak S, Gökçay, "8-Year Clinical Experience in Cerebral Palsy," 39(1), pp. 52–54, 1993 Feb.

[38] L. A. Gilman, *Coping with Cerebral Palsy,* 1st ed. New York: The Rosen Publishing Group, 2001.

[39] Y. Quijano-González, A. Melendez-Calderon, E. Burdet, J. E. Chong-Quero, D. Villanueva-Ayala, and J. C. Pérez-Moreno, "Upper Limb Functional Assessment of Children with Cerebral Palsy Using a Sorting Box," in *36th Annual International Conference of the IEEE Engineering in Medicine and Biology Society*, 2014, pp. 2330–2333.

[40] C. Thorogood, *Medscape: Rehabilitation and Cerebral Palsy*. [Online]. Available: http://emedicine.medscape.com/article/310740-overview

[41] O. Geman, "Data processing for Parkinson's disease: Tremor, speech and gait signal analysis," in *E-Health and Bioengineering Conference (EHB)*, 2011, pp. 1–4.

[42] R. Warner, "Palliative Nursing Care in other Neurological Conditions," in *Palliative Nursing: Across the Spectrum of Care*, E. Stevens, S. Jackson, and S. Milligan, Eds.: Blackwell Publishing Ltd, 2009.

[43] Mayo Clinic, *Mayo Clinic: Multiple sclerosis.* [Online]. Available: http://www.mayoclinic.org/diseases-conditions/multiple-sclerosis/home/ovc-20131882

[44] A. Compston and D. M. s. McAlpine, *McAlpine's multiple sclerosis*, 4th ed. Edinburgh: Elsevier Churchill Livingstone, 2006.

[45] E. Koutsouraki, V. Costa, and S. Baloyannis, "Epidemiology of multiple sclerosis in Europe: a review," *International review of psychiatry (Abingdon, England)*, vol. 22, no. 1, pp. 2–13, 2010, doi: 10.3109/09540261003589216.

[46] S. Beer, F. Khan, and J. Kesselring, "Rehabilitation interventions in multiple sclerosis: an overview," *Journal of Neurology*, 2012, pp. 1994–2008, 2012.

[47] J. H. Carr, R. B. Shepherd, J. Gordon, A. M. Gentile, and J. M. Held, "Movement Science: Foundations for physical therapy in rehabilitation," pp. 93–149, 1987.

[48] C. Nooijen, N. Ter Hoeve, and E. Field-Fote, "Gait quality is improved by locomotor training in individuals with SCI regardless of training approach," *Journal of NeuroEngineering and Rehabilitation*, vol. 6, no. 1, 2009, doi: 10.1186/1743-0003-6-36.

[49] S. J. Harkema, "Neural plasticity after human spinal cord injury: Application of locomotor training to the rehabilitation of walking," *Neuroscientist*, vol. 7, no. 5, pp. 455–468, 2001, doi: 10.1177/107385840100700514.

[50] H. B. Lim, K. H. Hoon, Y. C. Soh, A. Tow, and K. H. Low, "Effective gait planning for robotic rehabilitation - From normal gait study to application in clinical rehabilitation," *97814244*, pp. 1885–1890, 2009, doi: 10.1109/AIM.2009.5229764.

[51] P. Wang, K. H. Low, A. Tow, and P. H. Lim, "Initial system evaluation of an overground rehabilitation gait training robot (NaTUre-gaits)," *Advanced Robotics*, vol. 25, no. 15, pp. 1927–1948, 2011, doi: 10.1163/016918611X587214.

[52] S. Wist, J. Clivaz, and M. Sattelmayer, “Muscle strengthening for hemiparesis after stroke: A meta-analysis,” *Annals of physical and rehabilitation medicine*, vol. 59, no. 2, pp. 114–124, 2016, doi: 10.1016/j.rehab.2016.02.001.

[53] S. J. Harkema, A. L. Behrman, and H. Barbeau, *Locomotor training: Principles and practice / Susan J. Harkema, Andrea L. Behrman, Hugues Barbeau*. New York, NY, Oxford: Oxford University Press, 2011.

[54] H. Reimann, T. Fettrow, and J. J. Jeka, “Strategies for the Control of Balance During Locomotion,” *Kinesiology Review*, vol. 7, no. 1, pp. 18–25, 2018, doi: 10.1123/kr.2017-0053.

[55] S. B. O'Sullivan, T. J. Schmitz, and G. D. Fulk, Eds., *Physical rehabilitation*. Philadelphia: F.A. Davis Company, 2019.

[56] L. D. Weiss, J. Weiss, and T. Pobre, *Oxford American handbook of physical medicine and rehabilitation*. Oxford, New York: Oxford University Press, 2010.

[57] NEUROGYMTECH, “Parallel Bars Versus Dynamic Balance and Gait Training: Comparing Their Impact on Changes in Quality Measures/Indicators,” [Online]. Available: www.neurogymtech.com

[58] *Physical Therapy Parallel Bars.* [Online]. Available: https://www.medicalproductsdirect.com/phthpaba.html (accessed: Aug. 27 2020.550Z).

[59] D. Weiss and L. S. Krivickas, “Rehabilitation in Neuromuscular Disorders,” in *Neuromuscular Disorders: Treatment and Management*: Elsevier, 2011, pp. 115–136.

[60] K. Kaushik and K. Kumar, “Effect of Cage Therapy using Advanced Spider Suit Compared to Traditional Physical Therapy on Gross Motor Function in Children with Cerebral Palsy – An Indian Experience,” *Int J Neurorehabilitation Eng*, vol. 03, no. 01, 2016, doi: 10.4172/2376-0281.1000193.

[61] Believe Pediatric Physical Therapy, LLC, *Cage — Believe Pediatric Physical Therapy, LLC.* [Online]. Available: http://www.believetherapy.com/cage (accessed: Aug. 29 2020.166Z).

[62] N. Koceska and S. Koceski, “Review: Robot Devices for Gait Rehabilitation,” *International Journal of Computer Applications*, vol. 62, no. 13, pp. 1–8, 2013, doi: 10.5120/10137-4279.

[63] A. Wernig, A. Nanassy, and S. Müller, “Laufband (treadmill) therapy in incomplete paraplegia and tetraplegia,” *Journal of neurotrauma*, vol. 16, no. 8, pp. 719–726, 1999, doi: 10.1089/neu.1999.16.719.

[64] V. Dietz, MD, G. Colombo, DM, L. Jensen, DM, and L. Baumgartner, “Locomotor capacity of spinal cord in paraplegic patients,” *Ann. Neurol*, no. 37, pp. 574–582, 1995.

[65] Martha Visintin, Hugues Barbeau, Nicol Korner-Bitensky, Nancy E. Mayo, “A New Approach to Retrain Gait in Stroke Patients Through Body Weight Support and Treadmill Stimulation,” *Stroke*, vol. 29, pp. 1122–1128, 1998.

[66] S. Hesse, “Treadmill training with partial body weight support after stroke: A review,” *NRE*, vol. 23, no. 1, pp. 55–65, 2008, doi: 10.3233/NRE-2008-23106.

[67] P. Winchester and R. Querry, “Robotic orthoses for body weight-supported treadmill training,” *Physical Medicine and Rehabilitation Clinics of North America*, vol. 17, no. 1, pp. 159–172, 2006, doi: 10.1016/j.pmr.2005.10.008.

[68] S. Fisher, L. Lucas, and T. Adam Thrasher, “Robot-Assisted Gait Training for Patients with Hemiparesis Due to Stroke,” *Topics in Stroke Rehabilitation*, vol. 18, no. 3, pp. 269–276, 2011, doi: 10.1310/tsr1803-269.

[69] M. Pietrusinski *et al.*, “Gait Rehabilitation Therapy Using Robot Generated Force Fields Applied at the Pelvis,” *Measurement*, pp. 401–407.

[70] A. L. Behrman and S. J. Harkema, “Locomotor training after human spinal cord injury : a series of case studies,” *Phys Ther*, vol. 80, no. 7, pp. 688–700, 2000.

[71] J. Meuleman, E. van Asseldonk, G. van Oort, H. Rietman, and H. van der Kooij, “LOPES II - Design and Evaluation of an Admittance Controlled Gait Training Robot with Shadow-Leg Approach,” *IEEE Transactions on Neural Systems and Rehabilitation Engineering*, vol. 24, no. 3, pp. 352–363, 2016, doi: 10.1109/TNSRE.2015.2511448.

[72] L. L. Cai *et al.*, “Implications of assist-as-needed robotic step training after a complete spinal cord injury on intrinsic strategies of motor learning,” *The Journal of neuroscience : the official journal of the Society for Neuroscience*, vol. 26, no. 41, pp. 10564–10568, 2006, doi: 10.1523/JNEUROSCI.2266-06.2006.

[73] J. L. Emken, J. E. Bobrow and D. J. Reinkensmeyer, *9th International Conference on Rehabilitation Robotics, 2005: ICORR 2005 ; June 28 - July 1, 2005, [Chicago, IL*. Piscataway, NJ: IEEE Operations Center, 2005. [Online]. Available: http://ieeexplore.ieee.org/servlet/opac?punumber=10041

[74] S. Hesse, T. Sarkodie-Gyan, and D. Uhlenbrock, “Development of an Advanced Mechanised Gait Trainer, Controlling Movement of the Centre of Mass, for Restoring Gait in Non-ambulant Subjects - Weiterentwicklung eines mechanisierten Gangtrainers mit Steuerung des Massenschwerpunktes zur Gangrehabilitation,” *Biomedizinische Technik/Biomedical Engineering*, vol. 44, 7-8, pp. 194–201, 1999, doi: 10.1515/bmte.1999.44.7-8.194.

[75] Lars Lünenburger Tania Lam Robert Riener Gery Colombo, “"Gait Retraining After Neurological Disorders". In: Encyclopedia of Biomedical Engineering,”

[76] H. Schmidt, S. Hesse, C. Werner, A. Bardeleben, “UPPER AND LOWER EXTREMITY ROBOTIC DEVICES TO PROMOTE MOTOR RECOVERY AFTER STROKE - RECENT DEVELOPMENTS,” 2004.

[77] M. GIRONE, G. BURDEA, M. BOUZIT AND V. POPESCU, “A Stewart Platform-Based System for Ankle Telerehabilitation,”

[78] A. Goffer, “Gait-locomotor apparatus,” 7153 242, US.

[79] J. J. Eng and P. Fang Tang, “Gait training strategies to optimize walking ability in people with stroke: a synthesis of the evidence,” *01188623*, vol. 7, no. 10, pp. 1417–1436, 2011, doi: 10.1586/14737175.7.10.1417.Gait.

[80] M. Dzahir and S.-i. Yamamoto, “Recent Trends in Lower-Limb Robotic Rehabilitation Orthosis: Control Scheme and Strategy for Pneumatic Muscle Actuated Gait Trainers,” *Robotics*, vol. 3, no. 2, pp. 120–148, 2014, doi: 10.3390/robotics3020120.

[81] S. Hussain, S. Q. Xie, and G. Liu, “Robot assisted treadmill training: Mechanisms and training strategies,” *Medical Engineering and Physics*, vol. 33, no. 5, pp. 527–533, 2011, doi: 10.1016/j.medengphy.2010.12.010.

[82] S. Sargsyan, V. Arakelian, and S. Briot, “Robotic Rehabilitation Devices of Human Extremities: Design Concepts and Functional Particularities,” *Volume 3: Advanced Composite Materials and Processing; Robotics; Information Management and PLM; Design Engineering*, p. 245, 2012, doi: 10.1115/ESDA2012-82322.

[83] A. M. Callegaro, O. Unluhisarcikli, M. Pietrusinski, and C. Mavroidis, “Robotic Systems for Gait Rehabilitation,” pp. 265–283, 2014, doi: 10.1007/978-94-017-8932-5_10.

[84] Y. Şahin, F. M. Botsalı, M. Kalyoncu, and M. Tınkır, “Force Feedback Control of Lower Extremity Exoskeleton Assisting of Load Carrying Human,” vol. 598, pp. 546–550, 2014, doi: 10.4028/www.scientific.net/AMM.598.546.

[85] D. B. Fineberg *et al.*, “Vertical ground reaction force-based analysis of powered exoskeleton-assisted walking in persons with motor-complete paraplegia,” *The Journal of Spinal Cord Medicine*, vol. 36, no. 4, pp. 313–321, 2013, doi: 10.1179/2045772313Y.0000000126.

[86] W. Yang, C. J. Yang, and Q. X. Wei, “Design of an anthropomorphic lower extremity exoskeleton with compatible joints,” *2014 IEEE International Conference on Robotics and Biomimetics, IEEE ROBIO 2014*, pp. 1374–1379, 2014, doi: 10.1109/ROBIO.2014.7090525.

[87] J. F. Veneman, R. Kruidhof, E. E.G. Hekman, R. Ekkelenkamp, E. H.F. van Asseldonk, and H. van der Kooij, “Design and evaluation of the LOPES exoskeleton robot for interactive gait rehabilitation,” *IEEE Transactions on Neural Systems and Rehabilitation Engineering*, vol. 15, no. 1, pp. 379–386, 2007, doi: 10.1109/TNSRE.2007.903919.

[88] Z. Zhiyong *et al.*, “A Series Elastic- and Bowden-Cable-Based Actuation System for Use as Torque Actuator in Exoskeleton-Type Robots,” *The International Journal of Robotics Research*, vol. 1, no. 2, pp. 1–9, 2014, doi: 10.1177/0278364906063829.

[89] R. Ekkelenkamp, J. Veneman, and H. van der Kooij, “LOPES: A lower extremity powered exoskeleton,” *Proceedings - IEEE International Conference on Robotics and Automation*, pp. 3132–3133, 2007, doi: 10.1109/ROBOT.2007.363952.

[90] W. E. Ichinose *et al.*, “A robotic device for measuring and controlling pelvic motion during locomotor rehabilitation,” *Proceedings of the 25th Annual International Conference of the*

IEEE Engineering in Medicine and Biology Society (IEEE Cat. No.03CH37439), vol. 2, pp. 1690–1693, 2003, doi: 10.1109/IEMBS.2003.1279715.

[91] D. Aoyagi, W. E. Ichinose, S. J. Harkema, D. J. Reinkensmeyer, and J. E. Bobrow, "An assistive robotic device that can synchronize to the pelvic motion during human gait training," *Proceedings of the 2005 IEEE 9th International Conference on Rehabilitation Robotics*, vol. 2005, pp. 565–568, 2005, doi: 10.1109/ICORR.2005.1502026.

[92] D. Aoyagi, W. E. Ichinose, S. J. Harkema, D. J. Reinkensmeyer, and J. E. Bobrow, "A robot and control algorithm that can synchronously assist in naturalistic motion during body-weight-supported gait training following neurologic injury," *IEEE Transactions on Neural Systems and Rehabilitation Engineering*, vol. 15, no. 1, pp. 387–400, 2007, doi: 10.1109/TNSRE.2007.903922.

[93] K. P. Westlake *et al.*, "Pilot study of Lokomat versus manual-assisted treadmill training for locomotor recovery post-stroke," *Journal of NeuroEngineering and Rehabilitation*, vol. 6, no. 1, p. 18, 2009, doi: 10.1186/1743-0003-6-18.

[94] S.??o. Jezernik, G. Colombo, T. Keller, H. Frueh, and M. Morari, "Robotic Orthosis Lokomat: A Rehabilitation and Research Tool," *Neuromodulation*, vol. 6, no. 2, pp. 108–115, 2003, doi: 10.1046/j.1525-1403.2003.03017.x.

[95] A. Duschau-Wicke, A. Caprez, and R. Riener, "Patient-cooperative control increases active participation of individuals with SCI during robot-aided gait training," *Journal of NeuroEngineering and Rehabilitation*, vol. 7, no. 1, 2010, doi: 10.1186/1743-0003-7-43.

[96] S. K. Banala, S. H. Kim, S. K. Agrawal, and J. P. Scholz, "Robot assisted gait training with active leg exoskeleton (ALEX)," *97814244*, pp. 653–658, 2008, doi: 10.1109/BIOROB.2008.4762885.

[97] S. K. Banala, S. K. Agrawal, and J. P. Scholz, "Active Leg Exoskeleton (ALEX) for gait rehabilitation of motor-impaired patients," *2007 IEEE 10th International Conference on Rehabilitation Robotics, ICORR'07*, pp. 401–407, 2007, doi: 10.1109/ICORR.2007.4428456.

[98] S. H. Kim, S. K. Banala, E. A. Brackbill, S. K. Agrawal, V. Krishnamoorthy, and J. P. Scholz, "Robot-assisted modifications of gait in healthy individuals," *Experimental brain research*, vol. 202, no. 4, pp. 809–824, 2010, doi: 10.1007/s00221-010-2187-5.

[99] S. K. Banala, S. K. Agrawal, S. H. Kim, and J. P. Scholz, "Novel gait adaptation and neuromotor training results using an active leg exoskeleton," *IEEE/ASME Trans. Mechatron.*, vol. 15, no. 2, pp. 216–225, 2010, doi: 10.1109/TMECH.2010.2041245.

[100] S. Hussain, S. Q. Xie, P. K. Jamwal, and J. Parsons, "An intrinsically compliant robotic orthosis for treadmill training," *Medical Engineering and Physics*, vol. 34, no. 10, pp. 1448–1453, 2012, doi: 10.1016/j.medengphy.2012.02.003.

[101] S. Hussain, S. Q. Xie, and P. K. Jamwal, "Adaptive impedance control of a robotic orthosis for gait rehabilitation," *IEEE Transactions on Cybernetics*, vol. 43, no. 3, pp. 1025–1034, 2013, doi: 10.1109/TSMCB.2012.2222374.

[102] J. L. Emken, S. J. Harkema, J. A. Beres-Jones, C. K. Ferreira, and D. J. Reinkensmeyer, "Feasibility of manual teach-and-replay and continuous impedance shaping for robotic locomotor training following spinal cord injury," *IEEE Transactions on Biomedical Engineering*, vol. 55, no. 1, pp. 322–334, 2008, doi: 10.1109/TBME.2007.910683.

[103] J. L. Emken, J. H. Wynne, S. J. Harkema, and D. J. Reinkensmeyer, "A robotic device for manipulating human stepping," *IEEE Trans. Robot.*, vol. 22, no. 1, pp. 185–189, 2006, doi: 10.1109/TRO.2005.861481.

[104] D. Reinkensmeyer, J. H. Wynne, and S. J. Harkema, "A robotic tool for studying locomotor adaptation and rehabilitation," *Proceedings of the Second Joint 24th Annual Conference and the Annual Fall Meeting of the Biomedical Engineering Society] [Engineering in Medicine and Biology*, pp. 2353–2354, doi: 10.1109/IEMBS.2002.1053318.

[105] J. Zhang, "STRING-MAN: A New Wire Robotic System for Gait Rehabilitation," *The 8th International Conference on Rehabilitation*, pp. 64–66, 2003.

[106] M. Pietrusinski, I. Cajigas, G. Severini, P. Bonato, and C. Mavroidis, "Robotic gait rehabilitation trainer," *Mechatronics, IEEE/ASME Transactions on*, vol. 19, no. 2, pp. 490–499, 2014.

[107] M. Pietrusinski, I. Cajigas, M. Goldsmith, P. Bonato, and C. Mavroidis, "Robotically generated force fields for stroke patient pelvic obliquity gait rehabilitation," *97814244*, pp. 569–575, 2010, doi: 10.1109/ROBOT.2010.5509872.

[108] T. Susko, K. Swaminathan, and H. I. Krebs, "MIT-Skywalker: A Novel Gait Neurorehabilitation Robot for Stroke and Cerebral Palsy," *IEEE Transactions on Neural Systems and Rehabilitation Engineering*, vol. 24, no. 10, pp. 1089–1099, 2016, doi: 10.1109/TNSRE.2016.2533492.

[109] P. K. Artemiadis and H. I. Krebs, "On the potential field-based control of the MIT-skywalker," *IEEE International Conference on Intelligent Robots and Systems*, pp. 1427–1432, 2011, doi: 10.1109/ICRA.2011.5980063.

[110] R. B. Goldberg and E. Chargaff, "On the Control of the Induction of," *97814244*, vol. 68, no. 8, pp. 1702–1706, 1971.

[111] H. Schmidt, C. Werner, R. Bernhardt, S. Hesse, and J. Krüger, "Gait rehabilitation machines based on programmable footplates," *Journal of NeuroEngineering and Rehabilitation*, vol. 4, 2007, doi: 10.1186/1743-0003-4-2.

[112] S. Hesse and C. Werner, "Connecting research to the needs of patients and clinicians," *Brain Res Bull*, vol. 78, pp. 26–34, 2008, doi: 10.1016/j.brainresbull.2008.06.004.

[113] S. Hussein *et al.*, “Muscle coordination in healthy subjects during floor walking and stair climbing in robot assisted gait training,” *97814244*, 2008.

[114] S. Hesse, A. Waldner, and C. Tomelleri, “Innovative gait robot for the repetitive practice of floor walking and stair climbing up and down in stroke patients,” *Journal of NeuroEngineering and Rehabilitation*, vol. 7, no. 1, 2010, doi: 10.1186/1743-0003-7-30.

[115] O. Stoller, M. Schindelholz, L. Bichsel, and K. J. Hunt, “Cardiopulmonary responses to robotic end-effector-based walking and stair climbing,” *Medical Engineering and Physics*, vol. 36, no. 4, pp. 425–431, 2014, doi: 10.1016/j.medengphy.2013.12.016.

[116] C. Tomelleri, A. Waldner, C. Werner, and S. Hesse, “Adaptive locomotor training on an end-effector gait robot: Evaluation of the ground reaction forces in different training conditions,” *97814244*, 2011, doi: 10.1109/ICORR.2011.5975492.

[117] B. Novandy, J. Yoon, and Christiand, “A VR navigation of a 6-DOF gait rehabilitation robot with upper and lower limbs connections,” *97814244*, pp. 592–597, 2008, doi: 10.1109/ICHR.2008.4756010.

[118] J. Yoon, B. Novandy, C. H. Yoon, and K. J. Park, “A 6-DOF gait rehabilitation robot with upper and lower limb connections that allows walking velocity updates on various terrains,” *IEEE/ASME Trans. Mechatron.*, vol. 15, no. 2, pp. 201–215, 2010, doi: 10.1109/TMECH.2010.2040834.

[119] B. Novandy, J. Yoon, and A. Manurung, “Interaction control of a programmable footpad-type gait rehabilitation robot for active walking on various terrains,” *97814244*, pp. 372–377, 2009, doi: 10.1109/ICORR.2009.5209542.

[120] B. Novandy, Christiand, and J. W. Yoon, “Development of gait rehabilitation robot driven by upper limb motion,” *ICCAS 2007 - International Conference on Control, Automation and Systems*, pp. 2383–2388, 2007, doi: 10.1109/ICCAS.2007.4406760.

[121] T. Qin, L. Zhang, Y. Zou, C. Song, and S. Cheng, “Design and optimization of a footpad-type walking rehabilitation robot,” *2012 IEEE International Conference on Mechatronics and Automation, ICMA 2012*, pp. 290–295, 2013, doi: 10.1109/ICCME.2013.6548257.

[122] A. Taherifar, M. R. Hadian, M. Mousavi, A. Rassaf, and F. Ghiasi, “LOKOIRAN - A novel robot for rehabilitation of spinal cord injury and stroke patients,” *2012 IEEE International Conference on Mechatronics and Automation, ICMA 2012*, pp. 218–223, 2013, doi: 10.1109/ICRoM.2013.6510108.

[123] J. M. Burnfield, T. W. Buster, A. Taylor, S. Keenan, Y. Shu, and C. A. Nelson, “ICARE Intelligently Controlled Assistive Rehabilitation Elliptical,” *Revista Internacional de Medicina del Deporte*.

[124] B. Judith M, S. Yu, T. Adam P, B. Thad W, and N. Carl A, “Rehabilitation and Exercise Machine,” 20110294624.

[125] Judith M. BurnfieldYu ShuAdam P. TaylorThad W. BusterCarl A. Nelson, "Rehabilitation and exercise machine,"

[126] H. Yano, S. Tamefusa, N. Tanaka, H. Saitou, and H. Iwata, "Gait rehabilitation system for stair climbing and descending," *97814244*, pp. 393–400, 2010, doi: 10.1109/HAPTIC.2010.5444627.

[127] H. Yano, K. Kasai, H. Saitou, and H. Iwata, "Development of a gait rehabilitation system using a locomotion interface," *Journal of Visualization and Computer Animation*, vol. 14, no. 5, pp. 243–252, 2003, doi: 10.1002/vis.321.

[128] S. Hesse, D. Uhlenbrock, C. Werner, and A. Bardeleben, "A mechanized gait trainer for restoring gait in nonambulatory subjects," *Journal of Rehabilitation Research and Development*, vol. 81, no. 9, pp. 1158–1161, 2000, doi: 10.1053/apmr.2000.6280.

[129] S. Hesse, C. Werner, D. Uhlenbrock, S. V. Frankenberg, A. Bardeleben, and B. Brandl-Hesse, "An Electromechanical Gait Trainer for Restoration of Gait in Hemiparetic Stroke Patients: Preliminary Results," *Neurorehabilitation and Neural Repair*, vol. 15, no. 1, pp. 39–50, 2001, doi: 10.1177/154596830101500106.

[130] S. Hesse, C. Werner, and A. Bardeleben, "Electromechanical gait training with functional electrical stimulation: case studies in spinal cord injury," *Spinal Cord*, vol. 42, no. 6, pp. 346–352.

[131] R. F. Boian, M. Bouzit, G. C. Burdea, J. Lewis, and J. E. Deutsch, "Dual stewart platform mobility simulator," *Proceedings of the 2005 IEEE 9th International Conference on Rehabilitation Robotics*, vol. 2005, pp. 550–555, 2005, doi: 10.1109/ICORR.2005.1502023.

[132] Y. Stauffer *et al.*, "The WalkTrainer - A new generation of walking reeducation device combining orthoses and muscle stimulation," *IEEE Transactions on Neural Systems and Rehabilitation Engineering*, vol. 17, no. 1, pp. 38–45, 2009, doi: 10.1109/TNSRE.2008.2008288.

[133] M. Bouri *et al.*, "The WalkTrainerTM : A Robotic System for Walking," *Control*, pp. 1616–1621, 2006, doi: 10.1109/ROBIO.2006.340186.

[134] P. Wang, K. H. Low, and A. Tow, "Synchronized walking coordination for impact-less footpad contact of an overground gait rehabilitation system: NaTUre-gaits," *97814244*, 2011, doi: 10.1109/ICORR.2011.5975353.

[135] T. P. Luu, H. B. Lim, X. Qu, and K. H. Low, "Pelvic motion assistance of NaTUre-gaits with adaptive body weight support," *2011 8th Asian Control Conference ASCC*, pp. 950–955, 2011.

[136] H. B. Lim, T. P. Luu, K. H. Hoon, X. Qu, A. Tow, and K. H. Low, "Study of body weight shifting on robotic assisted gait rehabilitation with NaTUre-gaits," *IEEE International Conference on Intelligent Robots and Systems*, pp. 4923–4928, 2011, doi: 10.1109/IROS.2011.6048430.

[137] A. Olenšek, M. Zadravec, and Z. Matjačić, "A novel robot for imposing perturbations during overground walking: Mechanism, control and normative stepping responses," *Journal of NeuroEngineering and Rehabilitation*, vol. 13, no. 1, 2016, doi: 10.1186/s12984-016-0160-7.

[138] M. Peshkin *et al.*, "KineAssist: A robotic overground gait and balance training device," *Proceedings of the 2005 IEEE 9th International Conference on Rehabilitation Robotics*, vol. 2005, pp. 241–246, 2005, doi: 10.1109/ICORR.2005.1501094.

[139] J. Patton *et al.*, "KineAssist: Design and Development of a Robotic Overground Gait and Balance Therapy Device," *Topics in Stroke Rehabilitation*, vol. 15, no. 2, pp. 131–139, 2008, doi: 10.1310/tsr1502-131.

[140] K. H. Seo and J. J. Lee, "The development of two mobile gait rehabilitation systems," *IEEE Transactions on Neural Systems and Rehabilitation Engineering*, vol. 17, no. 2, pp. 156–166, 2009, doi: 10.1109/TNSRE.2009.2015179.

[141] A. Morbi, M. Ahmadi, and A. Nativ, "GaitEnable: An omnidirectional robotic system for gait rehabilitation," *2012 IEEE International Conference on Mechatronics and Automation, ICMA 2012*, pp. 936–941, 2012, doi: 10.1109/ICMA.2012.6283269.

[142] H. B. Lim, "Study and implementation of a gait rehabilitation system with capability for mobility and gait pattern generation,"

[143] S. Ayad, A. Megueni, H. Schiøler, M. Ayad, M. de Zee, and L. N.S.A. Struijk, "A control approach for a robotic ground walking platform," *Proceedings of the 9th International Conference on Electronics, Computers and Artificial Intelligence, ECAI 2017*, 2017-Janua, pp. 1–4, 2017, doi: 10.1109/ECAI.2017.8166446.

[144] E. Akdoğan and M. A. Adli, "The design and control of a therapeutic exercise robot for lower limb rehabilitation: Physiotherabot," *Mechatronics*, vol. 21, no. 3, pp. 509–522, 2011, doi: 10.1016/j.mechatronics.2011.01.005.

[145] S. Viteckova, P. Kutilek, and M. Jirina, "Wearable lower limb robotics: A review," *Biocybernetics and Biomedical Engineering*, vol. 33, no. 2, pp. 96–105, 2013, doi: 10.1016/j.bbe.2013.03.005.

[146] N. Aliman, R. Ramli, and S.?M. Haris, "Design and development of lower limb exoskeletons: A survey," *Robotics and Autonomous Systems*, July, pp. 1–17, 2017, doi: 10.1016/j.robot.2017.05.013.

[147] Y. M. Khalid, D. Gouwanda, and S. Parasuraman, "A review on the mechanical design elements of ankle rehabilitation robot," *Proceedings of the Institution of Mechanical Engineers -- Part H -- Journal of Engineering in Medicine (Sage Publications, Ltd.)*, vol. 229, no. 6, p. 452, 2015.

[148] M. X. Lyu, W. H. Chen, X. L. Ding, J. H. Wang, S. P. Bai, and H. C. Ren, "Design of a biologically inspired lower limb exoskeleton for human gait rehabilitation," *Review of Scientific Instruments*, vol. 87, no. 10, 2016, doi: 10.1063/1.4964136.

[149] Bing Chena et all, "Recent developments and challenges of lower extremity exoskeletons," 2015.

[150] F. Zhiguo, Q. Jinwu, Z. Yanan, S. Linyong, Z. Zhen, and W. Qiyuan, "Biomechanical design of the powered gait orthosis," *97814244*, pp. 1698–1702, 2007, doi: 10.1109/ROBIO.2007.4522421.

[151] P. Beyl, M. van Damme, R. van Ham, R. Versluys, B. Vanderborght, and D. Lefeber, "An exoskeleton for gait rehabilitation: Prototype design and control principle," *97814244*, pp. 2037–2042, 2008, doi: 10.1109/ROBOT.2008.4543506.

[152] P. Poli, G. Morone, G. Rosati, and S. Masiero, "Robotic technologies and rehabilitation: New tools for stroke patients' therapy," *BioMed Research International*, vol. 2013, 2013, doi: 10.1155/2013/153872.

[153] M. Frey, G. Colombo, M. Vaglio, R. Bucher, M. Jörg, and R. Riener, "A novel mechatronic body weight support system," *IEEE Transactions on Neural Systems and Rehabilitation Engineering*, vol. 14, no. 3, pp. 311–321, 2006, doi: 10.1109/TNSRE.2006.881556.

[154] R. N. Jazar, *Theory of Applied Robotics*, 2nd ed. New York: Springer US, 2010.

[155] Yuzhe Lu, Jianfeng Meng, Yunpeng Han, Xiaokang Shen, Jun Zhang, "Design and Walking Algorithm of a Foot-Pad Omni-directional Locomotion Interface," *Advances in Engineering Research*, 2016.

[156] S. T. McJunkin, "Transparency Improvement for Haptic Interfaces," Doctor of Philosophy, Rice University, 2007.

[157] M. Vukobratović, *Dynamics and robust control of robot-environment interaction*. Hackensack NJ: World Scientific Pub, 2009.

[158] R. Adams, M. Moreyra, B. Hannaford, Ed., *Stability and Performance of Haptic Displays: Theory and Experiments*, 1998.

[159] "Time-domain passivity control of haptic interfaces - Robotics and Automation, IEEE Transactions on,"

[160] A. Loria and H. Nijmeijer, "PASSIVITY IN CONTROL SYSTEMS," vol. 13, pp. 1–24.

[161] IEEE, "A Two-Port Framework for the Design of Unconditionally Stable Haptic Interfaces - Intelligent Robots and Systems, 1998. Proceedings., 1998 IEEE/RSJ International Conference on,"

[162] IEEE, "Factors affecting the Z-Width of a haptic display - Robotics and Automation, 1994. Proceedings., 1994 IEEE International Conference on,"

[163] Dinh-Son Vu, Simon Foucault, Clement Gosselin, and Jozsef Kovecses, *2015 IEEE International Conference on Robotics and Automation (ICRA 2015): Seattle, Washington, USA, 26 - 30 May 2015*. Piscataway, NJ: IEEE, 2015.

[164] Sciavicco, Lorenzo, Siciliano, Bruno, *Modelling and Control of Robot Manipulators,* 2nd ed.: CreateSpace Independent Publishing Platform, 2000.

[165] S. KİZİR and Z. BİNGÜL, "Fuzzy impedance and force control of a Stewart platform," *Turk J Elec Eng & Comp Sci*, vol. 22, pp. 924–939, 2014, doi: 10.3906/elk-1208-54.

[166] A. Campeau-Lecours, M. J.-D. Otis, and C. Gosselin, "Modeling of physical human–robot interaction," *International Journal of Advanced Robotic Systems*, vol. 13, no. 5, 172988141665816, 2016, doi: 10.1177/1729881416658167.

[167] A. Frisoli, E. Sotgiu, C. A. Avizzano, D. Checcacci, and M. Bergamasco, "Force-based impedance control of a haptic master system for teleoperation," *Sensor Review*, vol. 24, no. 1, pp. 42–50, 2004, doi: 10.1108/02602280410515815.

[168] Carignan, C.R, Cleary, K.R., "Closed-loop force control for haptic simulation of virtual environments," *haptics-e,* vol. 1, no. 2, 2000.

[169] Christian Ott, Ranjan Mukherjee, and Yoshihiko Nakamura, "Unified Impedance and Admittance Control,"

[170] M. C. Lin, A. Steed, and C. Cruz-Neira, *IEEE virtual reality 2008: Reno, Nevada, USA, March 8-12, 2008 proceedings*. Piscataway NJ: IEEE, 2008.

[171] L. V. Bruno Siciliano, *ROBOT FORCE CONTROL*, 1st ed.: Springer US, 1999.

[172] *Getting Started with Simscape.* [Online]. Available: https://www.mathworks.com/help/physmod/simscape/getting-started-with-simscape.html (accessed: Nov. 3 2019).

[173] *3D CAD Design Software.* [Online]. Available: https://www.solidworks.com/ (accessed: Nov. 4 2019).

[174] D. Cekus, B. Posiadała, and P. Warys, "Integration of Modeling in Solidworks and Matlab/Simulink Environments," *Archive of Mechanical Engineering*, vol. 61, no. 1, pp. 57–74, 2014, doi: 10.2478/meceng-2014-0003.

[175] "Dynamic Modeling of Human Gait Using a Model Predictive Control Approach,"

[176] Y. Xiang, J. S. Arora, and K. Abdel-Malek, "Physics-based modeling and simulation of human walking: a review of optimization-based and other approaches," *Struct Multidisc Optim*, vol. 42, no. 1, pp. 1–23, 2010, doi: 10.1007/s00158-010-0496-8.

[177] H. Geyer and U. Saranli, "Gait Based on the Spring-Loaded Inverted Pendulum," in *Humanoid Robotics: A Reference*, A. Goswami and P. Vadakkepat, Eds., Dordrecht: Springer Netherlands, 2019, pp. 923–947.

[178] J. Lanini, A. Duburcq, H. Razavi, C. G. Le Goff, and A. J. Ijspeert, “Interactive locomotion: Investigation and modeling of physically-paired humans while walking,” *PloS one*, vol. 12, no. 9, e0179989, 2017, doi: 10.1371/journal.pone.0179989.

[179] D.-S. Vu, “Synthèse sur la conception, commande et planification de trajectoire d'une interface de locomotion pour la réadaptation de la marche,”

[180] Hninn Wai Wai Hlaing, Aung Myo Thant Sin, Theingi, “Admittance Controller for Physical Human-Robot Interaction Using One-DOF Assist Device,”

[181] Araki M, “PID Control,” *Control Systems, Robotics, And Autimation*, vol. 2, 1984.

[182] N. Colonnese and A. M. Okamura, “M-Width: Stability, noise characterization, and accuracy of rendering virtual mass,” *The International Journal of Robotics Research*, vol. 34, no. 6, pp. 781–798, 2015, doi: 10.1177/0278364914559294.

[183] S. Amirkhani and A. Nahvi, “Design and implementation of an interactive virtual control laboratory using haptic interface for undergraduate engineering students,” *Comput Appl Eng Educ*, vol. 24, no. 4, pp. 508–518, 2016, doi: 10.1002/cae.21727.

[184] IEEE, “A Whole Body Kinesthetic Display Device For Virtual Reality Applications - Robotics and Automation, 1997. Proceedings., 1997 IEEE International Conference on,”

[185] Lynette A. Jones, “Kinesthetic Sensing,” *Human and Machine Haptics*, pp. 1–10, 2000.

[186] H. Takemura and K. Kiyokawa, *Proceedings: IEEE Virtual Reality 2001 13-17 March, 2001, Yokohama, Japan*. Los Alamitos Calif.: IEEE Computer Society Press, 2001.

[187] T. M. Bhaskar Dasguptaa, “The Stewart platform manipulator: a review,” *Mechanism and Machine Theory*, vol. 35, pp. 15–40, 2000.

[188] Ciprian-Radu Rad, Radu Balan, Sergiu-Dan Stan., Ed., *Numerical Implementation of The Kinematics For a 3-Dof Parallel Robot Using Matlab*, 2009.

[189] N. A. Pouliot, C. M. Gosselin, and M. A. Nahon, “Motion Simulation Capabilities of Three-Degree-of-Freedom Flight Simulators,” *Journal of Aircraft*, vol. 35, no. 1, pp. 9–17, 1998, doi: 10.2514/2.2283.

[190] Alexander Spinos, Devin Carroll, Terry Kientz, and Mark Yim., Ed., *Variable Topology Truss: Design and Analysis*, 2017.

[191] IEEE, “Development of a parallel link manipulator - Advanced Robotics, 1991. 'Robots in Unstructured Environments', 91 ICAR., Fifth International Conf,”

[192] J. E. Deutsch, J. Latonio, G. C. Burdea and R. Boian, “Post-Stroke Rehabilitation with the Rutgers Ankle System: A Case Study,” *Presence*, vol. 10, pp. 416–430, 2001.

[193] H. Rakhodaei, “Design and analysis of a 9 DOF: hybrid parallel robot,” Doctor of Philosophy, School of Mechanical Engineering, Birmingham, United Kingdom, 2013.

[194] H. Rakhodaei, M. Saadat, A. Rastegarpanah, and C. Z. Abdullah, “Path planning of the hybrid parallel robot for ankle rehabilitation,” *Robotica*, vol. 34, no. 1, pp. 173–184, 2016, doi: 10.1017/S0263574714001210.

[195] DAN ZHANG, “Kinetostatic Analysis and Optimization of Parallel and Hybrid Architectures for Machine Tools,” Doctor of Philosophy, Department of mechanical engineering, University of Laval, Quebec, Canada, 2000.

[196] D. L. J.CFaugère, “Combinatorial Classes of Parallel Manipulators,” *Mechanism and Machine Theory*, vol. 30, no. 6, pp. 765–776, 1995.

[197] Anders Lohmann Madsen, Søren Giessing Kristensen, “Design of Stewart Platform for Wave Compensation,” Master Thesis, Aalborg university, 2012.

[198] E. E. H. Martinez, S. I. V. Peña, and E. S. Soto, “Towards a Robust Solution of the Non-Linear Kinematics for the General Stewart Platform with Estimation of Distribution Algorithms,” *International Journal of Advanced Robotic Systems*, vol. 10, no. 1, p. 38, 2013, doi: 10.5772/52172.

[199] Alireza Rastegarpanah, Mozafar Saadat, Hamid Rakhodaei, Ed., *Analysis and simulation of various Stewart Platform configurations for lower limb rehabilitation*, 2013.

[200] J. Angeles, *Fundamentals of Robotic Mechanical Systems*. Cham: Springer International Publishing, 2014.

[201] “W. Khalil, E. Dombre - Modeling Identification and Control of Robots (2004, Butterworth-Heinemann),”

[202] D. C. Lay, S. R. Lay, and J. McDonald, *Linear algebra and its applications*. Boston: Pearson, 2016.

[203] T. Yoshikawa, “Manipulability of Robotic Mechanisms,” *The International Journal of Robotics Research*, vol. 4, no. 2, pp. 3–9, 1985, doi: 10.1177/027836498500400201.

[204] Z. Xie, G. Li, G. Liu, and J. Zhao, “Optimal design of a Stewart platform using the global transmission index under determinate constraint of workspace,” *Advances in Mechanical Engineering*, vol. 9, no. 10, 168781401772088, 2017, doi: 10.1177/1687814017720880.

[205] *Ball Joint DIN71802 C/CS--Wuerd Machinery CO.,LTD.* [Online]. Available: http://www.wuerdgroup.com/product/angled-ball-joint-ccs/ (accessed: Mar. 18 2020).

[206] O. Masory and J. Wang, “Workspace evaluation of Stewart platforms,” *Advanced Robotics*, vol. 9, no. 4, pp. 443–461, 1994, doi: 10.1163/156855395X00508.

[207] *Creating a Stewart Platform Model Using SimMechanics.* [Online]. Available: https://www.mathworks.com/company/newsletters/articles/creating-a-stewart-platform-model-using-simmechanics.html (accessed: Apr. 6 2020).